Cholesterol Dysregulation in Multiple Sclerosis: Implications for Pathogenesis and Opportunities for Monitoring and Treating Progressive Disease

Kristen Hawkins

Submitted to Swansea University in fulfilment of the requirements for the Degree of Doctor of Philosophy

Swansea University

2023

Abstract

Introduction

Multiple sclerosis (MS) is characterised by demyelination, neuroinflammation and neurodegeneration that contributes to a progressively worsening condition over time. Ongoing, chronic demyelination is an important hallmark of MS pathobiology; however the underlying drivers of progression have not been fully elucidated. Microglia mediate demyelination and contribute to continued lesion expansion. Phagocytosis and processing of myelin by microglia and macrophages results in the release of myelin-lipids – including cholesterol, and dysregulation of cholesterol homeostasis may drive a damaging microglial/macrophage response. The oxidised metabolites of cholesterol – oxysterols – are important ligands implicated in myelination, neuroinflammation and neuron survival and may represent a druggable target. Little is known about the abundance and location of cholesterol and the oxysterols in the MS brain, or how their dysregulation may contribute to a worsening progressive MS.

Objective

I aimed to identify whether cholesterol homeostasis and metabolism is dysregulated in pathologically relevant regions of the MS brain, and if so, to investigate whether its modulation could be beneficial in MS.

Methods

Postmortem, snap frozen brain tissue from progressive MS (n=7, male=3, age=49 years; REC 13/WA/0292) and controls (n=5, male=3, age=61 years) were immunostained for myelin, microglia and lipid markers. Regions of pathological interest (ROI) were macrodissected, oxysterols extracted, and quantified using enzyme-assisted derivatisation for sterol analysis - liquid chromatography – mass spectrometry (EADSA-LC-*MS*). Quantitative *in situ* hybridisation and immunostaining reported the relative expression of key enzymes of the cholesterol metabolic pathway. A primary human *in vitro* model of myelin phagocytosis by monocyte-

derived microglia-like cells was established to assess the effects of MS-related drugs on their ability to promote myelin clearance from lipid-laden cells.

Results

Key lipid metabolic systems differ between MS and control brain, and in regions of chronic demyelination, including cholesterol and 24S-hydroxycholestol (24S-HC; the major oxysterol of the human brain). 24S-HC: control WM – 20.44±2.87 ng/mg, slowly expanding lesion (SEL) edge – 3.27±1.59 ng/mg, SEL centre – 1.91±1.23 ng/mg. Evidence of altered cholesterol homeostasis was supported by the finding of abundant lipid droplet positive macrophages at SEL edge and a striking 98% reduction of the *CYP46A1* transcript in the MS brain, whose product metabolises cholesterol to 24S-HC ($p<0.0001$). MS-related drugs, including simvastatin, were shown to promote myelin clearance from lipid-laden macrophages *in vitro*.

Conclusion

Cholesterol is dysregulated in MS and an over accumulation of cholesterol in microglia/macrophages at sites of chronic, actively demyelinating tissue, such as the edge of SEL, may result in a failure of phagocytes to resolve inflammation. Interventions to restore cholesterol homeostasis, for example by increasing *CYP46A1* expression or activity, may resolve chronic inflammatory demyelination and reduce the severity of MS disease.

Declarations

This work has not previously been accepted in substance for any degree and is not being concurrently submitted in candidature for any degree.

Signed.....[redacted].....

Date.....30.03.2023.....

This thesis is the result of my own investigations, except where otherwise stated. Other sources are acknowledged by footnotes giving explicit references. A bibliography is appended.

Signed.....[redacted].....

Date.....30.03.2023.....

I hereby give my consent for my work, if relevant and accepted, to be available for photocopying and for inter-library loans **after expiry of a bar on access approved by the University**.

Signed.....[redacted].....

Date.....30.03.2023.....

The University's ethical procedures have been followed and, where appropriate, that ethical approval has been granted.

Signed.....[redacted].....

Date.....30.03.2023.....

Table of Contents

For Aunty Jane.

You are forever in our hearts.

Acknowledgements

First and foremost, I would like to thank Dr Owain Howell. I truly won the lottery of supervisors. I cannot thank you enough for sharing your seemingly endless knowledge and for all of your support and guidance throughout my project. I would not be the scientist I am today without you.

I would also like to thank Prof. Bill Griffiths and Prof. Yuqin Wang for sharing your specialist knowledge and welcoming me into your team as an honorary member.

I would like to thank The MS Society for funding this project – I am grateful to every single person who has donated. It has been an absolute pleasure to get to know some of the staff, volunteers and society members over the past 4 years.

Thank you to everyone on 2nd floor who has supported me with this project. In particular, I would like to say a huge thank you to Dr James Cronin and Prof. Cathy Thornton.

To my parents and my brother, Daniel, thank you for your unwavering support. Mum and Dad, thank you for inspiring me and for always encouraging me to chase my goals, without you this would not have been possible.

Oliver, thank you for always bouncing ideas around with me and for being my personal cheerleader. Thank you for feeding me whilst I wrote my thesis and for doing all the washing-up!

A big shout out has to go to my Meme Queens of the Sisterhud. Ladies, without you, PhD-land would not have been the same, and I cannot thank you enough.

Paige, thank you for every late night catch-up, and for endless laugher, even when times were tough.

Becky, Justin – thank you for "Therapy Thursday" and for generally being encouraging and uplifting.

Bea, Libby, Hannah, Chelsea, Sophie, Ellie - thank you for always checking in and constantly cheering me on.

Last, but absolutely not least, I would like to thank all the members, past and present, of the 3rd floor, particularly Dr Eylan Yutuc and Dr Rhian Evans, for your help and support, as well as for all the Pub Friday's and much needed coffee breaks.

List of Figures

List of Tables

Equation

Abbreviations

24S-HC: 24S-hydroxycholesterol

25-HC: 25-hydroxycholesterol

26-HC: (25R)26-hydroxycholesterol

7α,(25R)26-HC: 7α,(25R)26-dihydroxycholesterol

ABC: avidin-biotin complex

ABCA1: Adenosine triphosphate-binding cassette A1

AD: Alzheimer's disease

APOE: apolipoprotein E

CH25H: cholesterol 25-hydroxylase

CYP27A1: cytochrome P450 family 27 subfamily A member 1

CYP46A1: cytochrome P450 family 46 subfamily A member 1

CD68: cluster of differentiation 68

CIS: clinically isolated syndrome

CNS: central nervous system

CSF: cerebral spinal fluid

Ctrl: control

DAB: diamino benzidine

DAPI: 4',6'-diamidino-phenylindole

EADSA: enzyme-assisted derivatisation for steroid analysis

EAE: experimental autoimmune encephalomyelitis

EBV – Epstein-Barr virus

FBS: foetal bovine serum

GC: gas chromatography

GM: grey matter

GM-CSF: granulocyte/macrophage colony-stimulating factor

GML: grey matter lesion

GWAS: genome-wide association studies

GP: Girard's Reagent P

HLA: human leucocyte antigen

HMG-CoA: 3-hydroxy-3-methylglutaryl-CoA

HPLC: high performance liquid chromatography

IBA1: ionized calcium binding adapter molecule 1

IFN: interferon

IHC: immunohistochemistry

IL: interleukin

iNOS: inducible nitric oxide synthase

ISH: *in situ* hybridisation

iSTD: internal standard

LC: liquid chromatography

LDLR: low-density lipoprotein receptor

LFB: luxol fast blue

LIT: linear Ion trap

LXR: liver X receptor

MACS: magnetic-activated cell sorting

MAG: myelin-associated glycoprotein

MA/I – mixed active/inactive

MALDI: matrix-assisted laser desorption ionisation

MBP: myelin basic protein

MerTK: mer tyrosine kinase

MOG: myelin oligodendrocyte protein

MRI: magnetic resonance imaging

mRNA: messenger ribonucleic acid

MS: multiple sclerosis

MS: mass spectrometry

m/z: mass-to-charge ratio

NADPH: nicotinamide adenine dinucleotide phosphate

NAGM: normal appearing grey matter

NAWM: normal appearing white matter

NfL: neurofilament light chain

OPC: oligodendrocyte precursor cells

ORO: oil red O

P/S: penicillin/streptomycin

PBMC: peripheral blood mononuclear cells

PBS: phosphate buffered saline

PBS-T: phosphate buffered saline with 0.1% triton-x 100

PLN2: perilipin-2

PLP: proteolipid protein

PFA: paraformaldehyde

PMD: postmortem delay

PMS: progressive multiple sclerosis

PPAR: peroxisome proliferator-activated receptor

PPMS: primary progressive multiple sclerosis

RAR: retinoic acid receptor

RF: radio frequency

ROI: region of interest

ROS: reactive oxygen species

RORγT: RAR-related orphan receptor gamma t

RRMS: relapsing remitting multiple sclerosis

RT: room temperature

S1P: sphingosine-1-phosphate

SCAP: SREBP cleavage and activating protein

SEM: standard error of the mean

SPMS: secondary progressive multiple sclerosis

SPE: solid phase extraction

SREBP: sterol regulatory element binding protein

SSC: saline sodium citrate

TLC: thin layer chromatography

TMEM119: transmembrane protein 119

TNFα: tumour necrosis factor alpha

TREM2: triggering receptor expressed on myeloid cells 2

WM: white matter

WML: white matter lesion

Chapter 1 – Introduction

1.1 Multiple Sclerosis

Multiple sclerosis (MS) is a debilitating disease of the central nervous system (CNS), characterised by demyelination, neuroinflammation and neurodegeneration (Frohman, Racke, and Raine 2006). It affects around 130 000 people in the UK and around 2.5 million globally. It is the most common cause of non-traumatic brain injury in young people. (Browne et al. 2014; Compston and Coles 2002, 2008). MS adversely affects quality of life, and is associated with loss of motor control, reduced cognition and extreme fatigue (Confavreux and Vukusic 2014).

MS is currently incurable. Clinicians have a growing number of disease modifying therapies (DMTs) in their arsenal, however, the majority of these are only suitable for treating the earliest, most inflammatory phase of MS. The majority of available DMTs are centred on modifying the peripheral autoimmune response. Presence of progression independent of relapse activity (PIRA) indicates that there are other important drivers of disease worsening in many people with established, (or progressive) MS (PMS) (Confavreux and Vukusic, 2014; Elliott et al., 2019; Cree et al., 2019). Therefore, there is still a gap in our understanding of the neuropathic drivers through the clinical course of MS, and as a result, there is still an unmet need for drugs which can slow or stop disease progression.

1.1.1 – MS Disease, Diagnosis and Treatment

1.1.1.1 – MS Disease and Diagnosis

Diagnosis of MS is challenging due to the heterogeneous nature of the disease; often taking months/years from symptom onset before a diagnosis is confirmed. Diagnosis utilises the McDonald criteria and relies on a combination of the clinical manifestation of symptoms, presence of lesions on MRI (disseminated in anatomical space and time) and presence of cerebrospinal fluid (CSF)-specific oligoclonal bands (Thompson et al., 2018a; Travers et al., 2022).

There are 3 main clinical subtypes of MS disease – relapse remitting (RR), secondary progressive (SP) and primary progressive (PP) MS (figure 1.1). The majority of newly diagnosed MS patients present with the relapse remitting subtype of the disease. This is characterised by periods of relapse (new clinical disability onset/new radiologically defined attack) followed by remission (moderate or full return of physical function) (Confavreux and Vukusic, 2014; Dimitrov and Turner, 2014). Relapse remitting MS is associated with intermittent bouts of inflammatory attack in the CNS interspersed with periods of resolution of this inflammation and partial repair (remyelination and neuroplastic changes) such that a near full recovery is seen (Kamel, 2019) Today's DMTs are moderately to highly-effective at reducing new inflammatory attacks, to such an extent that the patient may become essentially relapse-free (Callegari et al., 2021). However, despite being on efficacious anti-inflammatory treatment, many people with RRMS still experience a slow worsening of disability, to such a point that the overriding clinical phenotype is that of a progressive neurological disease course – this is SPMS (Doshi and Chataway, 2016). Around 10% of MS patients experience a progressive neurological disability with limited relapses from onset - this is PPMS. Primary progressive and SPMS share many of the same pathological characteristics (Kuhlmann et al., 2017; Luchetti et al., 2018). They have considerably less overt, focal inflammation in the CNS but display a more widespread and chronic infiltration of the connective tissues, normal appearing white and grey matter, larger and more frequent demyelinating lesions, especially chronic active and slowly expanding lesions of the white and deep grey matter, and a sometimes very extensive demyelination of the cortical grey matter (Kutzelnigg et al., 2005; Magliozzi et al., 2007; Frischer et al., 2009; Howell et al., 2011; Frischer et al., 2015; Haider et al., 2016; Zrzavy et al., 2017; Luchetti et al., 2018). The nature of the chronic neuroinflammation, demyelination and extensive neuroal- and axonal-loss, that drives sustained atrophy, underlies the progressive and irreversible worsening in the later phase and is the presumed reason why current DMTs are less effective in PMS (Mahad et al., 2015; Correale et al., 2017).

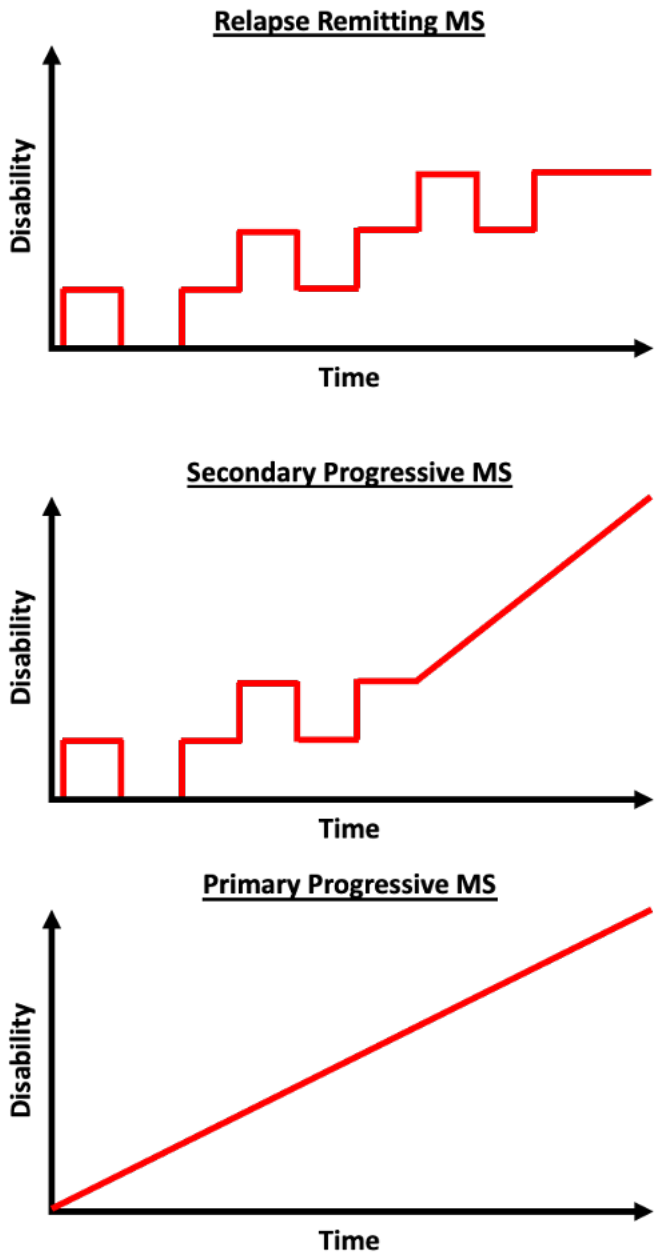

Figure 1.1 – Graphical Representation of the Main Subtypes of MS

Relapse remitting MS consists of periods of increased disability and periods of remission where symptoms resolve partially or completely (a). Secondary progressive disease begins with periods of increased disability and remission which gradually transitions into progressively worsening disease, with no improvement in symptoms (b). Primary progressive MS consists of worsening disability over time from onset (c). Created in Microsoft PowerPoint.

The clinical definition of MS as RR, SP or PP can be further refined based on the evidence of relapse activity, and findings from neuroimaging and clinical assessment. A relative assessment of disease inflammatory activity is made on the basis of the frequency of relapses and/or the finding of new lesions or unequivocally enlarging lesions (so that an individual can be said to be experiencing an 'active' or 'not active' inflammatory disease). An individual's MS can also be categorised as stable, or worsening, based on a longitudinal assessment of their neurological disability over time (has the patient got worse or remained stable). These modifiers are important criteria for the decision as to when to treat, what to treat with and provides a mechanism for monitoring how well a patient is responding to their treatment (Lublin et al., 2022).

There are a number of clinically useful biomarkers for MS. At present, the only biomarker for *in vivo* assessment of the entire CNS is MRI. This is very useful for identification of lesion activity, particularly demyelination with white matter (WM) involvement (Reich et al., 2018). The presence of CSF-specific oligoclonal bands can be used to aid diagnosis after a single attack, as their presence is prognostic of a higher risk of a second attack, i.e., conversion of clinically isolated syndrome (CIS; a 'one-off' attack) to an MS diagnosis (McGinley et al., 2021). There are also potential up-and-coming biomarkers such as neurofilament light chain (NfL) levels obtained in serum samples. NfL may correlate with increased inflammation; and potentially higher levels at diagnosis may be prognostic of an increased severity risk. However, NfL indicates neuronal damage and thus is not MS-specific, additionally its concentration can also be affected by confounding variables such as age and BMI – so its usefulness/prognostic meaning will have to be carefully considered (Yang et al., 2022). There is still a need for more diagnostic biomarkers and particularly more prognostic biomarkers to aid in the prediction of disease progression, which would ultimately improve patient care.

1.1.1.2 – Treatment of MS and the need for drugs that target neuroinflammation and neurodegeneration

MS disease modifying therapies target the peripheral immune system, modulating the immune response and sequestering lymphocytes to the periphery and preventing them from crossing the blood brain barrier (BBB) (Callegari et al., 2021; Correale et al., 2021). These treatments can be highly effective in RRMS and in some people with an active and worsening PMS (McGinley et al., 2021). A summary of available MS DMTs can be found in table 1.1.

To date, there are only two MS drugs suitable for the treatment of progressive disease – Ocrelizumab, for PPMS (and RRMS) and Siponimod (for SPMS). Importantly, these potent anti-inflammatory medicines are only effective (and can only be prescribed) for those people with evidence of ongoing disease activity (i.e., relapse activity or evidence of new and/or expanding lesions). Ocrelizumab is a monoclonal anti-CD20 antibody that depletes CD20 expressing B-cells. B-cells regulate inflammation via the production of pro-inflammatory and anti-inflammatory cytokines; a process that appears dysfunctional in MS. Additionally, B-cells can form follicular-like structures within the brain which correlate with a worse MS-prognosis (Magliozzi et al., 2007; Jakimovski et al., 2017; Riederer, 2017; Mulero et al., 2018).

Siponimod is a sphingosine-1-phosphate (S1P) modulator. S1P-receptors (subtypes 1-5) are expressed by a variety of cell types including lymphocytes and neuroglia. Siponimod can bind $S1P_1$ present on CD4+ T-cells, preventing egress from the thymus and lymph nodes, preventing T-cell infiltration into the blood, and thus CNS. Additionally, it can exert anti-inflammatory and anti-neurogenerative effects in pre-clinical models, by traversing the BBB and binding to $S1P_1$ and $S1P_5$ expressed by neuroglia, but whether this contributes significantly to Siponimod's efficacy in PMS is unclear (Behrangi et al., 2019; Dumitrescu et al., 2019; Cohan et al., 2022). The realisation that significant numbers of people with MS can experience PIRA (discussed in detail below, see 1.1.2) whilst still on active treatment, highlights the need for drugs which expressly target the other important components of this 'silent'

progression. It is thought that the shifting balance between systemic inflammation and central neuroinflammation, neurodegeneration and a variable extent of remyelination between individuals, and within the course of a person's MS, may explain the incomplete efficacy of today's DMTs. There is great need for drugs which act to slow or stop the progression of MS; and a need to understand the underlying mechanisms of silent progression to facilitate this (Cree et al., 2019; Cree et al., 2021).

Table 1.1 – UK Licenced Disease Modifying Therapies for the Treatment of MS

A list of approved DMTs for the treatment MS, their brief proposed mechanisms of action and which subtype of MS they are used to treat. There are also a number of unlicensed, experimental drugs at preclinical and clinical trial stage which have not been included in this table. RRMS – relapse remitting MS, SPMS – secondary progressive MS, PPMS – primary progressive MS, active – evidence of relapse activity.

Drug Name	Mechanism of Action	MS Subtype
Alemtuzumab (Bross *et al*, 2020)	Anti-CD52 monoclonal antibody, long-lived lymphocyte depletion	Active RRMS
Avonex (Bross *et al*, 2020)	Promotion of anti-inflammatory cytokines	RRMS
Betaferon (Bross *et al*, 2020)	Promotion of anti-inflammatory cytokines	RRMS
Cladribine (Bross *et al*, 2020)	Deoxyadenosine analogue, long-lived lymphocyte depletion	RRMS, active SPMS
Dimethyl fumerate (Bross *et al*, 2020; Mills *et al*, 2018)	Reduction of lymphocytes with a skew towards reducing pro-inflammatory T-cell (as well as B-cell) subsets	RRMS
Extavia (Bross *et al*, 2020)	Promotion of anti-inflammatory cytokines	RRMS
Fingolimod (Brinkmann *et al.*, 2002; Hait *et al.*, 2014; Kleiter *et al.*, 2016; Tiper *et al.*, 2016)	Sphingosine-1-phosphate receptor agonist, prevents ingress of lymphocytes into the CNS.	RRMS
Glatiramer acetate (Bross *et al*, 2020)	Anti-inflammatory	RRMS
Haematopoietic stem cell transplantation (Rush *et al*, 2019)	Remodeling of the immune system through chemotherapy and reintroduction of autologous stem cells	Aggressive RRMS/ progressive MS
Natalizumab (Bross *et al*, 2020)	Monoclonal antibody, sequesters T cells to the periphery	RRMS
Ocrelizumab (Bross *et al*, 2020)	Anti-CD20 monoclonal antibody, depletion of B cells	RRMS, PPMS
Ofatumumab (Kang and Blair, 2022)	Anti-CD20 monoclonal antibody, depletion of B cells	RRMS
Plegridy (Bross *et al*, 2020)	Promotion of anti-inflammatory cytokines	RRMS
Rebif (Bross *et al*, 2020)	Promotion of anti-inflammatory cytokines	RRMS
Siponimod (Behrangi *et al.*, 2019; Dumitrescu *et al.*, 2019; Cohan *et al.*, 2022)	Sphingosine-1-phosphate receptors 1 & 5 modulator, sequesters T cells to the periphery	RRMS, active SPMS
Teriflunomide (Bross *et al*, 2020)	Inhibitor of mitochondrial dihydro-orotate dehyderogenase	RRMS

1.1.2 – Progression Independent of Relapse Activity

The majority of people with RRMS convert to SPMS later in their disease course, irrespective of effective DMTs targeting acute inflammation and reducing annualised relapse rate (Lassmann et al., 2012; Callegari et al., 2021; Correale et al., 2021). This is likely due to a slow, underlying level of progression, which exists within the brains of people with MS - progression independent of relapse activity (PIRA). This 'silent' progression may be so slow that the patient and clinician may miss progression for a period of time, as ability accrual is gradual, and therefore progression is identified retrospectively (Cree et al., 2019; Kappos et al., 2020; Cree et al., 2021; Lublin et al., 2022).

PIRA appears to be driven by more diffuse inflammation, which contributes to neuroaxonal loss and subsequent accrual of seemingly irreversible physical and cognitive disability (Cree et al., 2019; Kappos et al., 2020; Cree et al., 2021; Lublin et al., 2022). Although the underlying cause of silent progression has yet to be elucidated, SP and PPMS share some common radiological/pathological features, which may suggest clues, including increased cortical demyelination and diffuse WM microglial activation and chronic demyelination (Frischer et al. 2009; Howell et al. 2011; Kutzelnigg et al. 2005; Luchetti et al. 2018; Magliozzi et al. 2010). For example, in WM, the presence of iron-rim, slowly expanding lesions, detected via MRI, associate with an elevated risk of increased disability. Their presence has been reported to be associated with an increased risk of conversion to secondary progression by 1.6 times, compared to those without iron-rim lesions (Absinta et al. 2019; Cree et al. 2021).

The later postmortem sampling of iron rim lesions imaged in the living demonstrated that they represent a mixed active/inactive (chronic) white matter lesion, which contain a rim of foamy macrophages, described extensively by others to associate with a more severe MS (Absinta et al., 2019). Continued, underlying neurodegeneration will also contribute to PIRA. Neuronal and axonal loss are a major component of tissue atrophy - whole brain, spinal cord and regional brain atrophy is an excellent correlate of disease severity and is prognostic for the rate of disease

worsening. The drivers of neuro-axonal damage will relate to loss of supporting oligodendrocytes and normal homeostatic astroglial and microglial responses. For example, in a rodent model of MS, experimental autoimmune encephalomyelitis (EAE), microglia, along with astrocytes, have been shown to produce damaging reactive oxygen species (ROS) and reactive nitrogen species (RNS) (Haider et al. 2011), alongside inflammatory cytokines, such as tumour necrosis factor-α (TNFα) and interferon-γ (IFN-γ), which can mediate temporary, as well as more long-term effects, on neuron and axon function and survival (Nikić et al., 2011). Oxidative injury may contribute to neurodegeneration because mitochondria are particularly sensitive to oxidation, and as discussed below (see 1.1.5.2) are essential for axonal/neuronal health through production of energy (Haider et al., 2011; Correale et al., 2019).

DMTs which specifically target compartmentalised CNS inflammation (the component of the immune response which is locked within the tissue, which includes widespread microglial activation, chronic actively demyelinating lesions and leptomeningeal inflammation) and neurodegeneration will be required to treat many cases of progressive MS (Callegari et al., 2021; Cree et al., 2021). A number of trials of agents which specifically target these central components of the disease are currently underway (Yong and Yong, 2021). For example, Ibudilast, a small molecule that can traverse the BBB, has been shown to reduce brain atrophy by 48% and slow progression in SP and PPMS in a phase 2 trial. Its action has been attributed to a reduction in diffuse CNS inflammation (Naismith et al., 2021). Similarly, efforts to use minocycline, an antibiotic that can cross the BBB, with long-described neuroimmune and microglia-specific modulating effects, in preventing conversion to clinically definite MS (Metz et al., 2017). Another target of interest is Bruton's tyrosine kinase (BTK). BTK is expressed by some B-cells and microglia, its inhibition by the brain penetrant Evobrutinib reduces their inflammatory activity, and is associated with a reduction in the volume of chronic actively demyelinating lesions (Arnold et al. 2022; Cree et al. 2021; García-Merino 2021). Efforts to modulate neuro-axonal processes, including protecting neurons from damage and destruction, are in a very early phase

and are yet to report any conclusive benefit on slowing or stopping disease progression (Chataway et al., 2020).

Other classes of drugs, which are not (at least directly) solely targeting inflammation are also being studied. For example, the phase 2 MS-STAT trial, has shown that high dose simvastatin (a statin which crosses the BBB), reduced total brain atrophy by 43% in SPMS patients (Chataway et al., 2014) and was associated with a relative preservation of cognitive function and higher quality of life indicators (Chan et al., 2017). This highlights, that the underlying mechanisms of PIRA may be multifactorial, and that by tackling components of this pathophysiology, including innate immune cell activation, slowly expanding demyelinating lesions and neuronal-axonal health, it may yet be possible to improve patient outcomes.

1.1.3 – Factors Affecting MS Susceptibility and Course

MS is a complex disease, associated with multiple environmental and genetic risk factors (Thompson et al., 2018b). Genome wide association studies (GWAS) have identified a range of risk, as well as protective, alleles. For example, carriers of the HLA DRB1*15:01 allele have around triple the risk of developing MS compared to a non-carrier (Patsopoulos et al., 2013). Additionally, a large GWAS study has shown that there is an enrichment of MS susceptibility genes, related to regulation of innate immunity, expressed specifically by microglia (as opposed to astrocytes or neurons) suggesting that microglia have a role in MS susceptibility (Patsopoulos et al., 2019). But as yet, little progress has been made in identifying common variants that link to disease subtype or severity (Jokubaitis et al., 2022).

The study of MS in family groups has identified rare heritable traits in these cohorts which do not map to larger studies using standard clinical cohorts (Patsopoulos, 2018). Nevertheless, these analyses do provide an insight into aspects of the disease aetiology and pathology. One such example is the description of a rare variant in CYP27B1 (Cytochrome P450 Family 27 Subfamily B Member 1), that encodes an enzyme important in steroid, lipid and cholesterol metabolism, and hydroxylates 25-hydroxyvitamin D_3 (Ramagopalan et al., 2011). Other work revealed a variant in NR1H3 (Nuclear Receptor Subfamily 1 Group H Member 3, also known as the

Oxysterols Receptor LXR-Alpha), which encodes liver X receptor (LXR-α), which together with its dimerization partner, retinoid X receptor (RXR), regulates the transcription of a host of important immune and metabolic-related genes, including those required for the catabolism of vitamin D and cholesterol. This coding variant in NR1H3 was associated with a particularly aggressive and atypical form of PPMS (Wang et al., 2016). These important, but not validated, studies highlight links between lipid metabolic processes, including those involving cholesterol, in MS risk and outcome.

There are a number of environmental risk factors which can increase someone's chance of developing MS, including smoking, obesity (especially in childhood/adolescence), vitamin D deficiency and infection. Obesity in early life has been associated with a two-fold increased risk of developing MS later in life (Gianfrancesco and Barcellos 2016; Thompson, Baranzini, et al. 2018). In addition to reducing overall health, the effect of obesity in MS has also been related to reduced vitamin D levels, often found in obese individuals (Thompson et al., 2018b). Vitamin D plays a role in the normal functioning of the immune system. Low levels have been shown to associate with an increased MS susceptibility risk, as well as a more severe disease course (Mark et al., 2018; Camu et al., 2020; Ao et al., 2021). Vitamin D deficiency may correlate with the reduced incidence of MS observed as you approach the equator, however, the reduction in these areas may also be due to sampling bias (e.g., reduced diagnosis in lower income countries).

Smoking is a risk factor for many morbidities, it has a profound effect on the immune system, increasing inflammation, and likely promotes autoimmunity (Arnson et al., 2010). Additionally, in MS, it has been shown to correlate with an increased rate of conversion to progressive disease (Ramanujam et al., 2015) and a more rapid disease evolution (Rodgers et al., 2022). Increased incidence of childhood infections may be protective against MS, whereas specific infection, such as with the Epstein-Barr Virus (EBV), has been shown to increase an individual's susceptibility risk (Bach, 2002; Levin *et al.*, 2005; Thompson *et al.*, 2018). For example, in a recent study Bjornevik and colleagues demonstrated a 32-fold increase in MS after infection with EBV, additionally this correlated to increased serum NfL concentration (Bjornevik et al.,

2022; Yang et al., 2022). EBV infection may increase MS risk due to a high molecular mimicry between EBV's transcription factor EBV nuclear antigen 1 (EBNA1) and the CNS protein glia cell adhesion molecule (GlialCAM) (Lanz et al., 2022).

MS is a multifactorial condition, the underlying cause has yet to be elucidated, but a combination of genetic and environmental factors which intersect at pathways that impact on immune regulation and metabolic pathways, likely contribute to MS risk.

1.1.4 – Experimental Models used in the Study of MS

There is no perfect model of MS which is capable of encompassing this complex disease as a whole. However, there are a number of *in vivo* and *in vitro* pre-clinical models which have helped to advance our knowledge of the underlying biology of MS. The most commonly used *in vivo* model for MS is EAE. Induction of EAE in susceptible mice is achieved by immunisation with self-myelin proteins such as MOG, MBP and PLP, along with reactive T cells and Freud's adjuvant and pertussis toxin (Munoz, Bernard, and Mackay 1984). This causes paralysis which ascends from the tail, similar to the ascending paralysis experienced by many MS patients. The genetic mouse model and myelin peptide used affects the clinical manifestation of EAE symptoms, with some variations of the model being more chronic in nature whilst others resemble a more relapsing remitting disease (Bernard et al. 2010). However, the commonality between each m2 model is its usefulness for the study of the immune response, with a skew towards T cell involvement (Ford and Evavold 2005; Procaccini et al. 2015). Despite this, EAE has limitations. To name a few, no EAE model captures a progressive form of MS, limiting the study of this prominent phase of disease; lesions mostly occur in spinal cord WM, whereas in human disease, lesions of the brain are most prevalent; EAE does not allow for extensive study of B-cell involvement, despite their known importance in human MS and lastly, study of remyelination is unsatisfactory due to lesion generation being sporadic (Procaccini et al. 2015).

Different models have been used to study other aspects of MS. For example, toxic *in vivo* rodent models of MS are better suited for the study of demyelination and remyelination, with a far lesser immune component – toxic models include the

cuprizone and lysolecithin models (Matsushima and Morell 2001). Cuprizone is a copper chelating compound, which when added into rodent chow results in the apoptosis of oligodendrocytes and subsequent demyelination – experimental factors can then be administered to test their effect on remyelination. It is of note that removal of cuprizone from the diet restores remyelination capacity, albeit to a lesser extent (Liu et al. 2010).

Lysolecithin can be used to produce reproducible focal lesions at injection sites. It acts directly on myelin, sparing surrounding axons and cells. This model has shown that T cells, B cells and macrophages infiltrate to sites of focal demyelination, highlighting their apparent importance in CNS repair in this model (Bieber, Kerr, and Rodriguez 2003). Additionally, there is evidence of slower/lesser capacity for remyelination in older animals, perhaps contributing to evidence surrounding inflammaging in MS (Cantuti-Castelvetri et al. 2018; Shields et al. 1999) . Although murine models of remyelination have helped to shed light on some of the molecular/cellular components of remyelination, remyelination in murine models is transient and repair occurs once the oligodendrocyte toxic stimulus is removed (Palavra et al. 2022) and therefore may not be truly comparable to human remyelination.

In addition to *in vivo* models, there are a number of established *in vitro* models to aid the study of MS pathomechanisms. Mechanisms related to neurons and glia have been modelled using cells of both murine and human origin, including immortalized cell lines, induced-primary cells, primary CNS cells and organotypic brain slices cultures. To give just a few examples – SK-N-SK and HOG are immortalized neuronal and oligodendrocytes cell lines, respectively, which have been used to help identify cellular contributions to MS. For example, they have been used to test whether MS patient sera/CSF preferentially binds to these cells, compared to control bio-fluids (Nazir et al. 2023). Induced microglia-like cells, generated from human peripheral monocytes, can be used to investigate myelin phagocytosis (Hendrickx et al. 2014). Primary cell cultures, such as primary microglia obtained from rapid autopsy, foetal or biopsy samples are ultimately true cells, however their inability to retain their endogenous state *ex vivo* limits their usefulness (Bohlen et al. 2017). Lastly, brain

slice cultures, thick slices of freshly dissected brain tissue (typically 100-400 µm), can be useful for the study of demyelination/remyelination. Cells obtained from young animals (<1 week old) are capable of myelinating *in vitro* when cultured on a porous membrane, in an air-media interface – the effect of various toxins/drugs can then be used to test effects on demyelination and remyelination (Madill et al. 2016; Muller, Buchs, and Stoppini 1993; Stoppini, Buchs, and Muller 1993; Zhang et al. 2011).

1.1.5 – Multiple Sclerosis Pathology

Inflammatory mediated myelin and neuronal damage is present in the brains of people with MS. Inflammatory infiltrates in the perivascular space and within the meninges produce seemingly soluble factors, yet to be fully identified, but which include TNF-α, IFN-γ, CXCL13 and lymphotoxin, which can induce demyelination and subsequent neurodegeneration via the activation of microglia and astrocytes in pre-clinical models (Lassmann, 2018).

1.1.5.1 – Molecular and Cellular Component of Demyelination

Demyelination is the inappropriate degradation of the myelin sheath (Dendrou, Fugger, and Friese 2015). The underlying cause has yet to be fully elucidated, however some of the key cellular/molecular mediators are known. Demyelination is orchestrated by activated CNS-resident cells, such as microglia and astrocytes, as well as infiltrating immune cells from the periphery (Dendrou et al. 2015). Microglial contribution to demyelination is complex. Microglia have a varied morphology and phenotype. At rest, microglia, with multiple fine processes, are constantly surveying the CNS environment for signs of immune threats. On detection of such threats, microglia undergo a morphological and phenotypic polarisation. Although oversimplified, microglia can be broadly categorised as one of two main phenotypes – M1 (typically proinflammatory and damaging) and M2 (typically anti-tinflammatory and protective). M1 microglia likely contribute to demyelination through the secretion of neurotoxic proteases (such as cathepsin C and matrix metalloproteinases), proinflammatory cytokines and chemokines (such as INF-γ, TNF-α and IL-6) and ROS. In turn, these secreted factors can promote and recruit

more microglia along with other damaging cell types such as neurotoxic se and reactive astrocytes (Dendrou et al. 2015; Mado, Adamczyk-Sowa, and Sowa 2023).

Products of the complement cascade (such as C1q and C3b) have been shown to be present within neurotoxic astrocytes found within WMLs, particularly in regions dense with complement positive microglia/macrophage-like cells. The presence of complement positive reactive astrocytes has been suggested to be unique to demyelination, therefore suggesting that complement activation can drive glia into a myelin-toxic and damaging state (Ingram et al. 2014; Saez-Calveras and Stuve 2022). The cycle then continues with neurotoxic astrocytes releasing microglial recruitment factors (such as CC-chemokine ligand 2 and granulocyte-colony macrophage stimulating factor). In addition, astrocytes can also act on OPCs, preventing them from maturing (Dendrou et al. 2015). A failure of OPC differentiation into mature, myelinating cells also causes a failure of myelin repair – remyelination – therefore reactive and damaging astrocytes likely also contribute to ongoing damage (Factor et al. 2020).

It is important to note that microglia are also required to allow for remyelination via the clearance of myelin debris (discussed in more detail in *1.1.5.4*) (Mado et al. 2023). Although demyelination is a dynamic process, with continued remyelination, in MS, demyelination ultimately dominates, eventually leading to the irreversible loss of axons and neuronal cell bodies (neurodegeneration) – presenting clinically as permanent disability.

As previously mentioned, the adaptative immune system also contributes to demyelination. Initially, T cells, specifically CD4+ Th1 and Th17, were considered the cellular drivers of demyelination. Peripheral autoreactive T-cells can cross the BBB and release a cascade of damaging cytokines including TNF-α and IFN-γ. Evidence for their contribution to demyelination is seen in EAE, which has been shown to be inducible through the passive transfer of CD4+ anti-myelin T-lymphocytes. In human disease, it is possible that CD4+ T-helper cells from the periphery inappropriately recognise and bind to self-myelin antigens, presented by CNS antibody-presenting

cells (ACPs), namely microglia and dendritic cells – thus promoting their entry to the CNS and subsequent production of myelin-toxic antibodies.

In addition to CD4+ T cells, CD8+ cells may contribute to demyelination. When stressed, CD8+ cytotoxic T cells can recognise self-myelin/oligodendrocyte antigens. Evidence for their damaging role has been shown in EAE as adoptive transfer of MBP CD8+ T cells has been shown to result in perivascular inflammation and WM demyelination. Postmortem analysis of the human MS brain has shown that CD8+ T cells are found in close proximity to the myelin sheath, suggesting that they play a role in myelin degradation (Lubetzki and Stankoff 2014). However, drugs which aim to exclusively target T-cells have had limited success in modulating MS, therefore highlighting that T cells are not the only drivers of MS disease (Segal et al. 2008).

B cells have been shown to have a role in demyelination. Evidence comes both from the presence of follicular tertiary lymphoid structures (composed of both B and T cells) found to be present within the brains of people with more severe MS; and additionally, from the success of B cell targeting drugs, such as CD20-targeting Ocrelizumab, in their ability to reduce both lesion formation as well as annualized relapse rate (Lubetzki and Stankoff 2014). In addition to antibody production by plasma cells, B cells are proficient APCs and regulate T cells (Van Meerhaeghe et al. 2023). However, longitudinal studies of patients treated with Ocrelizumab have unfortunately demonstrated that although annualized relapse rate is reduced, progression to a less inflammatory, neurodegenerative disease still prevails in the majority of those treated (Lubetzki and Stankoff 2014). There is still much to learn about demyelination (as well as remyelination) in MS, in order to develop drugs which will be capable of both preventing further damage, promoting repair and ultimately halting disease progression.

1.1.5.2 – White Matter Demyelination

Active white matter lesions (WML) are most typical during early/RRMS (Kuhlmann et al., 2017). During active demyelination, the site of injury is densely packed with phagocytic microglia/macrophage-like cells. At present, there is not a definitive

marker to distinguish between activated microglia, which have a macrophage-like morphology, and infiltrating macrophages from the periphery; to this end all activated microglia/macrophages will be referred to as macrophage-like cells (table 1.2). Demyelination likely occurs from the centre of the lesion outwards, with microglia/macrophage-like cells clustered around degenerating axons; as well as in adjacent NAWM. The centre of actively demyelinating lesions contain a higher proportion of macrophage-like cells (either generated from resident microglia or immune infiltrates) (Prineas et al., 2001; Kuhlmann et al., 2017; Lassmann, 2018. The myelin debris present within microglia/macrophage-like cells allows for activity staging, based on whether minor or major degradation products are present (Lucchinetti et al., 2000. At sites of active demyelination, microglia/macrophage-like cells have been found to have increased expression of nicotinamide adenine dinucleotide phosphate (NADPH) oxidase – suggesting oxidative tissue damage, alongside TMEM119 (a marker enriched in resident microglia), p22phox, iNOS (that both associate with oxidative stress), CD68, CD86 and HLA-DR (which are involved in phagocytosis and immune-cell co-activation) and a loss of the homeostatic marker, P2RY12 (Zrzavy et al., 2017). However, once ladened with myelin debris, their expression of NADPH oxidase is reduced/lost, perhaps suggesting that their ability to continue phagocytosing debris is diminished (Fischer et al., 2012; Lassmann, 2018).

In contrast to the actively demyelinating lesion described above, mixed active/inactive (MA/I) WML are predominantly seen in patients with long standing, progressive disease. These lesions have a hypocellular, inactive, demyelinated lesion centre, with a rim of demyelinating, activated (foamy) microglia/macrophage-like cells (Frischer et al., 2015; Lassmann, 2018). The microglia at sites of actively demyelinating tissue, including at the rim of MA/I WML, show a loss of a homeostatic signature, with a reduction of both P2RY12+ and TMEM119+ cells (Zrzavy et al., 2017). These WMLs have been associated with a worse MS prognosis (Absinta et al., 2019). Additionally, they are a useful pathological tool for the study of demyelination in postmortem tissues, which can provide context/further insight into *in vivo* studies of iron-rim lesions, detectable using MRI (Dal-Bianco et al., 2021). Although also present in other lesion types, astrocytic scarring is common in MA/I WML. Scar

formation in demyelinated areas is supposed to isolate inflammation, restrict damage and provide structural support for repair. However, there is also evidence that dysfunction in astrocytes may contribute to demyelination by recruiting lymphocytes and contributing to the defective innate immune response (Meinl et al., 2018) as well as being dysfunctional as a response to microglial-derived factors (Liddelow et al., 2017).

Inactive lesions, in comparison to actively demyelinating lesions, contain few/no microglia/macrophage-like cells and are considered an environment not supportive of remyelination or tissue remodelling (Lassmann 2018).

Axon damage and destruction occurs at all stages of MS lesion development. The frequency of transected neurites and end-bulb like structures are greatest in actively demyelinating lesions (active and chronic active lesions), however, after the acute phase of demyelination is complete, neurodegeneration still continues (Bitsch et al., 2000; Frischer et al., 2009). Axonal injury worsens, with further reductions in axonal transport speed and axonal end-bulb formation (Lassmann, 2018). Mitochondrial damage has been identified in MS. Mitochondria provide energy to cells, including axons, which they are transported along. Damage to mitochondria results in an energy deficiency: firstly, causing functional dysregulation of axonal transport required for signal transduction, and secondly, with prolonged energy deficiency, axonal degeneration (and neuronal cell death) (Correale et al., 2019. Demyelination of axons results in the axon becoming bioenergetically challenged. Sodium channels at the nodes of Ranvier are lost and more pressure is placed on sodium/potassium-ATPase to allow continued neuronal function. An increased reliance on ATP requires efficient mitochondrial ATP production and transport. Restoring mitochondrial transport experimentally is associated with neuroprotection and preserved axon function (Licht-Mayer et al., 2020). Click or tap here to enter text.

1.1.5.3 – Grey Matter Demyelination

Increased abundance of grey matter lesions (GML) is associated with a worse MS prognosis and correlates more with disability, compared to WML. However, current MRI technology, used in clinical practice, is unable to accurately identify GML

(Calabrese et al., 2007; Calabrese et al., 2010; Calabrese et al., 2013; Honce, 2013; Bevan et al., 2018; Filippi et al., 2019). As a result, at this time, GML are useful for aiding our understanding of MS pathomechanisms through pathological investigation, but are less useful for disease monitoring.

Studies have shown that there is widespread cortical and deep GM demyelination in MS (Calabrese et al., 2013). Cortical lesions can be further grouped into 4 distinct subtypes: type i, leukocortical lesions affecting the deep cortical laminae and subcortical WM; type ii, intracortical lesions, small lesions, typically surrounding a blood vessel and found within the margins of the GM; type iii, subpial lesions affecting the superficial cortical layers under the pia surface and type iv lesions which extend throughout the layers of the cortex without affecting the underlying subcortical WM (Bø et al., 2003; Kuhlmann et al., 2017). In comparisons to WML, GML are typically less inflammatory, with a 6^{th} of the number of CD68+ microglia found within cortical GML, compared to WML (Peterson et al., 2001). Nevertheless, inflammation still plays a role in cortical and deep GM demyelination, likely at least in part, independently of WM inflammation (Bö et al., 2007); with increased GM inflammation in early, RRMS, compared to long standing, progressive disease (Lucchinetti et al., 2011). Like WM demyelination, GM demyelination is only partially understood. One mechanism associated with GM pathology, and a more severe MS course, is the formation of B-cell follicle-like structures within the meninges. These structures associate with a gradient loss of neuroglia cells, suggesting that soluble factors produced at sites of B-cell follicle-like structures are pathogenic (Magliozzi et al., 2007; Magliozzi et al., 2010; Howell et al., 2011). Additionally, microglia within GML have also been shown to produce ROS, which are neurotoxic and contribute to GML pathogenesis (Gray et al., 2008; Haider et al., 2011).

1.1.5.4 – Molecular and Cellular Component of Remyelination

In contrast to demyelination, lesions in MS are capable of natural repair – remyelination (Franklin and Ffrench-Constant 2008; Lassmann 2018). Remyelination is the generation of new myelin sheaths around denuded axons, resulting in at least partially restored signal transduction and neurological function. A combination of animal studies, namely the murine cuprizone and lysolecithin models, along with

histological studies in human tissue, have helped to begin to unpick the underlying biology of remyelination (Castillo-Rodriguez et al. 2022; Kipp et al. 2012). Remyelination requires three main phases – first, myelin debris must be cleared, second, oligodendrocyte precursor cells (OPCs) must migrate to the site of demyelination and third, they must differentiate into mature, myelinating cells. The first step of this process is orchestrated by activated microglia/macrophages, which phagocytose the myelin debris. Whilst doing so, they release chemoattractants to recruit more phagocytes to the site to aid the clearance of the debris (Fu et al. 2014). The recruitment of OPCs is mediated by a number of molecular signalling pathways including Wnt/β-catenin, PI3K/AKT/mTOR, and ERK/MAPK (Maciak, Dziedzic, and Saluk 2023). Axons secrete signalling factors such as neuronal growth factor and glial cell growth factor, which promote pre-myelinating OPCs to make contact with denuded axons, and differentiate into mature myelinating cells; additionally, these signalling factors promote the migration of more OPCs to the site of demyelination. Mature oligodendrocytes then synthesise and assemble myelin proteins including PLP, MOG, MAG and MBP to form new insulating myelin sheaths around axons (Franklin and Ffrench-Constant 2008). It is of note, that new myelin generated to replace degraded myelin is inferior to the original. It appears thinner irrespective of the axonal circumference with an increased g-ratio compared to the original myelin. Remyelination restores the distribution of ion channels into clusters at the nodes of Ranvier, albeit with greater distances between internodes compared to the original, however, this still improves signal transduction (Franklin and Ffrench-Constant 2008; Keough and Yong 2013), likely manifesting as a clinical improvement. The capacity for remyelination varies between individuals and between lesions. In MS, remyelination ultimately becomes inadequate/fails to offset continued demyelination (Chari 2007).

1.1.6 – The Role of Astrocytes in MS Pathogenesis

Astrocytes are involved in many important processes during health. For example, astrocytes release regulators of neurotransmission such as glutamate and ATP (Volterra and Meldolesi 2005), they contribute to neuronal health by providing neurotrophic factors such as lactate and antioxidants (Ricci et al. 2009), their foot

processes contribute to the maintenance of the BBB, helping to prevent influx of peripheral immune cells (Horng et al. 2017) and additionally, they help to promote an anti-inflammatory environment through secretion of anti-inflammatory cytokines (Ponath, Park, and Pitt 2018).

In MS, astrocytes contribute to MS pathobiology. Astrocytes appear to become reactive and hypertrophic prior to demyelination in normal appearing tissue. Their foot-enlargement causes a reduction in BBB integrity, making it more permeable to peripheral infiltrates (Brambilla 2019; Brosnan and Raine 2013). Their morphology is also seen changed in active lesions, where they also become larger with less processes. These reactive cells can be seen at the margin of lesions, extending into the adjacent NAWM/NAGM. This observation in seen both in human MS lesions and also in EAE where they appear reactive prior to immune infiltration, and contain myelin debris, suggesting that they contribute to lesion expansion (D'Amelio, Smith, and Eng 1990; Ponath et al. 2017, 2018). Additional evidence for their contribution to lesion progression is their expression of microglia recruitment factors such as CCL2 and ICAM-1 (Bullard et al. 2007; Kim et al. 2014). Recruitment of microglia to lesions can be both damaging (continued degradation of the myelin sheath) and beneficial as they contribute to the removal of debris (which is required to permit remyelination) (Bogie et al. 2020; Lampron et al. 2015)).

At later stages of lesion progression, astrocytes form an astrocytic scar when demyelination is complete, i.e. in inactive lesions. Astroglial scars isolate regions of inflammation and can restrict damage to these areas (Voskuhl et al. 2009). Therefore, the presence of reactive astrocytes in MS lesions may contribute to both continued damage and expansion and/or reparative processes. The contribution of astrocytes to MS, aside from their role as CNS *de novo* cholesterol synthesisers, is beyond the scope of this thesis, but it is noted that their contribution to MS pathobiology is as important as it is varied.

1.1.7 – The Role of Microglia/Macrophage-Like Cells in MS Pathogenesis

Microglia are the resident immune cells of the human brain. In MS, resident microglia, alongside infiltrating macrophages are overwhelmingly responsible for the

inappropriate degradation of myelin and other cellular membranes (Luo et al., 2017). Microglia and macrophages are are similar in terms of their function (table 1.2). There is currently no single marker to distinguish activated brain resident microglia from infiltrating macrophages from the periphery. Highly sensitive techniques to characterise the transcriptome of cells, such as scRNA-seq, have helped to identify likely microglia-signatures using hierarchical clustering. However, there is still no definitive protein marker to distinguish activated microglia from infiltrating peripheral macrophages, but high throughput gene assays can help to identify similar cell types based on their global gene expression (Sellgren *et al*, 2017).

Table 1.2 – Comparison of Microglia and Macrophage Characteristics

Summary of microglia and macrophages: lineage (Cuadros et al. 2022; Ginhoux et al. 2010a; Lassmann, Brück, and Lucchinetti 2001), location (Goldmann et al. 2016; Gomez Perdiguero et al. 2015), morphology (Colonna and Butovsky 2017; Huang et al. 2015; Nimmerjahn 2012; Tremblay et al. 2011) function (Faust, Gunner, and Schafer 2021; Magnus et al. 2001a; Nayak et al. 2012; Paolicelli et al. 2011; Stevens et al. 2007a; Tremblay et al. 2011),role in MS (Cantuti-Castelvetri et al. 2018; Grajchen, Hendriks, and Bogie 2018; Haider et al. 2011; Lampron et al. 2015; Luo et al. 2017b) and related antibodies and related antibodies (Koso, Nishinakamura, and Watanabe 2018; Ruan and Elyaman 2022; Satoh et al. 2016; Zhang et al. 2006).

Characteristics	Microglia	Macrophages
Lineage (Ginhoux *et al.*, 2010; Cuadros *et al.*, 2022; Lassmann *et al.*, 2001).	Derived from yolk sac during embryogenesis and develop/mature and replicate in the CNS.	Derived from myeloid progenitors. Tissue resident cells derived from circulating monocytes
Endogenous Location (Gomez Perdiguero *et al.*, 2015; Goldmann et *al.*, 2016)	CNS.	Periphery. Sub-population may be CNS – studies using transgenic mice have provided evidence for yolk sac derived, CNS macrophages.
Morphology (Tremblay *et al.*, 2011; Nimmerjahn, 2012; Huang *et al.*, 2015; Colonna and Butovsky 2017).	Resting – small cells with multiple fine processes. Activated – soma enlarges, fewer fine processes. Reactive (macrophage-like) – amoeboid-like shape. Foamy - lipid-laden, amoeboid-like shape.	Typically amoeboid like shape - may differ depending on tissue type. Foamy - lipid-laden, amoeboid-like shape.
Function (Magnus *et al.*, 2001; Tremblay *et al.*, 2011; Stevens *et al.*, 2007; Paolicelli *et al.*, 2011; Faust *et al.*, 2021; Nayak *et al*, 2012).	Surveying CNS cells. Readily extend and retract processes to identify changes to local CNS environment. Non-inflammatory removal of apoptotic cellular debris. Synaptic pruning/remodelling. Activated upon stimuli such as pathogens, pro-inflammatory cytokines/chemokines. Promote inflammation and repair.	Phagocytosis of bacteria/other pathogens. Non-inflammatory removal of apoptotic cellular debris. Antigen-presentation. Production of pro- and anti-inflammatory cytokines. Wound healing and repair.
Role in MS (Cantuti-Castelvetri *et al.*, 2018; Luo *et al.*, 2017; Lampron *et al.*, 2015; Haider *et al.*, 2011; Grajchen *et al.*, 2018)	Phagocytosis of myelin debris to permit remyelination. Recruitment of other phagocytic/immune cells to the site of damage/inflammation.	Peripheral infiltrates to aid immune response. Phagocytosis of myelin debris to permit remyelination. Recruitment of other phagocytic/immune cells to the site of damage/inflammation.
Distinguishing antibody markers? (Staoh *et al.*, 2016; Ruan and Elyaman, 2022; Koso *et al.*, 2018; Zhang *et al.*, 2016)	To date, there is not a known antibody signature to differentiate between CNS resident macrophage-like cells and monocyte derived peripheral macrophages post-CNS infiltration. A few markers have been suggested, but still lack total specificity to microglia. For example, TMEM119 has been shown to be expressed exclusively by CNS resident microglia. Its usefulness is hampered though as It is not expressed by immature microglia and additionally it's expression is downregulated upon microglial activation - therefore it is still an inadequate marker to distinguish between microglia and CNS macrophages, particularly in an inflammatory CNS environment, such as in MS. Another potentially promising marker has been identified in mouse studies. Siglec-H in mice is homologous to human Siglec-L2 (albeit only by 42%). Siglec-H has been shown to be expressed almost exclusively by microglia at various maturities, but not by peripheral macrophages, however, this finding has not as yet been translated to humans.	

1.1.7.1 – In Vitro Phagocytosis Models of Microglia/Macrophage-Like Cells

There has been interest in the study of myelin phagocytosis in the context of MS for several decades. Early studies often used microglia extracted from rodent pups; these cells were advantageous for the study of phagocytosis, due to their involvement in early development, as they would have been actively involved in synaptic pruning (Faust et al. 2021) *in vivo*. Together with experiments utilising organotypic slice cultures, these earlier studies showed that it is primarily microglia with an ameboid-like morphology that phagocytose cellular debris, including myelin (Czapiga and Colton 1999; Giulian and Baker 1986; Reichert and Rotshenker 1999; Smith 1993; Smith and Hoerner 2000).

Due to the importance of myelin phagocytosis in MS, more recent studies have also studied myelin phagocytosis *in vitro*. Studies utilising murine bone marrow-derived macrophages have identified that excessive uptake of cholesterol, as a result of myelin phagocytosis, can be detrimental to microglia/macrophage-like cells, reducing their ability to act as phagocytosing cells and additionally promoting cell death.

Other literature has reported on mechanisms related to myelin phagocytosis. For example, Gitik *et al*, showed that myelin can regulate its own phagocytosis using primary murine microglia/macrophage cultures. They identified a pathway in which the presence of CD47+ myelin within microglia/macrophages activates SIRPα, resulting in a downregulation of myelin phagocytosis by these cells (Gitik et al. 2011). A mechanism which may be altered in MS (Han et al. 2012).

More recent studies have been conducted to look at myelin phagocytosis in human MS. For example, Hendrickx and colleagues used primary microglia obtained from post-mortem human brain tissue and post-mortem NAWM from people with and without MS. They used an *in vitro* myelin phagocytosis model to demonstrate that NAWM from people with MS was phagocytosed as an increased rate compared to WM from controls – suggesting that changes in myelin supersede myelin degradation in MS (Hendrickx et al. 2014).

Micro-alterations in myelin to promote its uptake by phagocytes along with evidence that microglia/macrophage-like cells are altered in MS, at different time points may both contribute to the on-going damage seen in MS. We still have not fully elucidated the underlying biology as to why myelin is inappropriately phagocytosed in human MS. Further study of this process is needed to permit the development of drugs to reduce inappropriate myelin phagocytosis and to promote remyelination (Grajchen et al. 2018).

1.1.7.2 – Contribution of Pro-inflammatory and Anti-inflammatory Processes of Microglia in MS

There is currently debate surrounding whether myelin debris clearance by foamy macrophages is beneficial or harmful in MS. The cause of inappropriate targeting, and subsequent, degradation of myelin by microglia/macrophages in MS is unknown, but some mechanisms of action have been suggested. Receptor-mediated endocytosis has been shown to be the mechanism of action driving myelin internalisation by phagocytic cells (Grajchen et al., 2018). Various receptors have been implicated in this process, including: Fc receptor binding of myelin-specific antibodies, after opsonisation to self-myelin epitopes (Prineas and Graham, 1981); complement receptor 3 regulated myelin internalisation (Reichert et al., 2001; Smith, 2001) and Mer tyrosine kinase (MerTK) driven myelin phagocytosis, which is suggested to be self-promoted by myelin debris via activation of liver X receptors (LXR) and peroxisome proliferator-activated receptor (PPAR)-dependent driven synthesis of MerTK (Bogie et al., 2012).

Microglia survey the CNS microenvironment and alter their morphology/secretion of cytokines in response to environmental cues. They are capable of secreting a wide variety of factors, some pro-inflammatory in nature, such as TNF-α, IL-6, and IL-1β, whilst others are anti-inflammatory including TGFα, IL-4 and IL-10 (Sasmono et al. 2003). The role of microglia and the pro/anti-inflammatory factors they produce does not categorise them simply as harmful or helpful; instead, the process is much more dynamic. For example, remyelination requires both anti/pro-inflammatory signals which are produced by microglia/macrophages, e.g., TNF-α and IL-4 have been shown to promote oligodendrocyte proliferation, an essential step for remyelination (Fenn et

al. 2014; Li and Barres 2018; Luo et al. 2017c; Muzio, Viotti, and Martino 2021; Voß et al. 2012).

1.1.7.3 – Defective Myelin Clearance may Contribution to MS

Degradation of intact myelin is clearly damaging in the CNS, however, myelin debris clearance by activated microglia/macrophages is believed to be necessary to produce an environment that can facilitate remyelination (Luo et al., 2017). Work by Lampron and colleagues showed defective myelin clearance, and reduced remyelinating capacity, using the toxin-induced cuprizone model of MS. They used CX3CR1 deficient mice. CXC3R1 is a receptor expressed by microglia which orchestrates crosstalk between microglia and neurons, and also controls microglial physiology. Mice, with CX3CR1 knock out microglia, displayed severely impeded phagocytosis, resulting in diffuse myelin debris throughout the WM and inefficient remyelination of axons (Lampron et al., 2015). Suggesting that myelin clearance is crucial for remyelination at this time in this model.

However, more recent work by Bogie and Hendriks has suggested that foamy macrophages are also detrimental in MS. They have suggested that polarisation of microglia/macrophages to either a pro-inflammatory or anti-inflammatory phenotype follows a triphasic pattern (Grajchen et al., 2018). Initial myelin phagocytosis pushes foamy macrophages towards a damaging phenotype, resulting in the release of pro-inflammatory mediators, such as TNF-α and ROS (Haider et al., 2011; Grajchen et al., 2018). Intracellular processing of cholesterol can then direct foamy macrophages into a more anti-inflammatory, and beneficial (reparative and pro-remyelinating) phenotype, which are likely involved in myelin debris clearance, as opposed to directed damage of intact myelin. This phenotypic switch to a less inflammatory state is likely LXR-driven. LXRs are activated by cholesterol metabolites (oxysterols), which are highly abundant in myelin (Mailleux et al., 2017) and are generated by the intracellular metabolism of endocytosed membranes. In addition to promoting the resolution of pro-inflammatory signalling, LXR activation results in the transcription, and subsequent translation, of cholesterol export transporters, such as apolipoprotein E (APOE) and adenosine triphosphate-binding cassette A1 (ABCA1), permitting the removal of excess cholesterol from foamy macrophages

(found in areas of actively demyelinating tissue) (Fukumoto et al., 2002; Tall, 2008). However, Bogie and Hendricks, along with others, have suggested that prolonged myelin phagocytosis coupled with defective cholesterol clearance from foamy macrophages can revert macrophages back to a pro-inflammatory phenotype (Grajchen et al., 2018). This proinflammatory state is seen in a model of the aged CNS, where foamy macrophages have been shown to have a dysfunctional capacity to clear myelin and support remyelination. The accumulation of unesterified, excess cholesterol, in foamy macrophages resulted in the formation of cholesterol crystals, which in turn caused lysosomal rupture and promoted inflammation via inflammasome activation (Cantuti-Castelvetri et al., 2018). This process has some relevance to MS as patient-derived microglia/macrophage-like cells have been shown to exhibit characteristics of premature aging (inflammaging) (Bolton, 2021) and ageing is an important variable in determining the risk of progression and the level of disability (Scalfari et al., 2011). This dynamic process of microglia/macrophage-like cell phenotype switching likely contributes to the continued and chronic inflammatory-driven demyelination, demonstrated by MA/I WML, and ultimately may reduce the success of remyelination whilst furthering glia and neuro-axonal damage. Ultimately, damage to myelin, resulting in direct/indirect neurodegeneration/injury to glia, underpins the loss of function in MS. Cholesterol is an essential lipid component of the myelin sheath and its degradation by microglia likely causes dyslipidaemia which may contribute to the continued innate immune dysregulation observed in progressive MS (Reynolds et al., 2011; Lampron et al., 2015; Grajchen et al., 2018).

1.2 Cholesterol and Oxysterols

Cholesterol is an important lipid involved in many biological functions (figure 1.2). It is essential for membrane structure, function and fluidity, cell signalling, and membrane trafficking (Brown and Goldstein, 1986; Cortes et al., 2014). It is also the precursor for other important biomolecules – oxysterols, bile acids and steroid hormones (Goedeke and Fernández-Hernando, 2011; Griffiths and Wang, 2019). Cholesterol disbalance is associated with a range of neurological disorders, including

Niemann-Pick disease, Huntington's, Alzheimer's and MS (Valenza *et al.*, 2007; Del Toro *et al.*, 2010; Griffiths and Wang, 2019; Varma *et al.*, 2021).

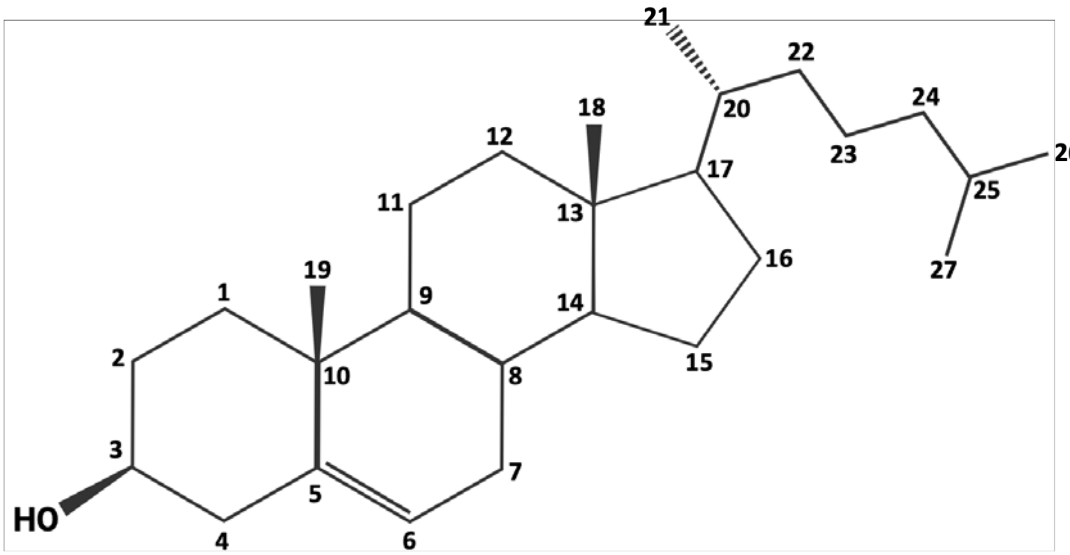

Figure 1.2 – Chemical Structure of Cholesterol

Created with BioRender.com.

1.2.1 – Cholesterol Biosynthesis

Cholesterol is unable to transverse the BBB and is synthesised *de novo* in the CNS (Zhang and Liu, 2015). The brain contains ~20% of the body's total cholesterol, with the majority unesterified and situated within the myelin sheath (Björkhem et al., 2004). The healthy adult human brain contains around 20 mg/g of cholesterol, with the majority present within the WM, due to the high density of myelinated axons (Dietschy and Turley, 2004). In adulthood, the concentration of cholesterol remains mostly constant, but a small fraction (around 0.7%) is turned over daily. This mechanism has to be tightly regulated to ensure that the supply of cholesterol always remains optimal (Dietschy, 2009).

Cholesterol is synthesised via a complex series of reactions. First, squalene is synthesised from acetyl-coenzyme A (acetyl-CoA) or acetoacetyl-CoA via the mevalonate pathway (figure 1.3). Squalene is then used as the first metabolite for

cholesterol synthesis by both neurons, which predominantly synthesise cholesterol via the Kandutsch-Russel pathway, and astrocytes which utilise the Bloch pathway (figure 1.4) (Mazein et al., 2013; Zhang and Liu, 2015). Synthesis starts with the conversion of 3-hydroxy-3-methylglutaryl-CoA (HMG-CoA) to mevalonate, via the action of HMG-CoA reductase – this is the rate limiting step of cholesterol biosynthesis. The amount of cholesterol produced can be reduced using statins, which act by inhibiting HMG-CoA reductase (Willey and Elkind, 2010).

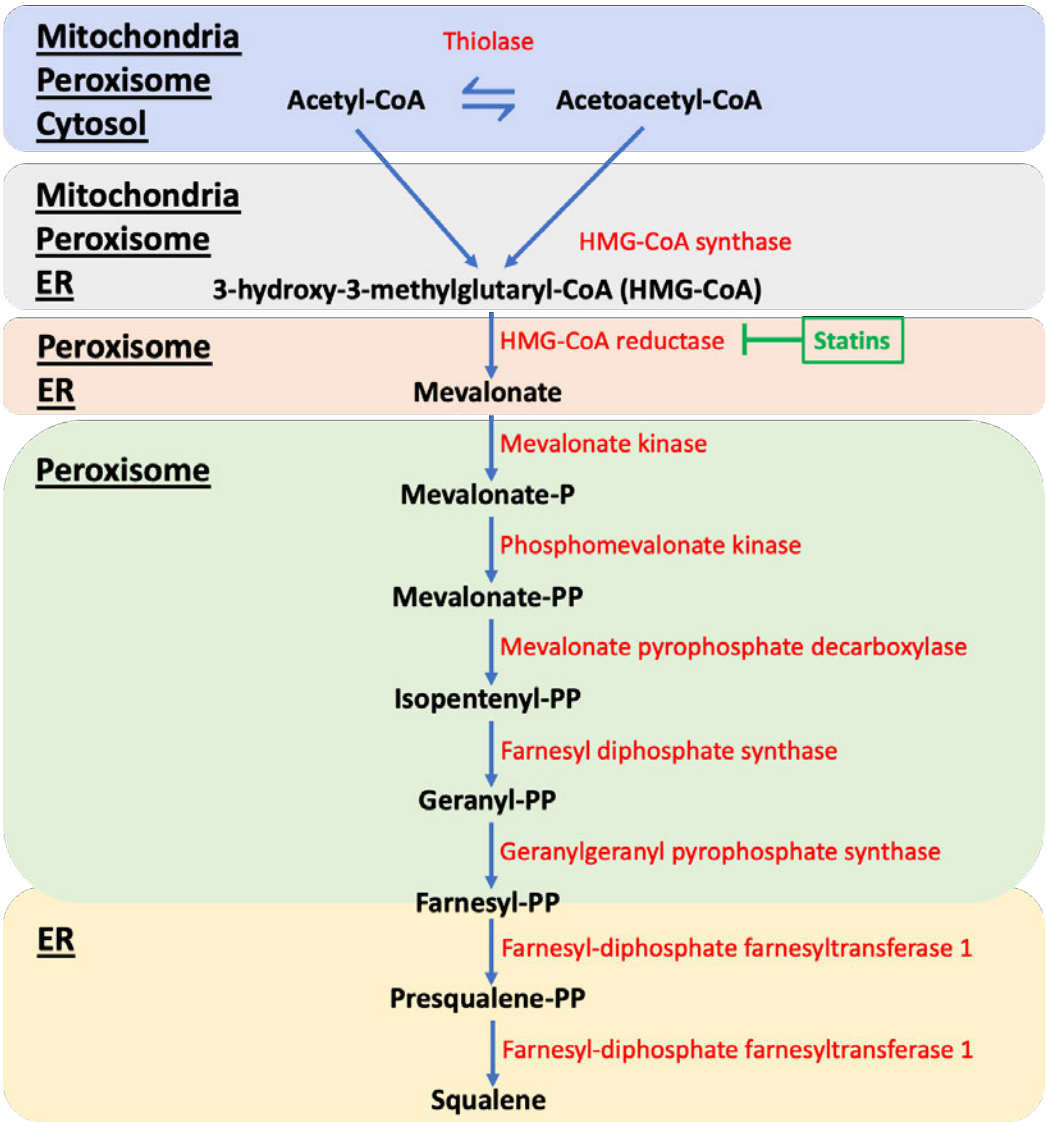

Figure 1.3 – Squalene Synthesis via the Mevalonate Pathway

The pathway starts with either the consumption of acetyl-CoA or enzymatic conversion of acetoacetyl-CoA to HMG-CoA. This occurs in the mitochondria, peroxisome, cytosol and endoplasmic reticulum (ER).

The rate limiting step in the pathway is the synthesis of mevalonate from HMG-CoA, via the enzymatic activity of HMG-CoA reductase; whose activity can be inhibited by statins. After mevalonate synthesis a further 7 enzymatic steps generate squalene in the ER Mazein et al., 2013). ER - endoplasmic reticulum, P – phosphate, PP-diphosphate, CoA – coenzyme A. Created in Microsoft PowerPoint.

Figure 1.4 – Bloch and Kandutsch-Russel Pathway for Cholesterol Synthesis

Squalene is used as the first metabolite in both the Kandutsch-Russel and Bloch pathways for cholesterol synthesis. Cholesterol is synthesised within the endoplasmic reticulum of neurons

(Kandutsch-Russel pathway) and astrocytes (Bloch pathway) (Mazein et al., 2013; Zhang and Liu, 2015). Created in Microsoft PowerPoint.

In the brain, cholesterol synthesis is predominantly carried out by astrocytes, which is then transferred to other cell types (Barber and Raben, 2019). Other cell types, including neurons, can synthesise cholesterol, but in adulthood this is significantly reduced; instead, mature neurons rely on astrocyte-derived cholesterol, accomplished by cholesterol horizontal transfer. Astrocytic cholesterol is loaded onto APOE, which is then transferred to neurons (and glia) via the action of ABC cholesterol transporters. Lipidated APOE is endocytosed by low-density lipoprotein receptor (LDLR) and LDLR-related protein 1 on neurons and other glia (Li et al., 2022).

The regulation of cholesterol biosynthesis is mediated by the action of regulatory binding element (SREBP) and SREBP cleavage-activating protein (SCAP), using a positive feedback mechanism (Shimano and Sato, 2017). SCAP is a sterol-sensing protein, located in the ER. In the absence of cholesterol, it chaperones SREBP from the ER to the Golgi apparatus. Once SREBP has entered the Golgi, its n-terminus is released via the protease action of site-1 protease and site-2 protease. This allows SREBP entry to the nucleus; once there it increases the production of cholesterol synthesis related gene products. In contrast, when cellular cholesterol in the ER is high, cholesterol inactivates the SCAP/SREBP complex, preventing SREBP's transport to the nucleus and subsequently decreases the transcription of cholesterol biosynthesis related genes (Horton et al., 2002; Goldstein et al., 2006; Lee et al., 2020).

1.2.2 – Cholesterol Homeostasis

The tight regulation of cholesterol homeostasis is imperative to the normal function of various processes within the brain. Both neurons and glia are important to this regulation. Astrocytes are primarily responsible for the biosynthesis of new cholesterol, whilst neurons are responsible for the majority of cholesterol turnover (Li et al., 2022). Neurons express *CYP46A1*, which regulates the enzymatic synthesis of 24S-hydroxycholeserol from cholesterol, the major metabolic product of cholesterol in the CNS. Unlike cholesterol, this oxidised product can then be removed

from cells and can also be transferred into the periphery across the BBB (Zhang and Liu, 2015) (see 1.2.2.1). Microglia and oligodendrocytes are also vital for maintaining cholesterol homeostasis (figure 1.5) (Li et al., 2022).

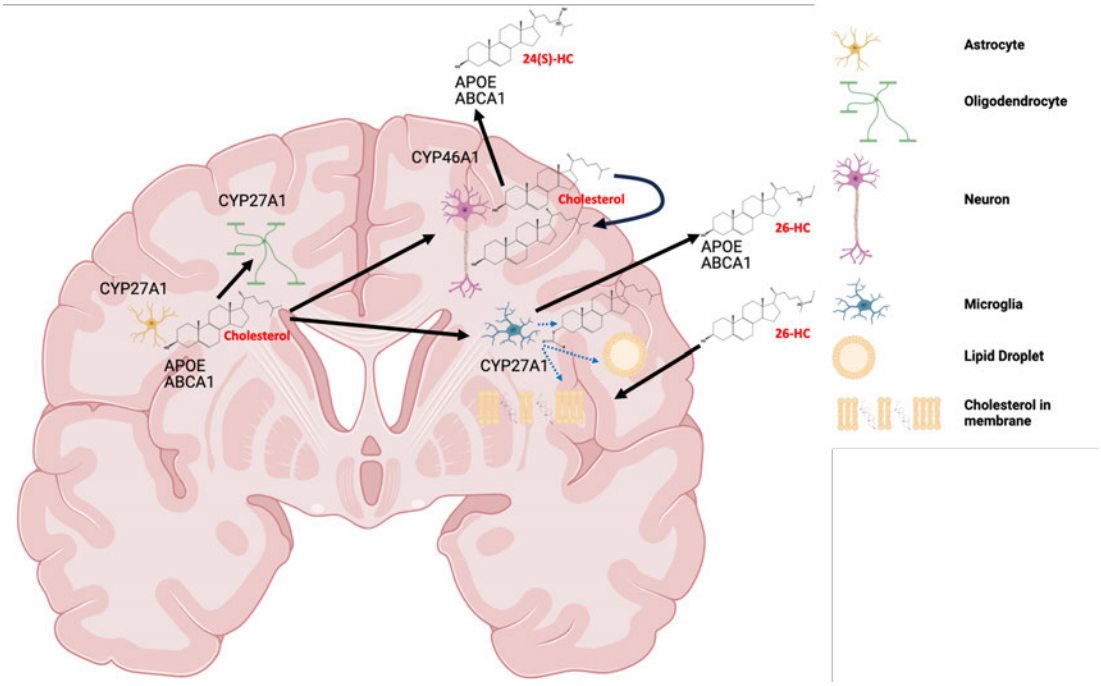

Figure 1.5 – Cholesterol Flux in the Human Brain

The majority of cholesterol is produced by astrocytes via the Bloch pathway. Astrocytic cholesterol is then transported via cholesterol transporters, such as APOE and ABCA1, to other cells including oligodendrocytes, microglia and neurons. Neurons can also produce cholesterol via the Kandutsch-Russel pathway – typically this is to support themselves and is most prominent during neonatal neurogenesis. Cholesterol is inserted into membranes, esterified (by acyltransferase), packaged into lipid droplets, or converted to oxysterols which can be effluxed from the brain, such as 24(S)-hydroxycholesterol (via neuronal CYP46A1) and 26-hydroxycholesterol (via ubiquitously expressed CYP27A1). In addition to oxysterol efflux from the brain, sterols such as 26-hydroxycholesterol can influx into the brain. 24(S)-hydroxycholesterol - 24(S)-HC; 26-hydroxycholesterol - 26-HC; CYP – cytochrome P450. Image produced using Biorender.com.

Oligodendrocytes support neuronal function and rely on high concentrations of cholesterol. Cholesterol is a key component of the myelin sheath, and is essential for allowing myelin sheath growth and axonal wrapping, which we now understand to be crucial to normal behaviours, such as learning and memory (Mathews and Appel, 2016; Bergles et al., 2019; Fields and Bukalo, 2020). Cholesterol deficiency in

oligodendrocytes has been associated with abnormal myelination, despite normal oligodendrocyte morphology (Saher et al., 2005; Mathews et al., 2014).

Microglia also require cholesterol for normal function; they are involved in supporting learning induced spine formation, synaptic plasticity and memory formation (Parkhurst et al., 2013), alongside immune defence and support of normal tissue homeostasis. Their endogenous cholesterol promotes survival and helps to regulate the expression of phagocytosis genes, which allows for mechanisms such as synaptic pruning (Paolicelli et al., 2011; Faust et al., 2021). Microglia express the protein triggering receptor expressed on myelin cells 2 (TREM2) (Qin et al., 2021). TREM2 facilitates the binding of lapidated APOE and its uptake by microglia. TREM2 is also involved in cholesterol clearance during demyelination; it senses lipid components and promotes lipid uptake and catabolism (Poliani et al., 2015; Yeh et al., 2016; Ulland and Colonna, 2018). A loss of TREM2 has been shown in areas of chronic demyelination, resulting in an inappropriate accumulation of cholesterol without the downregulation of phagocytosis related genes, causing continued phagocytosis (Yeh et al., 2016). Genetic variants mapping to APOE, TREM2 and lipid efflux transporters, including ABCA7, are associated with an altered risk of Alzheimer's disease (Karch and Goate, 2015).

1.2.2.1 – Cholesterol Metabolism Generates Signalling Molecules Called the Oxysterols

Synthesised cholesterol, which is not required is either packaged and stored within cells or is metabolised. Oxysterols are oxidised metabolites of cholesterol. They are important bioactive molecules in their own right and are functionally active within the brain Griffiths and Wang, 2019).

The main oxysterol of the human brain is 24S-hydroxycholesterol (24S-HC), also known as cerebrosterol. 24S-HC is synthesised from cholesterol via the action of 24-hydroxylase, which is encoded by *CYP46A1* (predominantly by neurons). Cholesterol is unable to traverse the BBB, whereas its oxidised products can; 24S-HC is the primary sterol which facilitates this. Additionally, 24S-HC is a potent ligand for the nuclear transcription factor liver X receptors (LXR)-α and LXR-β (Janowski et al.,

1999). Activation of LXR via ligand-receptor binding results in a signalling cascade causing the increased expression of many genes, including cholesterol efflux transporters, such as APOE and the ABC-family of lipid transporters (Lütjohann et al., 1996; Lund et al., 1999; Fukumoto et al., 2002; Lund et al., 2003; Tall, 2008; Matsuda et al., 2013).

In addition to 24S-HC, other oxysterols are also involved in maintaining cholesterol homeostasis. For example, (25R)26-hydroxycholesterol (26-HC, also known as 27-HC) and 25-hydroxycholesterol (25-HC) are also LXR-ligands and can promote cholesterol efflux transporter synthesis. 26-HC is synthesised from cholesterol by 27-hydroxylase, which is encoded for by ubiquitously expressed *CYP27A1.* 25-HC is synthesised by 25-hydroxylase activity, which is encoded by *CH25H*, expressed by macrophages and other immune cells (Fukumoto et al., 2002; Javitt, 2002; Jeitner et al., 2011; Liu et al., 2018).

In addition to mediating cholesterol homeostasis, oxysterols are also important for normal brain function, and are involved in myelination, neuronal health and inflammation (Mutemberezi et al., 2016). The rare developmental disease cerebrotendinous xanthomatosis (CTX) presents with complex peripheral and CNS pathology and the fatal degeneration of lower motor neurons. Mutations affecting *CYP27A1* cause CTX. *CYP27A1* is also required for the induction of Th17 T cells via 7β,(25R)26-dihydroxycholesterol (7β,26-diHC), a potent activator of RORγt. 24S,25-epoxycholesterol is neuroactive and supports neurogenesis (Theofilopoulos et al., 2013), whilst 8,9-unsaturated sterols can induce oligodendrocyte formation and remyelination (Hubler et al., 2018). 3β,7α-dihydroxycholestenoic acid is neuroprotective of motor neurons, whereas, others, such as 3β-hydroxycholestenoic acid are neurotoxic (Theofilopoulos et al., 2014).

Oxysterols are also involved in regulation of the immune system. For example, 25-HC is a mediator of negative feedback to interleukin-1 (IL-1) cytokine-mediated inflammation, therefore its production can be anti-inflammatory (Reboldi et al., 2014). 7α,25-dihydroxycholesterol (7α,25-diHC; synthesised from 25-HC via CYP7B1 activity) and 7α,(25R)26-dihydroxycholesterol (7α,26-diHC; synthesised from 26-HC

via 27-hydroxylase), are endogenous ligands for EBV induced G-protein coupled receptor 2 (EBI2), which contributes to B cell activation within lymphoid tissue. This can result in damaging inflammatory processes (Nair et al., 2015; Griffiths and Wang, 2019; Griffiths and Wang, 2020).

1.2.3 – Cholesterol and Oxysterol Dysregulation in Neurodegenerative disease

The regulation of cholesterol homeostasis is imperative for the proper function of the brain; dysregulation of cholesterol and oxysterols have been implicated in a variety of diseases, including neurodegenerative diseases (Griffiths and Wang, 2019; Griffiths and Wang, 2020).

For example, cholesterol dysregulation has been implicated in Alzheimer's Disease (AD). The most robust genetic risk factor for AD is the ε4 allele for $APOE_4$ (Corder et al., 1993). APOE is a cholesterol efflux transporter; lipidation of apolipoproteins is important for proper lipid transport and clearance. $APOE_4$ has been associated with decreased lipidation, and contributes to increased amyloid aggregation, a pathological hallmark of AD (Husain et al., 2021; Young et al., 2023). Additionally, 24S-HC has been found to be elevated in patient CSF, but reduced in serum and plasma. 24S-HC has also been reported to be reduced in AD brain (Heverin et al., 2004; Björkhem et al., 2009). A reduction in 24S-HC, and hypercholesterolaemia is damaging to the brain (Dias et al., 2014). Inhibition of *CYP46A1*, which encodes for 24-hydroxylase, has been shown to increase neuronal death in a mouse model of AD. Whereas increasing *CYP46A1* was neuroprotective, normalised 24S-HC concentration and also rescued cognitive defects in model systems (Burlot et al., 2015; Mast et al., 2017). 26-HC (the product of 27-hydroxylase) has been shown to be increased in the CSF and brains of people with AD (Heverin et al., 2004). High levels of 26-HC have been shown to impair neuronal morphology, hippocampal spine density and is also implicated in mechanisms related to synaptic maturation and plasticity. Therefore, inhibition of the enzyme responsible for the synthesis of 26-HC, via inhibition of the mRNA encoding for it, *CYP27A1*, may be protective in AD, whilst deficits cause CTX (see 1.2.2.1) (Merino-Serrais et al., 2019).

Another neurodegenerative disease associated with cholesterol and oxysterol dysregulation is Huntington's Disease (HD). Huntington's disease is characterised by an excess of 36 or more CAG repeats in the huntingtin gene (*HTT*) (McColgan and Tabrizi, 2018). A variety of sterols have been shown to differ in the brains of people with HD and in mouse models of HD, such as a reduction in lanosterol, lathosterol, desmosterol as well as cholesterol and 24S-HC Valenza et al., 2007). It has been demonstrated in mice that brain supplementation with cholesterol may be beneficial in HD (Valenza et al., 2015), additionally, increasing *CYP46A1* may be beneficial by increasing the rate of cholesterol metabolism, and consequently increasing the rate of cholesterol precursors and metabolite synthesis (collectively referred to as cholesterol flux), which were found to be reduced in HD-mice and patients (Boussicault et al., 2016).

Alterations in cholesterol metabolism have also been observed in MS. The concentration of several oxysterols differ in various biological fluids in RRMS patients compared to healthy controls. For example, Novakova *et al* have reported a decrease in 24S-HC in CSF and a reduction of 26-HC in serum. Additionally, Crick *et al* have shown that there is a reduced concentration of 25-HC and 26-HC in patient plasma (Novakova et al., 2015; Crick et al., 2017 but little attention has been paid to how MS-disease activity relates to these findings. There is also evidence that cholesterol homeostasis is altered in progressive MS. The MS STAT-2 phase II clinical trial showed that high dose treatment with simvastatin can reduce the rate of brain atrophy in people with SPMS, suggesting that mechanisms relating to cholesterol homeostasis are involved in this beneficial effect (Chataway et al., 2014).

It will be important to both identify any differences in cholesterol flux in progressive disease, and also to gain a better understanding of how changes observed in the periphery relate to changes in the brain and with disease activity. Work from our group, including work which will be presented in this thesis, has begun to address these questions. Of note, there are already existing drugs, alongside the brain penetrant statins, which have been shown to have inhibitory effects on cholesterol metabolism-related enzymes, some of which have already been suggested as potential therapies for neurodegenerative diseases, such as AD and HD (Burlot et al.,

2015; Boussicault et al., 2016; Kacher et al., 2019; Lerner et al., 2022). It will be imperative to ascertain whether modulating cholesterol flux in the CNS will benefit people with MS.

1.3 Mass Spectrometry

The strides which have been made in furthering our understanding of how cholesterol, and its oxidised metabolites, may relate to disease, including neurodegenerative disease, would not be possible without the advent of modern mass spectrometric techniques (Rampler et al., 2021).

Mass spectrometry (*MS*) is an analytical technique capable of identifying compounds in a mixture based on their mass to charge ratio. There are three main parts of a mass spectrometer. First, an ionisation source, which ionises compounds within a sample into gas phase ions; next, a mass analyser, which separates ions based on their mass-to-charge ratio (*m/z*) and lastly, an ion detector which converts the generated ion currents into amplified electrical signals, which are processed using a data management system to generate a mass spectrum (a plot of abundance against *m/z*) (Glish and Vachet, 2003) (figure 1.6).

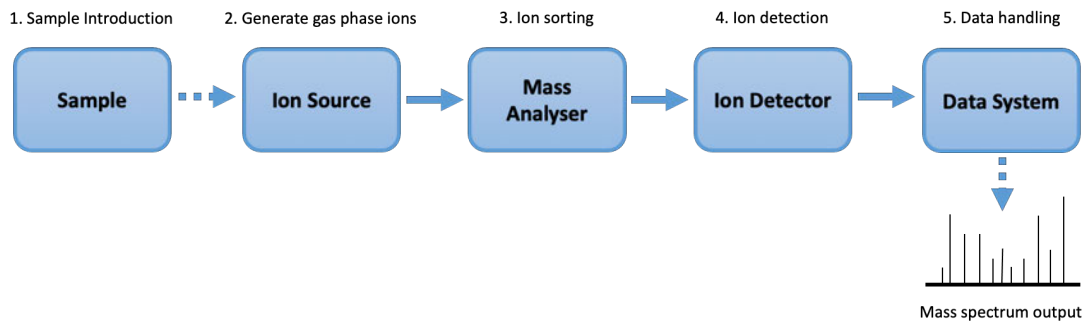

Figure 1.6 - Schema of Mass Spectrometry Workflow

Samples are loaded into the system. An ion source is used to confer a charge to molecules within the sample. Relevant ions are filtered by the mass analyser which are then transferred to, and measured by, the detector as electrical signals, which are then converted into readable data. Created in Microsoft PowerPoint.

1.3.1 – Mass Spectrometry Ionisation Sources and Mass Analysers

There a number of different ionisation methods and mass analysers that can be used, these are described below.

1.3.1.1 – Ionisation Methods

Compounds within a mixture are ionised under vacuum. Numerous ionisation sources are available including electron ionisation, chemical ionisation, electrospray ionisation and atmospheric pressure chemical ionisation (Smith, 2013).

Electron ionisation utilises a resistively heated filament which emits a beam of high-energy electrons. This interacts with molecules within the sample and results in an electron being expelled from the molecule, producing an ion. The first formed ion usually has a molecular mass of the sample molecule and is termed the molecular ion. Due to the high energy used, the molecular ion can be fragmented into fragment ions unique to the analyte. Positively charged ions are accelerated towards the mass analyser due to negative potential maintained by an ion focusing plate. Fragmentation of the molecular ion allows structural information about the analyte to be obtained (Hocart, 2010; Smith, 2013).

Chemical ionisation uses a reagent gas within the source to ionise molecules within the sample. First, the reagent gas undergoes electron ionisation. This gas is at a significantly higher concentration than that of the sample. The same molecules become ionised when they react with the pre-ionised reagent gas. This is 'soft' ionisation and does not result in a significant amount of fragmentation. This provides molecular mass information (Smith, 2013; Thomas, 2019).

Electrospray ionisation (ESI) pumps the liquid sample through a capillary. A potential difference is applied between the end of the capillary and an electrode, which results in the accumulation of charge on the surface of the sample liquid as it emerges from the capillary as charged droplets. A nebulising gas aids droplet formation, whilst a drying gas aids evaporation of solvent from the droplets. As solvent evaporates from the droplets, they become smaller, whereas the charge on the surface increases in density. Eventually, like charges repel each other and the droplet is split into smaller droplets; this process repeats until an ion is ejected from the droplet. The gas phase ion is then focused through a sampling cone before being transported to the mass analyser (Ho et al., 2003; Smith, 2013).

Atmospheric pressure chemical ionisation pumps the liquid sample through a pneumatic nebuliser, creating a fine spray. The droplets within the spray are vapourised and solvent is removed. The nebulising gas undergoes ionisation via electron ionisation by corona discharge (a highly charged electrode creates an electric field strong enough to ionise nearby molecules). These ions collide and interact with solvent molecules, such as those in the mobile phase, and form secondary ions. These secondary ions collide with sample molecules resulting in ionisation of the sample molecules, in a similar method as chemical ionisation. The ions are then passed to the mass analyser (Smith, 2013; Thomas, 2019).

1.3.1.2 – Mass Analysers

After ionisation, ions are transported to the mass analyser where they are separated according to their *m/z* before being transferred to the detector for measurement. There are different mass analysers which vary in their means by which to separate ions, their resolution and upper mass range (Smith, 2013).

For example, sector mass analysers separate ions using either an electric or magnetic field. Ions travel towards the detector under the influence of the electric/magnetic field. This applied field causes the ions to travel in a curved trajectory, with the radius of the curve dependent on the field strength and applied voltage; only ions with a specific *m/z* follow the correct curvature to reach the detector. Altering the electric/magnetic field strength and voltage allows ions with differing *m/z* to be detected (Bateman, 1999; Smith, 2013).

Another type of mass analyser is a time-of-flight (ToF) analyser. Ions are accelerated to the same kinetic energy and are sent towards the detector. Although the ions have the same kinetic energy, they take different times to reach the detector due to differences in their *m/z*; e.g., smaller ions have a greater velocity and reach the detector before larger ions with a lesser velocity. The time it takes for an ion to travel through the flight tube is measured and converted into the molecule's *m/z* (Bateman, 1999; Smith, 2013).

Quadrupole mass analysers consist of 4 parallel rods set around a central axis. Each opposing rod pair is connected electrically. A radio frequency (RF) and direct current

(DC) is applied to the rods; adjacent rods are of opposite RF. For a given RF/DC combination, only ions of a certain *m/z* have a stable trajectory and are able to pass through to the detector, all other ions collide with the rods and are neutralised. Altering the RF/DC allows ions with differing *m/z* to be sent to the detector (Mellon, 2003; Smith, 2013).

Ion trap mass analysers store ions within a trap before ejection for measurement. Linear ion traps (LIT) are constructed in a similar way to a quadrupole. The central quadrupole traps ions in a 2D-plane along the x/y axis. Unlike a quadrupole, the LIT traps ions within the analyser, prior to measurement. They are trapped along the axis of the trap (along the z axis) by a set of DC electrode segments positioned at either end, which are set to an appropriate voltage to cause the centre of the ion trap to be at a lower potential than the end sections. A gas is applied which causes ions to lose some kinetic energy, trapping them in the centre of the ion trap. This traps ions of all *m/z* values. Altering the RF potential facilitates ion oscillations with a stable trajectory, allowing ion accumulation, storage, focussing and ejection of ions of a particular *m/z* for measurement (Hocart, 2010; Dunn, 2011).

Orbitrap mass analysers work in a similar way to LIT and trap ions using an electrical field, however they employ a different *m/z* measurement. The Orbitrap consists of a spindle-shaped inner, central electrode, with an outer electrode at either end. In the case of a Thermo Scientific Orbitrap Elite, prior to entry to the Orbitrap, ions can be trapped using LIT, first using high pressure LIT and then a low pressure LIT. Ions (or fragmented ions) are then transferred into a curved linear trap (C-Trap). Nitrogen gas, present within the C-Trap, collides with ions and reduces their kinetic energy. These are then transferred to the high vacuum Orbitrap. The ions delivered to the Orbitrap consist of a range of *m/z* values, and begin to orbit the central electrode around the z-axis and also oscillate along the z-axis. Increasing the DC electrostatic field of the outer electrodes, forces the ions further towards the central electrode, stabilising their trajectory. Ions of differing *m/z* values will oscillate at differing frequencies along the central electrode. This principle is used to identify a single ion based on its specific frequency (Hocart, 2010; Gross, 2017).

1.3.1.3 – Tandem Mass Spectrometry

Tandem *MS* is the use of multiple stages of mass analysis, either in space (different mass analysers are physically coupled together) or in time (where the same instrument facilitates both storage and all mass analysis events) (de Hoffmann and Stroobant, 2007).

1.3.2 – Gas Chromatography and Liquid Chromatography

Prior to mass analysis via *MS*, molecules within a sample can be separated via chromatography, coupled to the mass spectrometer. The most common set-ups used for oxysterol analysis are gas chromatography-*MS* (GC-*MS*) and high-performance liquid chromatography-*MS* (HPLC-*MS*). Compounds within a complex mixture will have varying affinity for the stationary phase. In HPLC-*MS* the mobile phase is liquid and the stationary phase is solid, whereas in GC-*MS* the mobile phase is gas and the stationary phase can be either solid or a liquid. The mobile phase pushes the sample through the stationary phase column; the compounds are then separated - the higher the affinity a compound has for the stationary phase, the longer it will take to be eluted from the column, prior to injection into the mass spectrometer. GC is typically coupled to an ionisation system which utilises either electron or chemical ionisation, whereas LC is normally coupled with electrospray or atmospheric pressure chemical ionisation (see 1.3.1.1) (Smith, 2013; Gross, 2017).

1.3.3 – Application of Mass Spectrometry for the Identification of Oxysterols within the Human Brain

Mass spectrometry can utilise a variety of starting material, including tissue and biological fluid (Dzeletovic et al., 1995; Heverin et al., 2004; Leoni et al., 2005; Crick et al., 2017; Griffiths et al., 2019b). In order for compounds within a sample to be identified and quantified, they have to be extracted into a liquid medium. Alternatively, methods allowing on tissue *MS* imaging (*MS*I) can be utilised. *MS*I is discussed in chapter 2 (see *2.1.2*).

In this thesis I have utilised HPLC-electrospray ionisation (ESI)-*MS* using the Orbitrap Elite (Fisher Scientific) (figure 1.7), to provide both mass spectra and three rounds of fragmentation (MS^3) information, to identify and quantify sterols extracted from human brain tissue samples. Prior to HPLC-*MS* I utilised a method allowing for the

extraction, purification and identification of sterols within a sample - enzyme assisted derivatisation for sterol analysis (EADSA) (Crick et al., 2015). This method exploits the enzymatic reaction of cholesterol oxidase (CO) and Girard hydrazones. (Teng and Smith, 1995; Zhang et al., 2001). The addition of CO to the reaction mixture converts 3β-hydroxy-5-ene sterols to 3-oxo-4-ene equivalents – the 3-keto group is susceptible to derivatisation by Girard hydrazine (Girard P, GP). Once derivatised, sterols can be analysed by *MS*. EADSA is discussed in detail in chapter 2 (see 2.2.2.2).

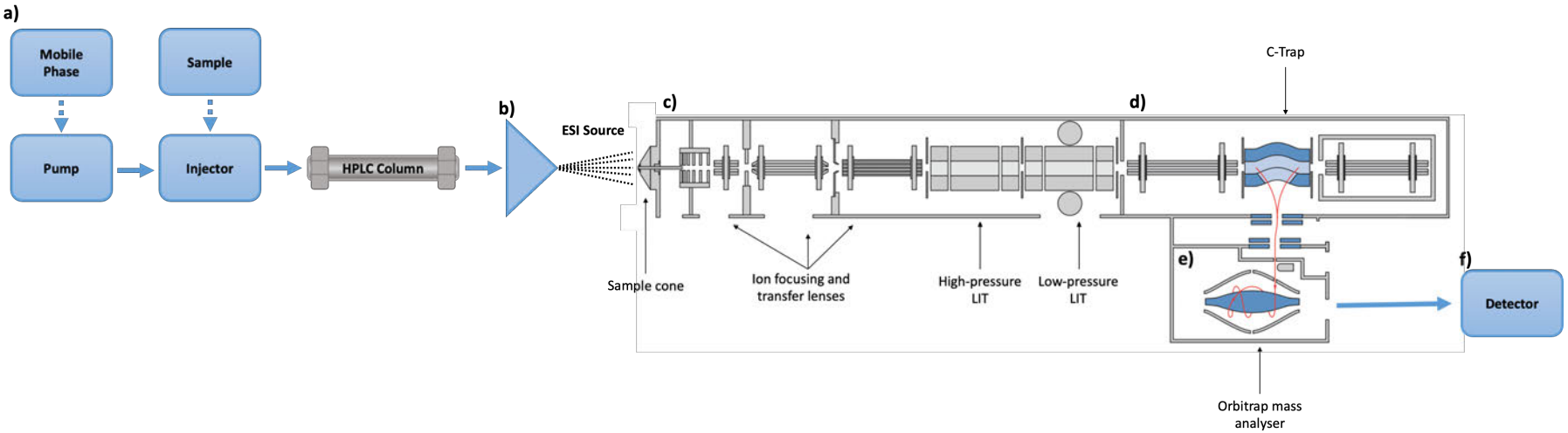

Figure 1.7 – Schema of HPLC-ESI-MS using the Orbitrap Elite Mass Analyser

The sample is pushed through the HPLC column by the mobile phase, the more affinity the sample has for the stationary phase column, the longer it will take to be eluted (a). The sample is pumped through the ESI source, before being collected by the sample cone (b). The ions are then focused and transported first to the high-pressure LIT followed by the low-pressure LIT (c). The ions then enter the C-trap® microscopy system (d) followed by the orbitrap mass analyser). The molecular ion and/or fragment ions are then sent to the detector for measurement (f). HPLC – high-performance liquid chromatography, LIT – linear iron trap. Image adapted and modified from http://planetorbitrap.com/orbitrap-elite (date accessed: 24/03/2023).

1.4 Hypothesis and Aims

There is an underlying, continuous progression independent of relapse activity (PIRA), affecting all phases of MS, which becomes clinically apparent in later disease (Cree *et al.*, 2019). PIRA-mechanisms have not been fully elucidated and more understanding of this important hallmark of disease is needed in order to stop, slow, or reverse MS progression. The results presented in this thesis focus on actively demyelinating tissue in MS, with a particular focus on MA/I WML, as these correlate with a worse MS-prognosis, contribute to PIRA and are prevalent in progressive disease (Elliott *et al.*, 2019; Absinta *et al.*, 2019; Ransohoff, 2023). Cholesterol is an important biomolecule and lipid component of the myelin sheath; its degradation by microglia/macrophages likely causes dyslipidaemia which may contribute to the continued innate immune dysregulation observed in progressive MS (Reynolds *et al.*, 2011; Grajchen *et al.*, 2018). Additionally, cholesterol oxidised metabolites, oxysterols, are important signalling lipids, and their dysregulation has been implicated in other neurodegenerative diseases – causing promotion of neuroinflammation and damaging neuronal health (Griffiths and Wang, 2019; Griffiths and Wang, 2020). To date, there has not been a systematic analysis of sterol abundance in the MS brain and there is limited data on foam-cell biology as pertaining to MA/I WML.

I hypothesise that cholesterol metabolism/homeostasis is altered in the human MS brain, at sites of ongoing, chronic inflammatory demyelination, and that this dysfunction contributes to neurodegeneration in MS disease. In order to test this, I will aim to:

1. Confirm that I can confidently identify and quantify cholesterol, its precursors and oxidised metabolites (oxysterols) in human brain tissue.
2. Identify and quantify changes in sterol concentration between pathologically relevant regions of the MS brain, as well as compared to demographically/regionally matched control brain.
3. Explore whether available drugs, relating to MS/cholesterol regulation, can reduce the number of lipid-laden foamy macrophage-like cells in an *in vitro* model of myelin phagocytosis.

Chapter 2 – Identification and Quantification of Low Abundance Oxysterols in the Human Multiple Sclerosis Brain

2.1 Introduction

Advancements in analytical methodologies has helped to highlight the emerging role of oxysterols in neurodegenerative disease. Information about oxysterols in the human brain is limited, and changes in the MS brain are unknown. Using cutting edge, mass spectrometric technology, I have begun to elucidate differences between the oxysterol profiles from the brains of people with and without MS.

2.1.1 – Challenges in Oxysterol Research

Previously, thin-layer chromatography (TLC) was used for the separation of oxysterols. TLC can separate oxysterols quickly and simply, however, resolution of side-chain isomers is poor, additionally, the method is unsuitable for the separation of complex mixtures of oxysterols, often present in biological samples (Shan et al., 2003; Griffiths et al., 2013). Modern studies favour the use of either gas-chromatography-*MS* (GC-*MS*) or liquid chromatography-*MS* (LC-*MS*). Both are valid methods for the detection of oxysterols, with neither technique superseding the other in their capability, however, GC-*MS* is traditionally considered the gold standard. Both are suitable for detection of oxysterols in a variety of biological mediums including plasma, CSF and tissue (Dzeletovic et al., 1995a; Heverin et al., 2004; Leoni et al., 2005; Crick et al., 2017; Griffiths et al., 2019b; Griffiths et al., 2019a).

Historically, GC- and LC-*MS* have shared some of the same challenges in oxysterol separation and quantification. Firstly, cholesterol is more highly abundant in biological samples compared to oxysterols; typically, there is at least 1000 times more cholesterol than any other oxysterol. High biological concentrations of cholesterol can lead to the formation of oxysterols via autoxidation during sample preparation/storage. It can be difficult to differentiate enzymatically formed oxysterols from those generated via autoxidation, therefore the abundance of a

measured oxysterol may differ from its true biological concentration. Although efforts have been made to avoid autoxidation in the current study, a number of oxysterols I have measured can be generated both enzymatically and via autoxidation - these sterols include 7α-hydroxycholesterol, 7β-hydroxycholesterol and 7-oxocholesterol. In addition, high cholesterol abundance can make the identification and quantification of very low abundant oxysterols more difficult. Groups have mitigated the risk of autoxidation (and the high cholesterol: oxysterol ratio) in a variety of ways, namely, the separation of cholesterol from other oxysterols at an early point during sample preparation. Both GC- and LC-*MS* sample preparation procedures utilise solid-phase extraction (SPE) and exploit the differing polarity of cholesterol and oxysterols to separate them (see 2.2.2.3). Additional steps are taken by groups utilising both GC- and LC-*MS* to further minimise autoxidation, these include avoiding the use of high temperatures, addition of metal chelators, addition of anti-oxidants, handling samples in an inert atmosphere and the use of solvents purged with argon or nitrogen (Dzeletovic et al., 1995a; McDonald et al., 2012). In addition to this, some have suggested that avoiding hydrolysis can reduce autoxidation (Kudo et al., 1989; Dzeletovic et al., 1995; Griffiths et al., 2013; Crick et al., 2015). Oxysterols can be free or esterified to fatty acids. The addition of a hydrolysis step allows for the fatty acid-esterified oxysterols to be quantified; omission of this step allows for free oxysterols to be quantified. The data presented in this chapter is of free, unesterified oxysterols. Free oxysterols are able to be transported from the brain to the periphery (blood/CSF) and therefore their measurement may be the most clinically useful.

Another challenge in oxysterol research is the resolution of isomers. Isomeric oxysterols may give similar spectra and their identification relies heavily on the production of suitable chromatograms and appropriate internal standards with similar chemical properties. Additionally, oxysterols are typically non-polar, neutral compounds, which are difficult to ionise – a property required for both GC- and LC-*MS*. To overcome these challenges groups have developed and utilised a variety of derivatisation procedures (Kudo et al., 1989; Jiang et al., 2007; Griffiths et al., 2008; Honda et al., 2008; Jiang et al., 2011; Griffiths et al., 2013). In the present study I

utilised a method allowing for the extraction, purification and identification of sterols within a sample - enzyme assisted derivatisation for sterol analysis (EADSA) (see 2.2.2.2) (Crick et al., 2015). EADSA exploits the enzymatic reaction of cholesterol oxidase (CO) and Girard hydrazones. (Teng and Smith, 1995; Zhang et al., 2001). The addition of CO to the reaction mixture converts 3β-hydroxy-5-ene sterols to 3-oxo-4-ene equivalents – the 3-keto group is susceptible to derivatisation by GP (figure 2.1). Once derivatised, sterols can be analysed by *MS*, in this case, by LC-electrospray ionisation (ESI)-*MS* and -MS^3.

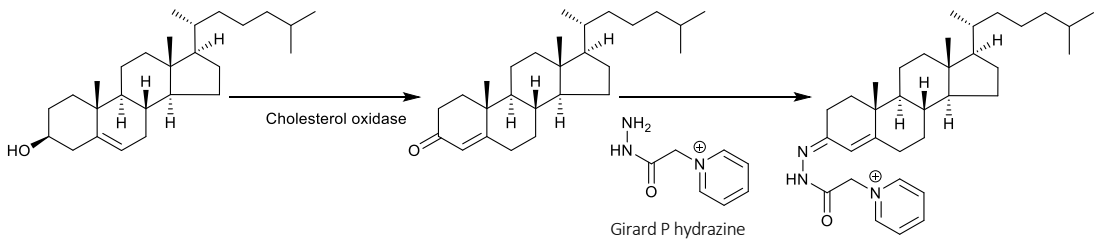

Figure 2.1 – Charged-tagging of Sterols

Cholesterol oxidase reacts with a 3β-hydroxyl group on sterols to produce a 3-oxo equivalent. Girard P hydrazine will react with the 3-oxo, resulting in a GP-tagged sterol with a positive charge. GP – Girard P. Image provided by Prof. William J Griffiths.

2.1.2 – On Tissue Mass Spectrometry Imaging using EADSA

There are a variety of technical approaches which can be used to quantify derivatised sterols. For example, enriched-tissue homogenates combined with LC-*MS*, or alternatively, on-tissue analysis using *MS* imaging (*MS*I). Two examples of *MS*I are liquid extraction for surface analysis (LESA) and matrix-assisted laser desorption/ionisation (MALDI).

Micro-LESA can be combined with EADSA to allow for the analysis of oxysterols on tissue – the EADSA methodology is modified to allow for surface derivatisation and internal standard addition via spraying, as opposed to the traditional method performed in solution. A capillary is then used to make contact with the tissue and deposits and aspirates the extraction solution, this is then run using LC-ESI-*MS*. For

on-tissue analysis of oxysterols in mouse brain, a spatial resolution of 400 μm has been achieved (Yutuc et al., 2019). This methodology is translatable to human tissues, and additionally can be used for the analysis of other compounds, such as proteins (Sarsby et al., 2014; Griffiths et al., 2020b).

The specificity of LESA-*MS*I is higher than MALDI-*MS*I, however MALDI-*MS*I can achieve higher spatial resolution (10 μM), which is highly beneficial when assessing pathological changes in varying tissue anatomy. Newer MALDI sources, including atmospheric pressure (AP)-MALDI, have been able to achieve a lateral resolution of 1.4 μm, and new technology will theoretically be able to achieve subcellular spatial resolution (Kompauer et al., 2016; Zhu et al., 2022). However, at present, MALDI-*MS*I is unsuitable for the analysis of low abundance oxysterols, but instead lends itself to the quantification of cholesterol. Cholesterol crystallises on the surface of the tissue and masks species with a similar spectral-finger print, such as low abundance oxysterols, currently preventing their detection. Like LESA-*MS*I, MALDI-*MS*I can be combined with a modification of EADSA allowing for on-tissue derivatisation; it also includes an additional step consisting of the addition of a suitable matrix, such as α-cyano-4-hydroxycinnamicacid. Unlike LESA-*MS*I, MALDI-*MS*I uses a laser to desorb and ionise molecules from the matrix-covered sample surface. The matrix aids in ionisation and also helps to protect the tissue surface by absorbing some of the laser's energy. The ions are then transported to the mass spectrometer to be measured (Gustafsson et al., 2011; Angelini et al., 2021).

Differences in cell type and number in the CNS are of importance in MS. People with MS typically have a reduced number of neuronal cell bodies, possibly up to as many as 13 billion less neurons within the cortex, compared to controls, as a result of neurodegenerative damage (Peterson et al., 2001; Carassiti et al., 2018). WML tend to be more inflammatory, with increased numbers of microglia/macrophage-like cells, compared to GML (Kuhlmann et al., 2017), which typically present as hypocellular lesions with few, if any, infiltrating macrophages. Therefore, the separation of WM and GM should both reduce any dilution effect from cell type differences as well as help us to elucidate location and abundance of sterols within the human MS brain.

.2.1.3 – Chapter Aims

At present, the location and abundance of oxysterols within the human MS brain is poorly understood. In order to address this, as well as explore the potential role of cholesterol and oxysterols in MS, it must first be confirmed which low abundance sterols are detectable in both control and MS brain. Secondly, any differences in the regional distribution of these sterols must be identified; and finally, whether there are differences in the abundance/location of sterols within the brains of people with and without MS needs to be assessed.

2.2 Methods

2.2.1 – Tissue Cohort

Snap-frozen, postmortem human brain tissue blocks from neuropathologically confirmed MS were provided by the UK MS Tissue Bank, Imperial College London (ethical approval, 08/MRE09/31+5). Age/gender matched control tissue blocks (anatomically matched where possible), with no history of neurological disease, were provided by the Thomas Willis Oxford Brain Bank, Oxford University (ethical approval, 13/wa/0292) (table 2.1). Tissue from 2 different tissue banks was used – the Oxford Brain Bank and the Imperial College London Brain Bank. Although there will be local differences, both tissue banks follow standard procedures in regard to tissue banking frozen samples – tissue is snap frozen on isopentane on dry ice and stored at -80°C. The choice to use tissue from two different tissue banks was made due to the type of tissue held by each tissue bank. Both tissue banks collect tissue from non-neurological disease, healthy controls. However, unlike the Imperial College London Brain Bank, the Oxford Brain Bank specifically collects brain tissue from controls, and as such, they have a larger selection of tissue from people with a younger age of death. The Imperial College London Brain Bank has more of a focus on collecting brains from people who lived with neurological disease, like MS – the control tissue they collect is typically from people who were much older compared to Oxford. Therefore, using tissue from two different brain banks allowed me to more closely age match the MS and control cases. Due to the differing nature of the tissue collected by the brain banks, the Oxford Brain Bank tissue has a longer PMD – this is due to the tissue being from control cases, who are younger and where their cause

of death may be sudden and require an investigation by a coroner – therefore delaying processing time after death. Typically, the cause of death for tissue from people with MS does not require extra investigation and therefore the PMD is shorter.

My overall project aim was to better understand the role of oxysterols in MS. I first sought to identify a cohort with evidence of an active inflammatory disease, from both a clinical and neuropathological perspective, defined as those who had had evidence of continued, active clinical disease progression (as diagnosed by clinical neurologists) and presence of pathologically confirmed lesions at death. Through my pre-screening, I also considered age, gender and MS subtype. The tissue blocks I screened came from an increased number of females, compared to males, reflecting the MS population and typically lived to at least middle-age. Additionally, the blocks were from those who had had progressive disease, with an increased number of blocks from people with SPMS, compared to PPMS, again reflecting the population. This was done as a pre-screening exercise to try to enrich for blocks likely to comprise of MA/I WMLs (see chapter 1 – 1.1.4.1). Photographs of unstained tissue blocks were provided, and blocks were reviewed and shortlisted if they contained a suspected active, inflammatory, WML based on the visible loss of myelin, with blurred or irregular edges, which was suggestive of recent demyelinating activity (Matthews et al., 2016). This exercise allowed me to request tissue blocks with an increased chance of containing the pathology I was most interested in (figure 2.2).

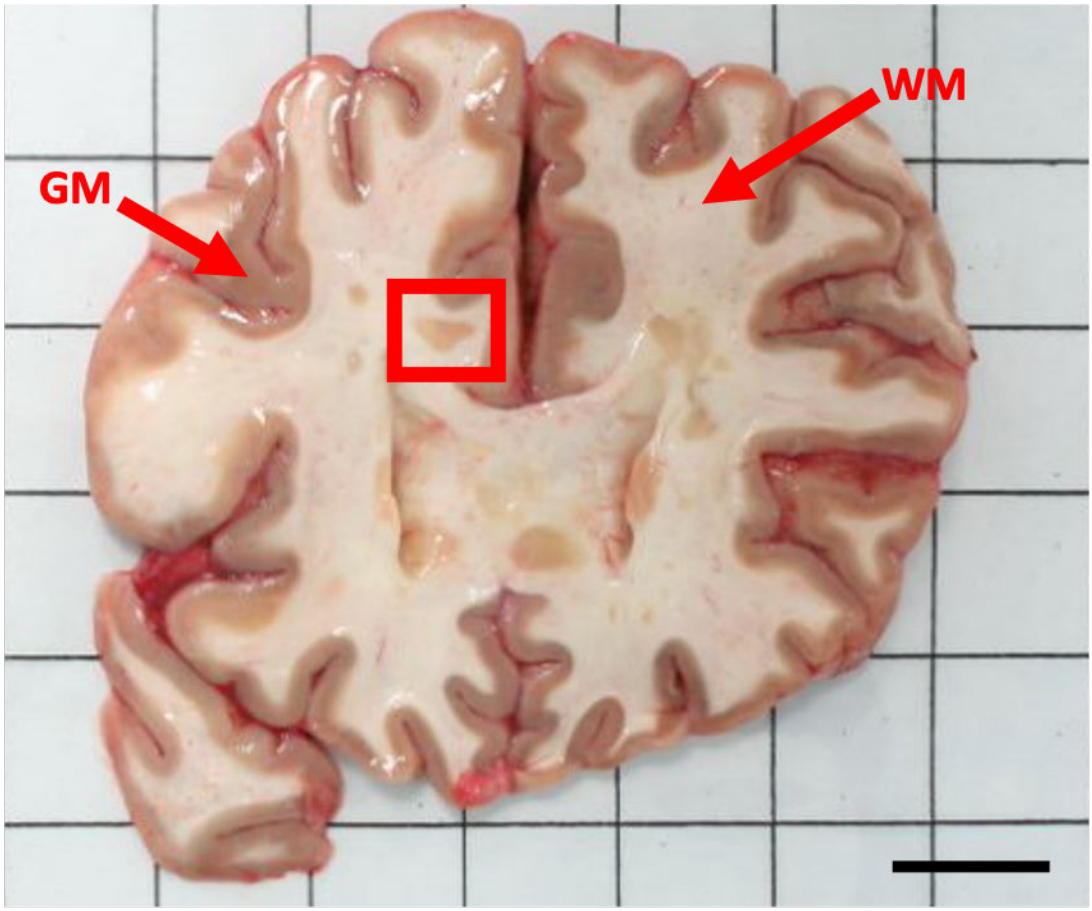

Figure 2.2 – White Matter Lesion Screening

A representative image of sliced brain tissue used to shortlist MS tissue blocks. Arrows point to grey matter (GM) and white matter (WM). Paler areas within the WM were deemed possible WM lesions. One example is highlighted by the red box. Scale bar = 2.5 cm. Image from UK MS Tissue Bank, Imperial College London.

Thirty-one MS tissue blocks, from 20 cases, and 5 tissue blocks from age and gender matched controls, without a history of neurological disease, were requested. At Swansea, the tissue blocks were cyrosectioned to 10 µm using a Leica CM1860 cryostat set to the appropriate temperature (-13°C to -16°C), and collected on Superfrost glass slides (Fisher Scientific). Sections were allowed to briefly airdry, prior to storage at -80°C, until use. All blocks selected were from the frontal lobe, temporal lobe or cingulate. Additional case demographics can be seen in table 2.1.

Table 2.1 – MS and Control Case Demographics

Samples highlighted in yellow were used to identify oxysterols present within the human MS brain. Tissue was provided by the UK MS Tissue Bank, Imperial College London, and the Thomas Willis Oxford Brain Bank, Oxford University. PMD = postmortem delay. Time progressive = number of years with a progressive disease diagnosis. Time wheelchair = number of years spent using a wheelchair.

Case Number	Sex	Age	PMD (hours)	Cause of Death	Brain Weight (g)	MS Subtype	Disease Duration (years)	Time Progressive (years)	Time Wheelchair (years)
MS 402	Male	46	12	Bronchopneumonia, MS	1246	SPMS	20	9	7
MS 407	Female	44	22	Septicaemia, pneumonia	1230	SPMS	19	11	10
MS422	Male	58	25	Chest infection, MS	1384	SPMS	13 (diagnosed)	Unknown	Unknown
MS 423	Female	54	10	Pneumonia	906	SPMS	30	21	18
MS 425	Female	46	25	Pneumonia, MS	992	SPMS	21	13	10
MS 438	Female	53	17	MS	1106	SPMS	18	Unknown	4
MS 461	Male	43	13	Bronchopneumonia	1116	SPMS	21	12	12
MS 473	Female	39	9	Bronchopneumonia, MS	1177	PPMS	13	10	6
MS 485	Female	57	24	Bronchopneumonia, MS	1109	PPMS	29	29	6+
MS 491	Female	64	9	Anaphylactic reaction	1217	SPMS	26	Unknown	Unknown
MS 492	Female	66	15	Sigmoid cancer	1234	PPMS	31	31	9
MS 497	Female	60	26	Aspiration pneumonia	1011	SPMS	29	12/13	12/13
MS 510	Female	38	19	Pneumonia, MS	1097	SPMS	22	15	15
MS 513	Male	51	17	Respiratory failure, MS	1033	SPMS	18	15	14
MS 523	Female	63	20	Bronchopneumonia, MS	1142	SPMS	32	9	9
MS 528	Female	45	17	MS	1137	SPMS	Unknown	Unknown	Unknown
MS 530	Male	42	15	Ab-ingestis pneumonia, MS	1357	SPMS	21	15	15
MS 538	Female	62	12	Pancreatic Cancer	1016	SPMS	31	17	3
MS 541	Female	67	Unknown	Unknown	Unknown	SPMS	49	17	13
MS 543	Female	66	Unknown	Unknown	Unknown	SPMS	40	8	20
NP 13/011	Female	62	24	Metastatic Colorectal Cancer	1261	N/A	N/A	N/A	N/A
NP 13/012	Female	60	48	Metastatic Breast Cancer	1423	N/A	N/A	N/A	N/A
NP 13/126	Male	56	40	Cardiac Arrest	1456	N/A	N/A	N/A	N/A
NP 13/127	Male	60	30	Cardiac Arrest	1168	N/A	N/A	N/A	N/A
NP 13/128	Male	68	48	Cardiac Arrest	1311	N/A	N/A	N/A	N/A

2.2.2 – Measurement of Sterols in Human Brain Tissue

2.2.2.1 – Macrodissection of Tissue for Sterol Analysis

The relative abundance of cholesterol, its metabolites and precursors in human MS and control brain tissue was measured. Five snap-frozen MS tissue blocks (from the frontal lobe, temporal lobe or cingulate) and 5 matched controls (superior frontal gyrus) were macrodissected to enrich for WM and GM, allowing for sterol analysis in these distinct anatomical regions. An n of 5 was chosen as a pilot study, allowing any sterol changes within gross anatomy to be identified, whilst reducing the cost and time of experimentation/analysis. Tissue sections (10 μm) were collected from each block and stained for luxol fast blue (LFB) (see 2.2.3.1). A corresponding LFB-stained tissue section for each block was then used to help identify the WM/GM border in each tissue block. Microscopic evaluation of each LFB section was carried out and an outline of the WM/GM was drawn. A combination of the stained LFB section and annotated drawings were used to identify WM/GM in the block prior to tissue sectioning. A scalpel was used to carefully score the tissue along the WM/GM border of each block, the tissue blocks were then cryosectioned, with slices enriched for either GM or WM carefully separated from each other using a paint brush. The enriched tissue fractions were collected in pre-weighed Eppendorf tubes, which were placed in the cryochamber, ensuring the tissue did not thaw as it was collected. Tissue scoring, sectioning and collection continued until at least 2 mg tissue per fraction was collected. The tissue was stored at -80°C until further processing. Tissue sections were collected after gross sectioning for homogenates, allowing the cases to be re-screened to identify any changes in pathology or to confirm lesion integrity further through the tissue block (see 2.2.3.1) (figure 2.3).

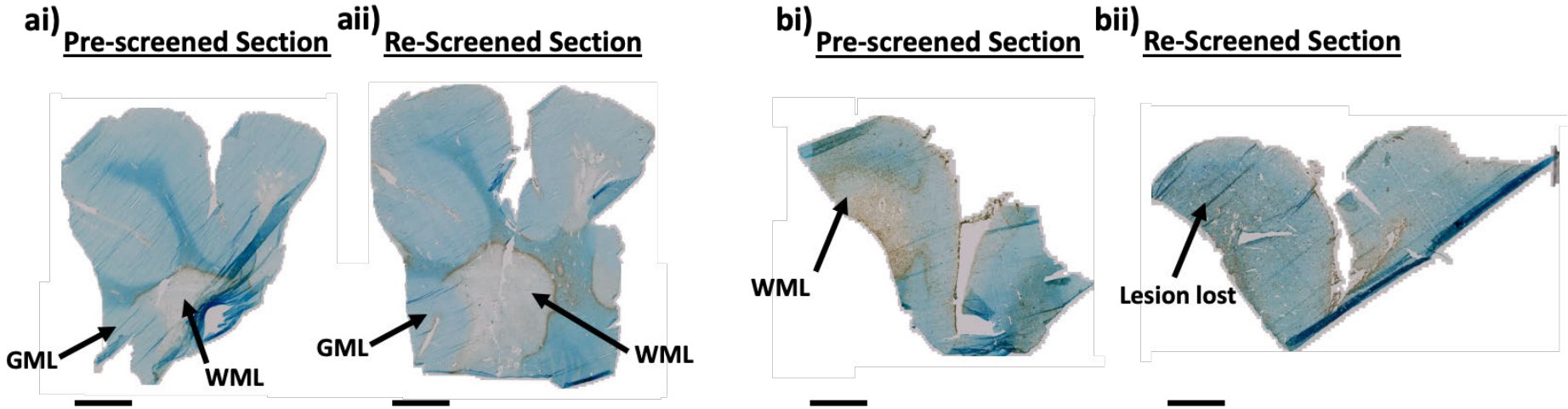

Figure 2.3 – Lesion Integrity Screening

LFB (blue) and HLA (brown) dual-stained 10 μm sections used for pre-screening (ai and bi). After gross sectioning, sections were re-screened to assess changes to pathology (aii and bii). Some blocks still contained similar pathology after gross sectioning (aii), others had altered pathology (bii). Representative images taken from MS 513 A3A3 (a) and MS 402 A1A3 (b). Scale bar = 0.50 cm.

2.2.2.2 – Enzyme-Assisted Derivatisation for Sterol Analysis – Liquid Chromatography – Mass Spectrometry

The extraction of sterols from brain tissue will be discussed in detail below, however other starting materials, such as plasma and CSF, can also be used. Once extracted, the sterols are purified from the sample via a SPE procedure, oxidised and derivatised to provide a 1+ charge, and finally undergo a second reversed-phased SPE procedure to further purify the sample and remove interferences. LC is then used to separate the sterols by their polarity and an Orbitrap mass spectrometer is used to produce a unique spectrum and chromatogram for each analyte; these are then used to identify and quantify the sterols in the sample.

2.2.2.3 – Extraction of Sterols from Brain Tissue and Preparation for LC-MS

WM and GM enriched brain tissue fractions from controls were manually homogenised in the presence of internal standards (iSTDs) (table 2.2) as follows. Internal standards were diluted in 4.2 ml 100% ethanol (Fisher Scientific), per sample. The tissue was manually homogenised in 2.1 ml iSTDs/ethanol solution using a 3 ml pestle and mortar. Thirty passes of the pestle were completed to homogenise the tissue. The solution was ultra-sonicated (Grant ultrasonic bath XB3, VWR) for 15 minutes, then 0.9 ml HPLC grade water (Fisher Scientific) was added dropwise under sonication, and the solution was ultra-sonicated for a further 15 minutes. The resulting 70% solution was transferred to a 12 ml Greiner tube. This process was repeated for the remaining tissue in the mortar; 2.1 ml iSTDs/ethanol solution was added and the solution was sonicated and diluted to 70% ethanol as above. The resulting extract-solution was added to the same Greiner tube. Details of the iSTDs can be found in table 2.2.

WM and GM enriched brain tissue from MS cases was mechanically homogenised using soft tissue homogenising CK14 Precellys tubes (Stretton Scientific). Internal standards were made up to a total volume of 4.2 ml in 100% ethanol, per sample. Brain tissue was transferred to a Precellys tube and 1.05 ml of iSTDs/ethanol solution was added. The sample was homogenised at 4.0 meters/second for 20 seconds,

followed by a 5 second break, and another homogenisation for 20 seconds using a FastPrep-24 homogeniser (M.P. Biomedicals). The supernatant was transferred to a 15 ml Falcon tube. Another 1.05 ml of iSTDs/ethanol solution was added to the Precellys tube and the homogenisation procedure was repeated. The resulting supernatant was transferred to the same 15 ml Falcon tube. This was repeated twice more to ensure maximum extraction for each sample. 1.8 ml of HPLC grade water was added dropwise under ultra-sonication, and the sample was ultra-sonicated for a further 15 minutes. Details of the iSTDs can be found in table 2.2.

Table 2.2 – Internal Standards used for Sterol Extraction

24R/S-Hydroxycholesterol-D_7 (24R/S-HC-D_7), 7α-Hydroxychoelsterol-D_7 (7α-HC-D_7), 22R-Hydroxycholest-4-en-3-one-D_7 (22R-HCO-D_7), 7α,25-Dihydroxycholesterol-D_6 (7α,25-diHC-D_6), 25-Hydroxyvitamin D3-D_6 (25-OHD_3-D_6). Internal standards purchased from Avanti Polar Lipids.

Internal Standard	Concentration (ng/ µl)	Mass per Sample (ng)
24R/S-HC-D_7	4	200
7α-HC-D_7	4	20
22R-HCO-D_7	5	200
7α,25-diHC-D_6	4	20
25-OHD_3-D_6	4	20
Cholesterol-D_7	200 000	1000

Both controls and MS samples were centrifuged at 4600 RPM for 1 hour at 4°C, using a Sorvall Legend RT centrifuge (Fisher Scientific). 600 µl of the supernatant (corresponding to 10% of the total brain tissue sample weight) was transferred to a 2 ml Eppendorf tube and 1.4 ml of 70% ethanol was added under ultra-sonication, the solution was further ultra-sonicated for 5 minutes. The solution was then centrifuged at 13000 RPM for 30 minutes at 4°C, using a Biofuge Fresco Heraeus centrifuge (Fisher Scientific).

Following sterol extraction from brain tissue, the sterols were fractionated using reversed-phase SPE. 200 mg Sep-Pak® Vac 3cc tC18 cartridges (Waters) were pre-conditioned using 4 ml 100% and 6 ml 70% ethanol, respectively. The extract-solution

was poured through the column under gravity, and the flow-through collected. The column was washed with 5.5 ml 70% ethanol; this column wash was collected in the same tube as the flow-through and deemed fraction 1 (Fr1). Next, a 4 ml 70% ethanol wash was performed, the flow-through collected in a second tube, Fr2. Next, two more column washes were performed with 2 ml 100% ethanol to elute cholesterol (and other similarly non-polar sterols); each flow-through was collected in a separate tube (Fr3 and Fr4). Fr1 and Fr3 were separated into two halves, A and B, and then all fractions were dried overnight using a Scanlaf scanspeed vacuum concentrator with scanvac coolsafe (Labogene) (25°C, 0.001 mbar) (figure 2.4).

After drying, Fr2 and Fr4 were stored at -20°C. Fr1 and Fr3 were processed further. Hereafter, Fr1 and Fr3 were processed separately to avoid potential cross-contamination (Fr3 A and Fr3 B were stored at -20°C prior to further use). Fr1 A and Fr1 B were reconstituted in 100 µl isopropanol. 1000 µl of 50 mM potassium phosphate buffer (pH 7), containing 3.0 µl of cholesterol oxidase (CO), was added to Fr1 A, converting 3β-hydroxyl groups to keto-groups. 1000 µl of 50 mM potassium phosphate buffer, without CO, was added to Fr1 B. The samples were incubated in a water bath at 37°C. After 1 hour, the oxidation reaction was stopped by the addition of 2000 µl of 100% methanol. 150 µl of glacial acetic acid was added as a catalyst. The samples were then derivatised overnight through Girard P reagent binding to the keto-groups to confer a positive charge. Fr1 A was derivatised with 190 mg of 5-deuterium Girard P reagent (D_5), whereas Fr1 B was derivatised using 150 mg of non-deuterated Girard P (D_0) (Tokyo Chemical Industrial) (figure 2.4). Girard P D_5 was kindly synthesised by former PhD students Alison Dickson and Manuela Pacciarini.

Next, a second reversed-phase SPE2 was used to further purify the sample and remove excess derivatisation reagent. 60 mg Oasis® HLB 3cc extraction cartridges (Waters Ltd) were pre-conditioned using 6ml 100%, 6ml 10% and 4ml 70% methanol, respectively. The 70% extract-sample was passed through the column under gravity and collected. The sample tube was washed with 1 ml 70% methanol, which was applied to the column, and collected with the sample effluent. HPLC grade water was

added to dilute the 70% effluent solution 1:1. The column was washed with 1 ml 35% methanol, which was collected and added to the effluent. This was then passed through the column again and collected. The 35% effluent was diluted 1:1 again to a 17.5% solution, the column was washed with 1 ml 17.5% methanol and the wash collected and added to the effluent. The effluent was applied to the column and then discarded. Following a final column wash with 6 ml 10% methanol, the sterols of interest were eluted and collected using three, 1 ml 100% methanol washes, and one, 1 ml ethanol wash. The samples were then either prepared for LC-*MS* or stored at -20°C until further use. The same oxidation, derivitisation and SPE2 procedure was repeated for Fr3 A and Fr3 B (figure 2.4).

A list of all reagents used during the SPE1, oxidation, derivisation and SPE2 procedures can be found in table 2.3.

Table 2.3 – List of Reagents for EADSA-LC-MS

Reagent	Purity	Manufacturer	Product Code
Absolute Ethanol	Analytical grade, 99.9+%	Fisher Scientific	E/0650DF/17
Acetonitrile	HPLC grade	Fisher Scientific	A/0626/17
Cholesterol Oxidase from *Streptomyces sp.*	0.088 units/µl	Merck	C8649
Formic Acid	Analytical grade, 99-100%	VWR	20318.297
Glacial Acetic Acid	Analytical grade, 99.8-100.5%	VWR	20104.334
Isopropanol	HPLC grade	Fisher Scientific	P/7507/17
Methanol	HPLC grade, 99.8+%	Fisher Scientific	M/4056/17
Potassium Phosphate Buffer (KH_2PO_4)	50 mM, pH 7.0	Merck	P9791
Water	HPLC grade	Fisher Scientific	W/0106/17

2.2.2.4 – Separation of Sterols Using Liquid Chromatography

Prior to separation and detection by LC-*MS*, samples were centrifuged for 30 minutes, 13000 RPM, 4°C (Biofuge Fresco Heraus). The first 2 methanol elutants for fraction A and fraction B were combined in equal parts, diluted to 60% methanol, then transferred to an HPLC vial (Waters). The samples were subjected to chromogenic separation using an UltilMate 3000 micro-HPLC system fitted with a Hypersil GOLD C18 selectivity HPLC column (Fisher Scientific). Samples were loaded onto an autosampler, their temperatures were maintained at 8°C prior to run and 35 µl of sample was injected onto the column per run.

Two mobile phases were used for the separation, mobile phase A (33.3% methanol, 16.7% acetonitrile, 50% HPLC grade water and 0.1% formic acid) and mobile phase B (63.3% methanol, 31.7% acetonitrile, 5% HPLC grade water and 0.1% formic acid). The analytes in each sample were separated by 2 LC gradients. The short gradient, 17 minutes, consisted of 20% mobile phase B: 80% mobile phase A for 1 minute, which was gradually increased to 80% B by 8 minutes; at 12 minutes the percentage returned to 20% B for the remainder of the sample run. The long gradient, 37 minutes, consisted of 20% mobile phase B: 80% mobile phase A for 10 minutes, before gradually being increased to 50% B at 20 minutes, remaining at 50% B for 6 minutes before being gradually increased to 80% B at 29 minutes; at 32 minutes mobile phase B returns to 20% for the remainder of the run. The column was washed between each loaded sample with two, 50:50 100% methanol: 100% propan-2-ol and 1, 95% methanol washes. The analytes within the sample were separated based on their polarity. Each subsequent eluant from the column was directed to the electrospray ionization source on the Orbitrap Elite mass spectrometer, running in positive ion mode (figure 2.4). The Orbitrap Elite was regularly calibrated to a mass accuracy of <5ppm using LTQ ESI positive calibration solution (Fisher Scientific), by another group member, Dr Eylan Yutuc.

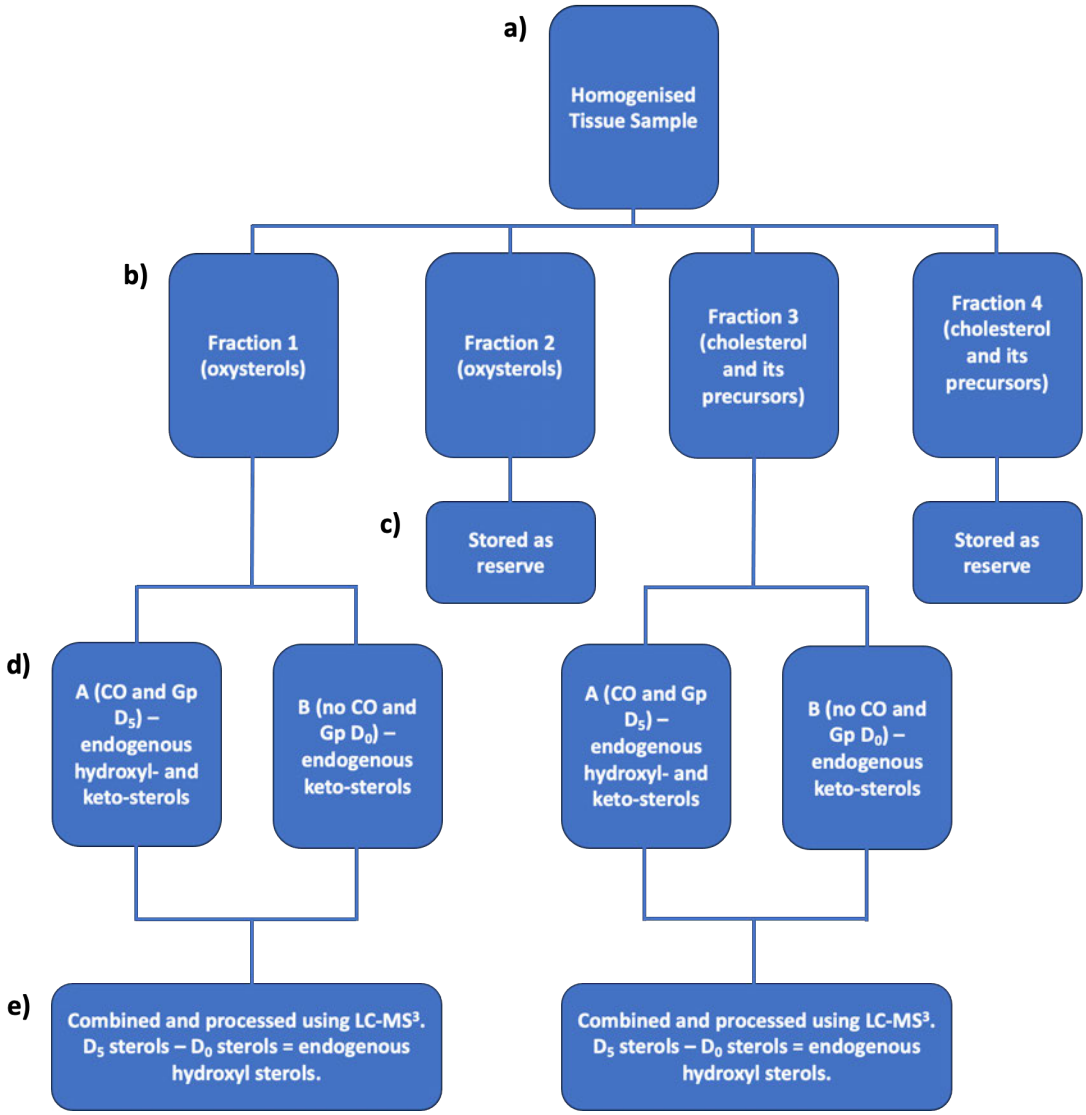

Figure 2.4 – Flow Diagram of Enzyme Assisted Derivatisation for Sterol Analysis

Tissue is homogenised with internal standards (a). The homogenate solution is passed through C18 cartridges, bound sterols are eluted using either 70% ethanol (Fraction 1 and 2) or 100% ethanol (fraction 3 and 4). Fractions 1 and 2 contain oxysterols and fraction 3 and 4 contain more non-polar sterols - cholesterol and its precursors (b). Fractions 2 and 4 are stored at -20°C for potential future use (c). Fractions 1 and 3 are split into 2 equal parts, A and B. Cholesterol oxidase is added to A which converts 3β-hydroxyl groups to a 3β-keto group. 5 deuterated Girard P (Gp D_5) is added to A whereas Girard P with no deuterium is added to B (Gp D_0), therefore all sterols in A have 3β-keto groups and are 5 mass units heavier than the equivalent 3β-keto sterol in B, allowing them to be distinguished (d). This also allows endogenous 3β-keto sterols to be identified from sterols with an endogenous 3β-hydroxyl group as 3β-hydroxyl sterols are only measured in A, therefore A-B = 3β-hydroxyl sterols (e). Created in Microsoft PowerPoint.

2.2.2.5 – Analysis of Sterols

Data was acquired using Thermo Xcalibur. Generated MS^3 spectra were used to identify oxysterols by matching their fragmentation pattern to a library of over 100 oxysterol species. Once identified, the corresponding chromatogram peaks were integrated and peak data exported. This provided the retention time and peak area, in counts, and analyte concentration was calculated (equation 2.1). The concentration of each sterol was calculated using an appropriate iSTD which had similar physical and chemical properties to the analyte of interest (table 2.4).

$$Q\ analyte = \frac{A\ analyte}{A\ iSTD} \times Q\ iSTD$$

Equation 2.1 – Calculating Analyte Amount

Formula for calculating relative endogenous analyte amount (*Q analyte*). *A analyte* – peak area (counts) of analyte; *A iSTD* – peak area (counts) of internal standard; *Q iSTD* – quantity (ng) of internal standard added during extraction.

Table 2.4 – List of Internal Standards used to Calculate Concentration of Analytes.
HC – hydroxycholesterol, HCO – hydroxycholest-4-en-3-one. Internal standards purchased from Avanti Polar Lipids.

Internal Standard	Analyte of Interest
24R/S-HC-D_7	• 24S-hydroxycholesterol • 25-hydroxycholesterol • (25R)26-hydroxycholesterol • 24R-hydroxycholesterol • 7α,(25R)26-dihydroxycholesterol • 3β-hydroxycholest-5-en-(26R)26-oic acid • 3β,7β-dihydroxycholestenoic acid
22R-HCO-D_7	• 7β-hydroxycholesterol • 7-oxocholesterol • 7α-hydroxycholesterol
Cholesterol-D_7	• Cholesterol • Desmosterol • 8,9-dehydrocholesterol

2.2.3 – Lesion Classification

Lesions were characterised based on their anatomical location, as either lesions of the WM or GM, following LFB histology and anti-MOG immunohistochemistry. Additionally, GML were subcategorised, using Kuhlmann *et al's* and Bø *et al's* classification, into type i lesions (leukocortical lesions, affecting deep cortical GM and underlying subcortical WM), type ii (small intracortical lesions surrounding vasculature, entirely within the GM), type iii (subpial lesions affecting the superficial cortical layers under the pia surface) or type iv (lesions which extend throughout the GM without affecting the underlying subcortical WM) (Bø et al., 2003; Kuhlmann et al., 2017).

2.2.3.1 – Histological and Immunochemical staining

Tissue sections were fixed for 1 hour with 4% paraformaldehyde (PFA), immediately after thawing. The sections were washed once with phosphate buffered saline (PBS) and then underwent either histological or immune-staining.

LFB staining was performed to allow for white/grey matter delineation and to identify areas of demyelination. After fixation, the sections were placed in pre-warmed LFB solution overnight at 60°C. Surplus stain was removed using a solution of excess lithium carbonate and 75% alcohol, until the white/grey matter border was clearly delineated (Klüver and Barrera, 1953).

In addition to LFB-only sections, sections were co-stained for LFB and HLA-DR. First, sections were stained with LFB as described above. Following the removal of excess stain, the sections were washed with PBS, then hydrogen peroxidase activity was quenched using 0.6% hydrogen peroxide for 8 minutes, followed by another PBS wash. Non-specific epitope sites were blocked by incubating with 10% normal goat serum for 30 minutes. Mouse anti-HLA-DR was then added and incubated overnight in a humid chamber. After washes with PBS, goat anti-mouse secondary antibody was added and incubated for 1 hour. After washes with PBS, the tissue was incubated with equilibrated avidin-biotin complex for 1 hour, diluted following the manufactures instructions. The tissue was washed with PBS and colour development

was achieved using 3,3'-diaminobenzidine (DAB) (components 1 and 2 combined in equal volumes).

Alternatively, sections were immune-stained. After fixation, peroxidase activity was quenched by incubating the sections with 0.6% hydrogen-peroxide, diluted in PBS containing 0.1% triton (PBS-T), for 8 minutes. Following 3 washes with PBS, the tissue was incubated for 30-60 minutes with 10% normal serum from an appropriate species, diluted in PBS-T, to block epitope sites. The tissue was then incubated with the appropriate concentration of primary antibody, diluted in PBS-T, overnight. Following washes with PBS, the tissue was incubated with the appropriate, species specific, secondary antibody conjugated to biotin, diluted in PBS-T to the appropriate concentration, for 1 hour. After washes with PBS, the tissue was incubated with equilibrated avidin-biotin complex for 1 hour, diluted following the manufactures instructions. The tissue was washed with PBS and colour development was achieved using DAB (components 1 and 2 combined in equal volumes).

Both LFB and immunostained sections were counterstained with cresyl violet and dehydrated through a graded series of alcohol (95%, 100%, fresh 100%). After overnight clearing in xylene the sections were mounted using DPX. Images were captured using a Zeiss AxioScope1 microscope (Carl Zeiss Ltd.) and Zeiss AcioCam black and white camera using the ZEN software suite (Carl Zeiss Ltd.). Unless otherwise stated, the described steps above were carried out at room temperature (RT). Details of the primary and secondary antibodies used can be found in table 2.5.

Table 2.5 – Primary and Secondary Antibodies used for Immunohistochemistry

Antigen	Target	Host Species	Working Concentration (µg/ml)	Supplier	Product Code	Monoclonal or Polyclonal
HLA-DR	Microglia	Mouse	1	Dako	F081701-2	Monoclonal
MOG	Myelin oligodendrocyte glycoprotein	Mouse	Stock conc. Unknown. 1 in 20 dilution.	Imperial College London (Prof. Reynolds)	-	Monoclonal
Secondary Antibody	**Target Species**	**Host Species**	**Working Concentration (µg/ml)**	**Supplier**	**Product Code**	**Monoclonal or Polyclonal**
Goat anti-mouse biotin	Mouse	Goat	3	Vector	BA-9200	Polyclonal

2.2.3.2 – Measuring Pathology

Stained tissue sections were digitised (ZEISS Axio Scanner (AxioScan. Z1)). The resulting annotated .czi files were managed with QuPath version 0.3.2 (https://qupath.github.io/) (Bankhead et al., 2017). Tissue sections were kindly digitised by staff at Cardiff University.

2.2.4 – Statistical Analysis

All statistical analysis was conducted using GraphPad Prism version 9.3.1. Due to small group sizes, I employed a more conservative, non-parametric statistical testing. Two-group comparisons were made by Mann Whitney testing with two-tailed distribution; greater than two-group comparisons were made by Kruskal-Wallis with Dunn's post-test. Values of <0.05 were considered significant.

2.3 Results

2.3.1 – Detecting Sterols in the Human Brain by Enzyme-Assisted Derivatisation by Sterol Analysis – Liquid Chromatography – Mass Spectrometry

EADSA-LC-*MS* was used to measure the relative abundance of sterols in WM- and GM-enriched tissue samples from both cases with confirmed MS and controls with no history of neurological disease. Fifteen sterols were identified and quantified. 7α-hydroxycholest-4-en-3-one was under the limit of detection and therefore was not quantified. Representative chromatograms and spectra can be seen in figure 2.5.

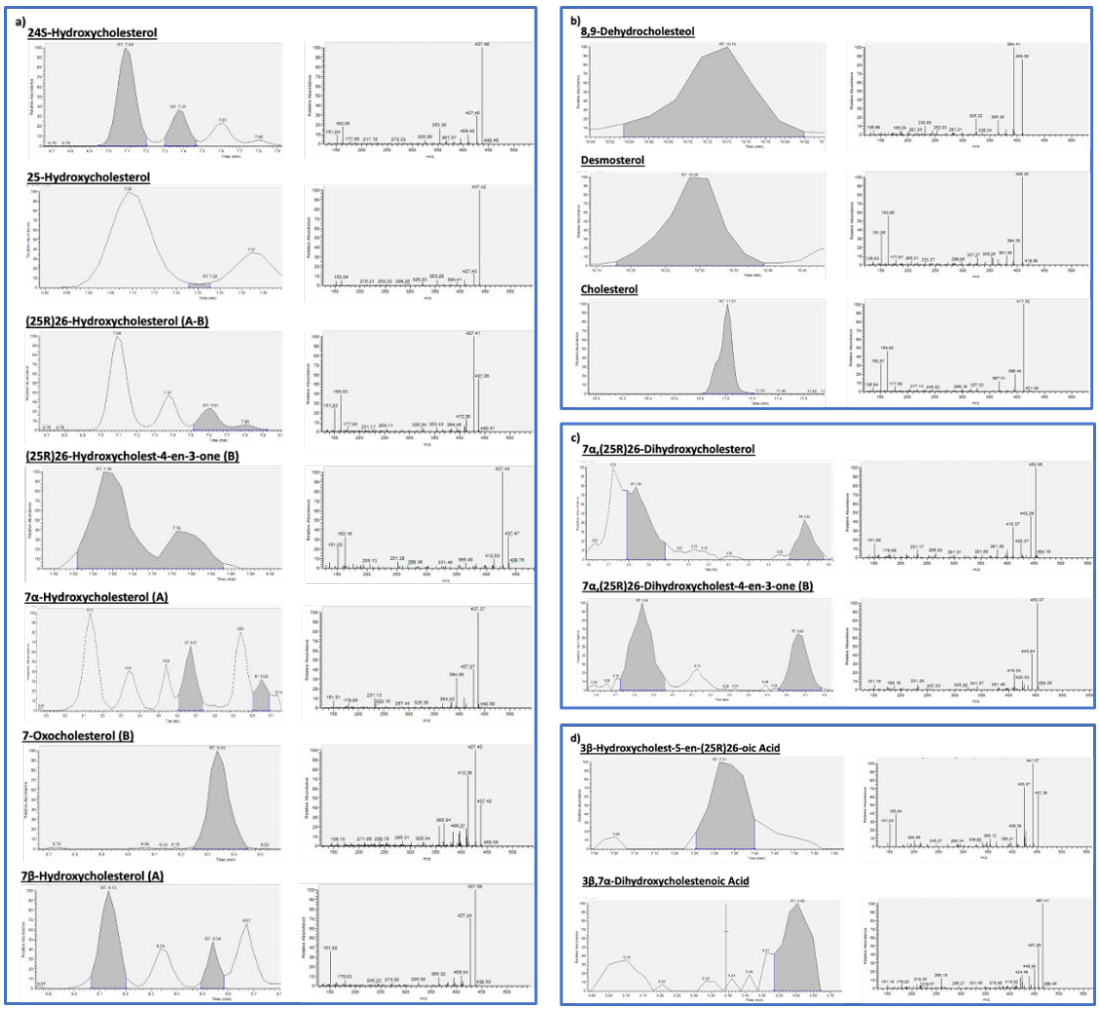

Figure 2.5 - Representative Spectra and Chromatograms of Measured Sterols

Representative chromatograms and spectra for confidently quantified analytes of interest, present in the human brain. Monohydroxy sterols (a), cholesterol and its precursors (b), dihydroxy sterols (c) and acids (d).

2.3.2 – Sterols Differ between MS and Control WM

Four sterols differed between MS and control WM: cholesterol, 24S-HC, 24R-hydroxycholesterol (24R-HC) and (25R)26-hydroxcholesterol (26-HC) ($p<0.05$). Each of the sterols were reduced in MS WM (cholesterol – MS WM 9.39±2.51 µg/mg (mean ±standard deviation), control WM 30.81±3.87 µg/mg; 24S-HC – MS WM 9.84±1.37 ng/mg, control WM 20.44±2.87 ng/mg; 24R-HC – MS WM 0.08±0.05 ng/mg, control WM 0.23±0.08 ng/mg; 26-HC – MS WM 1.86±1.17 ng/mg, control WM 5.06±1.05

ng/mg. 3β,7α-dihydroxycholestenoic acid (3β,7α-diHCA) followed the same trend, but did not reach statistical significance (figure 2.6, table 2.6).

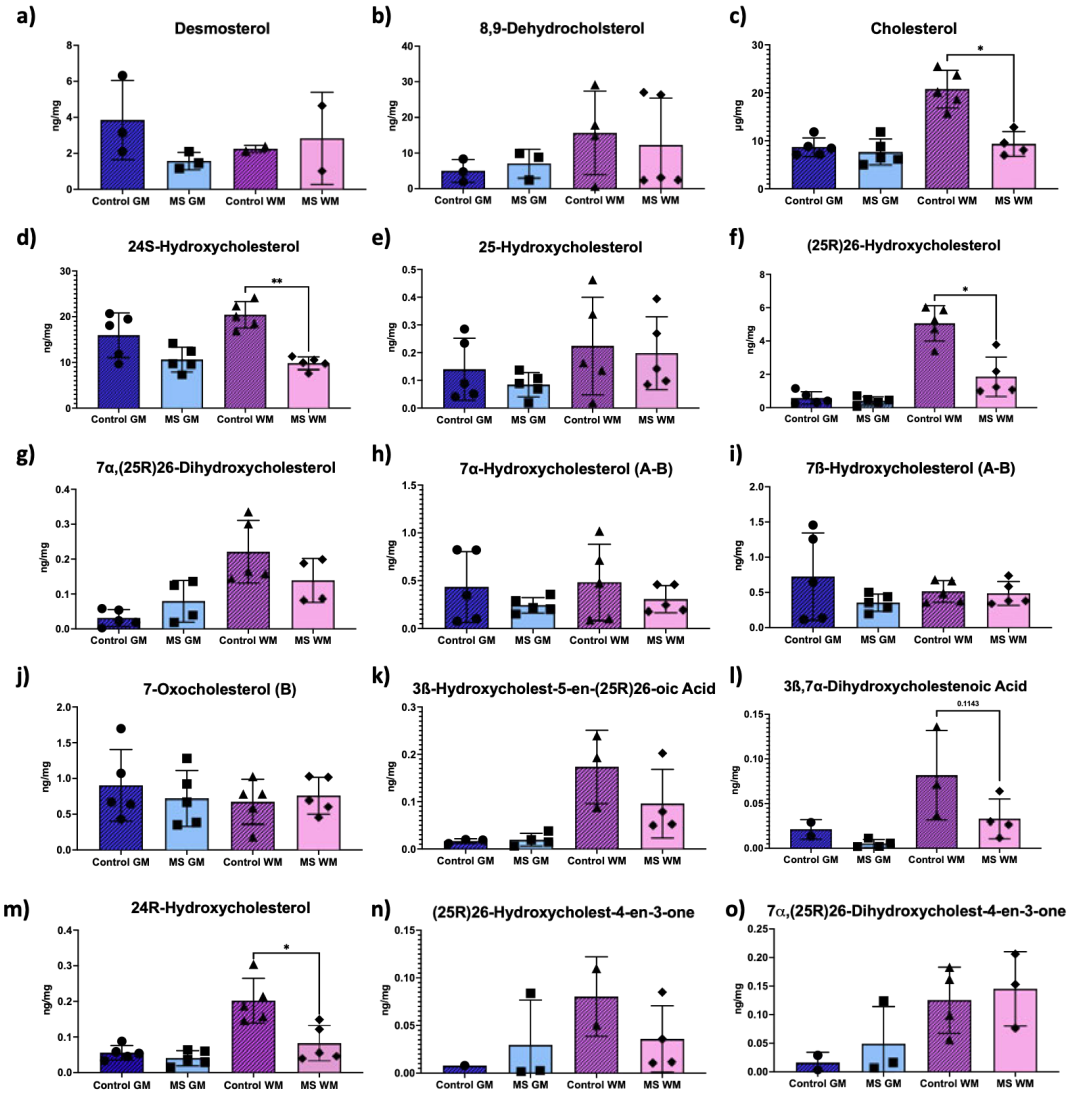

Figure 2.6 – Sterol Concentration in White and Grey Matter of the Human Brain

The relative abundance of sterols in human WM- and GM-enriched homogenates from the brains of people with (n = 5, male = 3) and without MS (n = 5, male = 3) (a-o). The abundance of four sterols were significantly reduced in MS WM compared to control WM – cholesterol (c), 24S-hydroxycholesterol (d), (25R)26-hydroxycholesterol (f) 24R-hydroxycholesterol (m). 3β,7α-dihydroxycholestenoic acid (l) followed the same trend, but did not reach statistical significance (*p<0.05, **p<0.01, Mann-Whitney U; GM/WM tested separately). Graphs show mean ± standard deviation.

Table 2.6 – Statistically Significantly Different Sterol Concentrations in MS WM

Mean ± standard deviation, Mann-Whitney U, n=5. 24S-HC – 24S-hydroxycholesterol, 26-HC – (25R)26-hydroxycholesterol.

Sterol	Concentration (ng/mg)		
	MS	Control	P Value
Cholesterol	9390±2510	30810± 3870	<0.05
24S-HC	9.84±1.37	20.44±2.87	<0.01
26-HC	1.86±1.17	5.06±1.05	<0.05

2.3.3 – Differing Concentrations of Sterols between Control and MS Brain

The MS brain contains areas of demyelinating, neuroaxonal and glial pathology, which will presumably contribute to the concentration differences measured between MS and control tissue for some oxysterols. Therefore, the gross pathology found in the sampled MS cases was identified and measured, including the number of lesions and percentage area of lesions/normal appearing tissue for each tissue block (figures 2.7 and 2.8), to better understand if the extent of lesion pathology in the sample associated with the abundance of the sterol of interest.

ai)

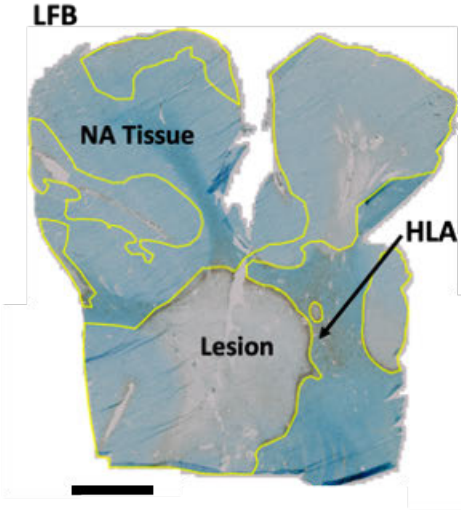

aii)

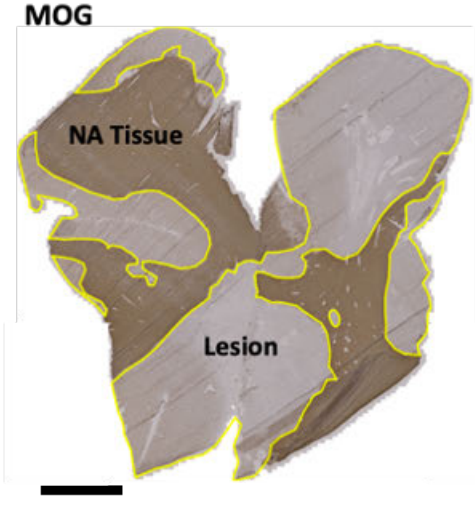

b)

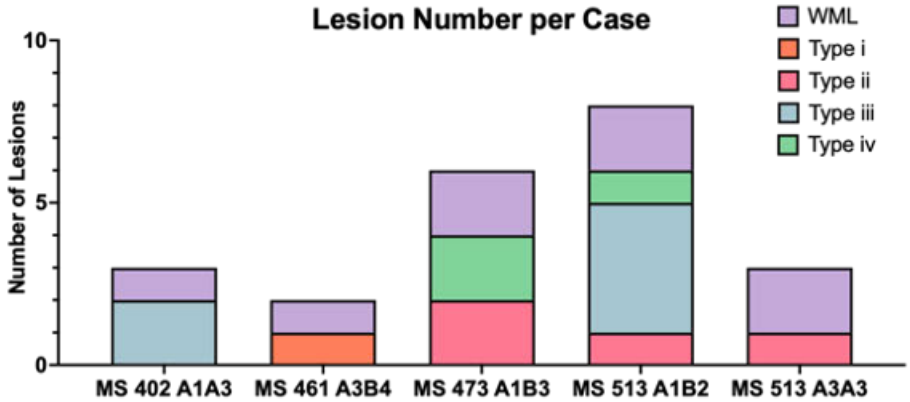

ci)

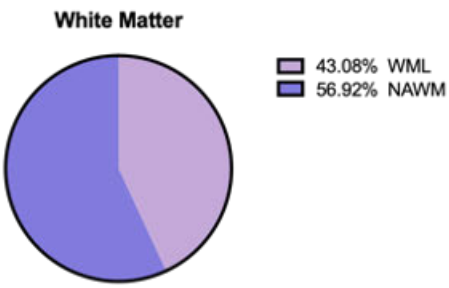

cii)

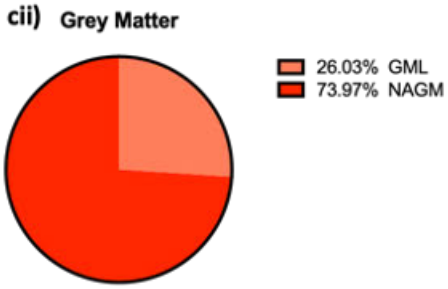

d)

Percentage of Lesions and Normal Appearing Tissue per Case (%)

Case	WML	NAWM	GML	NAGM
MS 402 A1A3	39.35	60.65	33.65	66.35
MS 461 A3B4	34.52	65.48	1.36	98.64
MS 473 A1B3	47.50	52.50	25.69	74.31
MS 513 A1B2	37.75	64.25	36.75	63.15
MS 513 A3A3	55.78	44.22	21.23	78.77

Figure 2.7 – Proportion of Demyelinated Tissue of Total Grey or White Matter Tissue Captured in the MS Tissue Homogenates

Tissue sections, from 5 MS cases were cut prior to homogenate collection. Areas devoid of myelin, shown by a lack of LFB/anti-MOG+ staining, were classed as lesions; areas positive for myelin were classed as normal appearing tissue. Lesion/normal appearing tissue borders are highlighted in yellow. Representative images taken from MS 513 A3A3 (ai & aii). Each MS tissue block was found to contain at least one WM, and 4 contained at least 1 GML, with a higher overall number of GML (b). The average percentage of WML load (ci) was about 9% higher than the GML load (cii). The percentage of the tissue containing lesions varied between MS cases. For example, MS 461 has a low percentage of both WML and GML, whereas MS 473 has a high WML/GML load (d). LFB – luxol fast blue, MOG – myelin oligodendrocyte glycoprotein, HLA – human leukocyte antigen, NA – normal appearing, WML – white matter lesion, GML – grey matter lesion, WM – white matter, GM – grey matter. Scale bars = 0.50 cm.

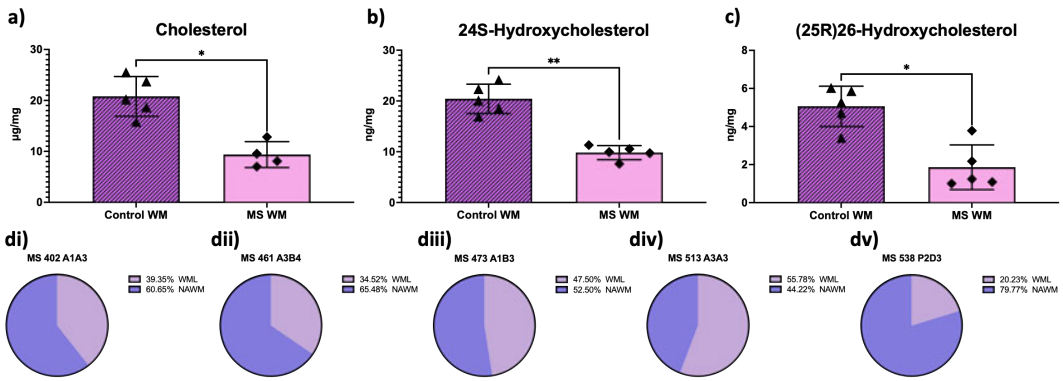

Figure 2.8 - The Extent of Demyelination in the Sampled Block Relates to the Concentration of Measured Sterols

Cholesterol (a) and 24S-hydroxycholesterol (b) were found to be decreased by ~50% in MS WM compared to control WM, and (25R)26-hydroxycholesterol (c) was found to be reduced by ~40% in MS WM (n = 5) compared to control WM (n = 5). The WM for each MS case used for homogenates contained a minimum of 20% lesioned tissue (di-v), broadly reflecting the decreased abundance of the measured sterols in each MS WM sample. Graphs show mean ± standard deviation; Mann-Whitney U *p<0.05, **p<0.01. WM – white matter, WML – white matter lesion.

2.4 Discussion

The aim of this chapter was to identify and quantify oxysterols in MS brain tissue; using EASDA-LC-*MS* methodology, 15 sterols were quantified.

2.4.1 – Detection of Oxysterols in Human Brain using Mass Spectrometry

Oxysterols have previously been implicated in neurodegenerative diseases including AD (Heverin et al., 2004), Huntington's disease (Leoni et al., 2008; del Toro et al., 2010) and Parkinson's disease (Björkhem et al., 2018; Huang et al., 2019). To date, the majority of research surrounding the role of oxysterols in neurodegenerative diseases has utilised serum, plasma and CSF samples (Leoni et al., 2008; Schüle et al., 2010; Abdel-Khalik et al., 2017; Marelli et al., 2018; Griffiths et al., 2019a)(Leoni et al., 2008; Schüle et al., 2010; Abdel-Khalik et al., 2017; Marelli et al., 2018; Griffiths et al., 2019a). These human sample types are accessible for research and may be most clinically useful in practise, however, they can only act as a surrogate to the changing oxysterol landscape of the human brain. To fully understand how oxysterols play a part in neurodegenerative disease, and how changing oxysterol abundance in the CSF and blood relates to disease pathology, their abundance and location within the brain must be investigated.

Postmortem human brain tissue has been utilised by the Björkhem and Turecki groups to identify sterols in the brains of AD patients and brains from non-neurological disease controls (who died via suicide), respectively. Both groups have utilised *MS*. The Björkhem study focused on 4 regions of the human brain, the frontal cortex, occipital cortex, basal ganglia and the pons. They have presented findings of 1 cholesterol precursor (lathosterol), cholesterol itself and 2 metabolites (24S-HC and 25R(26)-hydroxycholesterol (26-HC)). Due to the nature of AD, the Björkhem group only sampled from areas of the brain which contained either cortical or deep GM. The Turecki group also presented data on 24S-HC and 26-HC concentrations, in the Brodmann area 47, a GM structure associated with mood (Heverin et al., 2004; Freemantle et al., 2013). There is still a need for identification of oxysterol abundance in the WM of the human brain and other GM structures, and for a more comprehensive description of all of the sterols that can be identified. Additionally, there is a clear need to measure oxysterols in CNS tissue from MS donors.

EADSA-LC-*MS* differs to the technique used by the Björkhem and Turecki groups, who utilised gas chromatography–*MS* (GC-*MS*). At present, both GC-*MS* and LC-*MS* are

valid methods for the detection of oxysterols, with neither technique superseding the other (Griffiths et al., 2013). EADSA-LC-*MS* is a well described and proven method for oxysterol detection with a number of key attributes. Firstly, separating cholesterol from the other oxysterols ensures that oxysterols with a much lower abundance can be accurately measured, without being masked by cholesterol. Secondly, both sterols with an endogenous 3β-hydroxyl group and endogenous 3-keto group (such as 26-HC and 25R(26)-hydroxycholest-4-en-3-one) can be detected in the same sample run, speeding up detection. This is due to the combination of cholesterol oxidase addition/omission and Girard P reagents with a differing isotope label (Crick et al., 2015).

Using EADSA-LC-*MS* sterols that can be confidently identified in human control/MS brain were identified. Fifteen sterols within human WM/GM brain tissue were identified and quantified, at concentrations as low as 1 pg/mg. 7α-OHC was found to be below the limit of detection within the samples. Importantly, being able to accurately detect and determine the concentration of sterols such as 24S-HC, 25-HC and 26-HC is potentially very interesting given their roles in cholesterol homeostasis, brain health and neuroinflammation (Duc et al., 2019).

2.4.2 – Cholesterol Homeostasis is Altered in the MS Brain

The results show that cholesterol and three of its enzymatic downstream products, 24S-HC, 24R-HC and 26-HC were significantly reduced, by at least 40%, in MS WM compared to control WM. Additionally, 3β,7α-dihydroxycholestenoic acid followed the same trend in the WM, but did not reach statistical significance. No changes were found in MS GM compared to control GM. Additionally, no gender differences were identified, however, this may be due to the small number of samples, as opposed to gender not playing a role in brain cholesterol metabolism.

Mann Whitney U statistical testing was chosen as differences between MS and controls, in either WM or GM were tested for separately; separating these pathologically and functionally different brain regions. As the sample size was small, it could not assume that the data was parametric, therefore a non-parametric T-test

was chosen. Together, this implies that the reported differences are quite robust. Choosing to separate white and grey matter has allowed the identification of WM oxysterol differences between healthy controls and people with MS – these differences may have otherwise been masked, due to cellular and anatomical differences between these regions (Mercadante and Tadi, 2022).

Another consideration that must be made is the potential presence of pathology found within the MS brain, which is absent in controls. It was found that there was a mean WML percentage coverage of 42.98% and 23.74% GML coverage, across all cases used. How MS pathology may affect the concentrations of sterols in MS will be discussed in detail in the following chapter.

2.4.3 – Relating Sterol Changes in the Brain to the Periphery is Important

Although oxysterols have not previously been measured in the human MS brain, oxysterol concentrations have been investigated in MS serum, plasma and CSF. My results are supportive of Novakova *et al*'s study who measured 24S-HC and 26-HC in serum and CSF from healthy controls (n=16) and people with RRMS (n=31). They reported that 24S-HC was lower in CSF from people with RRMS compared to healthy controls, irrespective of whether they were experiencing a relapse or not at the time of sample collection (p=0.027). No difference was reported in CSF 26-HC levels; however, 26-HC was found to be significantly reduced in the serum of RRMS patients compared to healthy controls (p=0.044). No changes were reported for 24S-HC serum concentrations (Novakova et al., 2015).

My results showed that there was a decrease of both 24S-HC and 26-HC in MS WM compared to the WM of control brain. As both sterols are shuttled from the brain to the periphery (Meaney et al., 2002; Björkhem et al., 2004; Heverin et al., 2005; Björkhem, 2006), it's reasonable to assume that a lower brain concentration could result in lower peripheral concentrations, as less material is present to be removed. In addition to Novakova *et al*'s study, Crick *et al* have measured and reported a number of sterols which differ in the CSF and plasma from people with RRMS (n=17);

importantly, Crick *et al* utilised EADSA-LC-*MS* (Crick et al., 2017). They reported that 25-HC and 26-HC are reduced in RRMS plasma compared to control plasma (25-HC: $p<0.01$; 26-HC: $p<0.05$). Mine and Novakova *et al*'s study also found a reduction of 26-HC, although this was measured in different biological mediums, brain tissue and serum respectively. In the current study, a difference in 25-HC in human MS brain tissue compared to controls was not found. However, the sample size is small, and there is a need for the results to be validated in a larger cohort. Alternatively, 25-HC brain concentration may not correlate proportionally to circulating 25-HC in MS.

Crick *et al* and Novakova *et al* have reported differing results for 26-HC CSF concentrations. Crick *et al* reported an elevation in RRMS compared to controls ($p<0.05$), whereas Novakova *et al* reported no significant change. The lack of consensus could be due to the differing methodology used by the groups, or alternatively due to the large heterogeneity of RRMS and the reasonably small sample sizes used (Crick, RRMS=17; Novakova, RRMS=31). The decrease of 26-HC identified in this work in MS WM could relate to the sample size, or alternatively, 26-HC brain concentration may not be directly proportional to CSF-circulating 26-HC. Additionally, brain samples used in this study were from people who had had long-standing, progressive disease, as opposed to RRMS.

It will be important to understand the regional and tissue specific changes of these sterols in the brain and how changes in the MS brain may relate to changes within the periphery. Understanding the brain-effect of differences will be key to understanding the utility of any potential blood/CSF biomarkers. It is of note that this study was carried out on people who had progressive disease, whereas Novakova *et al* and Crick *et al's* studies were carried out on people with relapse remitting disease – as the neuro-environment differs between people with RRMS and progressive MS (Barnett and Prineas, 2004; Choi et al., 2012; Filippi et al., 2020; Jäckle et al., 2020) these results are not fully comparable. However, as the majority of the people with RRMS go on to develop progressive disease, work into oxysterols in both RRMS and

progression will be essential to furthering our understanding of MS and also our understanding of potential targets for treatment (Cree et al., 2021).

2.5 Limitations

The work presented in this chapter has shown that low abundance oxysterols can be identified and quantified in MS brain tissue homogenates, and that several sterols are at lower concentrations in MS WM compared to control WM, however, there are a number of limitations to this work which need to be addressed.

Firstly, the histological classification of samples, preparation, and measurement technique used (EADSA-LC-*MS*) is time consuming. EADSA sample preparation for oxysterols and cholesterol takes 3 days, plus the time taken to run samples using LC-*MS* (17-39 minutes per injection, per sample, with numerous injections used per sample to cover the array of masses which differing oxysterols localise at). Additionally, the analysis of cholesterol metabolites itself has limitations in terms of potential autoxidation, which has to be carefully managed to allow results to be trustworthy.

The analysis of sterols is based on the ability of the researcher to recognise fragmentation patterns and identify the correct corresponding sterol. Potential error arising from this was mitigated through training to ensure that my identification of sterols had a high inter-rater reliability with more experienced lab group members.

As this method is fairly low throughput, this study has only included a low number of cases. Consequently, the results are likely to be underpowered to determine statistical significance. Despite this, it has been shown that there is a difference between the concentration of a number of sterols, suggesting robust differences between MS and control brain tissue. However, these results will need to be validated in a larger cohort.

The extraction method for oxysterols and cholesterol differed between control and MS cases. During the completion of this thesis, a more efficient method of tissue homogenisation (mechanical homogenisation using Precellys tubes) was developed

by another student, Lauren Griffiths. This was deemed better practise than manual homogenisation, which was the method used to homogenise the control tissue. Due to its rarity and how precious control tissue is, in addition to the extensive time taken to extract and quantify sterols within tissue, the choice was made not to repeat sterol identification and quantification of the control tissue using mechanical homogenisation. Although the use of slightly different methodology between MS and control tissue cases is a limitation, the addition of iSTDs during the homogenisation step at least somewhat mitigates the risk of the methodology confounding the results, because the sterols within the tissue were normalised to the iSTDs prior to comparison between MS and controls. Therefore, the results presented in this pilot study still suggest that it is worthwhile repeating this in a larger cohort, however it would be optimal to use the same methodology throughout in future.

Macrodissection is a well-used technique and has been used by others to generate reproducible and useful results, however, tissue collected in this way can only be defined as 'enriched' for the tissue type of interest. It is possible that unintended GM or WM may have been collected as part of a sample, potentially confounding the results. In addition, this approach lacks the ability to correlate oxysterol content/concentration to pathologically defined regions. Adoption of this bulk approach of WM versus GM for analysis of human brain tissue was chosen because EADSA-LC-*MS* is a novel technique and therefore what to expect from the results was unknown. Although it would have been possible to only include NAWM/NAGM-enriched MS tissue differences may have been missed if oxysterol concentrations only differed in regions of MS pathology. This bulk approach successfully showed that it is worth further, more region-specific investigation. To further our understanding of where, and if certain pathology affects or is affected by oxysterols, it will be crucial to collect differing pathological regions as distinct sample types.

2.6 Conclusion

In this chapter it was demonstrated that low abundance oxysterols are both identifiable and quantifiable in human brain tissue, using Griffiths-Wang's EADSA-LC-*MS* technology. Importantly, it was demonstrated that a number of sterols differ

between MS and control brains. This suggests that alterations in oxysterol concentration may contribute to MS and therefore it is justifiable, and feasible, to conduct a larger, more systematic investigation of sterols in MS tissue. The major limitations of this work are the small sample size and lack of MS pathological specificity. I will interrogate the more precise location and abundance of sterols and relate the findings to detailed quantitative neuropathological assessments in the following chapters.

Chapter 3 – Quantification of Oxysterol Abundance in Pathological Regions of the Multiple Sclerosis Brain

3.1 Introduction

Having found evidence of cholesterol metabolism dysregulation in gross MS WM, investigations of the association between cholesterol and oxysterol abundance in actively demyelinating regions of the MS brain, to identify those enzymes and metabolites most associated with disease pathology, were carried out.

3.1.1 – Demyelination within the MS Brain

MS lesions can be classified based on their location within the brain, and also by the extent/pattern of inflammation. Pathological assessments and MRI have shown that WML types and their relative frequency evolve throughout disease and reflect the clinical outcome (Frischer et al., 2009).

The earliest stage of demyelination that is recognised in the central WM is the active lesion. Active WM lesions are most prevalent in people with a short disease duration or in those in the early relapse remitting stage (Brück et al., 1995; Lassmann et al., 1998; Barnett and Prineas, 2004; Frischer et al., 2015). They are also present in people with progressive disease, although their frequency declines with disease duration and age (Frischer et al., 2015). Active WMLs are hypercellular, characterised by a dense infiltration of microglia/macrophage-like cells, with a high proportion of foamy macrophages throughout the site of demyelination (Kuhlmann et al., 2017).

Additionally, a low number of T cells are found to localise around blood vessels and astroglial activation is marked (Popescu et al., 2013; Kuhlmann et al., 2017; Reich et al., 2018). Active lesions can be further separated into active and demyelinating lesions or active and post-demyelinating lesions based on the relative presence of myelin products within the macrophage-like cell after phagocytosis of myelin. Active and demyelinating lesions can be further sub-defined as early- or late-active lesions. Early active WMLs contain minor myelin protein degradation products, such as MOG+/MAG+ as inclusions, in addition to major myelin protein degradation products (PLP+) and lipids (LFB+). Active and demyelinating lesions which only contain major myelin degradation product inclusions, but lack minor myelin-proteins, are deemed late active and demyelinating lesions. Active and post-demyelinating WMLs are dense with foamy (lipid-laden) macrophages (see figure 3.4 cii and dii), which do not contain myelin debris; suggesting the initial wave of demyelination was complete prior to tissue sampling (Lucchinetti et al., 2000; Kuhlmann et al., 2017).

Some active lesions continue to enlarge and may become chronic active lesions. Chronic active or MA/I lesions (also defined as slowly expanding or smouldering lesions by others) have been correlated with increased disease progression and a worse MS-prognosis (Frischer et al., 2015; Absinta et al., 2019). Unlike the active lesions described above, this lesion type is more likely to be observed later in disease, typically after 10 years of disease duration. MA/I lesions are larger than active lesions and are characterised by a hypocellular lesion centre, with a rim of activated microglia/macrophage-like cells. The rim of MA/I lesions is highly heterogenous in terms of thickness and presence/absence of myelin degradation products in the microglia/macrophage-like cells. Like active lesions, the foamy macrophages lining the lesion may contain both early and late products of myelin breakdown (hence lesion classified as MA/I and demyelinating) or lack any evidence of recent myelin phagocytosis (and be termed MA/I and post-demyelinating). MA/I and post-demyelinating lesions may represent a later or less inflammatory stage of the evolving WML (Prineas et al., 2001; Frischer et al., 2009; Frischer et al., 2015; Kuhlmann et al., 2017; Elliott et al., 2019).

Lesions with little to no overt inflammatory cells are termed inactive (or silent) lesions. These lesions are hypocellular in their core, with few or no immune infiltrates throughout the lesion and microglia/macrophage-like cells at the border that are present at a density that is essentially no different to that seen in the peri-lesional and nearby NAWM (Kuhlmann et al., 2017). They contain hallmarks of seemingly irreversible neurodegeneration, such as axonal loss and astroglia scarring. Inactive lesions are most prevalent in long standing, progressive disease (Hametner et al., 2013; Frischer et al., 2015; Kuhlmann et al., 2017; Carassiti et al., 2018).

In comparison to WML, GML have been shown to link more closely with the clinical experience of MS; with increased lesion load correlating to increased disability (Calabrese et al., 2007; Calabrese et al., 2010; Calabrese et al., 2012; Honce, 2013; Bevan et al., 2018). However, the study of GML *in vivo* is currently challenging. Current MRI technology, suitable for clinical use, is unable to accurately identify all GM demyelination, therefore limiting their current usefulness for disease monitoring. In contrast, the majority of WML can be visualised quite effectively by standard clinical-grade MRI (Filippi et al., 2019).

In the present study efforts were focused on unpicking the changes in cholesterol metabolism in actively demyelinating WMLs (active and MA/I WML). The WM is most enriched in cholesterol and its metabolites; additionally, actively demyelinating WMLs are better resolved by MRI than GML. These lesions represent a frequently observed and dynamic site of ongoing tissue damage that is closely linked to ongoing and future measures of disease outcome (Absinta *et al.*, 2019).

3.1.2 – Myelin Debris Clearance by Macrophage-like Cells may be Damaging in the Chronically Inflamed MS Brain

Actively demyelinating lesions are dense with microglia/macrophage-like cells, either throughout the lesion or at the expanding edge (Kuhlmann et al., 2017). The action of these cells in clearing myelin debris is pro-reparative, as myelin debris must be cleared to allow efficient remyelination to take place (Lampron et al., 2015). However, work from Bogie and Hendriks has shown that foamy macrophages

(identified by an excessive lipid burden, determined using histological stains such as oil red O that stains esterified cholesterol and other lipids) can be damaging in MS and its models (Grajchen et al., 2018; Bogie et al., 2020). In the aged and chronically inflamed CNS, macrophage-like cells can lose their ability to effectively phagocytose debris, and instead can over accumulate lipids, such as cholesterol. A phenotypic-shift to a lesion-promoting and inflammatory macrophage phenotype of those cells enriched with stored lipids has been shown to be controlled by stearoyl-COA desaturase-1 (SCD1), an enzyme involved in the desaturation of fatty acids. Monosaturated fatty acid production has been shown to reduce the abundance of the cholesterol efflux transporter ABCA1, resulting in increased lipid and cholesterol accumulation, which is detrimental to the cell and can lead to a maladaptive immune response, including inflammasome activation, in the host (Cantuti-Castelvetri et al., 2018; Bogie et al., 2020). The abundance of cholesterol and its metabolites, and processes of cholesterol metabolism and flux, have not been systematically investigated in demyelinating MS lesions.

3.1.3 – Cholesterol Metabolism in the Human Brain

All cholesterol in the brain is synthesised by neurons and astrocytes. Neurons synthesise cholesterol via the Kandutsch-Russel pathway from the precursors lanosterol, 7-dehydrocholesterol and lathosterol; whereas astrocytes synthesise cholesterol via the Bloch pathway using the precursor desmosterol. Cholesterol synthesis via astrocytes is more efficient than by neurons, with neurons still relying on exogenous cholesterol supplies (see figures 1.3 and 1.4. (Nieweg et al., 2009; Zhang and Liu, 2015).

Regulation of cholesterol homeostasis within the CNS is imperative for healthy brain development and function. Neuronal cells are particularly sensitive to both a lack of, or an excess of, cholesterol and regulate their supply via a feedback mechanism to regulate cholesterol synthesis, import or removal (Ko et al., 2005; Pooler et al., 2006; Zhang and Liu, 2015). Cells continuously monitor their cholesterol concentrations via SREBPs, which regulate the transcription, and subsequent translation, of cholesterol biosynthesis/export-related regulators to maintain homeostasis (Brown and

Goldstein, 1999; Nohturfft et al., 2000). For example, when cholesterol levels reach their maximum cellular limit, excess cholesterol is either transported out of the brain to the periphery, or is esterified and stored as lipid droplets (Bryleva et al., 2010). Lipid droplet formation is facilitated by the esterification of cholesterol by acyl-coenzyme A: cholesterol acyltransferase 1 (ACAT1/SOAT1) (Melton et al., 2019). Excess cholesterol that is not stored, can be converted to oxidised products, oxysterols, whilst the excessive accumulation of stored lipids or the failure to remove excessive lipids, is associated with cellular dysfunction and pathology (e.g., the accumulation of pro-inflammatory, lipid-laden macrophages in the atherosclerotic plaque) (Moore et al., 2013).

Unlike cholesterol itself, oxysterols are able to exit the brain via the lipophilic BBB (Meaney et al., 2002). The major oxysterol of the brain, 24S-HC, is the main oxysterol which facilitates cholesterol efflux. 24S-HC is synthesised via the action of 24-hydroxylase, encoded by *CYP46A1* – which is predominately expressed by neurons (Lutjohann et al., 1996; Lund et al., 1999; Lund et al., 2003). 24S-HC also activates nuclear transcription factors, such as liver X receptors (LXR)-α and LXR-β via ligand-receptor binding, which in turn mediates the transcription of genes for – and subsequent translation of – cholesterol transporters, such as ABCA1 and APOE; increasing cholesterol export from both neuronal and glial cells (Fukumoto et al., 2002; Tall, 2008; Matsuda et al., 2013). Of note, the expression of *CYP46A1* is reduced in a number of neurodegenerative diseases, including Alzheimer's and Huntington's, and there is now much interest in modulating *CYP46A1* and 24-HC synthesis, for patient benefit (van der Kant et al., 2019).

3.1.4 – The Role of Oxysterols in the Brain

24S-HC is important for cholesterol export from both cells and the brain through LXR activation. 24S-HC regulation is also vital for neuronal cell health – removal of cholesterol, via conversion to 24S-HC, prevents a toxic build-up of cholesterol in neurons (Feringa and van der Kant, 2021). In addition to 24S-HC, other metabolites of cholesterol also act as ligands in a variety of signalling pathways, some of which are pertinent to MS, including myelination, inflammation and neuron survival (Duc et

al., 2019). For example, another LXR ligand is 25-HC, synthesised by macrophages, via cholesterol 25-hydroxylase (encoded by *CH25H*) (Liu et al., 2018). 25-HC has been shown to be reduced in RRMS patient plasma (Crick et al., 2017). Crick *et al* suggest that RRMS patient macrophages have a reduced capacity to synthesise 25-HC. 25-HC is a mediator of negative feedback to IL-1 cytokine-mediated inflammation. Therefore, a reduction of 25-HC in RRMS, as reported by Crick *et al*, may result in increased inflammation, driven by macrophages (Reboldi et al., 2014). The abundance of 25-HC in the MS brain has not been investigated.

Another oxysterol which may have relevance in MS-associated pathways is 26-HC. 26-HC is synthesised from cholesterol by the enzyme 27-hydroxylase (and is why 26-HC is often termed 27-HC by others), which is encoded by *CYP27A1*, a fairly ubiquitously expressed transcript (Javitt, 2002). 26-HC is a selective oestrogen receptor modulator (SERM) for oestrogen receptor β (Jeitner et al., 2011; Mast et al., 2015). Activation of oestrogen receptors, present on oligodendrocytes, are associated with differentiation and myelination capability of oligodendrocyte lineage cells (Khalaj et al., 2016). Compounds that can selectively bind to these oligodendrocyte-oestrogen receptors may permit oligodendrocyte precursor cell differentiation and aid remyelination efforts. Additionally, 26-HC may act alongside 24S-HC/25-HC as an LXR ligand, again promoting the synthesis of cholesterol efflux transporters (Fukumoto et al., 2002; Jeitner et al., 2011).

26-HC can be further metabolised to 7α, 26-diHC, by 27-hydroxylase. 7α,26-diHC may be implicated in RAR-related orphan receptor gamma t (RoRγ-t) signalling and EBI2 activation. 7α,26-diHC is an agonist ligand for RORγ-t; its binding elicits transcription/translation of gene products required for $CD4^+$ Th17 cell regulation (Soroosh et al., 2014). Pathogenic Th17 cells are important in MS risk and severity (Solt et al., 2011; Sonar and Lal, 2017). In addition, 7α,26-diHC has been identified as an EBI2 ligand, (Liu et al., 2011) which is a receptor involved in the directed migration of B cells into germinal follicles and secondary lymphoid organs (Pereira et al., 2010). B cell follicle-like structures form in the CNS of some people with MS, and their

presence has been shown to correlate with a more severe disease course (Magliozzi et al., 2007; Magliozzi et al., 2010; Howell et al., 2011; Bevan et al., 2018).

3.1.5 – Chapter Aims

Differences in the abundance of some sterols in WM of the MS brain, compared to the non-MS brain, have been confirmed in this work. Next, sterol abundance in different pathological regions of the brain, such as areas of actively demyelinating WMLs, will be explored, to assess if these differences correlate to such important pathological hallmarks of MS disease severity. Additionally, cellular expression of cholesterol metabolism related mechanisms and alterations in lipid storage at these sites of recently ongoing tissue destruction will be scrutinised to gain further biological insight.

3.2 Methods

3.2.1 – Identification and Characterisation of MS Pathology

3.2.1.1 – Shortlisting of MS Tissue Cases for Sterol Analysis Based on the Presence/Absence of Actively Demyelinating White Matter Lesions

Tissue sections were immunologically/histologically stained as described in 2.2.3.1 with markers for myelin (anti-MOG, anti-PLP, LFB), microglia/macrophage-like cells (anti-HLA-DR, anti-IBA1, anti-TMEM119), cholesterol biosynthesis related enzymes (CYP27A1, CYP46A1), neurons (anti-HuC-D) and perilipin-2+ (PLN2+) lipid droplets and oil red O (ORO+) to identify esterified-cholesterol rich droplets (table 3.1).

MA/I WML (Kuhlmann et al., 2017) were characterised by a rim of HLA-DR+ microglia/macrophage-like cells that had evidence of recently phagocytosed myelin debris (figure 3.1), with few immune cells at the centre of the lesion. Active lesions were characterised by an increased number of actively demyelinating microglia/macrophage-like cells in the centre of the lesion, compared to the surrounding normal appearing tissue. Lesions containing very few/no microglia/macrophage-like cells within the lesion were classified as inactive lesions (Kuhlmann et al., 2017). MS tissue blocks containing at least one WML with evidence of actively demyelinating tissue (MA/I/active WML) were shortlisted for further

characterisation and analysis. Although the presence of a WML was the focus, GM present within the shortlisted tissue blocks was also characterised. The lesions of the cortex were categorised according to well established criteria by Kuhlmann and Bø (Bø et al., 2003; Kuhlmann et al., 2017). See figure 3.7 – characterising extensive and variable demyelination of GM.

Table 3.1 – Primary and Secondary Antibodies

Antigen	Target	Host Species	Working Concentration (µg/ml)	Supplier	Product Code	Monoclonal or Polyclonal
CYP27A1	27-Hydroxylase	Rabbit	0.5	Abcam	ab227248	Polyclonal
CYP46A1	24-Hydroxylase	Mouse	2	Abcam	ab244241	Monoclonal
HLA-DR	Microglia/ macrophages	Mouse	1	Dako	F081701-2	Monoclonal
HuC-D	Neurons	Mouse	0.20	Fisher Scientific	MABN153	Monoclonal
IBA1	Microglia/ macrophages	Rabbit	0.20	Fujifilm	019-19741	Polyclonal
MOG	Myelin oligodendrocyte glycoprotein	Mouse	Stock conc., unknown 1 in 20 dilution.	Imperial College London (Prof. Reynolds)	-	Monoclonal
Perilipin-2	Lipid droplets	Rabbit	0.5	Merck	HPA016607	Polyclonal
PLP	Microglia/ macrophages	Mouse	0.20	BioRad	MCA839G	Monoclonal
TMEM119	Resident microglia	Rabbit	0.25	Merck	PA5-62505	Polyclonal
Secondary Antibody Fluorophore	**Target Species**	**Host Species**	**Working Concentration (µg/ml)**	**Supplier**	**Product Code**	**Monoclonal or Polyclonal**
Alexa Fluor-488	Mouse	Goat	3	Fisher Scientific	15607878	Polyclonal
Alexa Fluor-594	Rabbit	Donkey	3	Fisher Scientific	10798994	Polyclonal
Goat anti-mouse biotin	Mouse	Goat	3	Vector	BA-9200	Polyclonal

3.2.1.2 – Tissue Demographics of Shortlisted Cases

Eight MS tissue blocks (from the frontal lobe, temporal lobe or cingulate gyrus) from 7 MS cases (male=3), and 5 tissue blocks (from the superior frontal gyrus) from age/gender, and where possible, brain region, matched controls (males=3), without history of neurological conditions, were prepared for sterol analysis and quantitative neuropathological assessments. Case demographics can be seen in table 3.2.

Table 3.2 – MS and Control Case Demographics

PMD = postmortem delay. Time progressive = number of years with a progressive disease diagnosis. Time wheelchair = number of years spent using a wheelchair. N/A = not applicable.

Case Number	Sex	Age	PMD (hours)	Cause of Death	Brain Weight (g)	MS Subtype	Disease Duration (years)	Time Progressive (years)	Time Wheelchair (years)
MS402	Male	46	12	Bronchopneumonia, MS	1246	SPMS	20	9	7
MS407	Female	44	22	Septicaemia, pneumonia	1230	SPMS	19	11	10
MS438	Female	53	17	MS	1106	SPMS	18	Unknown	4
MS461	Male	43	13	Bronchopneumonia	1116	SPMS	21	12	12
MS473	Female	39	9	Bronchopneumonia, MS	1177	PPMS	13	10	6
MS513	Male	51	17	Respiratory failure, MS	1033	SPMS	18	15	14
MS541	Female	67	Unknown	Unknown	Unknown	SPMS	49	17	13
NP13/011	Female	62	24	Metastatic Colorectal Cancer	1261	N/A	N/A	N/A	N/A
NP13/012	Female	60	48	Metastatic Breast Cancer	1423	N/A	N/A	N/A	N/A
NP13/126	Male	56	40	Cardiac Arrest	1456	N/A	N/A	N/A	N/A
NP13/127	Male	60	30	Cardiac Arrest	1168	N/A	N/A	N/A	N/A
NP13/128	Male	68	48	Cardiac Arrest	1311	N/A	N/A	N/A	N/A

3.2.2 – Quantifying the Extent of White and Grey Matter Demyelination

White and grey matter lesions were stained and characterised as described in 3.2.1.1. Stained tissue sections were digitised (ZEISS Axio Scanner (AxioScan. Z1)). The resulting .czi files were annotated and managed with QuPath version 0.3.2 (Bankhead et al., 2017). The area of MA/I WML, active lesions, NAWM, GML (type i, type ii, type iii, type iv and deep GM) and NAGM was calculated.

The presence of actively demyelinating lesions was determined by the presence of LFB+, PLP+ and MOG+ inclusions. Co-localisation of HLA+ macroglia/macrophage-like cells with LFB, or IBA1+ microglia/macrophage-like cells with either MOG+ or PLP+ staining indicated the presence of an inclusion.

3.2.2.1 – Immunofluorescence

Tissue sections were fixed for 1 hour with 4% PFA, immediately after thawing. The sections were then washed once with PBS. For dual staining: epitope sites were blocked with 10% normal serum from an appropriate species, diluted in PBS-T. The tissue was then incubated with the appropriate concentration of primary antibody, diluted in PBS-T, overnight. Following PBS washes, the primary antibody was detected using an appropriate secondary antibody conjugated to a fluorophore for 1 hour. Following PBS washes, epitope sites were blocked with 10% normal serum from an appropriate species, diluted in PBS-T for 30 minutes. The tissue was then incubated with a second primary antibody, from an appropriate species, overnight. The sections were washed with PBS and incubated with a species specific biotinylated secondary antibody for 1 hour and washed with PBS. The secondary antibody was detected using a streptavidin (SAV) conjugated fluorophore. Finally, nuclei were visualised with 1 µg/ml 4',6-diamidino-2-phenylindole (DAPI), diluted in PBS-T, for 20 minutes. The tissue was incubated for 5 minutes with Sudan Black (Merck) to quench autofluorescence and rinsed with H_2O, before mounting with VectaMount H-5000. Images were captured using a Zeiss AxioScope1 microscope and Zeiss AcioCam black and white camera using the ZEN software suite (Carl Zeiss Ltd.). Details of the primary and secondary antibodies used can be found in table 3.1.

3.2.3 – Measurement of Sterols in Pathologically Distinct Regions of Interest within the Human MS Brain

3.2.3.1 – Macrodissection of Tissue for Sterol Analysis

Distinct areas of MS pathology and matched control tissue regions of interest (ROI), including NAWM, the MA/I lesion edge (high microglia/macrophage-like cell load), the MA/I lesion centre (low microglia/macrophage-like cell load), active WML, control WM, NAGM, GML and control GM were manually macrodissected using a scalpel to score the tissue block ROIs before sectioning on a cryostat to collect the separate portions of tissue, until >2 mg of ROI-enriched fractions were collected into Precellys tubes. Macrodissection was carried out as described in 2.2.2.1, and was guided using a combination of LFB, anti-HLA and anti-MOG-stained sections to identify each ROI (figures 3.1 and 3.7).

3.2.3.2 – Enzyme-Assisted Derivatisation for Sterol Analysis – Liquid Chromatography – Mass Spectrometry

Sterols were prepared for EADSA-LC-*MS* in Precellys tubes as previously described in 2.2.2.3. Sterol separation, quantification and analysis was carried out as described in 2.2.2.4 and 2.2.2.5.

3.2.4 – Quantification of Lipid Storage

3.2.4.1 – Quantification of Lipid Storage within Microglia/Macrophage-like Cells

The lipid-burden of WM and GM ROI were quantified using immunohistochemical co-staining for PLN2+ and HLA+ macrophage-like cells, or the presence of ORO+ esterified-cholesterol (table 3.1).

For anti-HLA and anti-PLN2: Cryosections were PFA fixed, quenched with a solution of hydrogen peroxide and blocked with normal horse serum prior to addition of the anti-HLA primary antibody. A biotinylated horse anti-mouse secondary antibody was then followed by the addition of the peroxidase-linked avidin-biotin complex (ABC Elite, Vector Laboratories Ltd.) and visualised with Immpact DAB (Vector Laboratories Ltd.) as the chromogen. Following PBS washing, and additional serum blocking, slides were incubated with anti-PLN2 antisera and detected with the one-step (avidin-

biotin free) ImmPRESS Alkaline Phosphatase Horse Anti-Rabbit IgG Polymer Detection Kit (Vectors Labs) with Vector Blue as the chromogen. Sections were then briefly rinsed in water before mounting (VectorMount).

ORO histology was carried out on thawed sections fixed with 4% PFA for 30 minutes and then washed with deionised water. Sections were then washed once with 60% isopropanol prior to incubation with filtered 0.5% ORO solution (Merck) for 20 minutes and then washed again with 60% isopropanol. Deionised water was used to removed excess stain until lipid droplets were clearly visible under the microscope. The sections were counterstained with filtered Gill's haematoxylin (Hx) and mounted with VectorMount.

The percentage area of HLA, PLN2 and ORO positive signal was calculated by colour deconvolution and thresholding using Fiji Image J version 2.3.0/1.53q. 5 snapshots per ROI were taken at 100X for measurement.

3.2.4.2 – Calculating the Percentage of Resident Microglia and Infiltrating Macrophages

After immunofluorescent staining for TMEM119 and HLA-DR, resident cells (TMEM119+, HLA+) and infiltrating and/or activated cells (HLA+, TMEM119-) were visualised using a Zeiss AxioScope microscope. Three representative snapshots were taken per ROI, per case. The number of co-labelled TMEM119+ and HLA+, and single labelled HLA+ cells were manually counted. The percentage of both TMEM119+/HLA+ and HLA+/TMEM119- cells were calculated as a proportion of the total cells counted per ROI.

3.2.5 – Quantification of Cholesterol Metabolism-Related Enzyme Transcripts

3.2.5.1 – In Situ Hybridisation

In situ hybridisation (ISH) was carried out using either RNAscope or BaseScope (ACD) following the manufacturer's instructions. This technique allows for specific on-tissue ISH – binding of 2, sequence specific, Z probes is required per target to permit the binding of amplifiers and chromogenic probes. The requirement of 2 Z probes to bind

RNA targets increases specificity and reduces background (Biotechne) (Wang et al., 2012).

Tissue sections were fixed with 4% PFA for 1 hour at RT, rinsed with water, dehydrated through a graded series of ethanol (50%, 70%, 100%) and dried for 15 minutes at RT followed by 15 minutes at 37°C. Peroxidase activity was quenched by incubating the sections in 0.06% hydrogen peroxide for 10 minutes at RT. Sections were washed in deionised water and then incubated with protease IV (ACD/Biotechne) for 20 minutes at RT. After washes with PBS, sections were incubated with the relevant probe, for 2 hours at 40°C in the HybEZ II oven (Biotechne). Table 3.3 contains details of the probes used, which were custom designed and validated by the manufacturer. The tissue sections were washed in 1X wash buffer (WB) and stored in 5X saline-sodium citrate (SSC) buffer overnight. Following washes with WB, sections were incubated with supplied Amp reagents (amplifier reagents; RNAscope 2.5 HD Detection Reagents-RED or Brown assays; kit #322360 or #322310 or Basescope detection reagents v2_red; #323910) and were washed with WB between each step. Amp temperatures and incubation times are listed in table 3.4 for RNAscope and BaseScope. Following the final amplification step and washes with WB, the sections were incubated with either DAB (50%-part A, 50%-part B) or Fast Red (1:60 dilution Fast Red part B into part A) chromogenic substrates to visualise mRNA puncta. Nuclei were visualised by incubating with freshly filtered Hx for 1-2 minutes. For tissue with puncta visualised with DAB, the sections were dehydrated through a graded series of ethanol (70%, 95%, 100%) and cleared in xylene prior to permanent mounting with DPX (Fisher Scientific). Tissue using the Fast Red detection system was air-dried for 5 minutes at RT followed by 25 minutes at 37°C before being mounted with VectaMount permanent mounting medium (Vector). Images were captured using the Zeiss AxioScope microscope and Zeiss 503 colour camera.

The percentage area of the generated mRNA puncta for *CYP46A1*, *CYP27A1* and *CH25H* was calculated using three representative snapshots per ROI, captured at 400X, per case using colour deconvolution and thresholding using Fiji Image J version

2.3.0/1.53q. After thresholding, the area of Fast Red (red channel) and Hx (blue channel) was calculated. The area of Fast Red was divided by the area of Hx to calculate the percentage of positive puncta, whilst also accounting for the differences in cell density that occur between MS and controls and between different areas of MS pathology.

3.2.5.2 – Immunostaining

Additionally, immunohistochemical staining, as described in 2.2.3.1, was carried out using anti-CYP46A1 and anti-CYP27A1, for the enzymes encoded for by *CYP46A1* and *CYP27A1*.

3.2.5.3 – Co-localisation of mRNA puncta and Neurons

Staining for *CYP46A1* mRNA puncta was carried out as described in 3.2.5.1, up to and including visualisation of puncta. Anti-HuC-D immunostaining was then carried out to detect co-localisation of *CYP46A1* and neurons. Sections were incubated with BLOXALL (Vector Ltd) for 10 minutes and blocked with 10% normal horse serum for 30 minutes. The primary antibody was then added and incubated overnight. After more washes with PBS, the sections were incubated with a biotinylated horse anti-mouse secondary antibody, for 1 hour. The sections were then incubated with the equilibrated avidin-biotin complex-alkaline phosphatase kit, following the manufacture's instructions (Vector Labs), for 1 hour. After washes with tris-buffered saline, the vector blue substrate (Vector Ltd) was used for colour development. The sections were then air-dried for 5 minutes at RT followed by 25 minutes at 37°C before being mounted with VectaMount permanent mounting medium (Vector Ltd). Images were captured using the Zeiss AxioScope microscope and Zeiss 503 colour camera. HuC-D information can be found in table 3.1.

Table 3.3 – In Situ Hybridisation Probes

Hs – homosapien. CYP46A1 - cytochrome P450 family 46 subfamily A member 1, CYP27A1 - cytochrome P450 family 27 subfamily A member 1, CH25H – cholesterol 25-hydrolase, ABCA1 – adenosine triphosphate-binding cassette A1, APOE – apolipoprotein E, SOAT1 – sterol O-acyltransferase 1.

Probe	System	Target	NCBI Reference	Target Species
Hs-CYP46A1	BaseScope	*CYP46A1*	NM_006668	Human
Hs-CYP27A1	RNAscope	*CYP27A1*	NM_000784	Human
Hs-CH25H	RNAscope	*CH25H*	NM_003956	Human
Hs-ABCA1	RNAscope	*ABCA1*	NM_005502	Human
Hs-APOE	RNAscope	*APOE*	NM_001302688	Human
Hs-SOAT1-C1	RNAscope	*SOAT1*	NM_003101	Human

Table 3.4 – Amplification Steps

System	Amp Number	Time (minutes)	Temperature (°C)
BaseScope	1	30	40
	2	30	40
	3	15	40
	4	30	40
	5	30	40
	6	15	40
	7	30	RT
	8	15	RT
RNAscope	1	30	40
	2	15	40
	3	30	40
	4	15	40
	5	30	RT
	6	15	RT

3.2.6 – Statistics

All statistical analysis was conducted using GraphPad Prism version 9.3.1. Due to small group sizes it could not be assumed that all samples were normally distributed, therefore, more conservative, non-parametric statistical testing procedures were employed throughout. Two-group comparisons were made by Mann Whitney testing with two-tailed distribution; greater than two-group comparisons were made by Kruskal-Wallis with Dunn's post-test. Values of <0.05 were considered significant.

3.3 Results

In this chapter MS brain tissue was separated into various regions of interest to assess which discrete areas of pathology best associate with the changes in cholesterol metabolism reported in homogenates of total MS grey and WM (chapter 2). The results of this chapter have been separated into first WM and then GM given the differences in lesion pathology and sterol abundance.

3.3.1 – Identifying and Characterising White Matter Pathology

MS cases which contained comparable, and clinically relevant, MS WM pathology were shortlisted as the principal interest was on mechanisms relating to lesion expansion. First, immunohistochemical staining was used to identify WMLs within the tissue cohort. Identified WMLs were then characterised as either active (A), MA/I or inactive. The focus was to profile ongoing actively demyelinating lesions (i.e those A or MA/I lesions), therefore, cases which had evidence of at least one A or MA/I lesion (figure 3.1) were shortlisted.

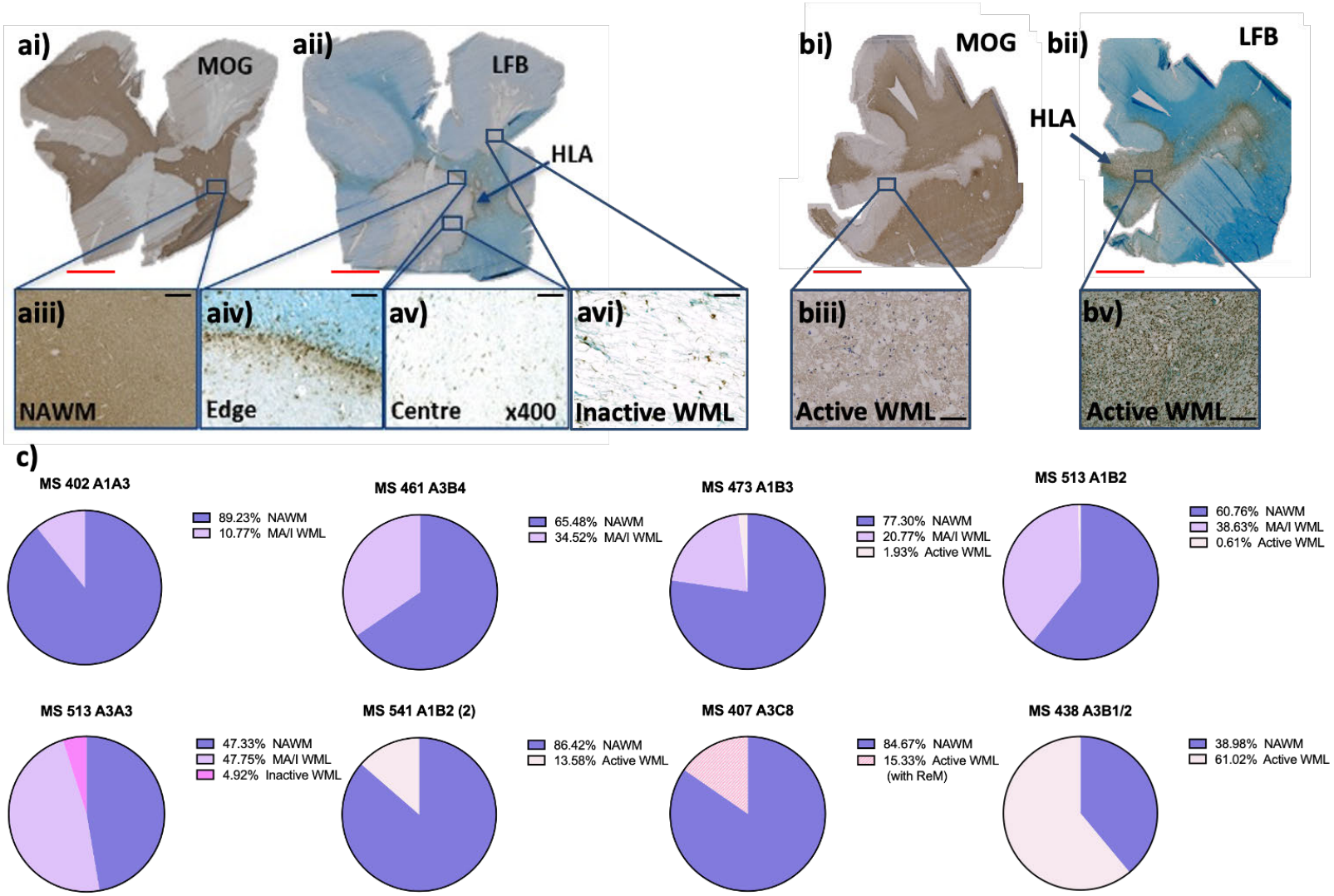
ai)
MOG
aii)
LFB
HLA
aiii)
NAWM
aiv)
Edge
av)
Centre
x400
avi)
Inactive WML
bi)
MOG
bii)
LFB
HLA
biii)
Active WML
bv)
Active WML
c)
MS 402 A1A3
89.23% NAWM
10.77% MA/I WML
MS 461 A3B4
65.48% NAWM
34.52% MA/I WML
MS 473 A1B3
77.30% NAWM
20.77% MA/I WML
1.93% Active WML
MS 513 A1B2
60.76% NAWM
38.63% MA/I WML
0.61% Active WML
MS 513 A3A3
47.33% NAWM
47.75% MA/I WML
4.92% Inactive WML
MS 541 A1B2 (2)
86.42% NAWM
13.58% Active WML
MS 407 A3C8
84.67% NAWM
15.33% Active WML
(with ReM)
MS 438 A3B1/2
38.98% NAWM
61.02% Active WML

Figure 3.1 – Characterising Extensive and Variable Demyelination of White Matter

Regions of NAWM and WMLs were identified by anti- MOG immunostaining and sub-categorised based on the presence and location of HLA+ microglia/macrophages (HLA/LFB stained sections). An example of a MA/I WML (a) - MOG (brown) with Hx counterstain (ai); LFB (blue) and HLA (brown), areas negative for LFB are lesions, cells positive for HLA rim the lesion (aii). A magnified image of NAWM (aiii), the lesion edge (aiv), lesion centre (av) and inactive WML (avi) can be seen. MS 513 A3A3 imaged (a). An example of an active WML (b) – MOG (brown) with Hx counterstain (bi); LFB (blue) and HLA (brown)-stained section, cells positive for HLA are seen within the lesions (bii) MS 473 A1B3 imaged (b). The relative area of WM demyelination of total WM was calculated per case following slide digitisation and QuPath assessment. Between all cases, n = 8, male = 3, the percentage of MA/I WML coverage ranged from 0-48% and active lesions ranged from 0-61% (c). MOG – myelin oligodendrocyte glycoprotein. LFB – luxol fast blue, HLA – human leukocyte antigen, NAWM – normal appearing white matter, WML – white matter lesion, MA/I – mixed active/inactive. Images captured using QuPath. Red scale bars = 0.50 cm, black scale bars = 100 μm.

Having shortlisted cases with suitable WM pathology, how homogenous the actively demyelinating lesions (A and MA/I) were in terms of their represention of early or late active demyelination was assessed. Demyelination can be time-stamped to a degree, based on the presence of minor (e.g. MOG) and major (e.g. PLP) myelin proteins and lipids (identified by LFB histology) contained within microglia/macrophage-like cells. LFB inclusions can be observed in phagocytes for around 1 month after phagocytosis, whereas PLP and MOG are degraded more quickly, at approximately 7 and 3-5 days, respectively (Lucchinetti et al., 2000; Kuhlmann et al., 2017). The presence of these inclusions was characterised to further detail the nature of the actively demyelinating lesions identified (figure 3.2).

Case	Lesion Type	Inclusion Summary
MS 402 A1A3	MA/I WML	LFB+, PLP+, MOG+
MS 407 A3C8	Re/DeM Active WML	LFB+, PLP+, MOG+
MS 461 A3B4 (1)	MA/I WML	LFB+, PLP+, MOG+
MS 473 A1B3	MA/I WML	LFB+, PLP+, MOG+
MS 513 A1B2	MA/I WML	LFB+, PLP+, MOG+
MS 513 A3A3	MA/I WML	LFB+, PLP+, MOG+
MS 541 A1B4 (2)	Active WML	LFB+, PLP+, MOG+

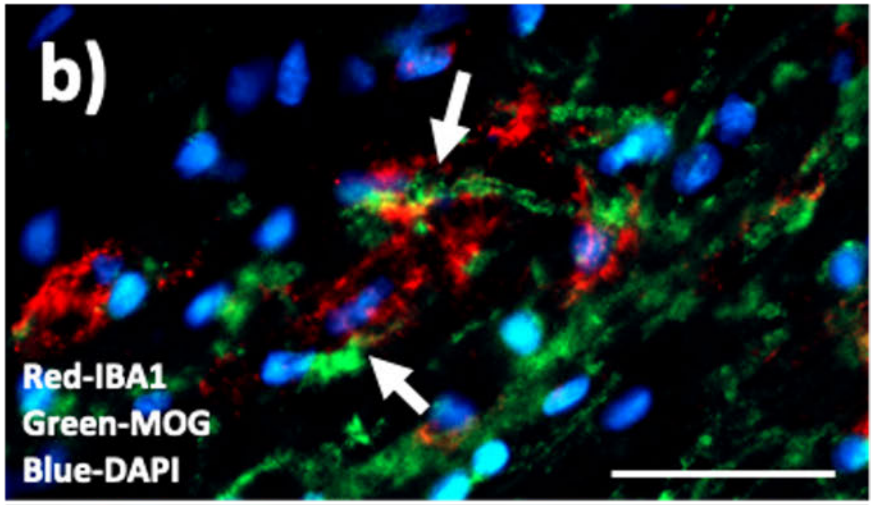

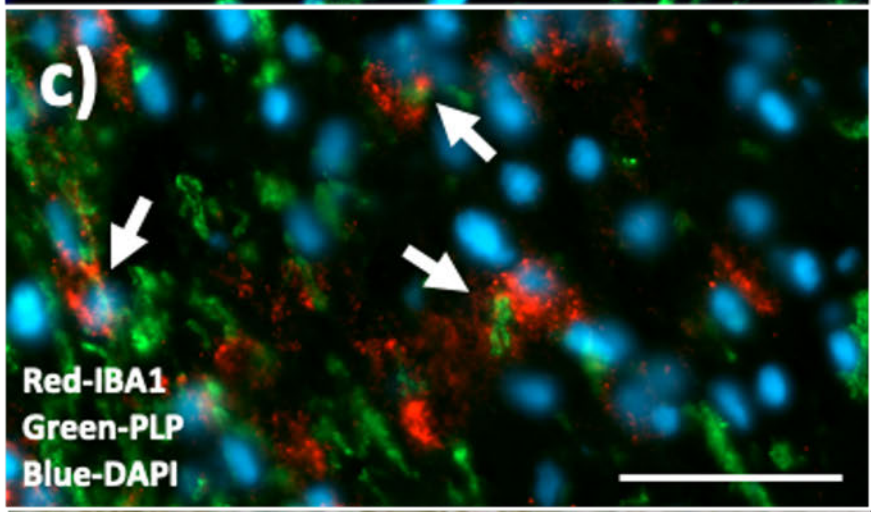

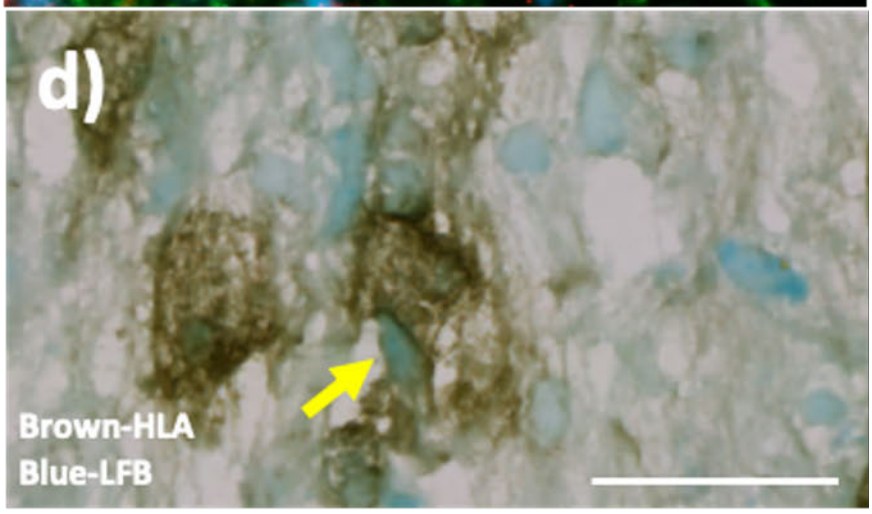

Figure 3.2 – Identifying Actively Demyelinating Lesions

The presence of microglia/macrophage-like cells positive for LFB+/PLP+/MOG+ inclusions were identified in shortlisted tissue blocks (a). Immunofluorochemistry for IBA1+ microglia/macrophage-like cells (red), MOG (green), DAPI nuclei (blue), arrows point to MOG inclusions (b). Immunofluorochemistry for IBA1+ microglia/macrophage-like cells (red), PLP (green), DAPI nuclei (blue), arrows point to PLP inclusions (c). Immunohistochemistry for HLA+ microglia/macrophage-like cells (brown) and LFB (myelin; blue), arrow points to an LFB inclusion (d). n = 8. Images captured using a Zeiss AxioScope microscope using either the Zeiss 503 colour camera (b and c) or AxioCam black and white camera (d). LFB – luxol fast blue, PLP – proteolipid protein, MOG – myelin oligodendrocyte glycoprotein. Representative images taken from MS 473 A1B3. Scale bars = 100 μm.

3.3.2 – Sterol Concentrations Differ Between Discrete Regions of MS WM Pathology

Having established that lesions present within the shortlisted blocks were comparable (by lesion type and activation stage), WM ROI were manually macrodissected for mass spectroscopy (see 3.2.3.1). MA/I WML lesions were separated into inactive centres and actively demyelinating edges, collecting tissue enriched for the MA/I WML edge, MA/I WML centre, active WML and NAWM. EADSA-LC-*MS* was then used to measure cholesterol, its precursors, and metabolites (figure 3.3). Four sterols differed in concentration between control WM and distinct regions of MS WM pathology: Cholesterol: control WM - 20.81±3.87 μg/mg (mean ± standard deviation), MA/I WML centre – 2.19±2.83 μg/mg; 24S-HC: control WM – 20.44±2.87 ng/mg, MA/I WML centre – 1.91±1.23 ng/mg, active WML – 1.47±0.59; 7β-HC: control WM – 0.32±0.11 ng/mg, MA/I WML centre – 0.10±0.06 ng/mg; 24R-HC: control WM – 0.20±0.06 ng/mg, MA/I WML centre – 0.01±0.01 ng/mg. In addition, 26-HC and 7-OC followed the same trend, but did not reach statistical significance (figure 3.3).

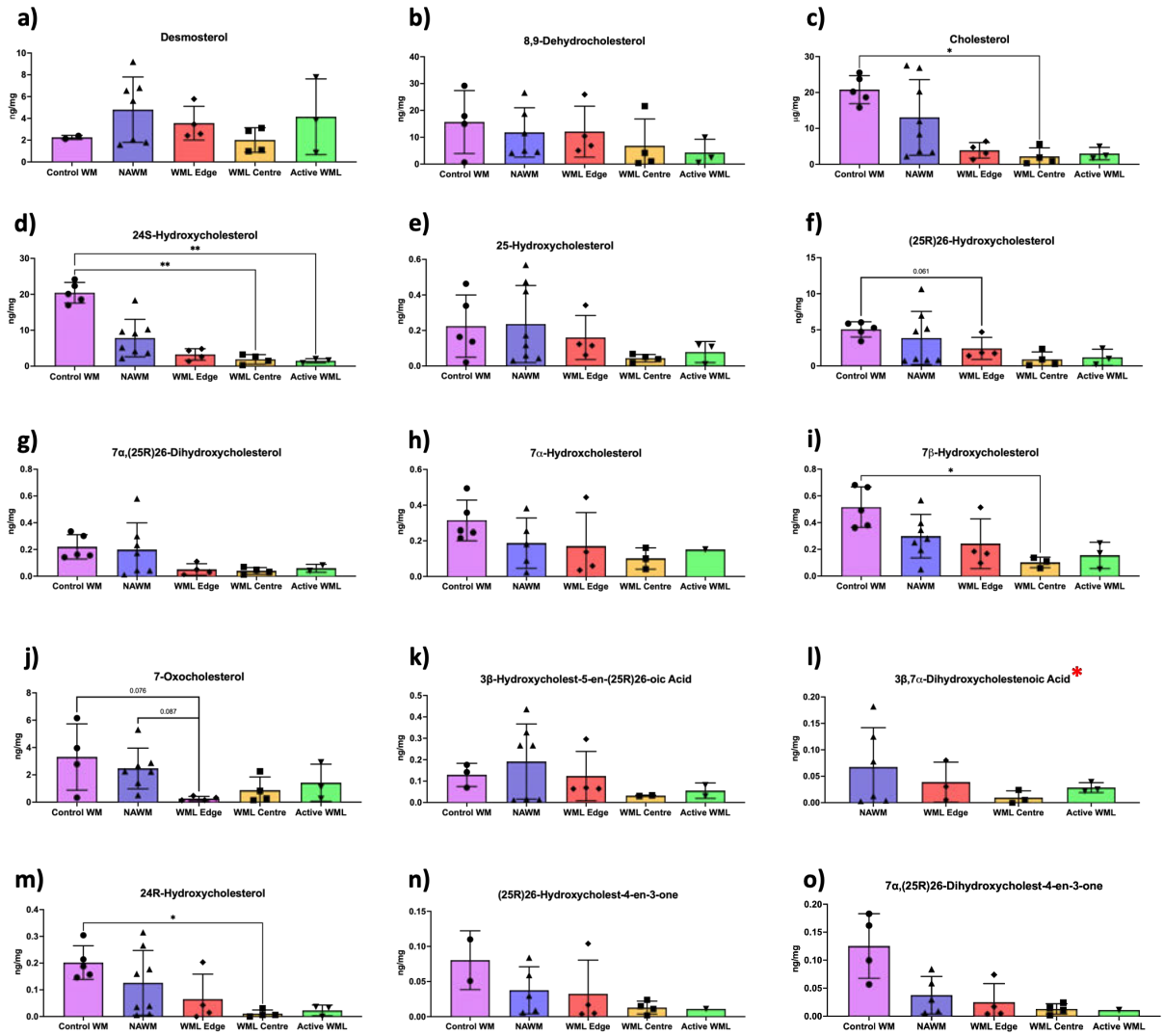

Figure 3.3 – Sterol Concentrations in Human Control White Matter and MS White Matter

The relative abundance of sterols in WM ROI-enriched homogenates from the brains of people with (n = 7) and without (n = 5) MS (a-o). Four sterols were significantly lower in MS WM pathological ROI compared to control WM – cholesterol (c), 24S-hydroxycholesterol (d), 7β-hydroxycholesterol (i) and 24R-hydroxycholesterol (m). Additionally, (25R)26-hydroxycholesterol (f) and 7-oxocholesterol (j) followed the same trend, but did not reach statistical significance. Kruskal-Wallis with Dunn's post-test, *p<0.05, **p<0.01,. Graphs show mean ± standard deviation. *Control WM under the limit of detection.

3.3.3 – Cholesterol Homeostasis is Altered in WM of the Human MS Brain

This work has provided evidence that cholesterol biosynthesis and metabolism is altered in distinct samples that represent WM pathological ROI of the MS brain. These ROI were further interrogated to investigate whether cholesterol storage is altered in WM ROI with altered cholesterol metabolism; more specifically whether lipid-storage was altered in microglia/macrophage-like cells in MS tissue.

Firstly, the proportion of HLA+ cells within the different ROI, was calculated, unsurprisingly the percentage of HLA-immunoreactivity was found to be increased at the MA/I WML edge and also within active WML compared to NAWM, MA/I WML centre and control WM. Control WM – 1.45±0.94% (mean ± standard deviation); NAWM – 3.52±6.50%; MA/I WML edge – 34.73±14.52%; MA/I WML centre – 1.46±0.99%; active WML – 28.95±20.50% (figure 3.4). Next, it was assessed whether there was a difference in the origin of the microglia/macrophages (infiltrating macrophages or resident microglia) by immunostaining for TMEM119 (widely expressed by homeostatic, resident microglia) and HLA-DR (expressed by both microglia and infiltrating macrophages) (Ruan and Elyaman, 2022). The number of resident cells (TMEM119+, HLA+) and infiltrating cells (HLA+, TMEM119-) were counted - there was an increased number of infiltrating macrophages at the MA/I WML edge, compared to the MA/I WML centre, active WML and NAWM; additionally, there was a higher number of infiltrating cells compared to resident cells at the MA/I WML edge. Resident cells: NAWM – 14.04±8.16%; MA/I WML edge – 5.18±2.46%; MA/I WML centre – 0.23%; active WML – 4.92±0.45%. Infiltrating cells: NAWM – 3.82±2.81%; MA/I WML edge – 22.41±6.95%; MA/I WML centre – 3.28±2.03%; active WML – 5.87±2.39% (figure 3.4). Additionally, the percentage immunoreactivity of ORO (esterified cholesterol and other hydrophobic lipids) and PLN2 (lipid droplets) was measured. ORO was found to be increased in the MA/I WML edge compared to NAWM, the MA/I WML centre and active WML, whereas it was found to be decreased in NAWM, the MA/I WML centre and active WML compared to control WM. Control WM – 1.56±1.02%; NAWM – 0.61±0.68%; MA/I WML edge 3.59±1.46%; MA/I WML centre 0.54±0.38%; active WML 0.18±0.22%. PLN2 storage

was found to be reduced in the MA/I WML centre compared to the edge. MA/I WML edge – 0.41±0.33%; MA/I WML centre – 0.11±0.19% (figure 3.4).

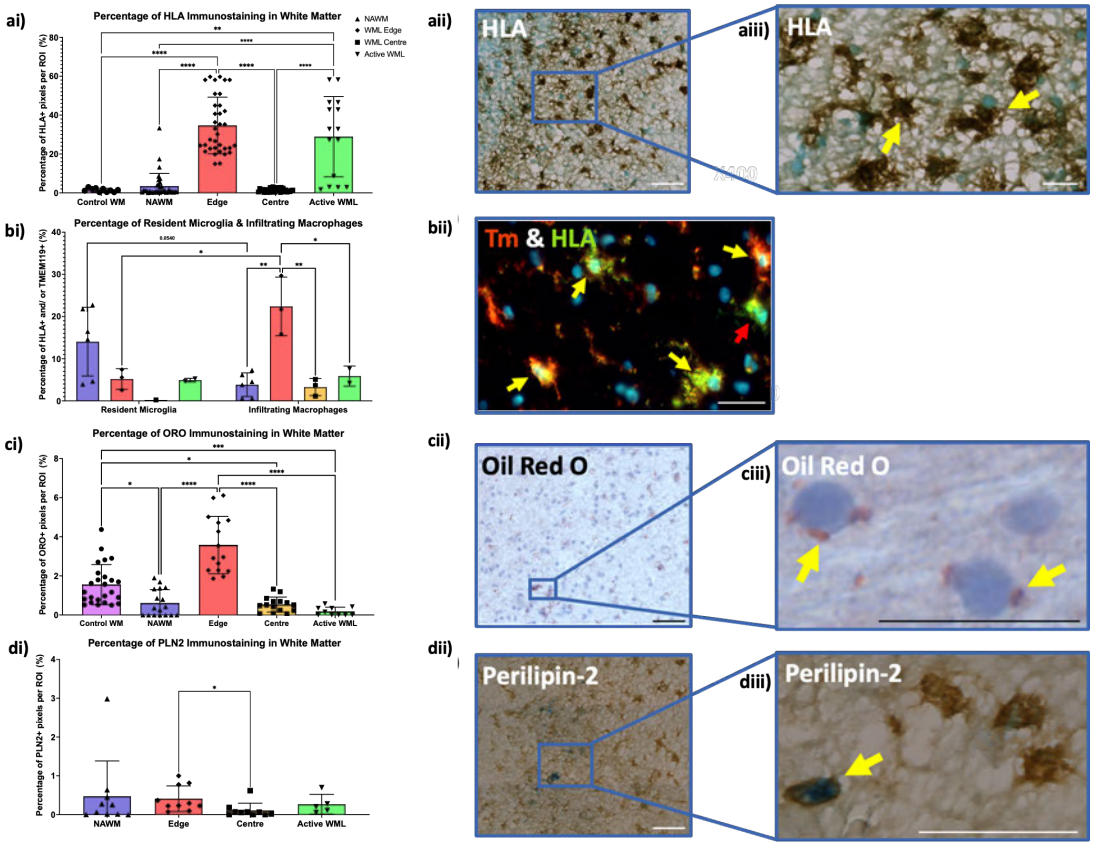

Figure 3.4 - Cholesterol and Lipid Droplets Selectively Accumulate at the Expanding Lesion Edge

HLA is increased at the MA/I WML edge and in active WML (ai), HLA+ macrophage-like cells (brown) (aii), arrows point to HLA+ macrophage-like cells (aiii). Immunofluorescence was used to identify resident microglia/infiltrating macrophages (b). An increased proportion of infiltrating macrophages accumulated at the MA/I WML edge compared to resident microglia; the inverse trend was seen for the NAWM, however this did not reach statistical significance ($p<0.1$). A higher proportion of infiltrating macrophages accumulated at the MA/I WML edge compared to the centre, active WML and NAWM (bi). Resident microglia were classed as cells dual positive for TMEM119 (red) and HLA (green); infiltrating cells were classed as those positive for HLA and negative for TMEM119, yellow arrows point to resident brain microglia; red arrow points to infiltrating macrophage (bii). Oil red O (ORO) is increased at the MA/I WML edge compared to NAWM, MA/I WML centre and active WML, whereas it is reduced in NAWM, the centre and active WML compared to WM from controls (ci) ORO+ droplets (red) (cii), arrows point to ORO+ droplets (ciii). Perilipin-2 (PLN2) is increased in the MA/I WML edge compared to the centre (di), PLN2+ stored lipids (blue), HLA+ macrophage-like cells (brown (dii), arrow points to stored PLN2 within an HLA+ macrophage-like cell (diii). Kruskal-Wallis with Dunn's post-test, *$p<0.05$,

***p<0.001, ****p<0.0001, (a, c, d); two-way ANOVA with Tukey's multiple comparisons test, *p<0.05, **p<0.01 (b). Graphs show mean ± standard deviation. Controls n = 5, MS n = 7. NAWM = normal appearing white matter, WML = white matter lesion, HLA – human leukocyte antigen, ORO – oil red O, PLN2 – perilipin-2. Images were captured using the Zeiss AxioScope microscope and Zeiss 503 colour camera (b) or Zeiss AxioCam black and white camera (a, c, d). Representative images taken from MS 513 A3A3. Scale bars = 50 μm.

Concentration changes of key sterols could partly be due to changes in the relative abundance of the enzymes responsible for their synthesis or metabolism. It was next assessed whether the transcripts encoding for these enzymes were altered in regions of WM demyelination. The relevant cholesterol biosynthesis/metabolism pathway, along with the enzymes involved, can be seen in figure 3.5. Four sterols were found to be significantly lower in regions of MS WM pathology - cholesterol, 24S-HC (and its epimer, 24R-HC) and 7β-HC. Additionally, 26-HC and 7-OC followed the same trend and were close to reaching significance (p<0.1). The enzymes involved in the production of these sterols are DHCR7, CYP46A1 (24-hydroxylase), HSD11B1, CYP27A1 (27-hydroxylase) and HSD11B2, respectively. To determine if the transcription of the genes that encode these enzymes was altered, ISH using the RNAScope method, was employed, which allows for the quantification and comparison of the relative expression of gene transcripts of interest in single cells and regions of interest (Wang et al., 2012).

24S-HC is the major oxysterol of the human brain; however, the current dogma dictates that *CYP46A1* is almost exclusively expressed by neurons (Petrov and Pikuleva, 2019). Expression of *CYP46A1* will be addressed in the GM section of this chapter.

CYP27A1, *CH25H, APOE, ABCA1* and *SOTA1* were probed for. As previously mentioned, CYP27A1 is responsible for the enzymatic conversion of cholesterol to 26-HC. This sterol potentially has relevance to mechanisms which may be involved in MS pathogenesis, and although nonsignificant, 26-HC followed the same trend as other sterols, being decreased in areas of MS WM pathology. *CYP27A1* mRNA expression was found to be decreased in areas of MS WM pathology (control WM – 3.36±3.27% (mean ±standard deviation); NAWM – 2.17±1.77%; MA/I WML edge –

1.63±2.16%; MA/I WML centre – 1.77±2.16%. Immunostaining revealed ubiquitous expression of the CYP27A1 protein in human WM (figure 3.6).

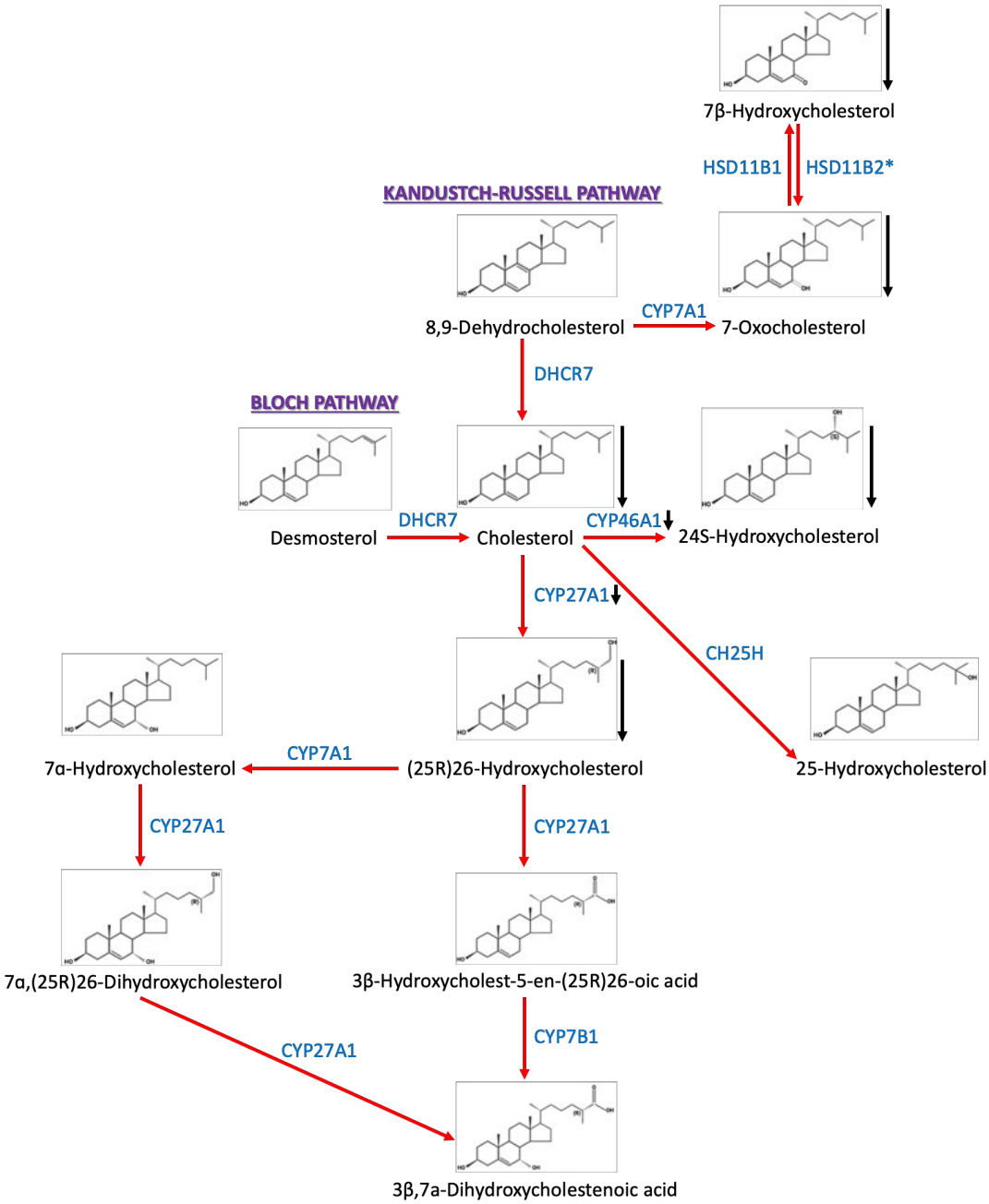

Figure 3.5 – Cholesterol Metabolism Pathway

Cholesterol can be synthesised via the Kandustch-Russell or Bloch Pathways, it is then metabolised into its oxysterol, downstream products (systematic names and structures in black). The enzymes responsible for metabolism of sterols are in blue (*= assumed enzyme). Black arrows indicate sterols/enzymes which were reduced in MS WM ROI. HSB11B1/2 – hydroxysteroid 11-beta dehydrogenase 1/2, CYP – cytochrome P450. DHCR7 – 7-dehysrocholesterol reductase, CH25H – cholesterol 25-hydroxylase.

CH25H is the enzyme responsible for the synthesis of 25-HC from cholesterol, and is known to be expressed by microglia/macrophages (Odnoshivkina *et al.*, 2022). Despite the 25-HC sterol appearing unchanged itself, its enzyme transcript expression was measured, as the concentration differences observed for other sterols occurred in areas with either increased/decreased microglia/macrophage-like cell load. *CH25H* was found to be unchanged between control and MS and within areas of MS WM pathology (figure 3.6), hence, validating the *MS* findings.

The percentage of mRNA transcripts were calculated using the area of puncta as a proportion of the area of Hx staining, therefore accounting for the changing cell density between the various compartments of the demyelinating lesion and adjacent normal appearing tissue.

A qualitative assessment of *APOE*, *ABCA1* and *SOAT1* showed widespread *APOE* expression at the actively demyelinating WML edge and positive cells in the adjacent WM. *ABCA1* and *SOAT1* transcripts were also present in WM, but were less frequent compared to APOE (figure 3.6).

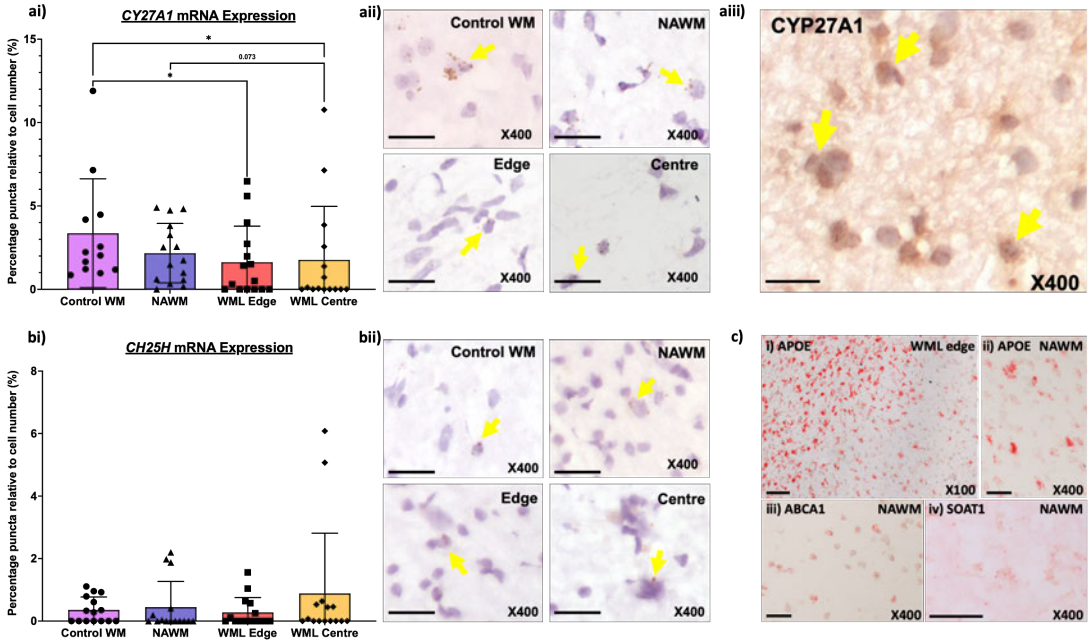

Figure 3.6 – Quantifying the Relative Expression of Cholesterol Metabolism-Related Enzyme Transcripts in WM

RNAScope was used to measure mRNA transcripts for *CYP27A1*, *CH25H, APOE, ABCA1 and SOAT1* (a-c). *CYP27A1* was reduced at the MA/I WML edge and centre compared to control WM; it was also lower at the MA/I WML centre compared to NAWM, although this did not reach statistical significance (ai). *In situ* hybridisation for *CYP27A1* mRNA expression with Hx counterstain in control WM, NAWM, MA/I WML edge and centre, arrows point to puncta (brown) (aii). Immunostaining for CYP27A1 (brown) with Hx counterstain, arrows point to CYP27A1+ cells (aiii). *In situ* hybridisation for *CH25H* mRNA showed no differences between controls and MS or within areas of MS WM pathology (bi), arrows point to *CH25H* puncta (brown) with Hx counterstain (bii). Representative ISH, using Fast Red as the chromogen, revealed widespread *APOE* expression at the active WML edge (ci) and positive cells in the adjacent white (cii). *ABCA1* (ciii) and *SOAT1* (civ) transcription was seen less frequently throughout the white matter ©. Kruskal-Wallis with Dunn's post-test, *p<0.05. Graphs show mean ± standard deviation. Controls n = 5, MS n = 5. WML – white matter lesion, CYP27A1 – cytochrome P450 27A1, CH25H – cholesterol 25-hydroxylase, NAWM – normal appearing WM, APOE – apolipoprotein E, ABCA1 – adenosine triphosphate-binding cassette transporter A1, SOAT1 – sterol O-acyltransferase 1. Representative images taken from MS 513 A3A3. Images were captured using the Zeiss AxioScope microscope a Zeiss AxioCam black and white camera. Scale bars = 50 μm.

3.3.4 – Identifying and Characterising Grey Matter Demyelination

As mentioned above, GM ROI were also collected, given their widespread presence in long-standing MS, however, the blocks were not expressly selected based on the presence/absence of GMLs (Griffiths et al., 2020a). Prior to tissue collection, the shortlisted cases were assessed for GM ROI via immunostaining. All identified GML were inflammatory inactive as is typical of long-standing MS, and were classed as cortical GML or deep GML (caudate, putamen) based on their location. Each of the shortlisted cases contained a proportion of NAGM and/or GML (figure 3.7).

3.3.5 –Sterol Concentrations Differ Between Regions of MS GM Pathology

After identification of GM ROI, tissue enriched for NAGM and GML was manually macrodissected. EADSA-LC-*MS* was then used to measure cholesterol, its precursors and metabolites. 7β-HC was found to be reduced in GML compared to GM from controls: control GM – 0.44±0.17 ng/mg (mean ± standard deviation), GML – 0.18±0.07 ng/mg. 7α-HC followed the same trend, but did not reach statistical significance ($p<0.1$), additionally, 24R-HC appeared lower in NAGM compared to control GM, but also did not reach significance ($p<0.1$) (figure 3.8).

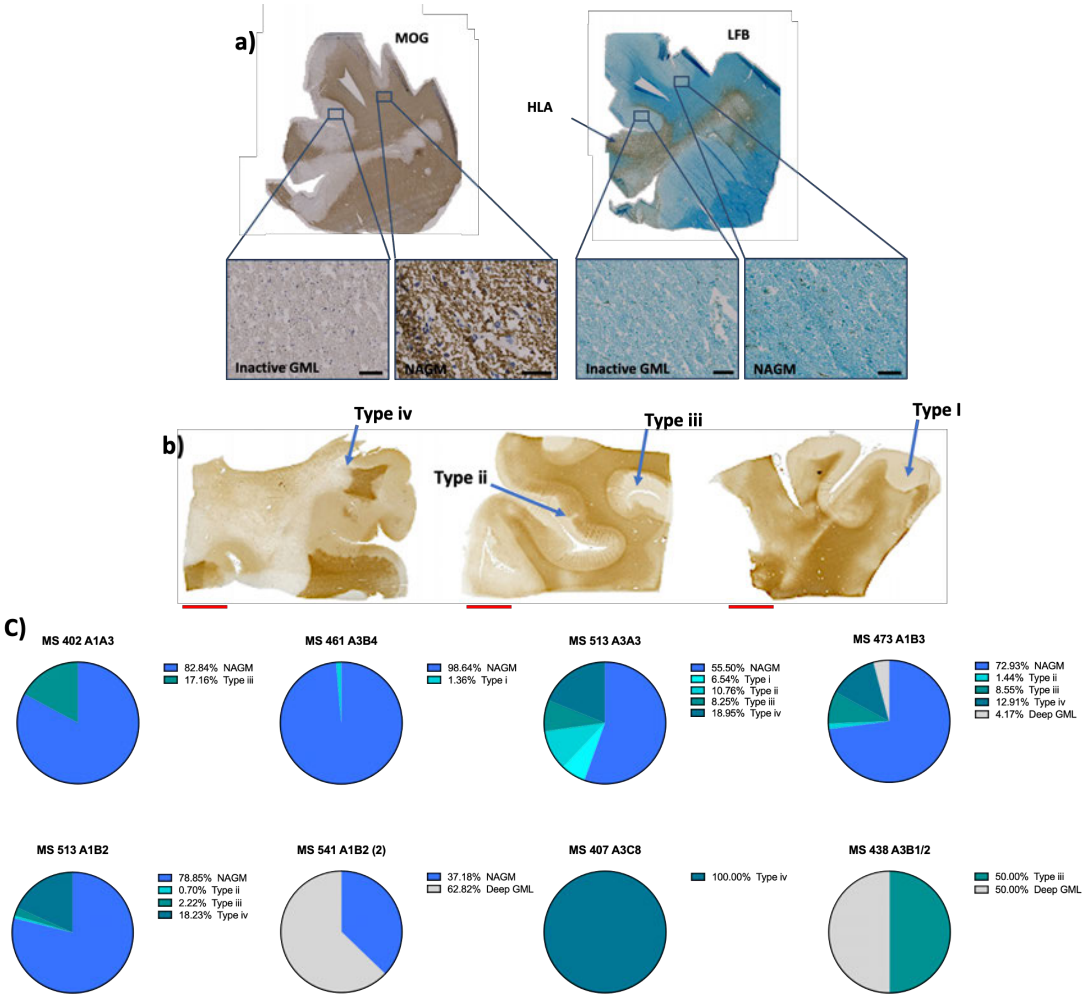

Figure 3.7 – Characterising Extensive and Variable Demyelination of Grey Matter

Regions of NAGM and GMLs were identified by the presence or absence of MOG/LFB staining. All lesions were classified as inactive (contained few HLA+ microglia/macrophage-like cells). Representative images taken from MS 473 A1B3 (a). GML were further classified based on their location within the GM, cortical or deep GML. Lesions affecting the cortex were further classified as either type i, type ii, type iii or type iv, arrows point to lesions. Images kindly provided by Owain Howell (b). The relative proportion of NAGM-lesion was calculated per case (n = 8). The percentage of type i lesions ranged from 0-7%; type ii range from 0-11%; type iii range from 0-50%; type iv ranged from 0-100% and deep GML ranged from 0-63%. Tissue images taken using QuPath version 0.3.2 (Bankhead et al., 2017). MOG – myelin oligodendrocyte glycoprotein, HLA – human leukocyte antigen, LFB – luxol fast blue, GML – grey matter lesion, NAGM – normal appearing grey matter. Red scale bars = 0.50 cm, black scale bars = 100 μm.

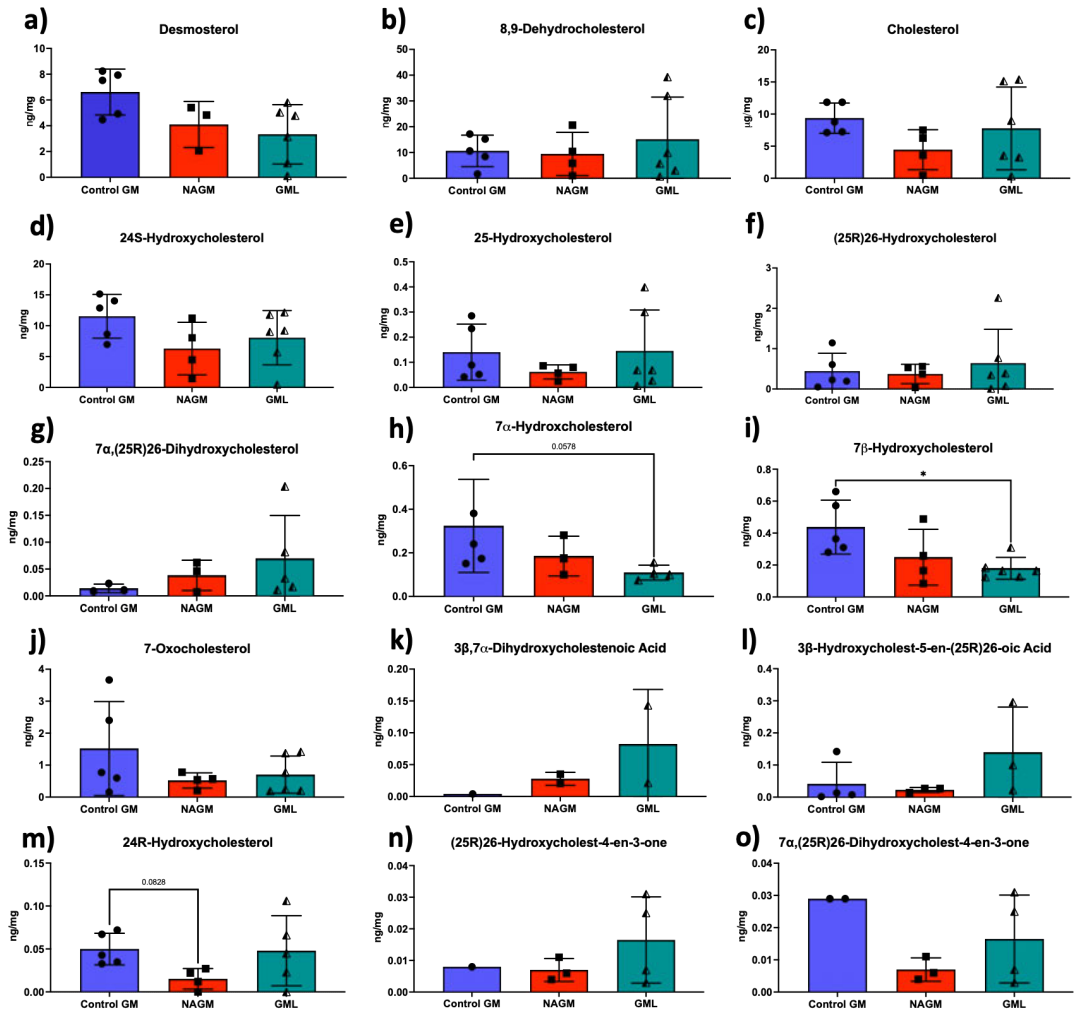

Figure 3.8 – Sterol Concentration in Human Control Grey Matter and MS Grey Matter

The relative abundance of sterols in GM ROI-enriched homogenates from the post-mortem brains of people with and without MS (a-o). 7β-hydroxycholesterol (i) was significantly lower in MS GML compared to control GM. Additionally, 7α-hydroxycholesterol (h) followed the same trend and 24R-hydroxycholesterol (m) appeared reduced in NAGM compared to GM from controls, however, neither reached statistical significance ($p<0.1$). Kruskal-Wallis with Dunn's post-test, *$p<0.05$). Graphs show mean ± standard deviation. Control n = 5, MS n = 6. NAGM – normal appearing GM, GML – grey matter lesion.

3.3.6 – Cholesterol Homeostasis is Altered in GM of the MS Brain

This work has provided evidence that cholesterol metabolism is also altered in areas of GM pathology within the MS brain. As with WM ROI, whether cholesterol storage is altered within GM ROI was investigated. Firstly, the proportion of HLA+ cells within the different GM ROI was calculated, no change was found between NAGM and

GMLs. Next, the percentage immunoreactivity of ORO and PLN2 was measured. ORO was found to be decreased in NAGM and GML compared to control GM. Control GM – 1.65±1.31% (mean ±standard deviation); NAGM – 0.33±0.49% GML – 0.72±1.17%. No change was found for PLN2+ lipid droplet storage, probably reflecting the lower overall abundance of myelin and myelin lipids in grey, in comparison to WM (figure 3.9).

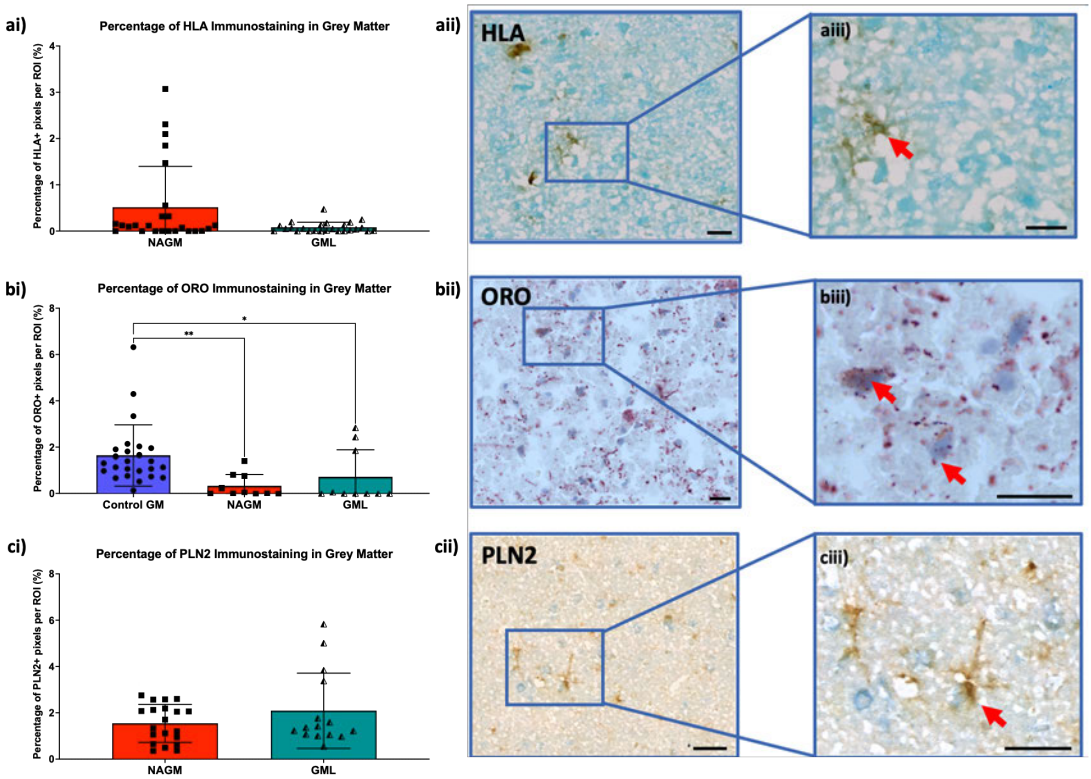

Figure 3.9 – Storage of Esterified Cholesterol Droplets are Decreased in MS GM

The percentage of HLA+ microglia were unchanged between NAGM and in GML (ai), HLA+ microglia (brown) (aii), arrow points to HLA+ microglia (aiii). ORO was found to be reduced in NAGM and GML compared to GM from controls (bi), ORO+ droplets red (bii), arrows point to ORO droplets (biii). PLN2 was unchanged between NAGM and GML (ci), PLN2 (blue) within an HLA+ microglia (brown) (cii), arrow points to stored HLA+PLN2+ microglia (ciii). *p<0.05, **p<0.01, Kruskal-Wallis with Dunn's post-test. Graphs show mean ± standard deviation. Controls n = 5, MS n = 5. NAGM = normal appearing grey matter, GML = grey matter lesion, HLA – human leukocyte antigen, ORO – oil red O, PLN2 – perilipin-2. Images were captured using the Zeiss AxioScope microscope and Zeiss AxioCam black and white camera. Representative images taken from MS 513 A1B2. Scale bar = 50 μm.

As cholesterol storage and metabolism also appeared altered in the GM, it was assessed if expression of the enzymes responsible for cholesterol metabolism were also altered in MS GM. As previously mentioned, CYP46A1 (24-hydroxylase) is responsible for the enzymatic conversion of cholesterol to 24S-HC. The dogma states that synthesis of CYP46A1 is driven by neurons (Petrov and Pikuleva, 2019). Using ISH, it was confirmed that *CYP46A1* mRNA is expressed by neurons in the GM, finding a significant decrease in expression in NAGM compared to GM from controls, with both a reduction in the number of immunopositive neurons and also the number of puncta per cell. Control GM – 0.28±0.24% (mean ± standard deviation); NAGM – 0.004±0.005%. Qualitative immunostaining for the CYP46A1 protein was also suggestive of a marked decrease of expression in MS compared to controls. Perhaps more surprisingly, immunostaining for HuC-D+ neurons, paired with ISH not only confirmed neuronal *CYP46A1* expression, but also revealed modest non-neuronal signal. The expression of *CYP27A1* and *CH25H* transcripts were also quantified; both were found to be significantly reduced in NAGM compared to GM from controls. *CYP27A1*: control GM – 3.65±2.84%; NAGM – 1.21±1.36%. *CH25H*: control GM – 1.63±1.96%; NAGM – 0.24±0.42%. Immunostaining for CYP27A1 confirmed protein expression in the GM (figure 3.10).

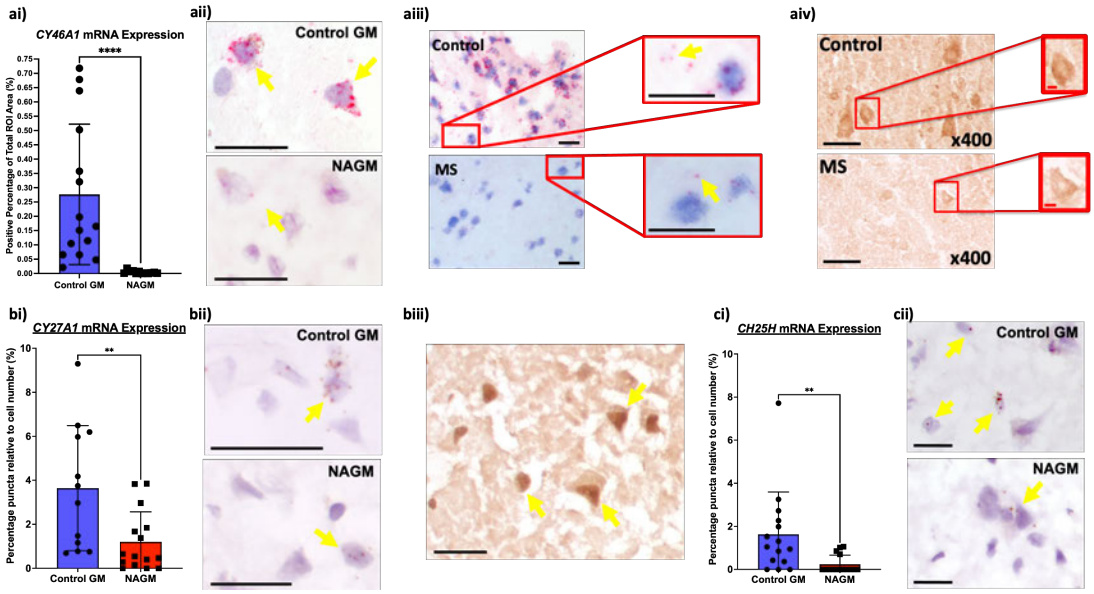

Figure 3.10 – Quantifying the Relative Expression of Cholesterol Metabolism-Related Enzyme Transcripts in GM

BaseScope was used to measure mRNA transcripts for *CYP46A1* and RNAScope was used to measure mRNA transcripts for *CYP27A1* and *CH25H* (a-c). *CYP46A1* was reduced in NAGM compared to controls (ai), arrows point to *CYP46A1* puncta (pink) with Hx counterstain (aii). Immunostaining for HuC-D+ neurons (blue) revealed both neuronal and non-neuronal *CYP46A1* puncta (pink) (aiii). Immunostaining for CYP46A1 showed a reduction in signal in MS compared to controls (aiv). *CYP27A1* (bi) and *CH25H* (ci) were both reduced in NAGM compared to controls, arrows point to *CYP27A1* puncta (brown) (bii) and *CH25H* puncta (brown) (cii). Immunostaining for CYP27A1 confirmed protein expression in GM (biii). Mann Whitney U, p<0.001***, p<0.0001****. Graphs show mean ± standard deviation. Controls n = 5, MS n = 5. Images were captured using the Zeiss AxioScope microscope and Zeiss AxioCam black and white camera. Representative images taken from MS 402 A1A3. CYP - cytochrome P450, CH25H – cholesterol 25-hydroxylase, NAGM – normal appearing GM. Black scale bars = 50 μm, red scale bars = 10 μm.

3.4 Discussion

Having identified sterol differences in gross anatomically distinct regions of the MS brain, compared to controls, It was next assessed if there were differences in demyelinated areas of the MS brain. As the initial study in chapter 2 showed differences in WM, efforts were focused on actively demyelinating WML – a lesion stage that is over-represented in a worsening disease course.

3.4.1 – Sterol Concentration is Altered in Areas of Demyelination

Cases which contained comparable, and clinically relevant, actively demyelinating lesions (both MA/I and active WML) were shortlisted, as the principal interest was on mechanisms relating to lesion expansion. Prior to tissue collection for sterol concentration analysis, the tissue was characterised to identify ROI - NAWM, MA/I WML edge, MA/I WML centre, active WML, NAGM, GML and WM/GM from controls. Actively demyelinating WMLs were further categorised as 'demyelinating', or 'post-demyelinating', based on the presence/absence of minor and major myelin degradation products – all sampled actively demyelinating lesions were categorised as 'demyelinating' and therefore could be grouped together for analysis (Kuhlmann et al., 2017).

EADSA-LC-MS was utilised to calculate the relative abundance of sterols within the WM and GM ROIs. This analysis revealed that some sterols differed in areas with marked demyelination. Cholesterol, 24S-HC, 7α-HC and 24R-HC were found to be reduced in the MA/I WML centre compared to WM from controls, in addition, 24S-HC was also reduced in the MA/I WML edge compared to control WM. 26-HC and 7-OXO also appeared reduced in the MA/I WML edge compared to control WM, however, they did not reach statistical significance ($p<0.1$), possibly reflecting the low power of this small study to identify statistically significant differences between groups. A reduction of these sterols at the hypocellular lesion centre, may be due to the loss of myelin, and therefore, cholesterol, resulting in a reduction of cholesterols' downstream products, due to decreased starting material (Saher and Stumpf, 2015). The reduction of 24S-HC and 26-HC at the lesion edge may also be due to reduced cholesterol, as a consequence of ongoing demyelination, but it may also correlate with changes in cholesterol storage/metabolism by macrophage-like cells (Cantuti-Castelvetri et al., 2018), discussed below. Some oxysterol concentrations also differed in GM - 7β-HC was reduced in GML compared to control GM. 7α-HC appeared lower in GML compared to control GM, and 24R-HC appeared reduced in NAGM compared to GM from controls, however they did not reach statistical significance ($p<0.1$). The 7-oxycholesterols (7α-HC, 7β-HC and 7-OXO) may also be reduced due to a lack of substrate in WM/GM. Their production has been shown to be cytotoxic to neurons, via the production of ROS. Others have also shown that an increase is associated with a worse AD course (Leonarduzzi et al., 2006; Dias et al., 2022). However, a decrease was found in the samples used in this study. It is of note that these sterols can also be formed as a result of autooxidation, so they could be an artefact of the oxysterol isolation procedure, as opposed to biologically-formed sterols (Griffiths et al., 2013).

3.4.2 – Dysfunctional Cholesterol Storage may Affect Sterol Concentrations in MS

Others have previously shown that aged/disease-affected macrophages may promote a proinflammatory environment as a result of a reduced capacity for lipid-

storage/efflux under certain pathological conditions (Cantuti-Castelvetri et al., 2018). Having identified differences in sterol abundance within areas of demyelination, which had either an increased or decreased microglia/macrophage-like cell load, cholesterol/lipid-storage was assessed using histology and immunostaining for components representative of stored lipids (Marschallinger et al., 2020). Firstly, anti-HLA immunostaining was confirmed to be increased at the MA/I WML edge and active WML (by at least 90% compared to NAWM and MA/I WML centre), confirming increased inflammation in these areas of recent demyelination. Additionally, the proportion of resident microglia (TMEM119+, HLA+) and infiltrating macrophages (HLA+, TMEM119-) were calculated, finding an increased number of single HLA+ infiltrating macrophages at the MA/I WML edge compared to other areas of MS WM ROI and 76% more compared to dual HLA+/TMEM119+ resident cells. This suggests that a higher proportion of macrophages from the periphery are present within actively demyelinating MA/I WML; however, this number maybe skewed to a certain extent. We now appreciate that when resident microglia, positive for TMEM119, are activated in response to inflammatory stress - such as occurs in MS, TMEM119 expression is downregulated. Therefore, although it's possible that a higher proportion of peripheral macrophages drive inflammatory demyelination, there is currently not a way to confidently assess this with our current array of phenotypic markers (Ruan and Elyaman, 2022).

Next, the percentage immunoreactivity of ORO and PLN2 staining, which corresponds to esterified-cholesterol rich droplets and lipid droplet storage, respectively, was calculated. In WM, both ORO and PLN2 were found to be selectively increased at the MA/I WML edge, reflecting the recent uptake of myelin, which in some instances may represent an excessive/inappropriate build-up of lipids/cholesterol at sites of demyelination. This build-up of intracellular lipids could be related to the decrease of 24S-HC/26-HC seen at the MA/I WML edge by EADSA-LC-MS. 24S-HC and 26-HC are LXR-α/LXR-β ligands. Activation of LXRs results in the transcription, and subsequent translation, of cholesterol efflux transporters, such as ABCA1 and APOE (Fukumoto et al., 2002; Tall, 2008). Microglia/macrophage-like cells are responsible for the

phagocytosis of debris, and it is thought that myelin-debris clearance is essential to create an environment suitable for repair. However, there is also evidence that cholesterol storage/clearance dysfunction by macrophage-like cells may also promote a detrimental inflammatory environment (Lampron et al., 2015; Bogie et al., 2020). In the context of the actively demyelinating MS lesion for example, this could mean that myelin debris that is ineffectively stored or not properly expelled from macrophage-like cells, could lead to the accumulation of excessive quantities of cholesterol within phagocytes, eventually leading to toxic and damaging responses, perhaps including cholesterol crystal formation and phagolysosomal membrane rupture (Cantuti-Castelvetri et al., 2018). Restoring normal cholesterol flux and oxysterol metabolism could represent one useful approach to alleviating this damaging reaction at sites of ongoing demyelination (Grajchen et al., 2018).

As 24S-HC/26-HC synthesis was shown to be dysregulated in MS WM, it was next assessed if there were differences in the transcripts encoding the enzymes which convert cholesterol to 24S-HC and 26-HC, *CYP46A1* and *CYP27A1*, respectively. *CYP46A1* is almost exclusively expressed by neurons, although some non-neuronal signal was also present within the samples (Petrov and Pikuleva, 2019). The expression of *CYP46A1* was found to be significantly reduced in NAGM by more than 98%, compared to control GM, reflecting a reduction of both the number of positive neurons, and the number of puncta present per neuron. Although RNA expression doesn't necessarily translate to protein expression (Greenbaum et al., 2003), a qualitative assessment of CYP46A1 (24-hydroxylase) immunostaining, showed a decrease in both the number of immunopositive neurons and a decreased staining intensity in MS GM compared to control GM. These findings are particularly interesting as *CYP46A1* has been reported to be down-regulated in a number of neurodegenerative diseases, including AD and HD. In a pre-clinical model of HD, knocking down *CYP46A1* expression reproduces a HD-like phenotype, whilst the restoration of neuronal *CYP46A1* expression is associated with improved motor function, less atrophy and improved cholesterol flux. This has promoted a gene therapy approach to be considered for HD treatment (Boussicault et al., 2016; Kacher

et al., 2019). Excitingly, *CYP46A1* is a druggable target. A small clinical pilot study of early AD has shown that efavirenza (an anti-HIV drug), can increase *CYP46A1*, and subsequently 24S-HC. The effect of efavirenza is also being tested as a therapeutic for epilepsy, where *CYP46A1* has been reported to be inhibited and 24S-HC decreased (Petrov and Pikuleva, 2019; van der Kant et al., 2019; Hanin et al., 2021; Lerner et al., 2022). These new findings of reduced brain 24S-HC, reduced transcript expression and reduced numbers of immunostained neurons strongly implies that cholesterol flux is altered in the MS brain and opens the door to testing some of these *CYP46A1* therapeutics in long-standing MS.

CYP27A1 is more ubiquitously expressed. Despite the decrease in 26-HC itself not reaching statistical significance ($p<0.1$), the transcript encoding its enzyme was found to be reduced in both white and grey matter. *CYP27A1* expression was reduced by 51% and 47% in MA/I WML edge and centre compared to control WM, respectively, and was decreased by 67% in NAGM compared to GM from controls. A reduction in the transcripts, which encode for the enzymes responsible for cholesterol metabolism, in areas of demyelination, further supports the hypothesis that cholesterol metabolism is dysregulated within the MS brain.

3.5 Limitations

The work presented in this chapter has shown that there is an association between demyelination and cholesterol metabolism dysregulation in MS, however, there are a number of limitations to this work which need to be addressed.

Firstly, the initial focus of this work was to assess whether discrete areas of WM demyelination associate with sterol concentrations, and although regions of GM interest were sampled, they were broadly grouped. Therefore, sterol changes which may associate with GML subtype/specific GM layer/cell type composition, may have been missed. For example, sterol changes in WM may relate in part to the composition of microglia/macrophage-like cells in areas of demyelination. Although less pronounced than in WM, the number/activation of microglia varies in different GML subtypes (Magliozzi et al., 2018), which would perhaps correlate to different

sterol abundances in these areas; an effect that this study has not tested for. GM pathology is extremely important in MS. GML are typically larger and more abundant than WML, and the presence of GML usually correlates with a worse MS prognosis (Calabrese et al., 2007; Calabrese et al., 2010; Calabrese et al., 2012; Honce, 2013; Bevan et al., 2018). Future studies with a focus to understand GML pathobiology and the contribution of sterol metabolism to this process are certainly needed.

The expression of a subset of transcripts which encode cholesterol metabolism-associated enzymes were shown to be reduced in MS WM and GM compared to controls. Due to time constraints, a number of other potentially useful transcripts, such as those encoding for cholesterol transporters, have not been quantitatively evaluated, and will need to be in the future. Additionally, RNA expression does not necessarily correspond to protein expression, so systematic analyses of the expression of the enzymes themselves will need to be conducted in the future.

Finally, due to a combination of time and tissue availability, this study has used a low number of cases. Future studies, with an increased sample size, will be needed to validate these findings. However, even with a small sample size, differences in the abundance of sterols, and relevant mRNA transcripts, have been shown between different regions of MS pathobiology, suggesting these differences are robust.

3.6 Conclusion

Cholesterol metabolism is altered in the human MS brain in areas of actively demyelinating tissue. A reduced concentration of some sterols was observed, which may be due to reduction in the enzymes responsible for their synthesis, as suggested by the stark reduction in the number of corresponding mRNA transcripts measured (Fukumoto et al., 2002; Tall, 2008). A reduction of these transcripts may associate with both a loss of cell number, as seen in MS (Peterson et al., 2001; Carassiti et al., 2018), and also cholesterol metabolism and storage dysfunction in the cells themselves (Cantuti-Castelvetri et al., 2018). Most noticeably, the *CYP46A1* transcript, whose product synthesises 24S-HC from cholesterol, was reduced by 98% in MS NAGM compared to control GM. 24S-HC is responsible for the efflux of

cholesterol from the CNS into the periphery, so its dysfunctional production may have a large implication on overall cholesterol flux in the brain. Sterols, including 24S-HC and 26-HC, were found to be reduced at sites of chronic demyelination, with an increased number of myelin-lipid rich microglia/macrophage-like cells. The over accumulation of myelin-lipids may relate to a reduction in the concentration of oxysterol-ligands for LXRs, resulting in a reduced number of cholesterol transporters, preventing cholesterol expulsion from the cells; potentially promoting a damaging microglial-phenotype (Cantuti-Castelvetri et al., 2018). In the following chapter, an attempt to model this dysregulation in culture will be made, to assess the role of inappropriate cholesterol storage by macrophage-like cells.

Chapter 4 – Lipid and Cholesterol Metabolism in Human Primary Microglia/Macrophages

4.1 Introduction

4.1.1 – The Role of Microglia in Health

Microglia are highly dynamic, specialised cells of the CNS. Unlike other neuroglia, microglia are derived from myeloid cell progenitors of the yolk sac during early development (Ginhoux et al., 2010; Cuadros et al., 2022). They readily extend and retract their processes, surveying the CNS and can detect and react to local changes in neural activity and the presence of pathogens, immune mediators and molecular patterns, promoting both inflammation and repair (Nayak et al., 2012). They facilitate phagocytosis of apoptotic cellular debris, which is a tightly regulated anti-inflammatory response that does not attract lymphocytes or induce inflammation (Magnus et al., 2001; Tremblay et al., 2011).

Microglia are important in modulating neuronal structure and function (Tremblay et al., 2011). For example, during early life, microglia modulate synaptic pruning, the degradation of immature synapses, allowing others to be formed and maintained (Stevens et al., 2007; Paolicelli et al., 2011; Faust et al., 2021). Signalling between

microglia and neurons is, in part, facilitated via the fractalkine axis. The fractalkine ligand (CX3CL1) is secreted by neurons, which then binds to the fractalkine receptor (CX3CR1) expressed by microglia, directing their engagement and phagocytosis of relevant synapses (Paolicelli et al., 2014). Additionally, microglia, are able to sense and respond to changes in neuronal activity, aiding modulation of excessive hyper/hypo-excitability, contributing to the maintenance of a homeostatic neural network (Umpierre and Wu, 2021). The expression and regulation of lipid metabolic machinery is central to microglial biology. In response to tissue injury, surveillant microglia undergo a series of complex phenotypical and morphological changes that are dependent on lipid-sensing. Polymorphisms in genes encoding for phagocytic and lipid-related proteins are associated with an increased risk of MS, such as the genes encoding MerTK (a regulator of phagocytosis) (Beecham et al., 2013), and TREM2 (required for the binding of lipidated APOE to promote cholesterol clearance) (Poliani et al., 2015; Yeh et al., 2016; Krasemann et al., 2017). Additionally, variants in genes including *ABCA7*, *BIN1 and CD33* are associated with risk variants for AD (Keren-Shaul et al., 2017; Prinz et al., 2019).

4.1.2 –Microglia and MS

In MS, the function of microglia is altered, and they phagocytose the myelin sheath (demyelination) and other cell membranes, in combination with peripheral immune infiltrating macrophages and dendritic cells (Luo et al., 2017). The cause of microglia inappropriately reacting to self-myelin antigens in MS is unclear, however, the physical act of degradation is mediated by receptor-ligand binding, causing internalisation of myelin (Grajchen et al., 2018). The loss of microglial homeostasis is a recognised hallmark of MS, as well as for a range of other complex neuroinflammatory and neurodegenerative diseases (Prinz et al., 2019). There is currently some debate around whether myelin debris uptake by microglia, is beneficial or damaging in MS. There is both evidence that myelin clearance is crucial for the promotion of an environment that can allow repair (remyelination of denuded axons) (Lampron et al., 2015; Luo et al., 2017); but also, evidence that suggests that this beneficial process is short lived, and instead mediates a change in microglia

phenotype from an anti-inflammatory, protective phenotype to a pro-inflammatory and destructive phenotype (Haider et al., 2011; Grajchen et al., 2018). This divergent view likely reflects the effects of the environment (i.e., whether the damage is acute or chronic) and age of the subject (microglia display a significant age-associated functional phenotype) (Loving and Bruce, 2020).

4.1.2.1 – Lipid Metabolism by Microglia/Macrophage-Like Cells

In atherosclerosis, an overload of cholesterol has been shown to be toxic to macrophages, driving the formation of lipid-laden foamy macrophages (Javadifar et al., 2021). In MS, microglia/macrophage-like cells phagocytose myelin/cellular debris. This debris is lipid (cholesterol)-rich (Berghoff et al., 2022a). Following phagocytic internalisation of myelin, myelin is degraded within lysosomes, which increases the availability of free-lipids, including cholesterol, which can be used in membranes, esterified and stored as lipid droplets, oxidised to cholesterol metabolites (oxysterols), or can be exported from the cell, via efflux transporters (Chausse et al., 2021). The synthesis of oxysterols contributes to activation of signalling pathways, including LXR and PPAR pathways. Activation of these pathways in health, pushes microglia back towards a more pro-regenerative phenotype following myelin phagocytosis, permitting future clearance of myelin (Bogie et al., 2012; Bogie et al., 2014; Chausse et al., 2021).

However, in the context of a neuroinflammatory disease, like MS, these systems may fail, and cholesterol efflux and effective storage becomes diminished. Defective cholesterol clearance has been modelled in a murine model of the aged CNS (Cantuti-Castelvetri et al., 2018), which may be relevant to MS, as patient microglia appear prematurely aged (Bolton, 2021) and disease severity is strongly linked to a person's age (Scalfari et al., 2011). Myelin phagocytosis assays, using murine bone marrow-derived macrophages, revealed that a defect in cholesterol clearance, after excessive myelin internalisation, can result from a downregulation of cholesterol efflux transporters, including APOE and ABCA1. Importantly, defective cholesterol clearance was shown to promote the formation of cholesterol crystals (as seen in

atherosclerosis (Duewell et al., 2010)). Build-up of cholesterol crystals induces phagolysosomal membrane rupture, subsequently stimulating the caspase-1-activating NLRP3 inflammasome response, resulting in the secretion of IL-1 beta (IL-1β) ((Duewell et al., 2010; de la Roche et al., 2018). IL-1β is a treatment target for MS and reflects wider NLRP3 inflammasome activation, which is commonplace in actively demyelinating MS lesions (Malhotra et al., 2020). Therefore, excessive build-up and defective clearance of cholesterol, may promote a pro-inflammatory and maladaptive microglial phenotype (Cantuti-Castelvetri et al., 2018) and contribute to the compartmentalisation of the immune response in established MS.

Importantly, in MS, foamy macrophages (lipid-laden, activated microglia and macrophages) are present in high numbers at the actively demyelinating rim of slowly expanding, MA/I WML (Frischer et al., 2015; Lassmann, 2018). Assuming these cells are in fact more damaging, than pro-reparative, cholesterol metabolism dysregulation, as a result of increased myelin phagocytosis, may contribute to this damaging phenotype, and therefore the continued expansion of clinically impactful actively demyelinating lesions (Grajchen et al., 2018).

4.1.3 –Studying microglial-like cells in vitro

There are several models which can be used to test microglial/macrophage and or monocyte cholesterol efflux/metabolism in vitro. The most easily obtainable are human immortalised monocyte derived cell line THP-1 and the derived human embryonic microglial/macrophage-like cells HMC-3. Upon stimulation, these cells express a number of monocyte/macrophage-like phenotypic markers and functions. THP-1 cells are a useful resource to investigate biological and lipid metabolic processes in a myeloid/macrophage-like cellular context. In contrast, HMC-3 express some phagocytic-related genes at a lower level than THP-1s, such as the phagocytosis regulator TREM2, so may not be as useful for investigation of phagocytosis. (Floden and Combs, 2007; Akhter et al., 2021; Zhang and Cui, 2021). In addition to human immortalised monocyte derived cells, there are murine models including SIM-A9 and BV-2 cells. SIM-A9 cells are spontaneously immortalised, semi-adherent cells,

purified from a mixed-glia culture of postnatal murine cortex, which have been shown to express macrophage/microglia-specific proteins including IBA1. BV-2 cells are a widely used murine model of microglia/macrophage-like cells and have a partly overlapping transcriptome/proteome to primary microglia, after stimulation with lipopolysaccharide (Blasi et al., 1990; Henn et al., 2009; Nagamoto-Combs et al., 2014). However, these cells still do not capture the full morphology/functionality of human, primary microglia. In addition, the process of immortalisation alters the cells' characteristics in comparison to endogenous microglia (Henn et al., 2009; Stansley et al., 2012).

Another *in vitro* model is induced microglia-like cells, which can be derived from the culturing of mature peripheral blood monocytes (Sellgren et al., 2017). These cells can be isolated from whole blood from healthy individuals, those with disease or those carrying a genetic variant of interest (Sellgren *et al.,* 2017). After isolation of the peripheral blood mononuclear cells (PBMCs), an immuno-magnetic sorting step can be used to screen and collect a cellular subset of interest, for example, CD14+ monocytes (Pan and Wan, 2020). Treatment with appropriate cytokines (IL-34 and granulocyte-macrophage colony-stimulating factor (GM-CSF)), for around a week transforms the monocytes into a microglia-like cell lineage. In the developing brain, IL-34 and GM-CSF polarise invading yolk-sac derived myeloid-cells into immature (foetal) microglia (Muñoz-Garcia et al., 2021). This method requires the availability of donor blood, and its preparation is more time consuming than microglia/macrophage-like cells obtained from immortalised cell lines, additionally these cells do not proliferate in culture. However, this model facilitates the use of patient derived cells. For example, induced microglia-like cells have been used to study phagocytosis capacity and inflammation related pathways in cells derived from patients with neurological diseases such as amyotrophic lateral sclerosis (ALS) and schizophrenia (Sellgren et al., 2017; Quek et al., 2022). There is a drive to move towards using patient derived cells for personalised medicine, where for example, a person's cells could be assessed on their response to a particular drug, prior to administering it to the patient (Quek and White, 2023).

A more complex culture model is the use of primary mixed glia models. Human brain microglia can be obtained from rapid autopsy, foetal or biopsy samples. A target brain region is digested into a single-cell suspension and the cells are cultured for around 2 weeks. The selectivity of cells collected via this method can be improved via the use of an immuno-magnetic sorting step (Gordon et al., 2011). Obtaining human brain microglia is outside of the scope of most laboratories due to a combination of ethics and the requirement for speed of sample processing post extraction. However, these cells are true, endogenous microglia; but even these cells do not retain their endogenous behaviour for long in culture (Bohlen et al., 2017). Studies have shown that engraftment of human-brain derived microglia into animal models is sufficient and necessary to re-enable more typical microglial behaviour (Bohlen et al., 2017).

Another very useful *in vitro* model of microglia are human pluripotent stem cell-derived microglia (pMGL). Induced pluripotent stem cells (iPSCs) first need to be differentiated into hematopoietic progenitor cells and then to microglia-like cells (Abud et al., 2017). This is a complicated, expensive and lengthy process, taking over 5 weeks to produce functionally useful microglia that essentially represent an immature microglia-like cell, more like those described in the foetal CNS (McQuade et al., 2018).

Each of the above methods are useful and valid for the study of microglia. In this study a combination of immortalised monocytes (THP-1) and induced microglia-like cells from mature primary human monocytes were used to model myelin phagocytosis.

4.1.4 – Lipid-Modulating Drugs and the Mode of Action of FTY720, Simvastatin and XBD173

Cholesterol metabolism and efflux dysregulation may contribute to important pathomechanisms, such as the generation of foamy macrophages, which may promote chronic and damaging inflammation and continued demyelination and neuro-axonal disruption (Lassmann, 2018; Grajchen et al., 2018). If so, cholesterol dysregulation may present as a novel druggable target to reduce inflammation and

neurodegeneration for people with MS. A selection of drugs are available which modulate cholesterol transport/metabolism. I have focused on FTY720 (fingolimod), simvastatin and XBD173. FTY720 is a licenced DMT for MS, simvastatin is currently at phase III clinical trial for SPMS and XBD173 is also an experimental drug being tested in SPMS, which may reduce inflammation; each regulates cholesterol and/or oxysterol metabolism in some way, either as their primary (simvastatin) or wider mode of action (FTY720, XBD173).

FTY720 is a widely used DMT for RRMS that targets the S1P lipid receptor. It was shown to be ineffective for the treatment for progressive MS (Lublin et al., 2016), however, this may partly be due to the wide range of subjects (in terms of age, disability and disease activity) included in the trials. Siponimod, which has a similar mode of action, is effective in reducing disability progression in active SPMS (Behrangi et al., 2019; Dumitrescu et al., 2019; Cohan et al., 2022). FTY720 has a wide range of biological effects, can cross the BBB and affects cholesterol efflux (via activation of signalling cascades which result in the increased expression of proteins involved in cholesterol trafficking (Vance et al., 2006; Newton et al., 2017). Its mode of action has not been fully elucidated, but its role in the periphery has been described. FTY720 is an orally prescribed, S1P receptor agonist, which modulates immune cell trafficking. Once ingested, it is readily phosphorylated into its active form via the action of nuclear sphingosine kinase 2 (SphK2) (Hait et al., 2014). On ligand-binding, the S1P receptor is internalised and degraded, which prevents the egress of lymphocytes from lymphoid organs in the periphery. This causes a reduction in circulating lymphocytes and as a result prevents the ingress of lymphocytes into the CNS. FTY720's potent immunosuppressive activity reduces annualised relapse rates in people with RRMS (Brinkmann et al., 2002; Hait et al., 2014; Kleiter et al., 2016; Tiper et al., 2016). There is evidence that FTY720 can stimulate 26-HC (an LXR-α/LXR-β-ligand) which can promote cholesterol efflux transporter synthesis. This has been shown to confer an atheroprotective effect to foamy macrophages. This may be pertinent to FTY720's possible mode of action in the MS CNS (Blom et al., 2010).

Statins are cholesterol lowering drugs, which are safe and well tolerated. A number of statins are able to traverse the BBB, and therefore may be beneficial in the regulation of cholesterol homeostasis in the brain. One such statin, simvastatin, has provided positive results in a phase II clinical trial of SPMS, when prescribed at a high dose (80 mg). Statins act by inhibiting HMG-CoA reductase, the enzyme responsible for the conversion of HMG-CoA into the cholesterol precursor, mevalonate. Ultimately, high dose simvastatin may have a positive effect on cholesterol metabolism in the brain (Stancu and Sima, 2001; Sirtori, 2014; Ramkumar et al., 2016).

XBD173 is a translocator protein 18 kDa (TSPO) ligand. TSPO is expressed predominantly on the outer mitochondrial membrane in steroid-synthesising tissues, including the brain, where it is highly expressed by activated microglia (Rupprecht et al., 2010; Yao et al., 2020). Its activation results in the translocation of cholesterol from the cytosol to the mitochondria, where it is then converted into neurosteroids and cholesterol hormones (Rupprecht et al., 2010; Lejri et al., 2019). Prior to use as an experimental drug, TSPO ligands, such as XBD173, were developed to be used as diagnostic tools to identify neuroinflammation via positron emission tomography (PET) imaging (Rupprecht et al., 2010). Increased TSPO expression by activated microglia/macrophages has been shown in models of neurodegenerative disease, including EAE, and correlates with neuroinflammation. Although the mechanistic action of TSPO is not fully understood, Bae and colleagues have shown that an increase of TSPO expression associates with a pro-inflammatory, damaging microglial phenotype, whereas ligand-TSPO receptor binding results in the expression of a more anti-inflammatory microglial phenotype (Bae et al., 2014). Therefore, treatment with XBD173 may act to suppress microglia-led inflammation by modulating cholesterol flux and metabolism.

4.1.5 – Chapter Aims

The work in this thesis has shown that cholesterol metabolism is dysregulated in the human MS brain at actively demyelinating sites, dense with lipid-laden

microglia/macrophage-like cells. I hypothesise that defective cholesterol and lipid clearance by these cells contributes to the altered cholesterol metabolism observed, and a dysfunctional and damaging microglial/macrophage response. Using a primary culture model of human induced microglia-like cells, I next attempted to model active myelin phagocytosis and inflammation, to investigate the expression of key cholesterol and lipid transporters and to test the effect of MS drugs on their ability to promote cholesterol clearance.

4.2 Methods

4.2.1 – Peripheral Blood Mononuclear Cell Isolation

Up to 108 ml of blood, from healthy volunteers (n=8, Females=3, mean age=30.1 years, age range=22-54 years), was collected in heparin vacutainers (Fisher Scientific) (Study approval: SUMS RESC 2022-0029). An equal amount of blood was layered onto lymphoprep (Stemcell Technologies) prior to centrifugation to separate blood constituents by density (2000 x g, 20 minutes, RT, accelerator and break off). The plasma layer was removed and discarded, without disturbing the buffy coat (layer containing PBMCs. The buffy coat was gently transferred to a universal tube. The PBMCs were washed twice by centrifugation (515 x g, 10 minutes; 7 minutes, RT, respectively) with media (RPMI-1640 glutaMAX; Fisher Scientific) pre-warmed to 37°C. Finally, the pellet was resuspended in 1 ml of the above media, and total cell number counted using a countess 3 automated cell counter (Fisher Scientific).

4.2.2 – CD14+ Monocyte Isolation

PBMCs were pelleted by centrifugation (300 x g, 10 minutes, RT). The pellet was resuspended in the appropriate volume of ice-cold MACS buffer (PBS (Gibco) containing 2% FBS (Fisher Scientific)), 80 µl per 10^7 cells, and CD14 microbeads (Miltenyi Biotec), 20 µl per 10^7 cells. After incubation at 4°C for 15 minutes, the cells were washed in MACS buffer by centrifugation (300 x g, 10 minutes, RT) and pelleted. The pellet was resuspended in 500 µl of MACS buffer; CD14+ cells were sorted by positive selection using an autoMACS (Miltenyi Biotec). The cells were sorted twice to collect a pure sample of CD14+ monocytes. Following centrifugation (300 x g, 10

minutes, RT) the pelleted cells were resuspended in day 0 media (RPMI-1640 glutaMAX containing 10% FBS and 1% penicillin streptomycin (pen-strep) (Fisher Scientific)). The cells were live counted and plated immediately.

4.2.3 – Differentiation to Microglia-like Lineage

Differentiation of CD14+ monocytes to microglia-like cells was achieved following work by Sellgren *et al* (Sellgren et al., 2017). 24-well plates (Greiner Bio-One) with 13 mm glass coverslips (Fisher Scientific) inserted into wells or 96-well plates (Fisher Scientific) were coated in poly-L-lysine (0.1mg/ml, Merck). On day 0, CD14+ monocytes were plated at a density of 100 000 – 650 000 cells per well in day 0 media (100 µl and 500 µl respectively). After 24 hours the media was aspirated and replaced with cytokine containing media (RPMI-1640 glutaMAX, 1% pen-strep, 0.1 µg/ml IL-34 (Bio-Techne) and 0.01 µg/ml GM-CSF (Bio-Techne). Every other day, half the media was aspirated and replaced with the same volume of fresh cytokine containing media. On day 8 or 10, the cells were fixed (see 4.2.5.2), lysed for RNA extraction (see *4.2.8.1*) or used for functional assays (see 4.2.6; 4.2.7). The cells were kept at 37°C with 5% CO_2 until fixation or lysis.

4.2.4 – THP-1 Culture

The initial stock of THP-1 cells were kindly gifted by the Griffiths-Wang group (Swansea University). Cryo-stored cells were warmed at 37°C in a water bath until almost fully thawed, 1 ml of prewarmed media (RPMI-1640 with glutaMAX + 10% FBS + 1% pen-strep (serum-containing media)) was added to fully thaw the cells, this was made to a final volume of 10 ml with media. The cells were pelleted by centrifugation (125 x g, 5 minutes, RT), resuspended in serum-containing media, at a density of 100 000 cells/ml, and transferred to a T-25 cell culture flask. The cells were kept at 37°C with 5% CO_2 for 48 hours. They were then passaged into 3 new T-25 flasks with the addition of fresh serum-containing media (7.5 ml media per flask). The THP-1s were passaged every 48 hours (once confluent, approx. 500 000 cells/ml) until use, or cryopreserved using the appropriate volume of freezing media (1:10 DMSO: serum-containing media) to allow for $1x10^6$ cells/ml.

4.2.5 – Morphology and Microglial Markers

4.2.5.1 – Morphology

The morphology of induced microglia-like cells was assessed using a bright-field EVOS XL Core microscope (Invitrogen) with phase-contrast. After 8 days of cytokine treatment, in serum-free culture media, most of the cells displayed increased adherence, ramified morphology and extended multiple fine processes. Each well of cells, for each donor, was assessed for morphology prior to proceeding with experimentation.

4.2.5.2 – Immunocytochemistry

Cell media was aspirated completely, cells washed with PBS, and fixed with 4% PFA for 30 minutes. Following washes with PBS, the cells were blocked with 10% normal goat serum (NGS) for 10 minutes at RT, then incubated with the appropriate concentration of primary antibody, diluted in PBS-T, for at least 3 hours at 4°C. Following washes with PBS, cells were incubated with the appropriate, species specific, secondary antibody conjugated to either biotin or a fluorophore, diluted in PBS-T to the appropriate concentration, for 1 hour at RT and washed with PBS. Table 4.1 contains details of the primary and secondary antibodies used. Biotinylated secondary antibodies were incubated with streptavidin (SAV) conjugated to a fluorophore, diluted to the appropriate concentration in PBS-T, for 1 hour at RT and washed with PBS. Nuclei were visualised with 1 µg/ml DAPI, diluted in PBS-T, for 1 minute at RT, followed by PBS washes. Cells grown onto coverslips were mounted with VectaMount permanent mounting medium (Vector). Images were captured at 200X magnification using an EVOS M5000 epifluorescence microscope (Invitrogen).

Table 4.1 – Primary and Secondary Antibodies Used for Immunocytochemistry

Antigen	Target	Host Species	Working Concentration (µg/ml)	Supplier	Product Code	Monoclonal or Polyclonal
C1Q	C1Q receptor	Rabbit	10	Fisher Scientific	F023402-2	Polyclonal
CD68	Microglia	Mouse	1	Dako	GA60961-2	Monoclonal
HLA-DR	Microglia	Mouse	1	Dako	F081701-2	Monoclonal
IBA1	Microglia	Rabbit	0.20	Fujifilm	019-19741	Polyclonal
TMEM119	Microglia	Rabbit	0.25	Merck	PA5-62505	Polyclonal
TREM2	Microglia	Mouse	10	Cardiff University (Prof. Morgan)	-	Monoclonal
Secondary Antibody Fluorophore	**Target Species**	**Host Species**	**Working Concentration (µg/ml)**	**Supplier**	**Product Code**	**Monoclonal or Polyclonal**
Alexa Fluor-488	Mouse	Goat	3	Fisher Scientific	15607878	Polyclonal
Alexa Fluor-594	Rabbit	Donkey	3	Fisher Scientific	10798994	Polyclonal

4.2.5.3 – In situ Hybridisation

ISH was carried out on cells as described in chapter 3, with slight modification. After peroxidase quenching, cells were treated with protease III prior to incubation with specific mRNA custom designed probes (ACD). All other steps remain as previously described (see 3.2.5.1).

4.2.6 – Myelin Phagocytosis Assays

4.2.6.1 – Fluro-Myelin Preparation

Human brain tissue was collected with a scalpel from available unfixed snap frozen tissue blocks from 2 control cases (1 male, mean age 59) and 1 MS case (female, 39, PPMS), until 1 mg of WM-enriched tissue had been collected. The tissue was kept on dry ice to prevent thawing. Isolation of myelin was achieved following Larocca and Norton's work (Larocca and Norton, 2007).The tissue was homogenised with 0.30 M sucrose using a Dounce homogeniser and pestle (VWR). The homogenate was layered over an equal volume of 0.83 M sucrose and ultracentrifuged (75 000 x g, 30 minutes, 4°C), resulting in crude myelin at the interface. The crude myelin was subjected to osmotic shock by resuspension in Tris-Cl buffer (0.2 M Tris-Cl in 100 ml dH_20, pH 7.45) followed by ultracentrifugation (75 000 x g, 15 minutes, 4°C). The resulting pellet was resuspended and homogenised in Tris-Cl buffer solution (20 mM Tris-Cl, 2 mM

Na_2EDTA, 1 mM dithiothreitol and protease inhibitor in 200 ml dH_20) and ultracentrifuged (12 000 x g, 15 minutes, 4°C). The resuspension and homogenisation in Tris-Cl buffer solution and ultracentrifugation was repeated, resulting in a crude myelin preparation. Following resuspension and a second homogenisation with 0.30 M sucrose, the crude myelin was further purified by repeating the above. The final purified myelin pellet was resuspended in Tris-Cl buffer solution prior to storage at -80°C.

Myelin protein concentration was calculated via Bradford assay. Six BSA standards, (ranging from 0 - 1 000 µg/ml) and isolated myelin were incubated with 50:1 BSA: copper sulphate solution for 30 minutes and measured using a POLARstar Omega plate reader (BMG Labtech). Following quantification of protein concentration, the myelin preparation was conjugated with pHrodo-red (Fisher Scientific). Lyophilised pHrodo-red was resuspended to 6.67 µg/µl in DMSO. Conjugation of myelin to pHrodo-red was achieved by incubating 15 mg/ml myelin with the appropriate volume of pHrodo-red and PBS (pH 7.4) for 50 minutes. Following centrifugation (6 000 x g, 12 minutes, 4°C), the resulting pellet was resuspended in PBS (pH 7.4) to obtain 1 µg/µl of pHrodo-red tagged myelin (Gómez-López et al., 2021).

4.2.6.2 – THP-1 Cells - Myelin Phagocytosis Assays

THP-1 cells were used to optimise myelin concentration and incubation times, prior to assays using primary induced microglia-like cells. Cells in media were transferred from T-25 flasks into a 12 ml tube and pelleted by centrifugation (125 x g, 5 minutes, RT). The pellet was resuspended in serum-containing media and cell counted. Prior to plating, 96-well plates were coated with poly-L-lysine (0.1 mg/ml) for 5 minutes, followed by at least 2 hours of drying. The THP-1s were seeded at a density of 75 000 cells per well in 7.5 ml serum-containing media, containing 100 nM phorbol-12-myristate-13-acetate (PMA) and incubated at 37°C, 5% CO_2. After 24 hours, the media was replaced with fresh serum-containing media and cells incubated for a further 24 hours. The phagocytosis ability of the cells was tested via the addition of pHrodo-red tagged myelin (1, 1.5, 2, 3 or 9µl of 1 µg/µl per well) at different time points (0, 2, 4,

8 and 24 hours). A control which omitted myelin was also used. The cells were washed with PBS and fixed in 4% PFA for 30 minutes prior to further washes with PBS. The cells were stained with actin-green for 30 minutes and counterstained using DAPI for 1 minute. Three technical replicates (3 wells) per condition were used with 3 images per well, per condition captured (a total of 9 snapshots captured per condition) for analysis using an EVOS M5000 epifluorescence microscope. The percentage area of pHrodo-red myelin staining, relative to actin-beta, was calculated by splitting the channels and thresholding in ImageJ version 1.52a. This was repeated 3 times using separate flasks of THP-1s.

4.2.6.3 – Induced Microglia-Like Cells - Myelin Phagocytosis Assays

After 8 days of culture, the induced microglia-like cells were stimulated by replacing the growth media with serum-containing media with cytokines (see 4.2.4). The phagocytosis ability of the cells was tested via the addition of pHrodo-red tagged myelin (1, 3, 4 or 9 µl of 1 µg/µl per well) at different time points (0, 2, 4, 8 and 24 hours), as well as a myelin negative control, were analysed as above (see 4.2.6.2). Three biological replicates were used to identify the optimal concentration of myelin.

4.2.7 – Drug Assays

Currently available MS-related drugs were tested on their ability to promote cholesterol efflux from myelin-lipid rich cells. THP-1 cells or induced microglia-like cells were challenged with 3 µg of pHrodo-red-tagged myelin, per well, after stimulation with PMA or serum-containing media respectively (see 4.2.6.2; 4.2.6.3). After 8 hours incubation with myelin, drugs of various concentrations were added: simvastatin (0.10 – 10.00 µM), FTY720 (0.001 - 0.100 µM) or XBD173 (0.10 – 10.00 µM), and the cells were incubated for a further 16 hours. Two controls were used, a cell only control (myelin negative, drug negative) and a vehicle control (myelin positive, drug negative control). After a total of 24 hours incubation, the cells were either fixed for 30 minutes in 4% PFA for analysis of phagocytosis (see 4.2.6.2), ISH (see 4.2.5.3) or lysed for RNA extraction (see 4.2.8.1). Three biological replicates (cells

from 3 different donors) were used to test drug concentrations. THP-1s from 3 flasks were used to test drug concentrations.

4.2.8 – Gene Assays

4.2.8.1 – RNA Extraction and cDNA Synthesis

RNA extraction from cultured cells was achieved using the RNeasy Plus Mini Kit (Qiagen) following the manufacturer's instructions. 10 µl dithiothreitol was added per 500 µl of Buffer RLT Plus, prior to lysis of cells. After cell lysis, the lysate was homogenised by passage through a 20-gauge needle 5 times. From this point, all steps were carried out at 4°C. The cell lysate was loaded onto a gDNA eliminator column and centrifuged at 16 000 x g for 30 seconds. An equal volume of 70% ethanol was added to the sample before transferring to a RNeasy spin column and centrifuging at 16 000 x g for 15 seconds. The spin column was washed twice using Buffer RPE by centrifuging at 16 000 x g for 15 seconds and 2 minutes, respectively. The sample was centrifuged again at 16 000 x g for 1 minute to eliminate any possible carryover of Buffer RPE. RNA was eluted from the RNeasy spin column using 30 µl RNase-free water. The concentration and purity of the RNA was measured using a nanodrop One (Fisher Scientific), prior to storage at -80°C.

cDNA synthesis was performed using the Precision nanoScript2 Reverse Transcription Kit (Primer Design). Up to 250 ng of total RNA was used as a template. 1 µl of oligo-dT primers and the appropriate volume of RNAse/DNAse free water was added per reaction, bringing the final volume to 10 µl. Annealing was achieved by heating to 65°C for 5 minutes, immediately followed by cooling to 4°C on ice. 10 µl of extension mastermix containing 5 µl nanoScript2 4X buffer, 1 µl dNTP mix (10 mM), 3 µl RNAse/DNAse free water and 1 µl nanoScript2 enzyme was added per reaction. For each synthesis, a nanoScript2 enzyme negative control and an RNA negative control were included. Extension was achieved by heating to 42°C for 20 minutes, followed by heat inactivation at 75°C for 10 minutes. The concentration and optical density (260/280 and 260/230) were measured using a nanodrop prior to storage at -80°C.

Cells from 12 wells per condition, from 3 biological replicates (3 donors) were combined for cDNA synthesis.

4.2.8.2 – Quantitative Polymerase Chain Reaction Analysis

Lyophilised forward and reverse primers (Merck) were resuspended to 100 μM in RNase/DNase-free water (see table 4.2 for sequences). A bulk reaction mix was prepared following the KiCqStart Universal SYBR Green quantitative polymerase chain reaction (qPCR) Protocol (Merck). Per well, 5.0 μl of KiCqStart SYBR Green qPCR ReadyMix (2X) (Merck) was combined with 0.5 μl of both forward and reverse primers of the same primer pair, diluted 1:20, to 5 μM, and 3 μl of nuclease-free water. This was then combined with 1 μl of template cDNA (THP-1 = 175 ng/μl; induced microglia-like cells = 250 ng/μl). Each reaction mixture contained 1X KiCqStart SYBR Green qPCR ReadyMix, 250 nM of forward/reverse primers and either 17.5 ng THP-1 cDNA or 25.0 ng induced microglia-like cells cDNA. The qPCR was performed using a CFX Connect Real-Time PCR detection system (Biorad) with the following cycle conditions: initial hot start and denaturation for 2 minutes at 95°C and 10 seconds at 95°C, followed by an extension/annealing step at 60°C for 1 minute, repeated for 39 cycles. Lastly, a melt curve analysis was performed within the 65-95°C range at 0.5°C increments, 5 seconds/step for 5 minutes.

Prior to quantification of target genes, all primers were subjected to a standard curve analysis to assess primer efficiency and that there was an absence of tertiary structure formation such as primer dimer. All data was quantified using the PFAFFL method.

Table 4.2 – Primer Sequences

Primer sequences for human samples.

Gene Target	Forward Primer Sequence	Reverse Primer Sequence
Hs-RPLP0	CGTCCTCGTGGAAGTGACAT	ATCTGCTTGGAGCCCACATT
Hs-HLA-DRA	CTGTAAGGCACATGGAGGTGA	GGTGGCTATAGGGCTGGAAA
Hs-TREM2	ACAGCATCTCCAGGGCTGA	TGCCAGAGCAGAACAAGGAG

4.2.9 – Statistical Analysis

All statistical analysis was conducted using GraphPad Prism version 9.3.1. Due to small group sizes, more conservative, non-parametric statistical testing was employed. Two-group comparisons were made by Mann Whitney testing with two-tailed distribution; greater than two-group comparisons were made by Kruskal-Wallis with Dunn's post-test. Values of <0.05 were considered significant.

4.3 Results

4.3.1 – Producing a Model of Phagocytic Induced Microglia-Like Cells

In order to understand how microglia may be involved in the propagation and continuation of cholesterol-metabolism dysregulation-led pathogenesis in MS, I designed and implemented a cell culture model using primary human induced microglia-like cells. Firstly, monocytes were isolated from control whole blood and were differentiated into microglia-like cells via the addition of IL-34 and GM-CSF over 8 days. By day 8 the cells had transformed into a more microglial-like morphology, having grown larger, less spherical and extended multiple fine processes. In addition to being more morphologically similar to endogenous human microglia, the cells were positive for markers typically expressed by microglia including HLA, TMEM119, TREM2, CD68 and C1Q (figure 4.1). Although these cells are not true endogenous microglia, having been differentiated from peripheral monocytes (which is not the typical pathway for microglia production *in vivo*), I used cytokines which are involved in endogenous microglial differentiation/homeostasis (Greter et al. 2012). GM-CSF is a crucial growth factor required for the generation of microglia, as displayed in murine knock-out studies, where homozygote GM-CSF-receptor negative mice have impaired microglia production (Ginhoux et al., 2010). In addition, IL-34 has been shown to be an alternative ligand for the GM-CSF receptor, as well as being important for mature microglial homeostasis (Greter et al. 2012). In contrast, others have demonstrated that macrophages can be differentiated from peripheral monocytes through the addition of GM-CSF and 10% FBS whilst omitting IL-34 (Sellgren et al. 2017). My use of both GM-CSF and IL-34 in culture, combined with the morphology

and antigen expression of the cells produced, gives me confidence that these cells are phenotypically closer to microglia compared to macrophages and can therefore be used to model microglia in an *in vitro* setting.

Next, it was assessed whether the microglia-like cells expressed relevant cholesterol metabolism/export machinery, which is expressed by endogenous microglia. Using RNAScope ISH, it was shown that the cells expressed the mRNA transcript for the enzyme responsible for converting cholesterol to (25R),26-hydroxycholesterol (CYP27A1, 27-hydroxylase), as well as the mRNA transcripts for several cholesterol transporters (ABCA1, APOE and SOAT1). Additionally, immunocytochemical staining revealed evidence that the induced microglia-like cells were capable of phagocytosing lipids, including human myelin, and therefore cholesterol (LFB+, filipin+). LFB+ and filipin+ signal was concentrated into small puncta, suggesting lysosomal storage of lipids, as expected. Prior to the addition of myelin to the cultures, the myelin was tagged with a pH sensitive dye - pHrodo-red. Under acidic conditions, such as within the lysosomes of phagocytic cells, pHrodo-red fluoresces, allowing it to be detected using fluorescence microscopy (excitation 560 nm, emission 585 nm) (figure 4.1).

Once confident that a microglia-like cell lineage could be induced from primary monocytes, which express relevant cholesterol metabolism/transport machinery, the cells ability to phagocytose human-brain derived myelin was investigated. A monocyte cell line (THP-1) was used to ascertain the optimal method and concentration-range to use for testing. Prior to the addition of pHrodo-red myelin, the THP-1s were stimulated with a 24-hour PMA treatment. Experimentation with PMA-stimulated THP-1 cells showed that 20-90% of cells would phagocytose myelin depending on the concentration (1-9 μg) and the length of incubation (2-24 hours) with the pHrodo-red tagged myelin. The use of 3 μg/well, for 8 hours, was found to promote the most optimal phagocytosis, whilst minimising cell lysis (figure 4.2).

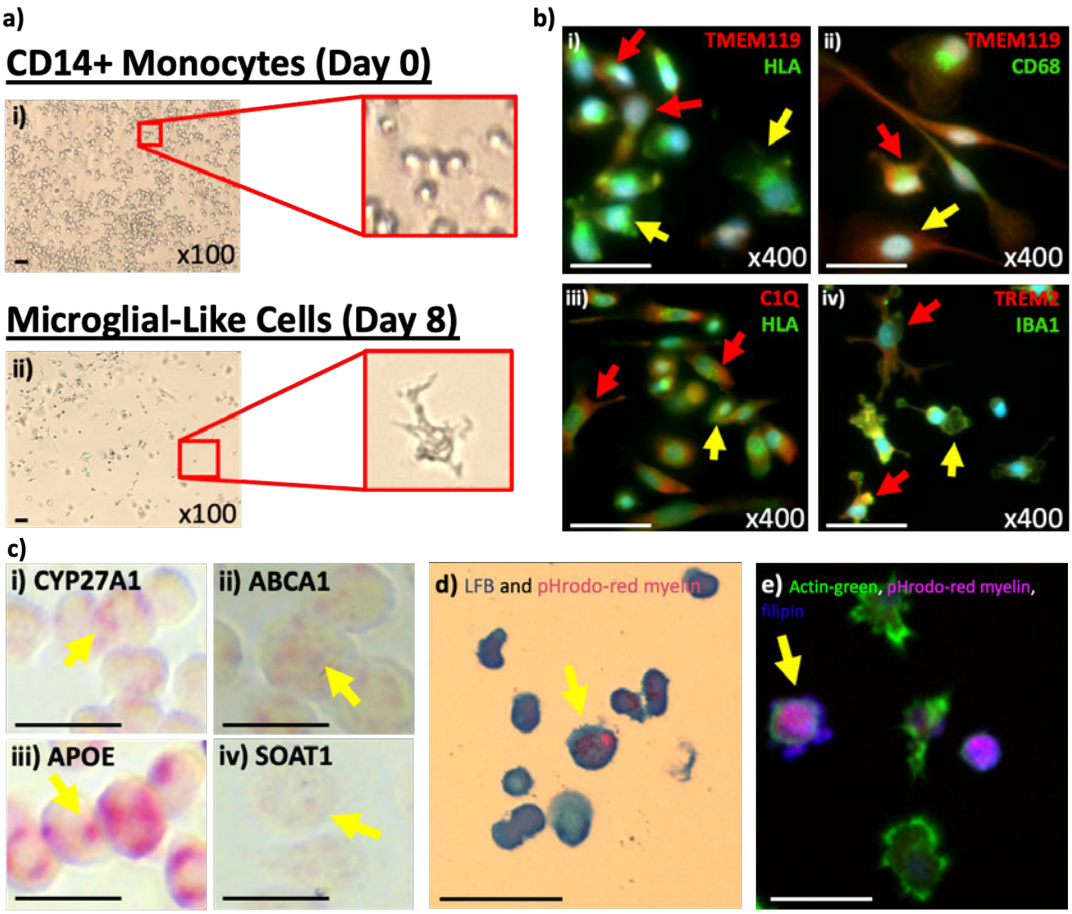

Figure 4.1 - Induced Microglia-like Cells from Monocytes Express Cholesterol Metabolism Machinery and Phagocytose Human Myelin

On day 0, the primary human peripheral blood derived monocytes had a typical monocyte morphology, being small and spherical (ai). After 8 days of cytokine treatment their morphology had altered – they were typically larger, ramified and extended multiple branching processes – more consistent with human microglial morphology (aii). Immunocytochemical staining showing that induced microglia express microglial-related markers (b) - TMEM119 (red), HLA (green), yellow arrow points to HLA+/TMEM119- cells, red arrows point to dual positive cells (bi); TMEM119 (red), CD68 (green), yellow arrow points to TMEM119+/CD68- cell, red arrow points to dual positive cell (bii); C1Q (red), HLA (green), yellow arrow points to HLA+/C1Q- cell, red arrows point to dual positive cells (biii); TREM2 (red), IBA1 (green), yellow arrow points to IBA1+/TREM2- cell, red arrows point to dual positive cells (biv). Induced microglia-like cells express cholesterol metabolism related machinery (c-e). Transcript detection for cholesterol metabolism related enzyme (ci) and cholesterol exporters (cii-iv) by *in situ* 132hybridization. Arrows point to puncta. Myelin-fed induced microglia-like cells dual-positive for LFB+ (blue)/pHrodo-red myelin+ cells (red), arrow points to co-labelled cell (d) and induced microglia-like cells (green) dual-positive for pHrodo-red myelin (red) and filipin (blue), arrow points to co-labelled cell

I. n = 1. Images from a and c were captured using a bright-field EVOS XL Core microscope. Images from b, d and e were captured using an EVOS M5000 epifluorescence microscope. CYP27–1 - cytochrome P450 27 A1; ABCA1 – adenosine trisphosphate binding cassette A1; APOE- apolipoprotein E; SOAT1 – sterol o-acyltransferase 1; TMEM119 – transmembrane protein 119; HLA – human leukocyte antigen; CD68 – cluster of differentiation 68; C1Q – complement component 1Q; TREM2 – triggering receptor expressed on myeloid cells 2; IBA1 – ionised calcium-binding adapter molecule 1. Scale bar = 50 μm.

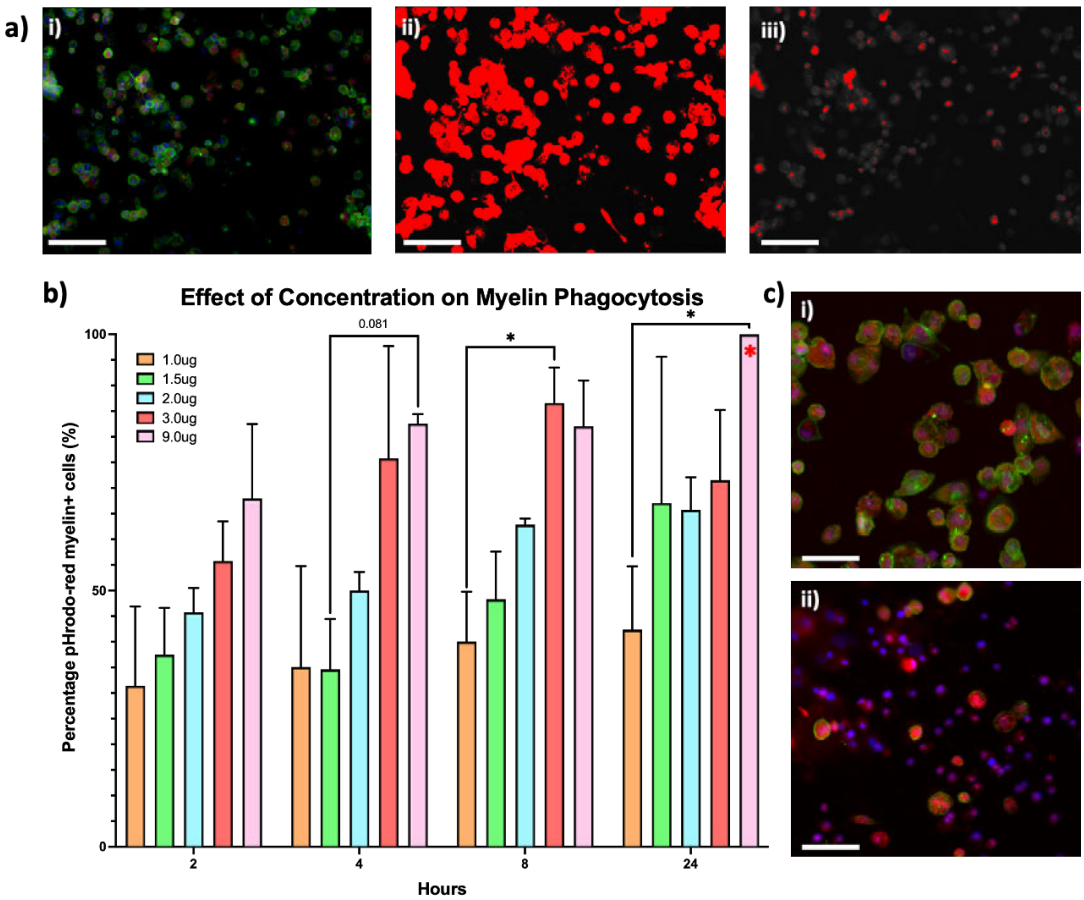

Figure 4.2 – Optimising the THP-1 Myelin Phagocytosis Assay

THP-1 cells were stimulated with PMA for 24 hours and then challenged with varying concentrations of pHrodo-red tagged myelin –1 - 9 μg) over different lengths of time –2 - 24 hours) (a-c). Original images were imported into Fiji ImageJ (ai). The colour channels were split into green (actin-green, cytoskeleton) (aii), red (pHrodo-red tagged myelin) (aiii) and blue (DAPI, nuclei stain). The green and red channels were thresholded to give the area of positive pixels, allowing the percentage area of myelin phagocytosis to be calculated, relative to cells positive for actin-green. Different incubation times, with different pHrodo-red tagged myelin concentrations were tested (b). After exposure to 3 μg of myelin, per well, for 8 hours, 87% of THP-1s contained myelin; representative image (ci). Exposure to 9 μg of myelin per well for 24 hours resulted in 100% myelin+ cells, however, this concentration and incubation

time was toxic to the cells resulting in increased cell lysis (*); representative image (cii). Graphs show mean ± standard deviation. N = 3 for each condition. Images were captured using an EVOS M5000 epifluorescence microscope. Scale bars = 50 μm.

As there were minimal differences between the percentage of THP-1 cells which phagocytosed myelin when treated with 1.5 μg and 2.0 μg myelin per well, the phagocytosis ability of the induced microglia-like cells was tested using 1 μg, 3 μg, 4μg and 9μg. Firstly, whether incubation time affects myelin-phagocytosis was assessed and it was found that the percentage of cells positive for pHrodo-red myelin increased with incubation time when exposed to 4 μg myelin from 0.5-24 hours. However, even after 24 hours, less than 7% of microglia were positive for myelin. Stimulation with 10% FBS was tested to assess if it would improve the phagocytosis capacity of the induced microglia-like cells, and although it did not reach statistical significance, a trend to increased myelin phagocytosis in the FBS-stimulated cells when treated with 1 μg myelin was found. Lastly, different concentrations of pHrodo-red+ myelin was tested over durations of time ranging from 2-24 hours. This showed that the use of 3 μg, for 8 hours, promoted the most optimal phagocytosis. However, it is of note that a considerably lower percentage of induced microglia-like cells phagocytosed myelin, compared to the THP-1 cells. (~8%) (figures 4.2 and 4.3).

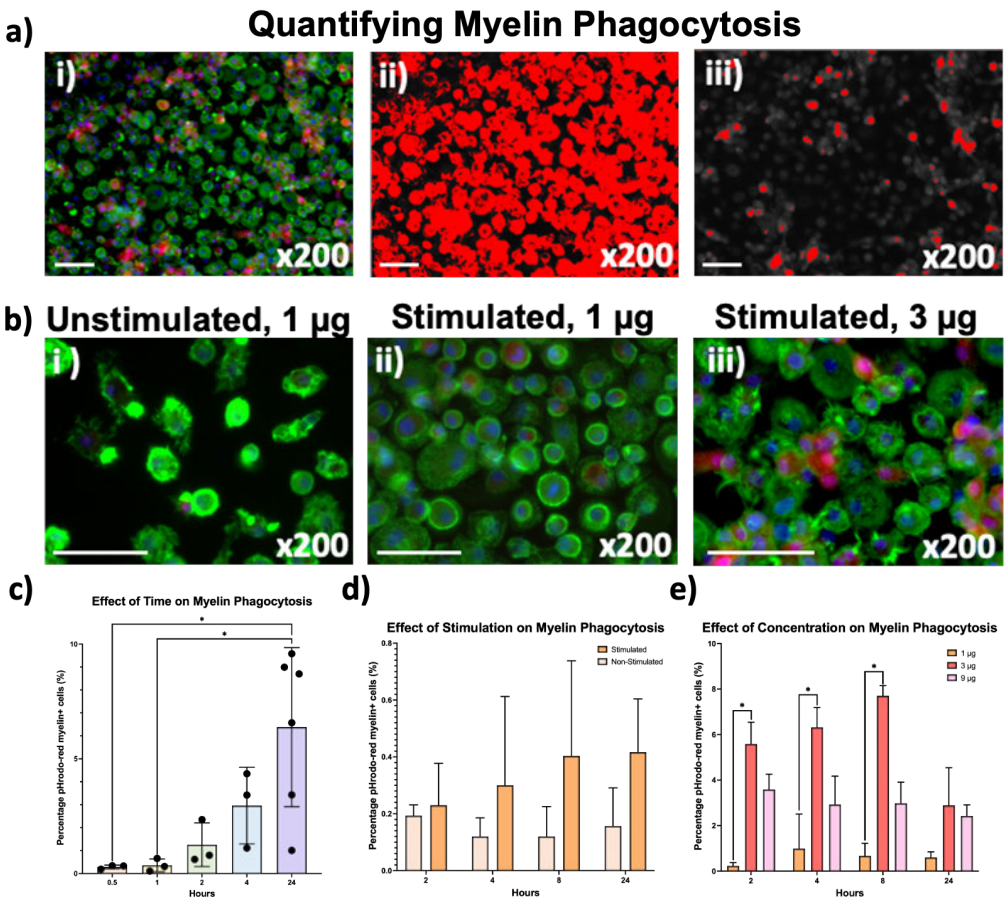

Figure 4.3 – Optimising the Induced Microglia-Like Cells Myelin Phagocytosis Assay

Myelin phagocytosis was measured using Fiji Image J Software (a). Original images were imported into the software. Blue=DAPI, red=pHrodo-red tagged myelin, green=actin green. (ai). The colour channels were split into green (actin-green, cytoskeleton), red (pHrodo-red tagged myelin) and blue (DAPI, nuclei stain). The green channel, cells (aii) and red channel, myelin (aiii) were thresholded (shown in red) to give the area of positive pixels, allowing the percentage of myelin phagocytosis to be calculated relative to cells positive for actin-green (a). Time, stimulation of cultured cells and myelin concentration affected phagocytosis (b-e). Representative images of immunocytochemical stains showing examples of cells treated with differing myelin concentrations and cell stimulation over an 8 hour treatment (b) - low myelin concentration fed to unstimulated cells (bi), low myelin concentration fed to cells stimulated with 10% FBS (bii) and higher myelin concentration fed to stimulated cells (biii). Unstimulated cells incubated with 4 µg of myelin for differing time periods ranging from 0.5–24 hours (c). Stimulated and unstimulated cells treated with 1 µg of myelin for differing times ranging from 2-24 hours (d). Three concentrations of myelin (1 µg, 3 µg and 9 µg) fed to stimulated cells for differing times ranging from 2-24 hours (e). *p<0.05, Kruskal-Wallis with Dunn's post-test. Graphs show mean ± standard deviation. n = 3 for each condition. Images were captured using an EVOS M5000 epifluorescence microscope. Scale bars = 50 µm.

4.3.2 – MS Related Drugs may Promote Myelin-Lipid Clearance

Having confirmed that the THP-1 cells and some induced microglia-like cells could phagocytose pHrodo-red labelled human myelin, it was investigated whether simvastatin, FTY720 and XBD173 could promote myelin clearance (see figure 4.4 for experimental design). These drugs were initially tested in THP-1s, but optimisation with induced microglia-like cells was required due to the large difference in myelin up-take between the cell line and human primary cells. After simulating the induced microglia with 10% FBS, the cells were incubated with 3 μg pHrodo-red myelin, for 8 hours. The cells ability to phagocytose myelin-lipids was assessed; this ranged from 14-43% of cells, between donors, highlighting that there are significant inter-person differences in the ability to phagocytose myelin (figure 4.5).

The cells were then treated with simvastatin, FTY720 or XBD173, at different concentrations (0-10 μM, simvastatin and XBD173 and 0-0.1 μM, FTY720), for 16 hours, to assess if they had an effect on myelin-lipid efflux, and if so, which concentration was optimal, i.e., resulted in the least number of pHrodo-red myelin+ cells. The percentage of pHrodo-red myelin+ cells, after myelin and drug treatment, were normalised to the number of pHrodo-red myelin+ cells treated with myelin and vehicle (DMSO or water). Each drug reduced the proportion of pHrodo-red myelin+ cells, the optimal concentration for simvastatin and XBD173 was 0.33 μM; and for FTY720 the optimal concentration was 0.003 μM. At these concentrations, simvastatin, FTY720 and XBD173 treatment resulted in more than a 50% decrease in the number of pHrodo-red myelin+ cells. The results followed a J-curve trend, suggesting that concentration above 0.33 μM for simvastatin and XBD173, and above 0.003 μM for FTY720, was toxic to the cells, or had off-target affects (Angeli et al., 2013) (figure 4.5).

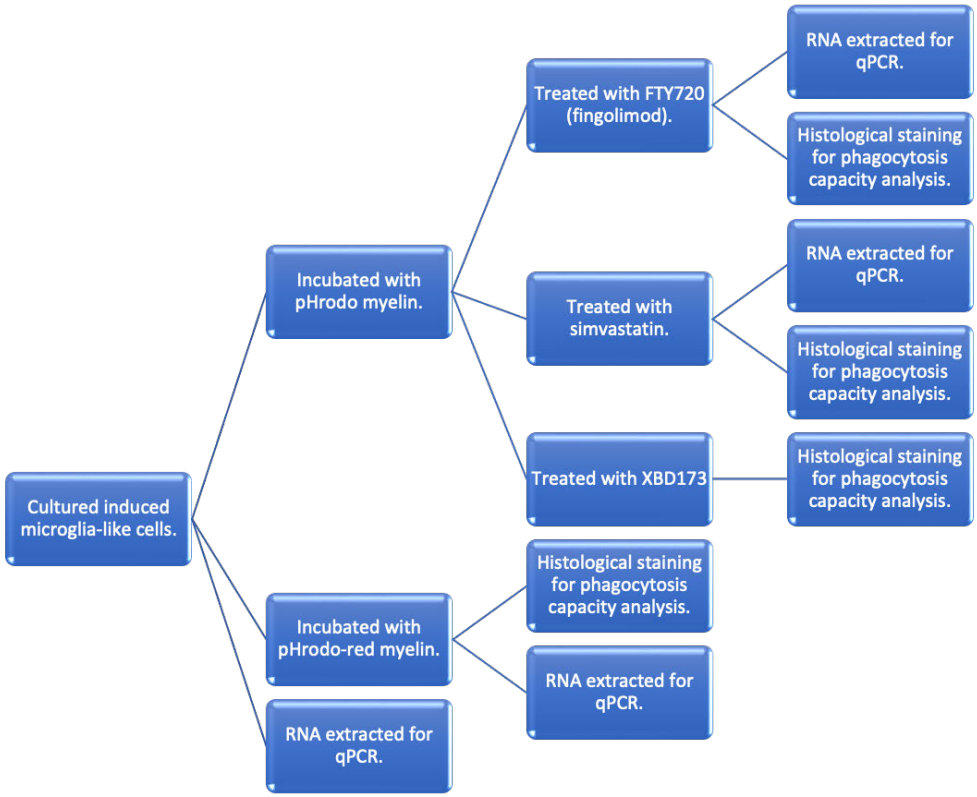

Figure 4.4 – Schema Illustrating Experimental Design

Induced microglia-like cells were cultured and then challenged with different experimental conditions. They were then processed for use in molecular or histological experiments. Created in Microsoft PowerPoint.

It was then assessed whether promoting myelin clearance altered the expression of relevant genes. FBS-stimulated induced microglia-like cells were challenged with either a vehicle (DMSO or water; control), 3 μg of myelin per well, for 24 hours (myelin) or 3 μg of myelin per well, for 8 hours, with either 0.33 μM of simvastatin or 0.003 μM FTY720 for 16 hours. After 24 hours, RNA was extracted from the cells and reverse transcribed to cDNA for use in qPCR experiments. The relative expression of *HLA* and *TREM2* was calculated and normalised to the untreated, control cells. Although nonsignificant, simvastatin reduced the expression of *HLA* by a fold change of 0.6 and FTY720 reduced the expression by a fold change of 0.5, compared to myelin treated cells. No differences were observed for *TREM2* relative expression (figure 4.6).

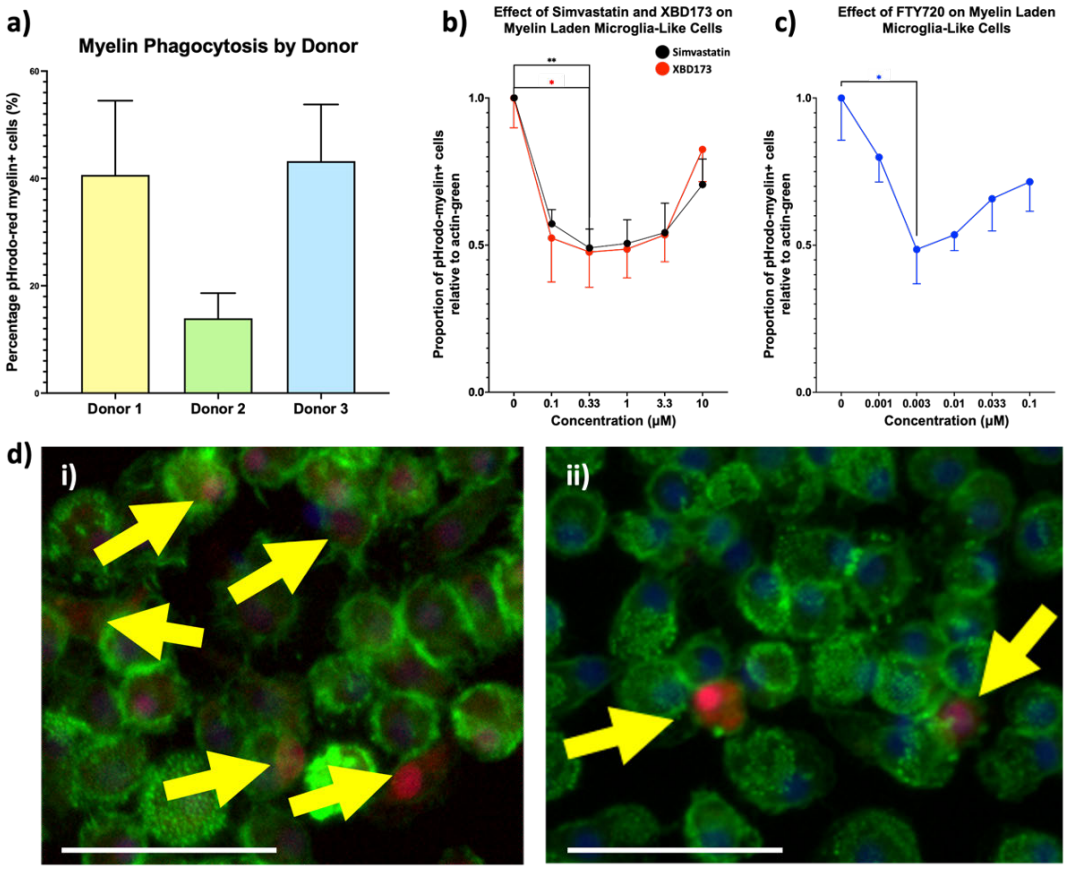

Figure 4.5 – Effect of MS-Related Drugs on Myelin Phagocytosis

Induced microglia-like cells were challenged with 3 μg per well of pHrodo-red tagged myelin for 8 hours. I assessed their baseline phagocytosis by treating with myelin plus drug vehicle (DMSO or water) for 24 hours (a). Simvastatin, XBD173 (b) or FTY720 (c) were added at various concentrations for 16 hours to assess their ability to improve myelin clearance. Staining of pHrodo-red myelin treated cells in the absence of drugs (green = cells, red = myelin, blue = nuclei) (di), the addition of simvastatin resulted in a reduction in the number of pHrodo-red myelin+ cells (bii). Arrows point to pHrodo-red myelin+ cells. All 3 drugs reduced the proportion of myelin-laden cells by up to 45% (b, c). *p<0.05, **p<0.01, Kruskal-Wallis with Dunn's post-test. Graphs show mean ± standard deviation. n = 3 donors. Images were captured using an EVOS M5000 epifluorescence microscope. Scale bars = 50 μm.

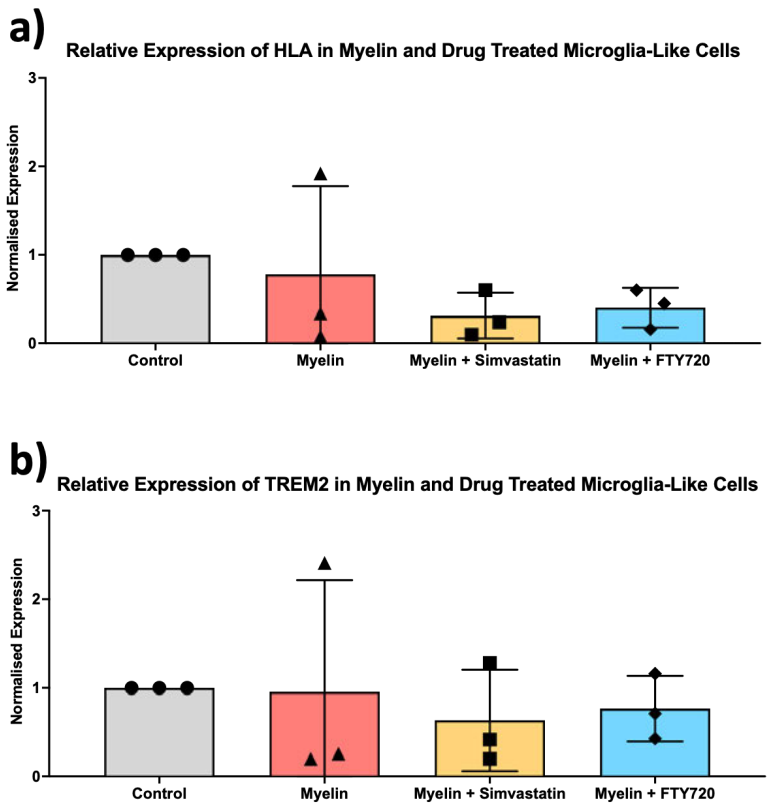

Figure 4.6 – Relative Expression of HLA and TREM2 in Myelin and Drug Treated Microglia-Like Cells

The relative expression of *HLA* (a) and *TREM2* (b) was calculated via qPCR. No significant differences were observed. Simvastatin and FTY720 reduced HLA expression with a fold change of 0.6 and 0.5 respectively, however this did not reach significance. Control – induced microglia-like cells treated with a vehicle for 24 hours (DMSO or water); myelin - induced microglia-like cells treated with pHrodo-red myelin for 24 hours; myelin + simvastatin - induced microglia-like cells treated with pHrodo-red myelin for 8 hours, with the addition of 0.33 μM simvastatin for 16 hours; myelin + FTY720 - induced microglia-like cells treated with pHrodo-red myelin for 8 hours, with the addition of 0.003 μM FTY720 for 16 hours. Graphs show mean ± standard deviation. n = 3 donors.

4.4 Discussion

4.4.1 – Induced Primary Microglia-Like Cells Phagocytose Human Myelin and Express Cholesterol-Related Metabolism and Export Machinery

Following methodology developed by Sellgren *et al* (Sellgren et al., 2017), I generated primary microglia-like cells from whole blood from healthy donors, in order to model myelin phagocytosis *in vitro*. First, it was determined whether these cells resembled endogenous microglia.

The induced microglia-like cells morphologically resembled endogenous microglia more closely, than the parent, blood derived monocytes; growing less spherical, larger and extending multiple fine processes. Additionally, immunocytochemical analysis confirmed that the induced microglia-like cells expressed immunomodulatory proteins, typically expressed by microglia and macrophages (HLA, TMEM119, TREM2, CD68 and C1Q) (Butovsky and Weiner, 2018. Due to the potential role of microglia in cholesterol homeostasis regulation (Lampron et al., 2015; Grajchen et al., 2018), I next confirmed that the induced microglia-like cells expressed relevant transcripts for the synthesis of cholesterol metabolism and transport machinery (*CYP27A1*, *APOE*, *ABCA1 and SOAT1*) (Griffiths and Wang, 2022) by ISH. Finally, I confirmed that a variable proportion of the induced microglia-like cells could phagocytose human myelin.

Interestingly, the myelin-lipid phagocytosis capacity of the induced microglia-like cells was significantly lower than that of cultured THP-1s, an immortalised human monocyte cell line. Up to 90% of PMA-stimulated THP-1 cells were shown to phagocytose myelin, whereas less than half (40%) of the FBS-stimulated induced microglia-like cells phagocytosed myelin. The capacity to phagocytose myelin was highly donor-dependent: cells isolated from some donors had an even more reduced myelin phagocytosis capacity, with less than 10% of cells positive for myelin-lipid debris, after incubation with pHrodo-red myelin; and may also differ to the THP-1s due to the different method of activation (PMA versus serum). A similar finding was reported by Hendrickx *et al* (Hendrickx et al., 2014), who found that THP-1 cells phagocyted myelin at a faster rate compared to their primary microglia model (primary, endogenous microglia obtained from unfixed brain at autopsy). They also presented findings which may shed light on the large inter-donor variability in myelin phagocytosis capacity reported here. They observed increased myelin uptake by aged microglia. I also observed this - for example, data presented in figure 4.5 shows 2 donors with increased myelin phagocytosis (donors 1 and 3), these donors were 55 and 54 respectively, whereas donor 2, who's cells had a lesser capacity for myelin phagocytosis, was 24 years old. Microglial senescence is a known age-associated

phenomenon (Spittau et al., 2017). Microglia in the MS brain present with a prematurely aged senescent phenotype (Musella et al., 2018) and age is a major determinant of the risk of transitioning to SPMS, being more disabled or being diagnosed with PPMS (Vaughn et al., 2019).

Together, these findings provided confidence that this model of primary induced microglia-like cells could be used to model the myelin debris phagocytosis present in the brains of people with MS.

4.4.1.1 – Relevance of the Lipid-Laden Microglia Model to MS Pathogenesis

Zrzavy *et al, 2017,* have shown that there is a shift towards an increase in microglia/macrophage-like cells with a dominant pro-inflammatory phenotype at the slowly expanding lesion edge of MA/I WML (Zrzavy et al., 2017). This agrees with the work by Bogie and Hendricks, which suggests that continuous myelin phagocytosis may generate damaging, lipid-laden foamy macrophages, as opposed to pro-reparative microglia described by Lampron and colleagues (Lampron et al., 2015; Grajchenet al., 2018). These foamy macrophages may contribute to the cholesterol metabolism/homeostasis dysregulation, which was identified at the slowly expanding MA/I WML edge. The continuous, chronic inflammation and demyelination measured at the edge of MA/I WML correlates clinically with a worse MS-prognosis and pathologically, with a more severe and aggressive disease (Luchetti et al., 2018). Many of these lesions can be measured *in vivo* by MRI as iron-rim lesions (Absinta et al., 2019). Attempts to model the dysfunctional lipid-laden phagocyte in culture will further our understanding of foamy macrophage biology, which could represent a viable treatment target to reduce active demyelination and improve clinical outcomes.

4.4.2 – Treatment with Simvastatin, FTY720 and XBD173 Promotes Myelin-Lipid Efflux from Induced Primary Microglia-Like Cells

As previously discussed, (see 4.1.2) phagocytosis of myelin-debris may either cause a proinflammatory and damaging, or an anti-inflammatory and pro-reparative, microglial phenotype (Grajchenet al., 2018). In chapters 2 and 3 of this thesis it was

demonstrated that cholesterol metabolism is dysregulated in the human MS brain, at sites of on-going, chronic inflammation. Having hypothesised that foamy macrophages are in fact damaging, due to the release of pro-inflammatory and damaging soluble factors, resulting from a failure to store or effectively efflux cholesterol, I tested whether current or experimental MS-relevant drugs affected this system.

Firstly, the optimal concentration and incubation time of pHrodo-red myelin was identified. These, and others', results have shown that myelin treatment for more than 24 hours can cause toxicity and excessive microglial cell death in culture (Hendrickx et al., 2014). The results in this thesis showed that treatment with 3 μg of tagged-myelin for 8 hours provided sufficient material and time for a significant level of phagocytosis within the culture well. The effects of drugs were also tested. The drugs were incubated with the myelin treated cells for 16 hours – ensuring that the total time the cells were exposed to myelin did not exceed 24 hours (8+16 hours), to mitigate excessive cell death. Hendrickx *et al* have also performed myelin-phagocytosis assays, using primary endogenous microglia. They incubated their cells with 12 μg of pHrodo-red myelin per well, for 24 hours – more than 4 times the pHrodo-red myelin concentration used in this study. Despite the large concentration difference, the number of pHrodo-red myelin positive cells, after 8 hours of treatment, were similar between this study (9-40%) and Hendrickx's assay (15%) (Hendrickx et al., 2014). The differences between the concentrations used and the proportion of positive cells are likely due to a high inter-variability of phagocytosis capacity between donor cells and/or the use of differing models of microglia.

Next, whether MS-related drugs could promote cholesterol efflux in this culture model was explored. Treatment with 0.001 and 0.003 μM FTY720, for 16 hours showed a reduction in the number of pHrodo-red myelin positive cells. The optimal dose was found to be 0.003 μM. FTY720 may have a mode of action which affects cholesterol homeostasis (Briard et al., 2011). For example, in an animal model of Niemann-Pick Type C disease (a fatal neurogenerative disorder), phosphorylated-

FTY720 was shown to increase the mRNA and protein expression of NPC1, a protein involved in intracellular trafficking of cholesterol. Its upregulation results in increased cholesterol efflux from lysosomes via apolipoproteins; experimentation in human cell lines also showed decreased cellular cholesterol (Vance et al., 2006; Newton et al., 2017)(Vance et al., 2006; Newton et al., 2017). Additionally, FTY720 may exert its affect by upregulating the synthesis of 26-HC, thus indirectly inducing the increased production of cholesterol efflux transporters, such as APOE and ABCA1, by 26-HC ligand-receptor binding to LXR-α/ LXR-β (Blom et al., 2010).

Simvastatin treatment also reduced the number of pHrodo-red myelin positive cells when used at a concentration of 0.1 and 0.33 μM; the optimum simvastatin concentration was 0.33 μM. Simvastatin is a lipophilic statin, capable of crossing the BBB. It is currently being tested in a phase III clinical trial of SPMS, after a positive outcome at phase II which showed that treatment with high-dose simvastatin significantly reduced annualised whole brain atrophy (Chataway et al., 2014). High dose simvastatin treatment reduces cholesterol synthesis in macrophages by competitively binding to HMG-CoA reductase, reducing cholesterol synthesis from mevalonate (Stancu and Sima, 2001). Simvastatin treatment has also been reported to modulate the reduction of esterified cholesterol accumulation in macrophages; additionally, it has been implicated in polarising macrophages towards a more anti-inflammatory phenotype in atherosclerosis (Bellosta et al., 2000; Stancu and Sima, 2001).

Lastly, treatment with a concentration of 0.1 and 0.33 μM XBD173 also reduced the number of pHrodo-red myelin positive cells. The least number of pHrodo-red myelin positive cells were present after treatment with 0.33 μM XBD173. XBD173, is an experimental MS drug, which may also be beneficial in the promotion of cholesterol homeostasis. XBD173 is a TSPO ligand. TSPO is a receptor expressed by microglia/macrophages which is involved in facilitating the transport of cholesterol from the cytosol to the mitochondria. It is then metabolised into steroid hormones and neurosteroid precursors. In the setting of cholesterol efflux, this shuttling and

later metabolism may be responsible for the reduction of myelin-lipids in cells treated with XBD173 (Rupprecht et al., 2010; Lejri et al., 2019). However, it is also likely to have off lipid-target affects, such as polarisation of microglia to an anti-inflammatory phenotype (see 4.1.4).

Treatment with each drug altered the number of pHrodo-red myelin+ cells in a J-curve manner. Concentrations above the optimal concentration for each drug resulted in an increase of myelin-lipid positive cells, suggesting that higher concentrations were either toxic to the cells, or that higher concentrations of these drugs had a non-lipid efflux related effect (Angeli et al., 2013). The dosage chosen for drug assays were similar to viable concentrations used by others in the literature (Lindberg et al., 2005; Noda et al., 2013).

Others have shown that diminished cholesterol efflux from macrophages can lead to a damaging microglia phenotype, due to the formation of cholesterol crystals and subsequent lysis of macrophages, resulting in the release of proinflammatory and damaging cytokines (Cantuti-Castelvetri et al., 2018). To date, cholesterol crystals have not been reported in MS lesions; it would be interesting to test for their presence in actively demyelinating lesions (active and the edge of MA/I lesions) in future. Nevertheless, over-accumulation of cholesterol and its altered metabolism or efflux is associated with inflammation and a reduced capacity for repair (Haider et al., 2011; Lampron et al., 2015; Grajchen et al., 2018). The results presented here have shown that each of the MS-related drugs discussed above can reduce the number of myelin-lipid laden primary induced microglia-like cells, in an *in vitro* model for myelin phagocytosis. Although each drug likely had effects outside of improving cholesterol efflux by macrophages, these results suggest that they also affect this system. In the context of MS, where dysregulation of cholesterol metabolism has been shown to be present in areas of important, damaging, chronic inflammation, these drugs may be clinically useful, and may possibly be beneficial in the regulation/ promotion of an anti-inflammatory microglial phenotype.

4.5 Limitations

The work presented in this chapter has demonstrated that induced human primary microglia-like cells, derivatised from monocytes, can be used to model active myelin phagocytosis in culture, and that MS-related drugs can promote cholesterol clearance. However, there are a number of limitations to this work which need to be addressed.

First and foremost, the cells utilised in this study were not endogenous microglia and were isolated from healthy donors and grown *in vitro*. Having shown that the primary induced microglia and THP-1 cells have greatly differing myelin phagocytosis capacity, the nature of the microglia model clearly needs careful consideration for future experiments, to best represent endogenous myelin clearance. Hendrickx *et al* have previously shown differences in the rate of myelin phagocytosis based on the origin of the isolated myelin (MS or control NAWM), which I did not account for in this study, instead the myelin used was pooled from both MS and control. (Hendrickx et al., 2014). Therefore, the findings from this study may not be fully representative of the endogenous activity of microglia or the effect of drugs on these cells in the MS brain. Additionally, a large inter-donor variability in terms of the cells ability to phagocytose myelin was observed. Hendrickx demonstrated that the age of the microglia donor impacts phagocytosis ability, which was also observed here, but due to the sample size this can only be taken as a qualitative observation. To attempt to account for these potentially confounding factors, a much larger cohort would need to be used in the future, where differences in donor age/gender/other demographics could be accounted for. Additionally, cell viability assays were not performed using a specially designed assay. Cells were inspected microscopically every day to inspect their changing growth and morphology. For the functional myelin phagocytosis studies, cells were judged on their phagocytic ability microscopically; DAPI nuclear staining was used to identify apoptotic bodies to ensure that dead cells were not included in analyses.

Next, different stimuli were used for the THP-1 and primary microglia-like cells. PMA is a typical stimulus used to activate THP-1 cells in the literature. A much 'gentler' stimulus for the primary cells - addition of 10% FBS for 24 hours – was chosen to attempt to keep the primary cells in as natural a state as possible *in vitro*, having shown that experiments without any stimulus to activate the cells resulted in little activation/phagocytic capability. Unlike the primary cells, which have limitations in regard to how many cells could be obtained per donor, the challenge of finding donors and the time taken to isolate and culture primary cells, the THP-1s were readily available. As such, the THP-1s were only used for optimisation of protocols and were never used as a comparison to the primary cells, therefore despite the use of different stimuli, this has not affected the primary cell experimentation/analyses.

Due to the acquisition of healthy blood donors, the time taken to isolate and derivatise primary monocytes to microglia-like cells and the time taken to optimise experimental conditions, the sample size for myelin phagocytosis and drug assays was small. Despite this, it has been shown that FTY720, simvastatin and XBD173 may promote cholesterol efflux in lipid (cholesterol)-laden, activated microglia, expressing a foamy macrophage-like phenotype. However, in order to confirm this, as well as identify any changes in gene expression between treatment groups, this will need to be repeated on a much larger scale using multiplex assays to provide an understanding of molecular changes between lipid-laden and drug treated microglia.

4.6 Conclusion

Myelin phagocytosis was successfully modelled, *in vitro*, using induced microglia-like cells, derived from primary human monocytes. Evidence in the literature suggests that the formation of foamy, lipid-laden macrophages, present at sites of chronic, inflammatory demyelination, are damaging in MS, and prevent remyelination. The formation of these foamy cells may be due to diminished cholesterol clearance. To this end I have investigated whether currently available MS-related drugs could promote cholesterol clearance, and the results presented here have demonstrated that FTY720, simvastatin and XBD173 may be suitable for this purpose. This will need

to be validated in a larger cohort, however, the findings in this chapter are proof of concept and warrant further investigation. Taken together, these results provide evidence that dysregulated cholesterol efflux may be a druggable target, capable of reducing persistent, chronic inflammation, in progressive MS.

Chapter 5 – Discussion and Future Directions

5.1 Discussion

5.1.1 – Validation and Resolution of Methodology

The use of highly precise *MS* has allowed for the confident identification and quantification of sterols within the human brain. This has revealed, for the first time, that cholesterol and some of its metabolites, including 24S-HC and 25R(26)-hydroxycholesterol (26-HC), are altered within areas of ongoing, chronic, inflammatory demyelination, in MS. Time was taken to thoroughly characterise tissue samples, allowing regions of actively demyelinated tissue to be well matched between cases. However, this has contributed to this study being low throughput, with only 18 (10 WM, 8 GM) lesions from 7 cases studied, plus matching normal appearing tissue and tissue from controls. In addition to the time taken to comprehensively characterise tissue samples, the EADSA preparation method for sterol extraction and charge-tagging, the time taken to run and quantify complex samples, as well as, *in vitro* mechanistic assays, were time consuming. Despite this, this work has provided evidence that cholesterol metabolism is altered within the MS brain, suggesting that the differences reported here are robust.

5.1.2 – 24S-Hydroxycholesterol as a Drug Target for the Treatment of Progressive MS

24S-HC is synthesised from cholesterol; its synthesis is primarily facilitated by neurons. It is then shuttled to relevant cells within the CNS (such as microglia) or is shuttled out of the brain, preventing over accumulation of cholesterol (Zhang and Liu, 2015). A striking reduction in the *CYP46A1* mRNA transcript, which encodes the

enzyme responsible for 24S-HC synthesis, 24-hydroxylase was observed. The expression of *CYP46A1* was decreased in MS NAGM by more than 98%, compared to control GM. Although a reduction at the mRNA level doesn't necessarily translate to the protein level, the enzyme product, 24S-HC, was found to be reduced in the same MS samples. This is suggestive of substantially altered and perhaps defective cholesterol metabolism by neurons in MS. Increasing *CYP46A1* expression and subsequent increase of its enzyme, 24-hydroxylase, and therefore 24S-HC, would likely improve cholesterol flux, reducing CNS cholesterol content via removal to the periphery, where it can be used as a substrate for other metabolites, such as bile acids (Wang et al., 2021). Excitingly, *CYP46A1* is a druggable target. It has been reported to be associated with AD, where a small clinical pilot study of early AD has tested the ability of efavirenza, a licenced anti-HIV drug, to increase *CYP46A1* activity, and subsequently increase the synthesis of 24-hydroxylase and 24S-HC. This pilot study confirmed that daily treatment with 200 mg of efavirenza increased 24S-HC in plasma, CSF and within the brain (Lerner et al., 2022). Investigation into the use of efavirenza in MS should be considered.

5.1.3 – Cholesterol Flux and Lipid-Induced Toxicity in Microglia

Microglia play an important role in brain health. They regulate the immune response, contribute to neuronal health and synaptic plasticity, and are heavily involved in the mechanisms regulating cholesterol homeostasis (Parkhurst et al., 2013). Additionally, astrocytes are also highly involved in cholesterol homeostasis and are the main suppliers of cholesterol to CNS neurons in adulthood. In MS, microglia are central to demyelination (and subsequently neurodegeneration) (Berghoff et al., 2022b). Microglia possess the machinery needed to allow phagocytosis; in MS the expression of phagocytosis related genes is upregulated in response to external stimuli, such as myelin debris (Zrzavy et al., 2017). Alterations in cholesterol, 24S-HC and 26-HC were found at the actively demyelinating rim of lesions, which contain a high number of foamy macrophages, suggesting that microglia and astrocytes have some involvement in cholesterol dysregulation at these sites of ongoing damage.

There is some debate surrounding whether foamy macrophages promote a beneficial or harmful environment (Lampron et al., 2015; Grajchen et al., 2018). It's probable that there is a switch from a pro-reparative, anti-inflammatory function, to a damaging, pro-inflammatory phenotype, at later stages of lesion development. As a consequence of myelin degeneration and processing by microglia and macrophage-like cells after phagocytosis, lipids, namely cholesterol, are released. (Berghoff et al., 2022b). At sites of new, active demyelination, phagocytosis of myelin facilitates downregulation of cholesterol synthesis related genes, by inhibition of the SREBP/SCAP complex. Horizontal transfer of cholesterol from microglia (and astrocytes) to other cell types, helps to facilitate myelination, myelin remodelling and neuron function. Additionally, cholesterol metabolism by all neural cells, increases the synthesis of oxysterols. Oxysterols, such as 24S-HC and 26-HC activate LXR-α and LXR-β by ligand-receptor binding, subsequently promoting the synthesis of cholesterol lipoproteins and efflux transporters, such as APOE and ABCA1. These lipoproteins and transporters facilitate a cycle of cholesterol export from the microglia and macrophage-like cells, which in turn provides more substrate for oxysterol synthesis (figure 5.1). Cholesterol flux also promotes an anti-inflammatory response. The beneficial effect of microglia/macrophage-like cells at earlier stages of MS disease is also supported by increased remyelination capacity by oligodendrocytes. Remyelination is impeded by myelin debris and therefore its removal is imperative for regenerative processes (Miron et al. 2013; Miron, Kuhlmann, and Antel 2011; Miron and Franklin 2014), adding to the importance of the need for cholesterol homeostasis. It's likely that this process occurs prior to symptomatic onset of MS, and in the early RR-phase, where reparative mechanisms are most effective and symptoms are at their mildest (Mailleux et al., 2017; Voskuhl et al., 2019; Berghoff et al., 2020; Berghoff et al., 2021; Berghoff et al., 2022b).

This process linking cholesterol flux with an anti-inflammatory and restorative microglial response is altered in areas of chronic, demyelination (present predominantly in the brains of people with longstanding, progressive MS, but also present in earlier disease) (Kuhlmann et al., 2017; Lassmann, 2018; Berghoff et al.,

2022b). Within the chronic demyelinating lesion, a prolonged exposure to myelin-lipids may have an opposite and damaging effect on microglia and macrophage-like cells, which contributes to lesion expansion and worsening of symptoms (Luchetti et al., 2018; Grajchen et al., 2018; Absinta et al., 2019). I have identified the presence of a high number of lipid-laden, foamy macrophages at the edge of slowly expanding, MA/I WML, positive for markers of esterified-cholesterol and lipid-rich droplets (oil-red O+ and perilipin-2+). Following myelin phagocytosis by these cells, cholesterol build-up likely downregulates cholesterol biosynthesis, then ineffective clearance of cholesterol by foamy macrophages prevents horizontal transfer of cholesterol, inhibiting remyelination efforts which rely on recycled cholesterol (figure 5.1) (Grajchen et al., 2018; Berghoff et al., 2020; Berghoff et al., 2022b).

In a model of inflammageing, cholesterol efflux failure by macrophages led to cholesterol storage as crystals causing subsequent cell lysis, and therefore the release of damaging soluble factors (Cantuti-Castelvetri et al., 2018). I have shown that 24S-HC and 26-HC (LXR-α/LXR-β ligands) are reduced in areas of chronic inflammation, such as at the MA/I WML edge. This supports the hypothesis that a reduction of LXR activation causes diminished cholesterol efflux and thus a maladaptive and continued inappropriate immune response by foamy macrophages in MS (Mailleux et al., 2017; Cantuti-Castelvetri et al., 2018; Berghoff et al., 2020). Others have shown that during chronic demyelination (particularly when this is coupled with astrocyte loss) other cell types, including neurons and oligodendrocytes, begin to upregulate cholesterol synthesis, presumably to counteract the lack of available recycled cholesterol, thus facilitating some remyelination (Berghoff et al., 2021). However, ultimately this is unable to keep up with continued demyelination, resulting in presently irreversible axonal damage and loss (Heß et al., 2020).

5.1.3.1 – Resolution of Defective Cholesterol Homeostasis Could be a Drug Target for Progressive MS

Current DMTs focus on regulating the peripheral immune response and act to prevent inflammatory infiltration into the CNS via the disrupted BBB. These DMTs have been successful in reducing annualised relapse rates in people with RRMS, but

the majority of these people still accumulate disability and many convert to the secondary progressive form of the disease over time (Callegari et al., 2021). This highlights that there are underlying important drivers of disease which cause worsening in many people with MS that are not effectively modified by today's medicines.

Cholesterol homeostasis dysregulation may contribute to the underlying mechanisms causing progression independent of relapse activity (PIRA). Although evident in later disease, it is likely that PIRA is occurring alongside the inflammatory driven, acute phase of the disease, and likely also prior to symptom onset – therefore modulation of this would likely benefit both people with early disease, as well as those who have already entered the progressive phase (Confavreux and Vukusic, 2014; Elliott et al., 2019; Cree et al., 2019; Tur et al., 2023). Understanding PIRA mechanisms, and identifying druggable targets, will be crucial for future MS treatment. Current and/or experimental MS drugs have an effect on cholesterol homeostasis, either directly, such as simvastatin, or indirectly, such as fingolimod (FTY720) (Stancu and Sima, 2001; Vance et al., 2006; Sirtori, 2014; Ramkumar et al., 2016; Newton et al., 2017). The investigation of their effect on myelin phagocytosis *in vitro* revealed that addition of these drugs to myelin-lipid-laden cells, reduced the number of cells positive for myelin, therefore suggesting that these drugs can promote cholesterol clearance. Further investigation into the mechanism behind improved clearance will be needed to appreciate if this contribution to enhanced cholesterol flux represents a meaningful mode of action of these drugs in the patient.

a) Early, Active Demyelination

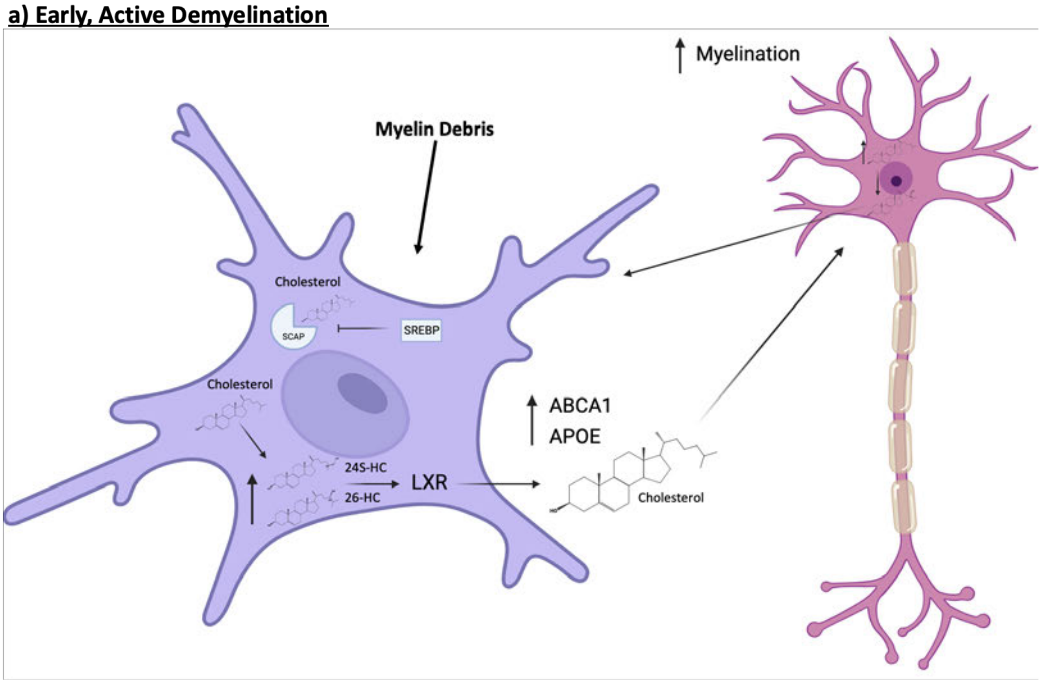

b) Prolonged, Chronic Demyelination

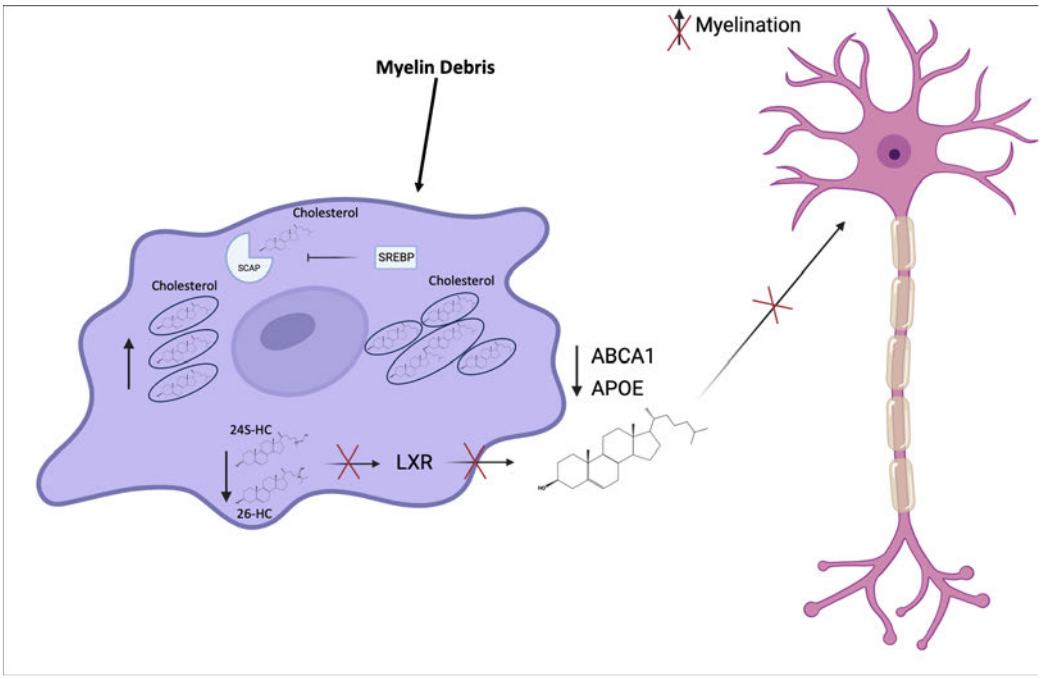

Figure 5.1 – Proposed Cholesterol Homeostasis Dysregulation

Early disease with active demyelination: myelin debris uptake results in increased cholesterol within the cell. Increased cellular cholesterol downregulates cholesterol synthesis by microglia by binding to SCAP, preventing the binding of SREBP. Cholesterol is oxidised to its products such as 26-HC, which along with neuron-generated 24S-HC, activates LXR, resulting in the upregulation of cholesterol transporters (e.g.,

ABCA1 and APOE) which allows for the horizontal transfer of cholesterol to neurons. This provides cholesterol to permit myelination and also provides a substrate for 24S-HC synthesis, which can be transferred back to microglia, allowing for continued clearance of cholesterol (a). Prolonged disease with continuous demyelination: continued myelin phagocytosis results in an overaccumulation of cholesterol within the cell, resulting in its storage as lipid-laden droplets. Cholesterol homeostasis is dysregulated. There is a reduction in the concentration of oxysterols including LXR-ligands. A decrease in LXR activation results in a reduction of cholesterol transporters, reducing horizontal transfer of cholesterol to neurons. This reduces available neuronal cholesterol for myelination and reduces the substrate for 24S-HC synthesis, thus further reducing the concentration of LXR-ligands within the foamy macrophage-like cell, ultimately contributing to inappropriate retention of cholesterol by the cell/ cholesterol homeostasis dysregulation. SCAP - SREBP cleavage and activating protein, SREBP - sterol regulatory element binding protein, 26-HC – 26-hydroxycholesterol, 24S-HC – 24S-hydroxycholesterol, LXR – liver X receptor, ABCA1 – adenosine trisphosphate-binding cassette A1, APOE - Apolipoprotein E. Image produced using Biorender.com.

5.1.3.2 – Improvement in Neuronal 24S-Hydroxycholesterol Could Promote Microglia Homeostasis Resolution

The cells within the CNS are very dynamic and are in constant communication with each other (Vainchtein and Molofsky, 2020). This work has shown that 24S-HC is reduced in the WM of the MS brain, in regions of actively demyelinating tissue. Targeting neuronally-synthesised 24S-HC production, via upregulation of *CYP46A1* (see 5.1.2), could potentially aid resolution of foamy macrophage-led cholesterol homeostasis dysfunction. Increasing neuronal 24S-HC, and therefore available 24S-HC for uptake by foamy macrophages, could possibly facilitate a phenotypic shift in microglia from pro-inflammatory and damaging, back towards an anti-inflammatory and myelin-lipid recycling phenotype, consequently improving remyelination efforts (Lutjohann et al., 1996; Lund et al., 1999; Fukumoto et al., 2002; Lund et al., 2003; Tall, 2008; Matsuda et al., 2013; Zhang and Liu, 2015).

5.2 Future Directions

The findings presented in this thesis have identified cholesterol and oxysterol dysregulation in the MS brain. The next step will be to confirm these findings in a larger cohort. There is a need to ascertain how this foundation knowledge of alteration in the brain can be practically used clinically. Oxysterols, such as 24S-HC,

are able to traverse the BBB and are exported from brain into the periphery (Zhang and Liu, 2015). Work within our group is currently ongoing to identify If circulating levels of oxysterols in the CSF and plasma correlate to the change in concentration of cholesterol and key oxysterols identified in the brain. One such potentially valuable biomarker would be 24S-HC. 24S-HC is only generated in the CNS and 24S-HC could provide a real-time measure of neuron health to monitor the effectiveness of a DMT in later stages of the disease, at a time when the disease may be worsening but where neuroimaging is less informative. Biomarkers of the worsening progressive phase are urgently needed as serum neurofilament-light levels do not accurately reflect this component of the disease (Masanneck et al., 2022; Ransohoff, 2023). If so, oxysterols may serve as biomarkers, able to act as a surrogate to identify alterations to processes in the CNS. This could be useful both as a method to monitor the effectiveness of cholesterol metabolism-related trial drugs and/or to identify people who may benefit from cholesterol homeostasis restoring drugs in the future (Leoni and Caccia, 2011).

This work has demonstrated that it would be justifiable to continue this research, to aid our understanding of cholesterol flux dysregulation in MS. This work could be furthered in a variety of ways. It will be necessary to understand oxysterol dysregulation in other regions of pathological interest, such as remyelinating lesions and shadow plaques. This work has also only touched upon dysfunction in the GM, understanding cholesterol homeostasis dysregulation in specific GML, as well as within different layers of the normal appearing cortex, will be essential to further our understanding of defective cholesterol flux in the MS brain, in a more holistic manner. Employing LESA (see 2.1.2), a *MS*I technique, would theoretically allow multiple lesion types/brain regions to be simultaneously sampled to measure the abundance of a variety of oxysterols. In addition to expanding the lesion types included for analysis, it will be important to increase the sample number, so that comparisons between different demographics, such as gender and chronological age, can be made.

Eventually, this work has the potential to be clinically translatable. The mechanism of action of high-dose simvastatin needs to be elucidated. Induced microglia-like cells could be generated from the blood of participants of the MS-STAT trial. The phagocytic capacity of cells derived from those treated with and without simvastatin could be compared. In addition to comparisons of cholesterol efflux, an array of the cells genetic profile could be compared; for example, via either cellular RNA extraction, or supernatant collection, which would allow transcriptomic profiling using a platform such as Nanostring. This would permit large scale identification of individual genes or pathways which may be altered by simvastatin treatment, shedding light on its mode of action. Additionally, the plasma from simvastatin treated and simvastatin naïve patients could also be assayed to assess changes at the gene-level in the periphery. This could also be applied to identify the mechanism of action of other cholesterol homeostasis-related drugs, such as fingolimod, which could be compared to DMTs which do not affect cholesterol homeostasis.

Together, this highlights that furthering this research is justifiable and valuable for the enhancement of our understanding of cholesterol homeostasis in MS, with the hope of identifying true druggable targets.

5.3 Conclusion

There is currently an unmet need for drugs which are able to slow, stop or reverse progressive MS (Hollen et al., 2020). Identification of PIRA has highlighted a need for therapeutics which treat the underlying cause of progression, in addition to acute inflammation. This progression likely contributes to MS disease from, or even prior to, clinical presentation (Tur et al., 2023). The results presented in this thesis provide evidence that cholesterol metabolism/oxysterol dysregulation may contribute to mechanisms which permit continued chronic demyelination and neurodegeneration, present in the brains of people with MS. Identification that oxysterols (including 24S-HC) and cholesterol-metabolism related transcripts (such as *CYP46A1*) are reduced in the MS brain at sites of chronic, inflammatory demyelination, may partly explain why foamy macrophages fail to successfully process myelin debris post-phagocytosis,

contributing to a failure to resolve damage. Currently available drugs have been shown to promote myelin efflux *in vitro* and excitingly others have shown that *CYP46A1* expression can be modulated to improve 24S-HC synthesis. Taken together, the findings presented in this thesis support the theory that cholesterol homeostasis is dysregulated in the MS brain and that treatment to restore cholesterol homeostasis may be beneficial for people with progressive MS.

Appendix

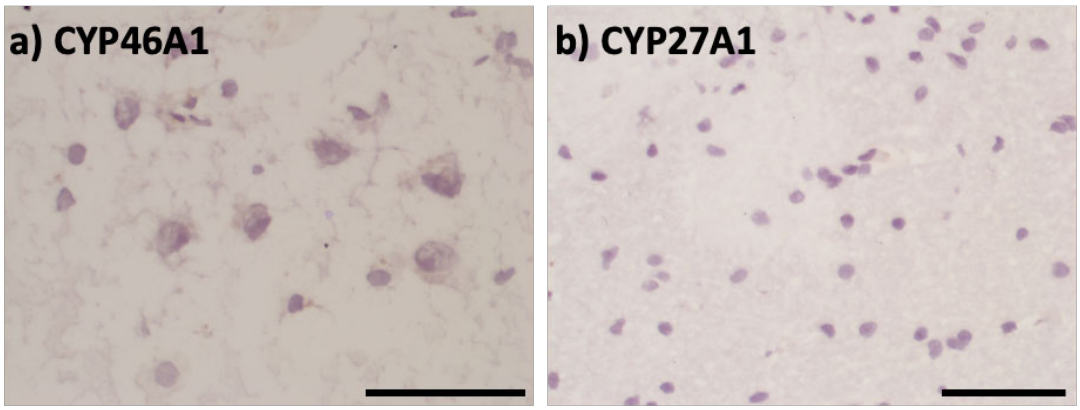

Supplementary Figure 1.1 – Negative Antibody Controls

Novel antibodies to the group were tested using antibody negative controls, CYP46A1 (a) and CYP27A1 (b). All other antibodies used had been validated previously. Scale bars = 100 μm. CYP27A1 - Cytochrome P450 family 27 subfamily A member 1, CYP46A1 - Cytochrome P450 family 27 subfamily A member 1.

Supplementary Table 1.1 – General Materials and Suppliers

Reagents and Consumables	Supplier	Product Code
1.5 ml Eppendorf Tubes	Star Lab	S1615-5550
12 ml Greiner Tubes	Greiner Bio-One	163270
13 mm circular glass coverslips	Fisher Scientific	12392128
15 ml Falcon Tubes	Merck	430052
20-Gauge Needles	Fisher Scientific	12399169
60 mg Oasis® HLB 3cc Extraction Cartridges	Waters	WAT094226
200 mg Sep-Pak® Vac 3cc tC18 Cartridges	Waters	WAT054925
24-well plates	Greiner Bio-One	662160D186
3,3'-diaminobenzidine	Vector Laboratories Ltd	SK-4103
50 ml Falcon Tubes	Fisher Scientific	430921
96-well plates	Fisher Scientific	10564581
Avidin-Biotin Complex	2B Scientific	SK-4103-400
Basescope v2, Kit	Biotechne	323910
Blades	Fisher Scientific	12074088
BLOXALL	Vector Laboratories Ltd	SP-6000
Bovine Serum Albumin	Merck	A7030-10G
CD14 microbeads	Miltenyi Biotec	130-050-201
CK14 Precellys Tubes	Stretton Scientific	P000912-LYSK0-A
Copper Sulphate	Fisher Scientific	10695482
Cresyl Violet	Fisher Scientific	10045203
Cyrovials	Fisher Scientific	10545601
Dimethyl Sulfoxide	Fisher Scientific	10103483
Dithiothreitol	Fisher Scientific	10699530
DPX Mountant	Fisher Scientific	15538321
Fetal Bovine Serum	Fisher Scientific	12350273
FTY720	Merck	S6196-5MG
Gill's Haematoxylin	Merck	GHS132-1L
GM-CSF	Bio-Techne	215-GM-010/CF
Heparin Vacutainers	Fisher Scientific	13171543
HPLC Vials	Waters	186002639
Hydrogen Peroxide, 30%	Vector Laboratories Ltd	OKRA00049
IL-34	Bio-Techne	215-GM-010/CF
Immortalised THP-1 Cell Line	Gifted by Griffiths-Wang Group, Swansea Univeristy	-
ImmPRESS Alkaline Phosphatase	Vector Laboratories Ltd	mp-7452-15
Industrial Methylated Spirit	Fisher Scientific	11442874
KiCqStart SYBR Green qPCR ReadyMix (2X)	Merck	KCQS00-1250RX
Lithium Carbonate	Fisher Scientific	10741281
LTQ ESI Positive Calibration Solution	Fisher Scienific	11340360
Lymphoprep	Stemcell Technologies	07801
Nondeuterated Girard P	Tokyo Chemical Industrial	G0030
Normal Goat Serum	Merck	G9023-5ML
OCT	Fisher Scientific	1254271
PBS, 1x	Fisher Scientific	11593377
Penicillin Streptomycin	Fisher Scientific	11528876
Phorbol-12-myristate-13-acetate	Fisher Scientific	10515491
pHrodo-Red	Fisher Scientific	10676983
Poly-L-lysine Hydrobromide	Merck	P1274-25MG
PrecisionPLUS qPCR Master Mix (5ml - with SYBR green)	Primer Design	PPLUS-machine type-5ML
Precision nanoScript2 Reverse Transcription Kit	Primer Design	RT-NanoScript2
Protease Inhibitor Cocktail	Merck	11836170001
RNAscope 2.5 HD Kit	Biotechne	225394
RNAse/DNAse Free Water	Fisher Scientific	11538646
RNeasy Plus Mini Kit	Qiagen	217004
RPMI-1640 glutaMAX	Fisher Scientific	1202759
Scalpels	Fisher Scientific	12397999
Simvastatin	Merck	S6196-5MG
Sucrose	Fisher Scientific	11487417
Superfrost Adhesion Slides	Fisher Scientific	10149870
T-25 Culture Flasks	Merck	CLS431463-200EA
Triton-X-100	Fisher Scientific	11488696
Vector Blue	Vector Laboratories Ltd	SK-5300
VectorMount	Vector Laboratories Ltd	H-1000
XBD173	Merck	SML1223-5MG
Xylene	Fisher Scientific	10784001

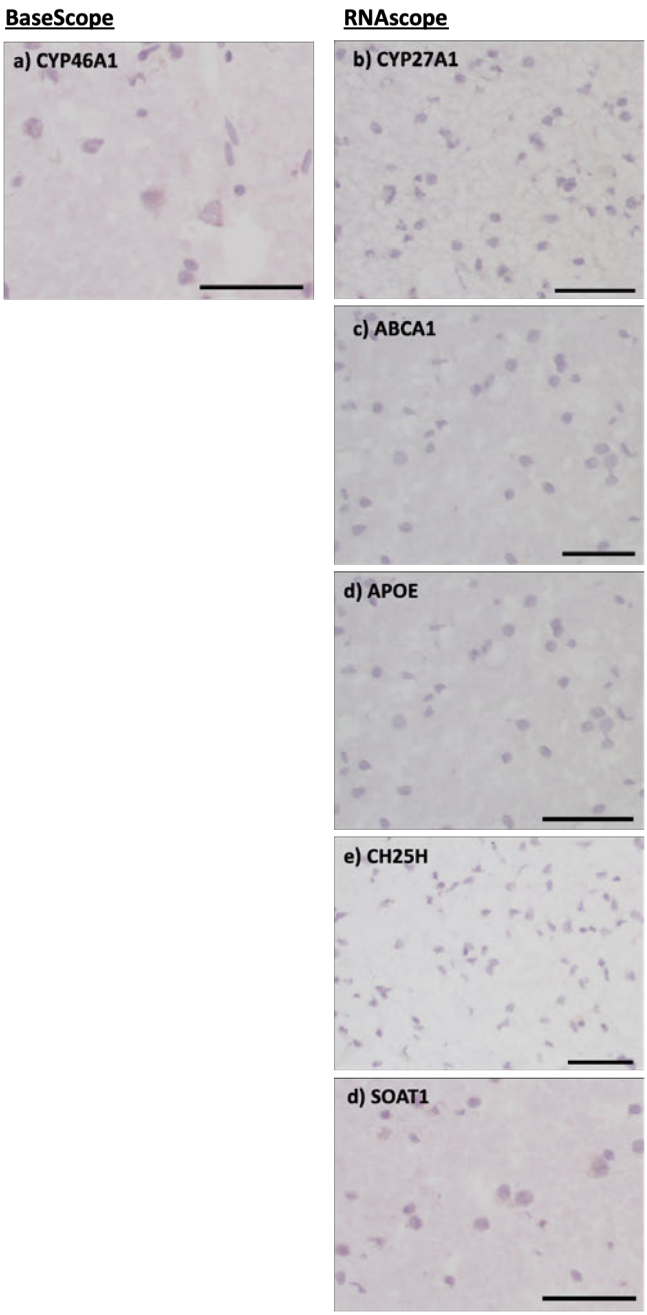

Supplementary Figure 1.2 – Negative RNAscope and BaseScope Controls

The probes used for BaseScope (a) and RNAscope (b-d) were tested using probe-negative controls. Representative images negative for CYP46A1 (a), CYP27A1 (b), ABCA1 (c), APOE (d), CH25H (e) and SOAT1 (d) are shown. n = 1 case tested. Images were captured using the Zeiss AxioScope microscope and Zeiss AxioCam black and white camera. Scale bars = 100 μm. CYP27A1 - Cytochrome P450 family 27 subfamily A member 1, CYP46A1 - Cytochrome P450 family 27 subfamily A member 1, ABCA1 - ATP-binding cassette A1, APOE - Apolipoprotein E, CH25H - Cholesterol 25-hydroxylase.

Bibliography

Abdel-Khalik, Jonas, Eylan Yutuc, Peter J. Crick, Jan-Åke Gustafsson, Margaret Warner, Gustavo Roman, Kevin Talbot, Elizabeth Gray, William J. Griffiths, Martin R. Turner, and Yuqin Wang. 2017. "Defective Cholesterol Metabolism in Amyotrophic Lateral Sclerosis." *Journal of Lipid Research* 58(1):267–78. doi: 10.1194/jlr.P071639.

Absinta, Martina, Pascal Sati, Federica Masuzzo, Govind Nair, Varun Sethi, Hadar Kolb, Joan Ohayon, Tianxia Wu, Irene C. M. Cortese, and Daniel S. Reich. 2019. "Association of Chronic Active Multiple Sclerosis Lesions with Disability In Vivo." *JAMA Neurology* 76(12):1474–83. doi: 10.1001/JAMANEUROL.2019.2399.

Abud, Edsel M., Ricardo N. Ramirez, Eric S. Martinez, Luke M. Healy, Cecilia H. H. Nguyen, Sean A. Newman, Andriy V. Yeromin, Vanessa M. Scarfone, Samuel E. Marsh, Cristhian Fimbres, Chad A. Caraway, Gianna M. Fote, Abdullah M. Madany, Anshu Agrawal, Rakez Kayed, Karen H. Gylys, Michael D. Cahalan, Brian J. Cummings, Jack P. Antel, Ali Mortazavi, Monica J. Carson, Wayne W. Poon, and Mathew Blurton-Jones. 2017. "IPSC-Derived Human Microglia-like Cells to Study Neurological Diseases." *Neuron* 94(2):278–93. doi: 10.1016/j.neuron.2017.03.042.

Adams, D.O., and Hamilton, T.A. (1984) The cell biology of macrophage activation. *Annu Rev Immunol* **2**: 283–318.

Angeli, Fabio, Gianpaolo Reboldi, and Paolo Verdecchia. 2013. "Hypertension and the J-Curve Phenomenon: Implications for Tight Blood Pressure Control." *Hypertension Research* 36(2):109–11. doi: 10.1038/hr.2012.165.

Angelini, Roberto, Eylan Yutuc, Mark F. Wyatt, Jillian Newton, Fowzi A. Yusuf, Lauren Griffiths, Benjamin J. Cooze, Dana El Assad, Gilles Frache, Wei Rao, Luke B. Allen, Zeljka Korade, Thu T. A. Nguyen, Rathnayake A. C. Rathnayake, Stephanie M. Cologna, Owain W. Howell, Malcolm R. Clench, Yuqin Wang, and William J. Griffiths. 2021. "Visualizing Cholesterol in the Brain by On-Tissue Derivatization and Quantitative Mass Spectrometry Imaging." *Analytical Chemistry* 93(11):4932–43. doi: 10.1021/acs.analchem.0c05399.

Ao, Tomoka, Junichi Kikuta, and Masaru Ishii. 2021. "The Effects of Vitamin D on Immune System and Inflammatory Diseases." *Biomolecules* 11(1624). doi: 10.3390/BIOM11111624.

Arnold, Douglas, Colm Elliott, Xavier Montalban, Emily Martin, Yann Hyvert, and Davorka Tomic. 2022. "Effects of Evobrutinib, a Bruton's Tyrosine Kinase Inhibitor, on Slowly Expanding Lesions: An Emerging Imaging Marker of Chronic Tissue Loss in Multiple Sclerosis." *Neurology* 98(18 Supplement).

Arnson, Yoav, Yehuda Shoenfeld, and Howard Amital. 2010. "Effects of Tobacco Smoke on Immunity, Inflammation and Autoimmunity." *Journal of Autoimmunity* 34(3):J258–65. doi: 10.1016/j.jaut.2009.12.003.

Bach, Jean-François,. 2002. "Effect of Infections on Susceptibility to Autoimmune and Allergic Diseases." *N Engl J Med* 347(12):911–20.

Bae, Keun-Ryung, Hyun-Jung Shim, Deebika Balu, Sang Ryong Kim, and Seong-Woon Yu. 2014. "Translocator Protein 18 KDa Negatively Regulates Inflammation in Microglia." *Journal of Neuroimmune Pharmacology* 9(3):424–37. doi: 10.1007/s11481-014-9540-6.

Bankhead, Peter, Maurice B. Loughrey, José A. Fernández, Yvonne Dombrowski, Darragh G. McArt, Philip D. Dunne, Stephen McQuaid, Ronan T. Gray, Liam J. Murray, Helen G. Coleman, Jacqueline A. James, Manuel Salto-Tellez, and Peter W. Hamilton. 2017. "QuPath: Open Source Software for Digital Pathology Image Analysis." *Scientific Reports* 7(1):1–7. doi: 10.1038/s41598-017-17204-5.

Barber, Casey N., and Daniel M. Raben. 2019. "Lipid Metabolism Crosstalk in the Brain: Glia and Neurons." *Frontiers in Cellular Neuroscience* 13(212). doi: 10.3389/FNCEL.2019.00212/BIBTEX.

Barnett, Michael H., and John W. Prineas. 2004. "Relapsing and Remitting Multiple Sclerosis: Pathology of the Newly Forming Lesion." *Annals of Neurology* 55(4):458–68. doi: 10.1002/ana.20016.

Bateman, R. 1999. "Sector Mass Spectrometers." *Encyclopedia of Spectroscopy and Spectrometry* 2511–17.

Bauman, David R., Andrew D. Bitmansour, Jeffrey G. McDonald, Bonne M. Thompson, Guosheng Liang, and David W. Russell. 2009. "25-Hydroxycholesterol Secreted by Macrophages in Response to Toll-like Receptor Activation Suppresses Immunoglobulin A Production." *Proceedings of the National Academy of Sciences of the United States of America* 106(39):16764–69. doi: 10.1073/PNAS.0909142106.

Beecham, Ashley H., Nikolaos A. Patsopoulos, Dionysia K. Xifara, Mary F. Davis, Anu Kemppinen, Chris Cotsapas, Tejas S. Shah, Chris Spencer, David Booth, An Goris, Annette Oturai, Janna Saarela, Bertrand Fontaine, Bernhard Hemmer, Claes Martin, Frauke Zipp, Sandra D'Alfonso, Filippo Martinelli-Boneschi, Bruce Taylor, Hanne F. Harbo, Ingrid Kockum, Jan Hillert, Tomas Olsson, Maria Ban, Jorge R. Oksenberg, Rogier Hintzen, Lisa F. Barcellos, Cristina Agliardi, Lars Alfredsson, Mehdi Alizadeh, Carl Anderson, Robert Andrews, Helle Bach Søndergaard, Amie Baker, Gavin Band, Sergio E. Baranzini, Nadia Barizzone, Jeffrey Barrett, Céline Bellenguez, Laura Bergamaschi, Luisa Bernardinelli, Achim Berthele, Viola Biberacher, Thomas M. C. Binder, Hannah Blackburn, Izaura L. Bomfim, Paola Brambilla, Simon Broadley, Bruno Brochet, Lou Brundin, Dorothea Buck, Helmut Butzkueven, Stacy J. Caillier, William Camu, Wassila Carpentier, Paola Cavalla, Elisabeth G. Celius, Irène Coman, Giancarlo Comi, Lucia Corrado, Leentje Cosemans, Isabelle Cournu-Rebeix, Bruce A. C. Cree, Daniele Cusi, Vincent Damotte, Gilles Defer, Silvia R. Delgado, Panos Deloukas, Alessia Di Sapio, Alexander T. Dilthey, Peter Donnelly, Bénédicte Dubois, Martin Duddy, Sarah Edkins, Irina Elovaara, Federica Esposito, Nikos Evangelou, Barnaby Fiddes, Judith Field, Andre Franke, Colin Freeman, Irene Y. Frohlich, Daniela Galimberti, Christian Gieger, Pierre Antoine Gourraud, Christiane Graetz, Andrew Graham, Verena Grummel, Clara Guaschino, Athena Hadjixenofontos, Hakon Hakonarson, Christopher Halfpenny, Gillian Hall, Per Hall, Anders Hamsten, James Harley, Timothy Harrower, Clive Hawkins, Garrett Hellenthal, Charles Hillier, Jeremy Hobart, Muni Hoshi, Sarah E. Hunt, Maja Jagodic, Ilijas Jelcic, Angela Jochim, Brian Kendall, Allan Kermode, Trevor Kilpatrick, Keijo Koivisto, Ioanna Konidari,

Thomas Korn, Helena Kronsbein, Cordelia Langford, Malin Larsson, Mark Lathrop, Christine Lebrun-Frenay, Jeannette Lechner-Scott, Michelle H. Lee, Maurizio A. Leone, Virpi Leppä, Giuseppe Liberatore, Benedicte A. Lie, Christina M. Lill, Magdalena Lindén, Jenny Link, Felix Luessi, Jan Lycke, Fabio Macciardi, Satu Männistö, Clara P. Manrique, Roland Martin, Vittorio Martinelli, Deborah Mason, Gordon Mazibrada, Cristin McCabe, Inger Lise Mero, Julia Mescheriakova, Loukas Moutsianas, Kjell Morten Myhr, Guy Nagels, Richard Nicholas, Petra Nilsson, Fredrik Piehl, Matti Pirinen, Siân E. Price, Hong Quach, Mauri Reunanen, Wim Robberecht, Neil P. Robertson, Mariaemma Rodegher, David Rog, Marco Salvetti, Nathalie C. Schnetz-Boutaud, Finn Sellebjerg, Rebecca C. Selter, Catherine Schaefer, Sandip Shaunak, Ling Shen, Simon Shields, Volker Siffrin, Mark Slee, Per Soelberg Sorensen, Melissa Sorosina, Mireia Sospedra, Anne Spurkland, Amy Strange, Emilie Sundqvist, Vincent Thijs, John Thorpe, Anna Ticca, Pentti Tienari, Cornelia Van Duijn, Elizabeth M. Visser, Steve Vucic, Helga Westerlind, James S. Wiley, Alastair Wilkins, James F. Wilson, Juliane Winkelmann, John Zajicek, Eva Zindler, Jonathan L. Haines, Margaret A. Pericak-Vance, Adrian J. Ivinson, Graeme Stewart, David Hafler, Stephen L. Hauser, Alastair Compston, Gil McVean, Philip De Jager, Stephen J. Sawcer, and Jacob L. McCauley. 2013. “Analysis of Immune-Related Loci Identifies 48 New Susceptibility Variants for Multiple Sclerosis.” *Nature Genetics* 45(11):1353–60. doi: 10.1038/ng.2770.

Behrangi, Newshan, Felix Fischbach, and Markus Kipp. 2019. “Mechanism of Siponimod: Anti-Inflammatory and Neuroprotective Mode of Action.” *Cells* 8(24). doi: 10.3390/cells8010024.

Bellosta, Stefano, Nicola Fed, Franco Bernini, Rodolfo Paoletti, and Alberto Corsini. 2000. “Non-Lipid-Related Effects of Statins.” *Annals of Medicine* 32(3):164–76. doi: 10.3109/07853890008998823.

Berard, Jennifer L., Kevin Wolak, Sylvie Fournier, and Samuel David. 2010. “Characterization of Relapsing-Remitting and Chronic Forms of Experimental Autoimmune Encephalomyelitis in C57BL/6 Mice.” *GLIA* 58(4):434–45. doi: 10.1002/glia.20935.

Berghoff, Stefan A., Lena Spieth, and Gesine Saher. 2022a. “Local Cholesterol Metabolism Orchestrates Remyelination.” *Trends in Neurosciences* 45(4):272–83. doi: 10.1016/J.TINS.2022.01.001.

Berghoff, Stefan A., Lena Spieth, and Gesine Saher. 2022b. “Local Cholesterol Metabolism Orchestrates Remyelination.” *Trends in Neurosciences* 45(4):272–83. doi: 10.1016/J.TINS.2022.01.001.

Berghoff, Stefan A., Lena Spieth, Ting Sun, Leon Hosang, Constanze Depp, Andrew O. Sasmita, Martina H. Vasileva, Patricia Scholz, Yu Zhao, Dilja Krueger-Burg, Sven Wichert, Euan R. Brown, Kyriakos Michail, Klaus Armin Nave, Stefan Bonn, Francesca Odoardi, Moritz Rossner, Till Ischebeck, Julia M. Edgar, and Gesine Saher. 2021. “Neuronal Cholesterol Synthesis Is Essential for Repair of Chronically Demyelinated Lesions in Mice.” *Cell Reports* 37(4). doi: 10.1016/J.CELREP.2021.109889.

Berghoff, Stefan A., Lena Spieth, Ting Sun, Leon Hosang, Lennart Schlaphoff, Constanze Depp, Tim Düking, Jan Winchenbach, Jonathan Neuber, David Ewers, Patricia Scholz, Franziska van der Meer, Ludovico Cantuti-Castelvetri, Andrew O. Sasmita, Martin Meschkat, Torben

Ruhwedel, Wiebke Möbius, Roman Sankowski, Marco Prinz, Inge Huitinga, Michael W. Sereda, Francesca Odoardi, Till Ischebeck, Mikael Simons, Christine Stadelmann-Nessler, Julia M. Edgar, Klaus Armin Nave, and Gesine Saher. 2020. “Microglia Facilitate Repair of Demyelinated Lesions via Post-Squalene Sterol Synthesis.” *Nature Neuroscience 2020 24:1* 24(1):47–60. doi: 10.1038/s41593-020-00757-6.

Bergles, Dwight E., Johns Hopkins, Penelope Dimas, Laura Montani, Jorge A. Pereira, Daniel Moreno, Martin Trö tzmü ller, Joanne Gerber, Clay F. Semenkovich, Harald C. Kö feler, and Ueli Suter. 2019. “CNS Myelination and Remyelination Depend on Fatty Acid Synthesis by Oligodendrocytes.” *ELIFE* 8(e44702). doi: 10.7554/eLife.44702.001.

Bevan, Ryan J., Rhian Evans, Lauren Griffiths, Lewis M. Watkins, Mark I. Rees, Roberta Magliozzi, Ingrid Allen, Gavin McDonnell, Rachel Kee, Michelle Naughton, Denise C. Fitzgerald, Richard Reynolds, James W. Neal, and Owain W. Howell. 2018. “Meningeal Inflammation and Cortical Demyelination in Acute Multiple Sclerosis.” *Annals of Neurology* 84(6):829–42. doi: 10.1002/ana.25365.

Bieber, Allan J., Scott Kerr, and Moses Rodriguez. 2003. “Efficient Central Nervous System Remyelination Requires T Cells.” *Annals of Neurology* 53(5):680–84. doi: 10.1002/ana.10578.

Bitsch, A., J. Schuchardt, S. Bunkowski, T. Kuhlmann, and Wolfgang Brück. 2000. “Acute Axonal Injury in Multiple Sclerosis. Correlation with Demyelination and Inflammation.” *Brain : A Journal of Neurology* 123(6):1174–83. doi: 10.1093/BRAIN/123.6.1174.

Björkhem, I. 2006. “Crossing the Barrier: Oxysterols as Cholesterol Transporters and Metabolic Modulators in the Brain.” *Journal of Internal Medicine* 260(6):493–508. doi: 10.1111/j.1365-2796.2006.01725.x.

Björkhem, Ingemar. 2007. “Rediscovery of Cerebrosterol.” *Lipids* 42(1):5–14. doi: 10.1007/S11745-006-1003-2.

Björkhem, Ingemar, Angel Cedazo-Minguez, Valerio Leoni, and Steve Meaney. 2009. “Oxysterols and Neurodegenerative Diseases.” *Molecular Aspects of Medicine* 30(3):171–79.

Björkhem, Ingemar, Steve Meaney, and Alan M. Fogelman. 2004. “Brain Cholesterol: Long Secret Life behind a Barrier.” *Arteriosclerosis, Thrombosis, and Vascular Biology* 24(5):806–15. doi: 10.1161/01.ATV.0000120374.59826.1b.

Björkhem, Ingemar, Kalicharan Patra, Adam L. Boxer, and Per Svenningsson. 2018. “24S-Hydroxycholesterol Correlates with Tau and Is Increased in Cerebrospinal Fluid in Parkinson’s Disease and Corticobasal Syndrome.” *Frontiers in Neurology* 9(756). doi: 10.3389/fneur.2018.00756.

Bjornevik, Kjetil, Marianna Cortese, Brian C. Healy, Jens Kuhle, Michael J. Mina, Yumei Leng, Stephen J. Elledge, David W. Niebuhr, Ann I. Scher, Kassandra L. Munger, and Alberto Ascherio. 2022. “Longitudinal Analysis Reveals High Prevalence of Epstein-Barr Virus Associated with Multiple Sclerosis.” *Science (New York, N.Y.)* 375(6578):296–301. doi: 10.1126/SCIENCE.ABJ8222.

Blom, Tomas, Nils Bäck, Aino-Liisa Mutka, Robert Bittman, Zaiguo Li, Angel De Lera, Petri T. Kovanen, Ulf Diczfalusy, and Elina Ikonen. 2010. "FTY720 Stimulates 27-Hydroxycholesterol Production and Confers Atheroprotective Effects in Human Primary Macrophages." *Circulation Research* 106(4):720–29. doi: 10.1161/CIRCRESAHA.109.204396.

Bö, Lars, Jeroen J. G. Geurts, Paul Van Der Valk, Chris Polman, and Frederik Barkhof. 2007. "Lack of Correlation Between Cortical Demyelination and White Matter Pathologic Changes in Multiple Sclerosis." *Archives of Neurology* 64(1):76–80. doi: 10.1001/ARCHNEUR.64.1.76.

Bø, Lars, Christian A. Vedeler, Harald I. Nyland, Bruce D. Trapp, and Sverre J. Mørk. 2003. "Subpial Demyelination in the Cerebral Cortex of Multiple Sclerosis Patients." *Journal of Neuropathology & Experimental Neurology* 62(7):723–32. doi: 10.1093/JNEN/62.7.723.

Bogie, Jeroen F. J., Elien Grajchen, Elien Wouters, Aida Garcia Corrales, Tess Dierckx, Sam Vanherle, Jo Mailleux, Pascal Gervois, Esther Wolfs, Jonas Dehairs, Jana van Broeckhoven, Andrew P. Bowman, Ivo Lambrichts, Jan Åke Gustafsson, Alan T. Remaley, Monique Mulder, Johannes V. Swinnen, Mansour Haidar, Shane R. Ellis, James M. Ntambi, Noam Zelcer, and Jerome J. A. Hendriks. 2020. "Stearoyl-CoA Desaturase-1 Impairs the Reparative Properties of Macrophages and Microglia in the Brain." *Journal of Experimental Medicine* 217(5). doi: 10.1084/jem.20191660.

Bogie, Jeroen F. J., Winde Jorissen, Jo Mailleux, Philip G. Nijland, Noam Zelcer, Tim Vanmierlo, Jack Van Horssen, Piet Stinissen, Niels Hellings, and Jerome J. A. Hendriks. 2014. "Myelin Alters the Inflammatory Phenotype of Macrophages by Activating PPARs." *Acta Neuropathologica Communications* 2(1):1–13. doi: 10.1186/2051-5960-1-43/FIGURES/6.

Bogie, Jeroen F. J., Silke Timmermans, Vân Anh Huynh-Thu, Alexandre Irrthum, Hubert J. M. Smeets, Jan Åke Gustafsson, Knut R. Steffensen, Monique Mulder, Piet Stinissen, Niels Hellings, and Jerome J. A. Hendriks. 2012. "Myelin-Derived Lipids Modulate Macrophage Activity by Liver X Receptor Activation." *PLOS ONE* 7(9). doi: 10.1371/JOURNAL.PONE.0044998.

Bohlen, Christopher J., F. Chris Bennett, Andrew F. Tucker, Hannah Y. Collins, Sara B. Mulinyawe, and Ben A. Barres. 2017. "Diverse Requirements for Microglial Survival, Specification, and Function Revealed by Defined-Medium Cultures." *Neuron* 94(4):759-773.e8. doi: 10.1016/J.NEURON.2017.04.043.

Bolton, Christopher. 2021. "An Evaluation of the Recognised Systemic Inflammatory Biomarkers of Chronic Sub-Optimal Inflammation Provides Evidence for Inflammageing (IFA) during Multiple Sclerosis (MS)." *Immunity & Ageing* 18(18). doi: 10.1186/S12979-021-00225-0.

Boussicault, Lydie, Sandro Alves, Antonin Lamazière, Anabelle Planques, Nicolas Heck, Lara Moumné, Gaëtan Despres, Susanne Bolte, Amélie Hu, Christiane Pagès, Laurie Galvan, Francoise Piguet, Patrick Aubourg, Nathalie Cartier, Jocelyne Caboche, and Sandrine Betuing. 2016. "CYP46A1, the Rate-Limiting Enzyme for Cholesterol Degradation, Is Neuroprotective in Huntington's Disease." *Brain* 139(3):953–70. doi: 10.1093/BRAIN/AWV384.

Brambilla, Roberta. 2019. “The Contribution of Astrocytes to the Neuroinflammatory Response in Multiple Sclerosis and Experimental Autoimmune Encephalomyelitis.” *Acta Neuropathologica* 137(5):757–83.

Briard, Emmanuelle, David Orain, Christian Beerli, Andreas Billich, Markus Streiff, Marc Bigaud, and Yves P. Auberson. 2011. “BZM055, an Iodinated Radiotracer Candidate for PET and SPECT Imaging of Myelin and FTY720 Brain Distribution.” *ChemMedChem* 6(4):667–77. doi: 10.1002/CMDC.201000477.

Brinkmann, Volker, Michael D. Davis, Christopher E. Heise, Rainer Albert, Sylvain Cottens, Robert Hof, Christian Bruns, Eva Prieschl, Thomas Baumruker, Peter Hiestand, Carolyn A. Foster, Markus Zollinger, and Kevin R. Lynch. 2002. “The Immune Modulator FTY720 Targets Sphingosine 1-Phosphate Receptors.” *Journal of Biological Chemistry* 277(24):21453–57. doi: 10.1074/JBC.C200176200.

Brosnan, Celia F., and Cedric S. Raine. 2013. “The Astrocyte in Multiple Sclerosis Revisited.” *Glia* 61(4):453–65. doi: 10.1002/GLIA.22443.

Brown, Michael, and Joseph Goldstein. 1986. “A Receptor-Mediated Pathway for Cholesterol Homeostasis.” *Science* 232(4746):34–47.

Brown, Michael S., and Joseph L. Goldstein. 1999. “A Proteolytic Pathway That Controls the Cholesterol Content of membranes, Cells, and Blood.” *Proceedings of the National Academy of Sciences of the United States of America* 96(20):11041. doi: 10.1073/PNAS.96.20.11041.

Browne, Paul, Dhia Chandraratna, Ceri Angood, Helen Tremlett, Chris Baker, Bruce V. Taylor, and Alan J. Thompson. 2014. “Atlas of Multiple Sclerosis 2013: A Growing Global Problem with Widespread Inequity.” *Neurology* 83(11):1022–24. doi: 10.1212/WNL.0000000000000768.

Brück, Wolfgang, Phyllis Porada, Sigrid Poser, Peter Rieckmann, Folker Hanefeld, Hans A. Kretzschmarch, and Hans Lassmann. 1995. “Monocyte/Macrophage Differentiation in Early Multiple Sclerosis Lesions.” *Annals of Neurology* 38(5):788–96. doi: 10.1002/ANA.410380514.

Bryleva, Elena Y., Maximillian A. Rogers, Catherine C. Y. Chang, Floyd Buen, Brent T. Harris, Estelle Rousselet, Nabil G. Seidah, Salvatore Oddo, Frank M. Laferla, Thomas A. Spencer, William F. Hickey, and Ta Yuan Chang. 2010. “ACAT1 Gene Ablation Increases 24(S)-Hydroxycholesterol Content in the Brain and Ameliorates Amyloid Pathology in Mice with AD.” *Proceedings of the National Academy of Sciences of the United States of America* 107(7):3081–86. doi: 10.1073/PNAS.0913828107.

Bullard, Daniel C., Xianzhen Hu, Trenton R. Schoeb, Robert G. Collins, Arthur L. Beaudet, and Scott R. Barnum. 2007. “Intercellular Adhesion Molecule-1 Expression Is Required on Multiple Cell Types for the Development of Experimental Autoimmune Encephalomyelitis.” *The Journal of Immunology* 178(2):851–57. doi: 10.4049/jimmunol.178.2.851.

Burlot, Marie Anne, Jérôme Braudeau, Kristin Michaelsen-Preusse, Brigitte Potier, Sophie Ayciriex, Jennifer Varin, Benoit Gautier, Fathia Djelti, Mickael Audrain, Luce Dauphinot, Francisco Jose Fernandez-Gomez, Raphaëlle Caillierez, Olivier Laprévote, Ivan Bièche, Nicolas Auzeil, Marie Claude Potier, Patrick Dutar, Martin Korte, Luc Buée, David Blum, and

Nathalie Cartier. 2015. “Cholesterol 24-Hydroxylase Defect Is Implicated in Memory Impairments Associated with Alzheimer-like Tau Pathology.” *Human Molecular Genetics* 24(21):5965–76. doi: 10.1093/HMG/DDV268.

Butovsky, Oleg, and Howard L. Weiner. 2018. “Microglial Signatures and Their Role in Health and Disease.” *Nat Rev Neurosci* 19(10):622–35. doi: 10.1038/s41583-018-0057-5.

Calabrese, Massimiliano, Alice Favaretto, Valeria Martini, and Paolo Gallo. 2013. “Grey Matter Lesions in MS.” *Prion* 7(1):20–27. doi: 10.4161/pri.22580.

Calabrese, Massimiliano, Valentina Poretto, Alice Favaretto, Sara Alessio, Valentina Bernardi, Chiara Romualdi, Francesca Rinaldi, Paola Perini, and Paolo Gallo. 2012. “Cortical Lesion Load Associates with Progression of Disability in Multiple Sclerosis.” *Brain : A Journal of Neurology* 135(Pt 10):2952–61. doi: 10.1093/BRAIN/AWS246.

Calabrese, Massimiliano, Maria A. Rocca, Matteo Atzori, Irene Mattisi, Alice Favaretto, Paola Perini, Paolo Gallo, and Massimo Filippi. 2010. “A 3-Year Magnetic Resonance Imaging Study of Cortical Lesions in Relapse-Onset Multiple Sclerosis.” *Annals of Neurology* 67(3):376–83. doi: 10.1002/ANA.21906.

Calabrese, Massimiliano, Nicola De Stefano, Matteo Atzori, Valentina Bernardi, Irene Mattisi, Luigi Barachino, Aldo Morra, Luciano Rinaldi, Chiara Romualdi, Paola Perini, Leontino Battistin, and Paolo Gallo. 2007. “Detection of Cortical Inflammatory Lesions by Double Inversion Recovery Magnetic Resonance Imaging in Patients with Multiple Sclerosis.” *Archives of Neurology* 64(10):1416–22. doi: 10.1001/ARCHNEUR.64.10.1416.

Callegari, Ilaria, Tobias Derfuss, and Edoardo Galli. 2021. “Update on Treatment in Multiple Sclerosis.” *La Presse Médicale* 50(2):104068. doi: 10.1016/J.LPM.2021.104068.

Camu, William, Hôpital Gui De Chauliac, Trygve Holmøy, Andrei Miclea andreimiclea, Andrei Miclea, Maud Bagnoud, Andrew Chan, and Robert Hoepner. 2020. “A Brief Review of the Effects of Vitamin D on Multiple Sclerosis.” *Front. Immunol* 11(781). doi: 10.3389/fimmu.2020.00781.

Cantuti-Castelvetri, Ludovico, Dirk Fitzner, Mar Bosch-Queralt, Marie-Theres Weil, Minhui Su, Paromita Sen, Torben Ruhwedel, Miso Mitkovski, George Trendelenburg, Dieter Lütjohann, Wiebke Möbius, and Mikael Simons. 2018. “Defective Cholesterol Clearance Limits Remyelination in the Aged Central Nervous System.” *Science* 359(6376):648–88.

Carassiti, D., D. R. Altmann, N. Petrova, B. Pakkenberg, F. Scaravilli, and K. Schmierer. 2018. “Neuronal Loss, Demyelination and Volume Change in the Multiple Sclerosis Neocortex.” *Neuropathology and Applied Neurobiology* 44(4):377–90. doi: 10.1111/NAN.12405.

Castillo-Rodriguez, Maria de los Angeles, Stefan Gingele, Lara Jasmin Schröder, Thiemo Möllenkamp, Martin Stangel, Thomas Skripuletz, and Viktoria Gudi. 2022. “Astroglial and Oligodendroglial Markers in the Cuprizone Animal Model for De- and Remyelination.” *Histochemistry and Cell Biology* 158(1):38. doi: 10.1007/S00418-022-02096-Y.

Chan, Dennis, Sophie Binks, Jennifer M. Nicholas, Chris Frost, M. Jorge Cardoso, Sebastien Ourselin, David Wilkie, Richard Nicholas, and Jeremy Chataway. 2017. “Effect of High-Dose

Simvastatin on Cognitive, Neuropsychiatric, and Health-Related Quality-of-Life Measures in Secondary Progressive Multiple Sclerosis: Secondary Analyses from the MS-STAT Randomised, Placebo-Controlled Trial." *The Lancet. Neurology* 16(8):591–600. doi: 10.1016/S1474-4422(17)30113-8.

Chari, Divya M. 2007. "Remyelination In Multiple Sclerosis." *International Review of Neurobiology* 79:589–620. doi: 10.1016/S0074-7742(07)79026-8.

Chataway, Jeremy, Floriana De Angelis, Peter Connick, Richard A. Parker, Domenico Plantone, Anisha Doshi, Nevin John, Jonathan Stutters, David MacManus, Ferran Prados Carrasco, Frederik Barkhof, Sebastien Ourselin, Marie Braisher, Moira Ross, Gina Cranswick, Sue H. Pavitt, Gavin Giovannoni, Claudia Angela Gandini Wheeler-Kingshott, Clive Hawkins, Basil Sharrack, Roger Bastow, Christopher J. Weir, Nigel Stallard, Siddharthan Chandran, Thomas Williams, Tiggy Beyene, Vanessa Bassan, Alvin Zapata, Dawn Lyle, James Cameron, Daisy Mollison, Shuna Colville, Baljean Dhillon, Richard A. Parker, Sharmilee Gnanapavan, Richard Nicholas, Waqar Rashid, Julia Aram, Helen Ford, James Overell, Carolyn Young, Heinke Arndt, Martin Duddy, Joe Guadagno, Nikolaos Evangelou, Matthew Craner, Jacqueline Palace, Jeremy Hobart, David Paling, Seema Kalra, and Brendan McLean. 2020. "Efficacy of Three Neuroprotective Drugs in Secondary Progressive Multiple Sclerosis (MS-SMART): A Phase 2b, Multiarm, Double-Blind, Randomised Placebo-Controlled Trial." *The Lancet Neurology* 19(3):214–25. doi: 10.1016/S1474-4422(19)30485-5.

Chataway, Jeremy, Nadine Schuerer, Ali Alsanousi, Dennis Chan, David MacManus, Kelvin Hunter, Val Anderson, Charles R. M. Bangham, Shona Clegg, Casper Nielsen, Nick C. Fox, David Wilkie, Jennifer M. Nicholas, Virginia L. Calder, John Greenwood, Chris Frost, and Richard Nicholas. 2014. "Effect of High-Dose Simvastatin on Brain Atrophy and Disability in Secondary Progressive Multiple Sclerosis (MS-STAT): A Randomised, Placebo-Controlled, Phase 2 Trial." *The Lancet* 383(9936):2213–21. doi: 10.1016/S0140-6736(13)62242-4.

Chausse, Bruno, Pamela A. Kakimoto, and Oliver Kann. 2021. "Microglia and Lipids: How Metabolism Controls Brain Innate Immunity." *Seminars in Cell and Developmental Biology* 112:137–44. doi: 10.1016/J.SEMCDB.2020.08.001.

Choi, Sung R., Owain W. Howell, Daniele Carassiti, Roberta Magliozzi, Djordje Gveric, Paolo A. Muraro, Richard Nicholas, Federico Roncaroli, and Richard Reynolds. 2012. "Meningeal Inflammation Plays a Role in the Pathology of Primary Progressive Multiple Sclerosis." *Brain* 135(10):2925–37. doi: 10.1093/brain/aws189.

Cohan, Stanley L., Ralph H. B Benedict, Bruce A. C Cree, John DeLuca, Le H. Hua, Jerold Chun, and Stanley L. Cohan StanleyCohan. 2022. "The Two Sides of Siponimod: Evidence for Brain and Immune Mechanisms in Multiple Sclerosis." *CNS Drugs* 36:703–19. doi: 10.1007/s40263-022-00927-z.

Colonna, Marco, and Oleg Butovsky. 2017. "Microglia Function in the Central Nervous System During Health and Neurodegeneration." doi: 10.1146/annurev-immunol.

Compston, Alastair, and Alasdair Coles. 2002. "Multiple Sclerosis." *Lancet* 359(9313):1221–31. doi: 10.1016/S0140-6736(02)08220-X.

Compston, Alastair, and Alasdair Coles. 2008. “Multiple Sclerosis.” *The Lancet* 372(9648):1502–17. doi: 10.1016/S0140-6736(08)61620-7.

Confavreux, Christian, and Sandra Vukusic. 2014. *The Clinical Course of Multiple Sclerosis*. Vol. 122. 1st ed. Elsevier B.V.

Corder, E. H., A. M. Saunders, W. J. Strittmatter, D. E. Schmechel, P. C. Gaskell, G. W. Small, A. D. Roses, J. L. Haines, and M. A. Pericak-Vance. 1993. “Gene Dose of Apolipoprotein E Type 4 Allele and the Risk of Alzheimer’s Disease in Late Onset Families.” *Science* 261(5123):921–23. doi: 10.1126/SCIENCE.8346443.

Correale, Jorge, María I. Gaitán, María C. Ysrraelit, and Marcela P. Fiol. 2017. “Progressive Multiple Sclerosis: From Pathogenic Mechanisms to Treatment.” *Brain* 140(3):527–46. doi: 10.1093/BRAIN/AWW258.

Correale, Jorge, Mario Javier Halfon, Dominic Jack, Adrián Rubstein, and Andrés Villa. 2021. “Acting Centrally or Peripherally: A Renewed Interest in the Central Nervous System Penetration of Disease-Modifying Drugs in Multiple Sclerosis.” *Multiple Sclerosis and Related Disorders* 56. doi: 10.1016/J.MSARD.2021.103264.

Correale, Jorge, Mariano Marrodan, and Maria Ysrraelit. 2019. “Mechanisms of Neurodegeneration and Axonal Dysfunction in Progressive Multiple Sclerosis.” *Biomedicines* 7(14).

Cortes, Victor A., Dolores Busso, Alberto Maiz, Antonio Arteaga, Flavio Nervi, and Attilio Rigotti. 2014. “Physiological and Pathological Implications of Cholesterol.” *Frontiers in Bioscience - Landmark* 19(3):416–28. doi: 10.2741/4216.

Cree, Bruce A. C., Douglas L. Arnold, Jeremy Chataway, Tanuja Chitnis, Robert J. Fox, Angela Pozo Ramajo, Niamh Murphy, and Hans Lassmann. 2021. “Secondary Progressive Multiple Sclerosis: New Insights.” *Neurology* 97(8):378–89. doi: 10.1212/WNL.0000000000012323.

Cree, Bruce A. C., Jill A. Hollenbach, Riley Bove, Gina Kirkish, Simone Sacco, Eduardo Caverzasi, Antje Bischof, Tristan Gundel, Alyssa H. Zhu, Nico Papinutto, William A. Stern, Carolyn Bevan, Andrew Romeo, Douglas S. Goodin, Jeffrey M. Gelfand, Jennifer Graves, Ari J. Green, Michael R. Wilson, Scott S. Zamvil, Chao Zhao, Refujia Gomez, Nicholas R. Ragan, Gillian Q. Rush, Patrick Barba, Adam Santaniello, Sergio E. Baranzini, Jorge R. Oksenberg, Roland G. Henry, and Stephen L. Hauser. 2019. “Silent Progression in Disease Activity–Free Relapsing Multiple Sclerosis.” *Annals of Neurology* 85(5):653–66. doi: 10.1002/ANA.25463.

Crick, Peter J., T. William Bentley, Jonas Abdel-Khalik, Ian Matthews, Peter T. Clayton, Andrew A. Morris, Brian W. Bigger, Chiara Zerbinati, Luigi Tritapepe, Luigi Iuliano, Yuqin Wang, and William J. Griffiths. 2015. “Quantitative Charge-Tags for Sterol and Oxysterol Analysis.” *Clinical Chemistry* 61(2):400–411. doi: 10.1373/clinchem.2014.231332.

Crick, Peter J., William J. Griffiths, Juan Zhang, Martin Beibel, Jonas Abdel-Khalik, Jens Kuhle, Andreas W. Sailer, and Yuqin Wang. 2017. “Reduced Plasma Levels of 25-Hydroxycholesterol and Increased Cerebrospinal Fluid Levels of Bile Acid Precursors in Multiple Sclerosis Patients.” *Molecular Neurobiology* 54(10):8009–20. doi: 10.1007/s12035-016-0281-9.

Cuadros, Miguel A., M. Rosario Sepulveda, David Martin-Oliva, José L. Marín-Teva, and Veronika E. Neubrand. 2022. “Microglia and Microglia-Like Cells: Similar but Different.” *Frontiers in Cellular Neuroscience* 16(816439).

Cuzner, M.L., and Norton, W.T. (1996) Biochemistry of Demyelination. *Brain Pathology* **6**: 231–242 https://onlinelibrary.wiley.com/doi/full/10.1111/j.1750-3639.1996.tb00852.x.

Czapiga, Meggan, and Carol A. Colton. 1999. “Function of Microglia in Organotypic Slice Cultures.” *Journal of Neuroscience Research* 56(6):644–51. doi: 10.1002/(SICI)1097-4547(19990615)56:6<644::AID-JNR10>3.0.CO;2-9.

Dal-Bianco, A., R. Schranzer, G. Grabner, M. Lanzinger, S. Kolbrink, G. Pusswald, P. Altmann, M. Ponleitner, M. Weber, B. Kornek, K. Zebenholzer, C. Schmied, T. Berger, H. Lassmann, S. Trattnig, S. Hametner, F. Leutmezer, and P. Rommer. 2021. “Iron Rims in Patients with Multiple Sclerosis as Neurodegenerative Marker? A 7-Tesla Magnetic Resonance Study.” *Frontiers in Neurology* 12(632749). doi: 10.3389/FNEUR.2021.632749/BIBTEX.

D’Amelio, Fernando E., Marion E. Smith, and Lawrence F. Eng. 1990. “Sequence of Tissue Responses in the Early Stages of Experimental Allergic Encephalomyelitis (EAE): Immunohistochemical, Light Microscopic, and Ultrastructural Observations in the Spinal Cord.” *Glia* 3(4):229–40. doi: 10.1002/GLIA.440030402.

Dendrou, Calliope A., Lars Fugger, and Manuel A. Friese. 2015. “Immunopathology of Multiple Sclerosis.” *Nature Reviews Immunology* 15(9):545–58.

Dias, Irundika H. K., Maria C. Polidori, and Helen R. Griffiths. 2014. “Hypercholesterolaemia-Induced Oxidative Stress at the Blood–Brain Barrier.” *Biochemical Society Transactions* 42(4):1001–5. doi: 10.1042/BST20140164.

Dias, Irundika H. K., Hala Shokr, Freya Shephard, and Lisa Chakrabarti. 2022. “Oxysterols and Oxysterol Sulfates in Alzheimer’s Disease Brain and Cerebrospinal Fluid.” *Journal of Alzheimer’s Disease* 87(4):1527–36. doi: 10.3233/JAD-220083.

Diczfalusy, Ulf. 2013. “On the Formation and Possible Biological Role of 25-Hydroxycholesterol.” *Biochimie* 95(3):455–60. doi: 10.1016/J.BIOCHI.2012.06.016.

Dietschy, John M. 2009. “Central Nervous System: Cholesterol Turnover, Brain Development and Neurodegeneration.” *Biol Chem* 390(4):287–93. doi: 10.1515/BC.2009.035.

Dietschy, John M., and Stephen D. Turley. 2004. “Cholesterol Metabolism in the Central Nervous System during Early Development and in the Mature Animal.” *Journal of Lipid Research* 45(8):1375–97. doi: 10.1194/jlr.R400004-JLR200.

Dimitrov, Lilia G., and Benjamin Turner. 2014. “Editorials: What’s New in Multiple Sclerosis?” *British Journal of General Practice* 64(629):612–13. doi: 10.3399/bjgp14X682609.

Doshi, Anisha, and Jeremy Chataway. 2016. “Multiple Sclerosis, a Treatable Disease.” *Clinical Medicine (London, England)* 16(Suppl 6):s53–59. doi: 10.7861/CLINMEDICINE.16-6-S53.

Duc, Donovan, Solenne Vigne, and Caroline Pot. 2019. “Oxysterols in Autoimmunity.” *International Journal of Molecular Sciences* 20(18). doi: 10.3390/ijms20184522.

Duewell, Peter, Hajime Kono, Katey J. Rayner, Cherilyn M. Sirois, Gregory Vladimer, Franz G. Bauernfeind, George S. Abela, Luigi Franchi, Gabriel Nuñez, Max Schnurr, Terje Espevik, Egil Lien, Katherine A. Fitzgerald, Kenneth L. Rock, Kathryn J. Moore, Samuel D. Wright, Veit Hornung, and Eicke Latz. 2010. "NLRP3 Inflammasomes Are Required for Atherogenesis and Activated by Cholesterol Crystals." *Nature* 464:1357–63. doi: 10.1038/nature08938.

Dumitrescu, Laura, Cris S. Constantinescu, and Radu Tanasescu. 2019. "Siponimod for the Treatment of Secondary Progressive Multiple Sclerosis." *Expert Opinion on Pharmacotherapy* 20(2):143–50. doi: 10.1080/14656566.2018.1551363.

Dunn, Warwick B. 2011. "Mass Spectrometry in Systems Biology: An Introduction." *Methods in Enzymology* 500:15–35. doi: 10.1016/B978-0-12-385118-5.00002-5.

Dzeletovic, Susanna, Olof Breuer, Erik Lund, and Ulf Diczfalusy. 1995. "Determination of Cholesterol Oxidation Products in Human Plasma by Isotope Dilution-Mass Spectrometry." *Analytical Biochemistry* 225(1):73–80. doi: 10.1006/ABIO.1995.1110.

Elliott, Colm, Shibeshih Belachew, Jerry S. Wolinsky, Stephen L. Hauser, Ludwig Kappos, Frederik Barkhof, Corrado Bernasconi, Julian Fecker, Fabian Model, Wei Wei, and Douglas L. Arnold. 2019. "Chronic White Matter Lesion Activity Predicts Clinical Progression in Primary Progressive Multiple Sclerosis." *Brain* 142:2787–99. doi: 10.1093/brain/awz212.

Factor, Daniel C., Anna M. Barbeau, Kevin C. Allan, Lucille R. Hu, Mayur Madhavan, An T. Hoang, Kathryn E. A. Hazel, Parker A. Hall, Sagar Nisraiyya, Fadi J. Najm, Tyler E. Miller, Zachary S. Nevin, Robert T. Karl, Bruna R. Lima, Yanwei Song, Alexandra G. Sibert, Gursimran K. Dhillon, Christina Volsko, Cynthia F. Bartels, Drew J. Adams, Ranjan Dutta, Michael D. Gallagher, William Phu, Alexey Kozlenkov, Stella Dracheva, Peter C. Scacheri, Paul J. Tesar, and Olivia Corradin. 2020. "Cell Type-Specific Intralocus Interactions Reveal Oligodendrocyte Mechanisms in MS." *Cell* 181(2):395. doi: 10.1016/J.CELL.2020.03.002.

Faust, Travis E., Georgia Gunner, and Dorothy P. Schafer. 2021. "Mechanisms Governing Activity-Dependent Synaptic Pruning in the Developing Mammalian CNS." *Nat Rev Neurosci* 22:657–73. doi: 10.1038/s41583-021-00507-y.

Fenn, Ashley M., Jodie C. E. Hall, John C. Gensel, Phillip G. Popovich, and Jonathan P. Godbout. 2014. "IL-4 Signaling Drives a Unique Arginase+/IL-1β+ Microglia Phenotype and Recruits Macrophages to the Inflammatory CNS: Consequences of Age-Related Deficits in IL-4Rα after Traumatic Spinal Cord Injury." *The Journal of Neuroscience : The Official Journal of the Society for Neuroscience* 34(26):8904–17. doi: 10.1523/JNEUROSCI.1146-14.2014.

Feringa, Femke M., and Rik van der Kant. 2021. "Cholesterol and Alzheimer's Disease; From Risk Genes to Pathological Effects." *Frontiers in Aging Neuroscience* 13(690372). doi: 10.3389/FNAGI.2021.690372/BIBTEX.

Fields, R. Douglas, and Olena Bukalo. 2020. "Myelin Makes Memories." *Nature Neuroscience 2020 23:4* 23(4):469–70. doi: 10.1038/s41593-020-0606-x.

Filippi, Massimo, Paolo Preziosa, Brenda L. Banwell, Frederik Barkhof, Olga Ciccarelli, Nicola De Stefano, Jeroen J. G. Geurts, Friedemann Paul, Daniel S. Reich, Ahmed T. Toosy, Anthony Traboulsee, Mike P. Wattjes, Tarek A. Yousry, Achim Gass, Catherine Lubetzki, Brian G.

Weinshenker, and Maria A. Rocca. 2019. “Assessment of Lesions on Magnetic Resonance Imaging in Multiple Sclerosis: Practical Guidelines.” *Brain* 142:1858–75. doi: 10.1093/brain/awz144.

Filippi, Massimo, Paolo Preziosa, Dawn Langdon, Hans Lassmann, Friedemann Paul, Àlex Rovira, Menno M. Schoonheim, Alessandra Solari, Bruno Stankoff, and Maria A. Rocca. 2020. “Identifying Progression in Multiple Sclerosis: New Perspectives.” *Annals of Neurology* 88(3):438–52. doi: 10.1002/ana.25808.

Fischer, Marie T., Rakhi Sharma, Jamie L. Lim, Lukas Haider, Josa M. Frischer, Joost Drexhage, Don Mahad, Monika Bradl, Jack Van Horssen, and Hans Lassmann. 2012. “NADPH Oxidase Expression in Active Multiple Sclerosis Lesions in Relation to Oxidative Tissue Damage and Mitochondrial Injury.” *Brain* 135:886–99. doi: 10.1093/brain/aws012.

Ford, Mandy L., and Brian D. Evavold. 2005. “Specificity, Magnitude, and Kinetics of MOG-Specific CD8+ T Cell Responses during Experimental Autoimmune Encephalomyelitis.” *European Journal of Immunology* 35(1):76–85. doi: 10.1002/eji.200425660.

Franklin, Robin J. M., and Charles Ffrench-Constant. 2008. “Remyelination in the CNS: From Biology to Therapy.” *Nature Reviews Neuroscience 2008 9:11* 9(11):839–55. doi: 10.1038/nrn2480.

Freemantle, Erika, Gary Gang Chen, Cristiana Cruceanu, Naguib Mechawar, and Gustavo Turecki. 2013. “Analysis of Oxysterols and Cholesterol in Prefrontal Cortex of Suicides.” *International Journal of Neuropsychopharmacology* 16(6):1241–49. doi: 10.1017/S1461145712001587.

Frischer, Josa M., Stephan Bramow, Assunta Dal-Bianco, Claudia F. Lucchinetti, Helmut Rauschka, Manfred Schmidbauer, Henning Laursen, Per Soelberg Sorensen, and Hans Lassmann. 2009. “The Relation between Inflammation and Neurodegeneration in Multiple Sclerosis Brains.” *Brain* 132:1175–89. doi: 10.1093/brain/awp070.

Frischer, Josa M., Stephen D. Weigand, Yong Guo, Nilufer Kale, Joseph E. Parisi, Istvan Pirko, Jay Mandrekar, Stephan Bramow, Imke Metz, Wolfgang Brück, Hans Lassmann, and Claudia F. Lucchinetti. 2015. “Clinical and Pathological Insights into the Dynamic Nature of the White Matter Multiple Sclerosis Plaque.” *Ann Neurol* 78(5):710–21. doi: 10.1002/ana.24497.

Frohman, Elliot M., Michael K. Racke, and Cedric S. Raine. 2006. “Multiple Sclerosis — The Plaque and Its Pathogenesis.” *New England Journal of Medicine* 354(9):942–55. doi: 10.1056/nejmra052130.

Fu, Ruying, Qingyu Shen, Pengfei Xu, Jin Jun Luo, and Yamei Tang. 2014. “Phagocytosis of Microglia in the Central Nervous System Diseases.” *Molecular Neurobiology* 49(3):1434. doi: 10.1007/S12035-013-8620-6.

Fukumoto, Hiroaki, Amy Deng, Michael Irizarry, Michael Fitzgerald, and William Rebeck. 2002. “Induction of the Cholesterol Transporter ABCA1 in Central Nervous System Cells by Liver X Receptor Agonists Increases Secreted AB Levels.” *J Biol Chem* 13(277):48508–13.

García-Merino, Antonio. 2021. “Bruton’s Tyrosine Kinase Inhibitors: A New Generation of Promising Agents for Multiple Sclerosis Therapy.” *Cells* 10(2560). doi: 10.3390/CELLS10102560.

Gianfrancesco, M. A., and L. F. Barcellos. 2016. “Obesity and Multiple Sclerosis Susceptibility: A Review.” *J Neurol Neuromed* 1(7):1–5.

Ginhoux, Florent, Melanie Greter, Marylene Leboeuf, Sayan Nandi, Peter See, Solen Gokhan, Mark F. Mehler, Simon J. Conway, Lai Guan Ng, E. Richard Stanley, Igor M. Samokhvalov, and Miriam Merad. 2010a. “Fate Mapping Analysis Reveals That Adult Microglia Derive from Primitive Macrophages.” *Science* 330(6005):841–45. doi: 10.1126/SCIENCE.1194637.

Ginhoux, Florent, Melanie Greter, Marylene Leboeuf, Sayan Nandi, Peter See, Solen Gokhan, Mark F. Mehler, Simon J. Conway, Lai Guan Ng, E. Richard Stanley, Igor M. Samokhvalov, and Miriam Merad. 2010b. “Fate Mapping Analysis Reveals That Adult Microglia Derive from Primitive Macrophages.” *Science (New York, N.Y.)* 330(6005):845. doi: 10.1126/SCIENCE.1194637.

Gitik, Miri, Sigal Liraz-Zaltsman, Per Arne Oldenborg, Fanny Reichert, and Shlomo Rotshenker. 2011. “Myelin Down-Regulates Myelin Phagocytosis by Microglia and Macrophages through Interactions between CD47 on Myelin and SIRPα (Signal Regulatory Protein-α) on Phagocytes.” *Journal of Neuroinflammation* 8(1):1–11. doi: 10.1186/1742-2094-8-24/FIGURES/4.

Giulian, D., and T. J. Baker. 1986. “Characterization of Ameboid Microglia Isolated from Developing Mammalian Brain.” *The Journal of Neuroscience* 6(8):2178. doi: 10.1523/JNEUROSCI.06-08-02163.1986.

Glish, Gary L., and Richard W. Vachet. 2003. “The Basics of Mass Spectrometry in the Twenty-First Century.” *Nature Reviews Drug Discovery* 2(2):140–50. doi: 10.1038/NRD1011.

Goedeke, Leigh, and Carlos Fernández-Hernando. 2011. “Regulation of Cholesterol Homeostasis.” *Cellular and Molecular Life Sciences 2011 69:6* 69(6):915–30. doi: 10.1007/S00018-011-0857-5.

Goldmann, Tobias, Peter Wieghofer, Marta Joana Costa Jordão, Fabiola Prutek, Nora Hagemeyer, Kathrin Frenzel, Lukas Amann, Ori Staszewski, Katrin Kierdorf, Martin Krueger, Giuseppe Locatelli, Hannah Hochgerner, Robert Zeiser, Slava Epelman, Frederic Geissmann, Josef Priller, Fabio M. V. Rossi, Ingo Bechmann, Martin Kerschensteiner, Sten Linnarsson, Steffen Jung, and Marco Prinz. 2016. “Origin, Fate and Dynamics of Macrophages at Central Nervous System Interfaces.” *Nature Immunology* 17(7):797–805. doi: 10.1038/ni.3423.

Goldstein, Joseph L., Russell A. DeBose-Boyd, and Michael S. Brown. 2006. “Protein Sensors for Membrane Sterols.” *Cell* 124(1):35–46. doi: 10.1016/J.CELL.2005.12.022.

Gomez Perdiguero, Elisa, Kay Klapproth, Christian Schulz, Katrin Busch, Emanuele Azzoni, Lucile Crozet, Hannah Garner, Celine Trouillet, Marella F. De Bruijn, Frederic Geissmann, and Hans Reimer Rodewald. 2015. “Tissue-Resident Macrophages Originate from Yolk-Sac-Derived Erythro-Myeloid Progenitors.” *Nature* 518(7540):547–51. doi: 10.1038/nature13989.

Gómez-López, Ariadna Regina, Gemma Manich, Mireia Recasens, Beatriz Almolda, Berta González, and Bernardo Castellano. 2021. “Evaluation of Myelin Phagocytosis by Microglia/Macrophages in Nervous Tissue Using Flow Cytometry.” *Current Protocols* 1(3):1–18. doi: 10.1002/cpz1.73.

Gordon, Richard, Colleen E. Hogan, Matthew L. Neal, Vellareddy Anantharam, Anumantha G. Kanthasamy, and Arthi Kanthasamy. 2011. “A Simple Magnetic Separation Method for High-Yield Isolation of Pure Primary Microglia.” *Journal of Neuroscience Methods* 194(2):287. doi: 10.1016/J.JNEUMETH.2010.11.001.

Grajchen, Elien, Jerome J. A. Hendriks, and Jeroen F. J. Bogie. 2018. “The Physiology of Foamy Phagocytes in Multiple Sclerosis.” *Acta Neuropathologica Communications* 6(124).

Gray, Elizabeth, Taya L. Thomas, Samar Betmouni, Neil Scolding, and Seth Love. 2008. “Elevated Activity and Microglial Expression of Myeloperoxidase in Demyelinated Cerebral Cortex in Multiple Sclerosis.” *Brain Pathology* 18(1):86–95. doi: 10.1111/J.1750-3639.2007.00110.X.

Greenbaum, Dov, Christopher Colangelo, Kenneth Williams, and Mark Gerstein. 2003. “Comparing Protein Abundance and MRNA Expression Levels on a Genomic Scale.” *Genome Biology* 4(117).

Greter, Melanie, Iva Lelios, Pawel Pelczar, Guillaume Hoeffel, Jeremy Price, Marylene Leboeuf, Thomas M. Kündig, Karl Frei, Florent Ginhoux, Miriam Merad, and Burkhard Becher. 2012. “Stroma-Derived Interleukin-34 Controls the Development and Maintenance of Langerhans Cells and the Maintenance of Microglia.” *Immunity* 37(6):1050–60. doi: 10.1016/j.immuni.2012.11.001.

Griffiths, Lauren, Richard Reynolds, Rhian Evans, Ryan J. Bevan, Mark I. Rees, Djordje Gveric, James W. Neal, and Owain W. Howell. 2020. “Substantial Subpial Cortical Demyelination in Progressive Multiple Sclerosis: Have We Underestimated the Extent of Cortical Pathology?” *Neuroimmunology and Neuroinflammation* 7(1):51–67. doi: 10.20517/2347-8659.2019.21.

Griffiths, Rian L., James W. Hughes, Susan E. Abbatiello, Michael W. Belford, Iain B. Styles, and Helen J. Cooper. 2020. “Comprehensive LESA Mass Spectrometry Imaging of Intact Proteins by Integration of Cylindrical FAIMS.” *Analytical Chemistry* 92(4):2885–90. doi: 10.1021/ACS.ANALCHEM.9B05124/ASSET/IMAGES/LARGE/AC9B05124_0002.JPEG.

Griffiths, William J., Jonas Abdel-Khalik, Eylan Yutuc, Gustavo Roman, Margaret Warner, Jan Åke Gustafsson, and Yuqin Wang. 2019. “Concentrations of Bile Acid Precursors in Cerebrospinal Fluid of Alzheimer’s Disease Patients.” *Free Radical Biology and Medicine* 134:42–52. doi: 10.1016/j.freeradbiomed.2018.12.020.

Griffiths, William J., Peter J. Crick, Anna Meljon, Spyridon Theofilopoulos, Jonas Abdel-Khalik, Eylan Yutuc, Josie E. Parker, Diane E. Kelly, Steven L. Kelly, Ernest Arenas, and Yuqin Wang. 2019. “Additional Pathways of Sterol Metabolism: Evidence from Analysis of Cyp27a1-/- Mouse Brain and Plasma.” *Biochimica et Biophysica Acta. Molecular and Cell Biology of Lipids* 1864(2):191–211. doi: 10.1016/J.BBALIP.2018.11.006.

Griffiths, William J., Peter J. Crick, and Yuqin Wang. 2013. “Methods for Oxysterol Analysis: Past, Present and Future.” *Biochemical Pharmacology* 86(1):3–14. doi: 10.1016/J.BCP.2013.01.027.

Griffiths, William J., Martin Hornshaw, Gary Woffendin, Sharon F. Baker, Andrew Lockhart, Sibylle Heidelberger, Magnus Gustafsson, Jan Sjövall, and Yuqin Wang. 2008. “Discovering Oxysterols in Plasma: A Window on the Metabolome Europe PMC Funders Group.” *J Proteome Res* 7(8):3602–12. doi: 10.1021/pr8001639.

Griffiths, William J., and Yuqin Wang. 2019. “Oxysterol Research : A Brief Review.” *Biochemical Society Transactions* 0:1–10.

Griffiths, William J., and Yuqin Wang. 2020. “Oxysterols as Lipid Mediators: Their Biosynthetic Genes, Enzymes and Metabolites.” *Prostaglandins and Other Lipid Mediators* 147. doi: 10.1016/J.PROSTAGLANDINS.2019.106381.

Griffiths, William J., and Yuqin Wang. 2022. “Cholesterol Metabolism: From Lipidomics to Immunology.” *Journal of Lipid Research* 63(2).

Gross, Jürgen H. 2017. *Mass Spectrometry*. 3rd ed.

Gustafsson, Johan O. R., Martin K. Oehler, Andrew Ruszkiewicz, Shaun R. McColl, and Peter Hoffmann. 2011. “MALDI Imaging Mass Spectrometry (MALDI-IMS)—Application of Spatial Proteomics for Ovarian Cancer Classification and Diagnosis.” *International Journal of Molecular Sciences* 12(1):773–94. doi: 10.3390/IJMS12010773.

Haider, Lukas, Marie T. Fischer, Josa M. Frischer, Jan Bauer, Romana Hö, Gergö Botond, Harald Esterbauer, Christoph J. Binder, Joseph L. Witztum, and Hans Lassmann. 2011. “Oxidative Damage in Multiple Sclerosis Lesions.” *A JOURNAL OF NEUROLOGY* 134(7):1914–24. doi: 10.1093/brain/awr128.

Haider, Lukas, Tobias Zrzavy, Simon Hametner, Romana Höftberger, Francesca Bagnato, Günther Grabner, Siegfried Trattnig, Sabine Pfeifenbring, Wolfgang Brück, and Hans Lassmann. 2016. “The Topograpy of Demyelination and Neurodegeneration in the Multiple Sclerosis Brain.” *Brain* 139(3):807–15. doi: 10.1093/BRAIN/AWV398.

Hait, Nitai C., Laura E. Wise, Jeremy C. Allegood, Megan O’brien, Dorit Avni, Thomas M. Reeves, Pamela E. Knapp, Junyan Lu, Cheng Luo, Michael F. Miles, Sheldon Milstien, Aron H. Lichtman, and Sarah Spiegel. 2014. “Active, Phosphorylated Fingolimod Inhibits Histone Deacetylases and Facilitates Fear Extinction Memory.” *Nat Neurosci* 17(7):971–80. doi: 10.1038/nn.3728.

Hametner, Simon, Isabella Wimmer, Lukas Haider, Sabine Pfeifenbring, Wolfgang Brück, and Hans Lassmann. 2013. “Iron and Neurodegeneration in the Multiple Sclerosis Brain.” *Annals of Neurology* 74(6):848–61. doi: 10.1002/ANA.23974.

Han, May H., Deborah H. Lundgren, Siddhartha Jaiswa, Mark Chao, Kareem L. Graham, Christopher S. Garris, Robert C. Axtell, Peggy P. Ho, Christopher B. Lock, Joslyn I. Woodard, Sara E. Brownell, Maria Zoudilova, Jack F. V. Hunt, Sergio E. Baranzini, Eugene C. Butcher, Cedric S. Raine, Raymond A. Sobe, David K. Han, Irving Weissman, and Lawrence Steinman.

2012. “Janus-like Opposing Roles of CD47 in Autoimmune Brain Inflammation in Humans and Mice.” *The Journal of Experimental Medicine* 209(7):1325–34. doi: 10.1084/JEM.20101974.

Hanin, Aurélie, Paul Baudin, Sophie Demeret, Delphine Roussel, Sarah Lecas, Elisa Teyssou, Maria Damiano, David Luis, Virginie Lambrecq, Valerio Frazzini, Maxens Decavèle, Isabelle Plu, Dominique Bonnefont-Rousselot, Randa Bittar, Foudil Lamari, and Vincent Navarro. 2021. “Disturbances of Brain Cholesterol Metabolism: A New Excitotoxic Process Associated with Status Epilepticus.” *Neurobiology of Disease* 154:105346. doi: 10.1016/J.NBD.2021.105346.

Healy, Luke M., Gabrielle Perron, So-Yoon Won, Mackenzie A. Michell-Robinson, Ayman Rezk, Samuel K. Ludwin, Craig S. Moore, Jeffery A. Hall, Amit Bar-Or, and Jack P. Antel. 2016. “MerTK Is a Functional Regulator of Myelin Phagocytosis by Human Myeloid Cells.” *The Journal of Immunology* 196(8):3375–84. doi: 10.4049/JIMMUNOL.1502562.

Hendrickx, Debbie A. E., Karianne G. Schuurman, Michael van Draanen, Jörg Hamann, and Inge Huitinga. 2014. “Enhanced Uptake of Multiple Sclerosis-Derived Myelin by THP-1 Macrophages and Primary Human Microglia.” *Journal of Neuroinflammation* 11(64). doi: 10.1186/1742-2094-11-64.

Heß, Katharina, Laura Starost, Nicholas W. Kieran, Christian Thomas, Maria C. J Vincenten, Jack Antel, Gianvito Martino, Inge Huitinga, Luke Healy, and Tanja Kuhlmann. 2020. “Lesion Stage-Dependent Causes for Impaired Remyelination in MS.” *Acta Neuropathologica* 140:359–75. doi: 10.1007/s00401-020-02189-9.

Heverin, Maura, Nenad Bogdanovic, Dieter Lütjohann, Thomas Bayer, Irina Pikuleva, Lionel Bretillon, Ulf Diczfalusy, Bengt Winblad, and Ingemar Björkhem. 2004. “Changes in the Levels of Cerebral and Extracerebral Sterols in the Brain of Patients with Alzheimer’s Disease.” *Journal of Lipid Research* 45(1):186–93. doi: 10.1194/jlr.M300320-JLR200.

Heverin, Maura, Steve Meaney, Dieter Lütjohann, Ulf Diczfalusy, John Wahren, and Ingemar Björkhem. 2005. “Crossing the Barrier: Net Flux of 27-Hydroxycholesterol into the Human Brain.” *Journal of Lipid Research* 46(5):1047–52. doi: 10.1194/jlr.M500024-JLR200.

Ho, C. S., C. W. K. Lam, M. H. M. Chan, R. C. K. Cheung, L. K. Law, L. C. W. Lit, K. F. Ng, M. W. M. Suen, and H. L. Tai. 2003. “Electrospray Ionisation Mass Spectrometry: Principles and Clinical Applications.” *The Clinical Biochemist Reviews* 24(1):3–12.

Hocart, Charles H. 2010. “Mass Spectrometry: An Essential Tool for Trace Identification and Quantification.” *Comprehensive Natural Products II: Chemistry and Biology* 9:327–88. doi: 10.1016/B978-008045382-8.00187-8.

de Hoffmann, Edmond, and Vincent Stroobant. 2007. *Mass Spectrometry Principles and Applications*.

Hollen, Chris W., M. Mateo Paz Soldán, II John R. Rinker, and Rebecca I. Spain. 2020. “The Future of Progressive Multiple Sclerosis Therapies.” *Federal Practitioner* 37(Suppl 1):S43–49.

Honce, Justin Morris. 2013. “Gray Matter Pathology in MS: Neuroimaging and Clinical Correlations.” *Multiple Sclerosis International* 2013:1–16. doi: 10.1155/2013/627870.

Honda, Akira, Kouwa Yamashita, Hiroshi Miyazaki, Mutsumi Shirai, Tadashi Ikegami, Guorong Xu, Mitsuteru Numazawa, Takashi Hara, and Yasushi Matsuzaki. 2008. “Highly Sensitive Analysis of Sterol Profiles in Human Serum by LC-ESI-MS/MS.” *Journal of Lipid Research* 49(9):2063–73. doi: 10.1194/JLR.D800017-JLR200.

Horng, Sam, Anthony Therattil, Sarah Moyon, Alexandra Gordon, Karla Kim, Azeb Tadesse Argaw, Yuko Hara, John N. Mariani, Setsu Sawai, Per Flodby, Edward D. Crandall, Zea Borok, Michael V. Sofroniew, Candice Chapouly, and Gareth R. John. 2017. “Astrocytic Tight Junctions Control Inflammatory CNS Lesion Pathogenesis.” *The Journal of Clinical Investigation* 127(8):3136–51. doi: 10.1172/JCI91301.

Horton, Jay, Joseph Goldstein, and Michael Brown. 2002. “SREBPs: Activators of the Complete Program of Cholesterol and Fatty Acid Synthesis in the Liver.” *J. Clin. Invest.* 109:1125–31.

Howell, Owain W., Cheryl A. Reeves, Richard Nicholas, Daniele Carassiti, Bishan Radotra, Steve M. Gentleman, Barbara Serafini, Francesca Aloisi, Federico Roncaroli, Roberta Magliozzi, and Richard Reynolds. 2011. “Meningeal Inflammation Is Widespread and Linked to Cortical Pathology in Multiple Sclerosis.” *Brain* 134(9):2755–71. doi: 10.1093/brain/awr182.

Huang, Hai, Samer Tohme, Ahmed B. Al-Khafaji, Sheng Tai, Patricia Loughran, Li Chen, Shu Wang, Jiyun Kim, Timothy Billiar, Yanming Wang, and Allan Tsung. 2015. “Damage-Associated Molecular Pattern-Activated Neutrophil Extracellular Trap Exacerbates Sterile Inflammatory Liver Injury.” doi: 10.1002/hep.27841/suppinfo.

Huang, Xuemei, Nicholas W. Sterling, Guangwei Du, Dongxiao Sun, Christina Stetter, Lan Kong, Yusheng Zhu, Jeffery Neighbors, Mechelle M. Lewis, Honglei Chen, Raymond J. Hohl, and Richard B. Mailman. 2019. “Brain Cholesterol Metabolism and Parkinson’s Disease.” *Movement Disorders* 34(3):386–95. doi: 10.1002/mds.27609.

Hubler, Zita, Dharmaraja Allimuthu, Ilya Bederman, Matthew S. Elitt, Mayur Madhavan, Kevin C. Allan, H. Elizabeth Shick, Eric Garrison, Molly T. Karl, Daniel C. Factor, Zachary S. Nevin, Joel L. Sax, Matthew A. Thompson, Yuriy Fedorov, Jing Jin, William K. Wilson, Martin Giera, Franz Bracher, Robert H. Miller, Paul J. Tesar, and Drew J. Adams. 2018. “Accumulation of 8,9-Unsaturated Sterols Drives Oligodendrocyte Formation and Remyelination.” *Nature* 560(7718):372–76. doi: 10.1038/s41586-018-0360-3.

Husain, Mohammed Amir, Benoit Laurent, and Mélanie Plourde. 2021. “APOE and Alzheimer’s Disease: From Lipid Transport to Physiopathology and Therapeutics.” *Frontiers in Neuroscience* 15. doi: 10.3389/FNINS.2021.630502/BIBTEX.

Ingram, Gillian, Sam Loveless, Owain W. Howell, Svetlana Hakobyan, Bethan Dancey, Claire L. Harris, Neil P. Robertson, James W. Neal, and B. Paul Morgan. 2014. “Complement Activation in Multiple Sclerosis Plaques: An Immunohistochemical Analysis.” *Acta Neuropathologica Communications* 2(1):1–34. doi: 10.1186/2051-5960-2-53.

Jäckle, Katharina, Thomas Zeis, Nicole Schaeren-Wiemers, Andreas Junker, Franziska van der Meer, Nadine Kramann, Christine Stadelmann, and Wolfgang Brück. 2020. “Molecular Signature of Slowly Expanding Lesions in Progressive Multiple Sclerosis.” *Brain* 143(7):2073–88. doi: 10.1093/brain/awaa158.

Jakimovski, Dejan, Bianca Weinstock-Guttman, Murali Ramanathan, Channa Kolb, David Hojnacki, Alireza Minagar, and Robert Zivadinov. 2017. “Ocrelizumab: A B-Cell Depleting Therapy for Multiple Sclerosis.” *Expert Opinion on Biological Therapy* 17(9):1163–72. doi: 10.1080/14712598.2017.1347632.

Janowski, Bethany A., Michael J. Grogan, Stacey A. Jones, G. Bruce Wisely, Steven A. Kliewer, Elias J. Corey, and David J. Mangelsdorf. 1999. “Structural Requirements of Ligands for the Oxysterol Liver X Receptors LXR and LXR.” *Proc. Natl. Acad. Sci* 96:266–71.

Javadifar, Amin, Sahar Rastgoo, Maciej Banach, Tannaz Jamialahmadi, Thomas P. Johnston, and Amirhossein Sahebkar. 2021. “Molecular Sciences Foam Cells as Therapeutic Targets in Atherosclerosis with a Focus on the Regulatory Roles of Non-Coding RNAs.” *Int. J. Mol. Sci* 22(2529). doi: 10.3390/ijms22052529.

Javitt, Norman B. 2002. “25R,26-Hydroxycholesterol Revisited: Synthesis, Metabolism, and Biologic Roles.” *Journal of Lipid Research* 43(5):665–70. doi: 10.1016/S0022-2275(20)30106-1.

Jeitner, T. M., I. Voloshyna, and A. B. Reiss. 2011. “Oxysterol Derivatives of Cholesterol in Neurodegenerative Disorders.” *Current Medicinal Chemistry* 18(10):1515–25. doi: 10.2174/092986711795328445.

Jiang, Xuntian, Daniel S. Ory, and Xianlin Han. 2007. “Characterization of Oxysterols by Electrospray Ionization Tandem Mass Spectrometry after One-Step Derivatization with Dimethylglycine.” *Rapid Commun Mass Spectrom* 21(2):141–52.

Jiang, Xuntian, Rohini Sidhu, Forbes D. Porter, Nicole M. Yanjanin, Anneliese O. Speak, Danielle Taylor Te Vruchte, Frances M. Platt, Hideji Fujiwara, David E. Scherrer, Jessie Zhang, Dennis J. Dietzen, Jean E. Schaffer, and Daniel S. Ory. 2011. “A Sensitive and Specific LC-MS/MS Method for Rapid Diagnosis of Niemann-Pick C1 Disease from Human Plasma.” *Journal of Lipid Research* 52(7):1435–45. doi: 10.1194/JLR.D015735.

Jokubaitis, Vilija G., Maria Pia Campagna, Omar Ibrahim, Jim Stankovich, Pavlina Kleinova, Fuencisla Matesanz, Daniel Hui, Sara Eichau, Mark Slee, Jeannette Lechner-Scott, Rodney Lea, Trevor J. Kilpatrick, Tomas Kalincik, Philip L. De Jager, Ashley Beecham, Jacob L. McCauley, Bruce V Taylor, Steve Vucic, Louise Laverick, Karolina Vodehnalova, Maria-Isabel García-Sanchéz, Antonio Alcina, Anneke van der Walt, Eva Kubala Havrdova, Guillermo Izquierdo, Nikolaos Patsopoulos, Dana Horakova, and Helmut Butzkueven. 2022. “Not All Roads Lead to the Immune System: The Genetic Basis of Multiple Sclerosis Severity.” *MedRxiv*. doi: 10.1093/BRAIN/AWAC449.

Kacher, Radhia, Antonin Lamazière, Nicolas Heck, Vincent Kappes, Coline Mounier, Gaëtan Despres, Yulia Dembitskaya, Elodie Perrin, Wilhelm Christaller, Satish Sasidharan Nair, Valérie Messent, Nathalie Cartier, Peter Vanhoutte, Laurent Venance, Frédéric Saudou, Christian Néri, Jocelyne Caboche, and Sandrine Betuing. 2019. “CYP46A1 Gene Therapy Deciphers the Role of Brain Cholesterol Metabolism in Huntington’s Disease.” *Brain* 142(8):2432–50. doi: 10.1093/BRAIN/AWZ174.

Kamel, Fatemah Omar. 2019. “Factors Involved in Relapse of Multiple Sclerosis.” *Journal of Microscopy and Ultrastructure* 7(3). doi: 10.4103/JMAU.JMAU_59_18.

van der Kant, Rik, Vanessa F. Langness, Cheryl M. Herrera, Daniel A. Williams, Lauren K. Fong, Yves Leestemaker, Evelyne Steenvoorden, Kevin D. Rynearson, Jos F. Brouwers, J. Bernd Helms, Huib Ovaa, Martin Giera, Steven L. Wagner, Anne G. Bang, and Lawrence S. B. Goldstein. 2019. "Cholesterol Metabolism Is a Druggable Axis That Independently Regulates Tau and Amyloid-β in IPSC-Derived Alzheimer's Disease Neurons." *Cell Stem Cell* 24(3):363–75. doi: 10.1016/J.STEM.2018.12.013.

Kappos, Ludwig, Jerry S. Wolinsky, Gavin Giovannoni, Douglas L. Arnold, Qing Wang, Corrado Bernasconi, Fabian Model, Harold Koendgen, Marianna Manfrini, Shibeshih Belachew, and Stephen L. Hauser. 2020. "Contribution of Relapse-Independent Progression vs Relapse-Associated Worsening to Overall Confirmed Disability Accumulation in Typical Relapsing Multiple Sclerosis in a Pooled Analysis of 2 Randomized Clinical Trials." *JAMA Neurology* 77(9):1132–40. doi: 10.1001/jamaneurol.2020.1568.

Karch, Celeste M., and Alison M. Goate. 2015. "Alzheimer's Disease Risk Genes and Mechanisms of Disease Pathogenesis." *Biological Psychiatry* 77(1):43–51. doi: 10.1016/J.BIOPSYCH.2014.05.006.

Keough, Michael B., and V. Wee Yong. 2013. "Remyelination Therapy for Multiple Sclerosis." *Neurotherapeutics* 10(1):44. doi: 10.1007/S13311-012-0152-7.

Keren-Shaul, Hadas, Amit Spinrad, Assaf Weiner, Orit Matcovitch-Natan, Raz Dvir-Szternfeld, Tyler K. Ulland, Eyal David, Kuti Baruch, David Lara-Astaiso, Beata Toth, Shalev Itzkovitz, Marco Colonna, Michal Schwartz, and Ido Amit. 2017. "A Unique Microglia Type Associated with Restricting Development of Alzheimer's Disease." *Cell* 169(7):1276–90. doi: 10.1016/J.CELL.2017.05.018.

Khalaj, Anna, J., Jonathan Hasselmann, Catherine Augello, Spencer Moore, and Seema, K. Tiwari-Woodruff. 2016. "Nudging Oligodendrocyte Intrinsic Signaling to Remyelinate and Repair: Estrogen Receptor Ligand Effects." *J Steroid Biochem Mol Biol.* 160:43–52. doi: doi:10.1016/j.jsbmb.2016.01.006.

Kim, Roy Y., Alexandria S. Hoffman, Noriko Itoh, Yan Ao, Rory Spence, Michael V. Sofroniew, and Rhonda R. Voskuhl. 2014. "Astrocyte CCL2 Sustains Immune Cell Infiltration in Chronic Experimental Autoimmune Encephalomyelitis." *Journal of Neuroimmunology* 274(1–2):53–61. doi: 10.1016/j.jneuroim.2014.06.009.

Kipp, Markus, Marion Victor, Gianvito Martino, and Robin J.M. Franklin. 2012. "Endogeneous Remyelination: Findings in Human Studies." *CNS & Neurological Disorders Drug Targets* 11(5):598–609. doi: 10.2174/187152712801661257.

Kleiter, Ingo, Ilya Ayzenberg, and Robert Hoepner. 2016. "Fingolimod for Multiple Sclerosis and Emerging Indications: Appropriate Patient Selection, Safety Precautions, and Special Considerations." *Therapeutics and Clinical Risk Management* 12:261–72. doi: 10.2147/TCRM.S65558.

Klüver, Heinrich, and Elizabeth Barrera. 1953. "A Method for the Combined Staining of Cells and Fibers in the Nervous System." *Journal of Neuropathology and Experimental Neurology* 12(4):400–403. doi: 10.1097/00005072-195312040-00008.

Ko, Mihee, Kun Zou, Hirohisa Minagawa, Wenxin Yu, Jian Sheng Gong, Katsuhiko Yanagisawa, and Makoto Michikawa. 2005. “Cholesterol-Mediated Neurite Outgrowth Is Differently Regulated between Cortical and Hippocampal Neurons.” *Journal of Biological Chemistry* 280(52):42759–65. doi: 10.1074/JBC.M509164200.

Kompauer, Mario, Sven Heiles, and Bernhard Spengler. 2016. “Atmospheric Pressure MALDI Mass Spectrometry Imaging of Tissues and Cells at 1.4-Mm Lateral Resolution.” *Nature Methods* 14(1):90–96. doi: 10.1038/NMETH.4071.

Koso, Hideto, Ryuichi Nishinakamura, and Sumiko Watanabe. 2018. “Sall1 Regulates Microglial Morphology Cell Autonomously in the Developing Retina.” *Advances in Experimental Medicine and Biology* 1074:209–15. doi: 10.1007/978-3-319-75402-4_26/COVER.

Krasemann, Susanne, Charlotte Madore, Ron Cialic, Caroline Baufeld, Narghes Calcagno, Rachid El Fatimy, Lien Beckers, Elaine O’Loughlin, Yang Xu, Zain Fanek, David J. Greco, Scott T. Smith, George Tweet, Zachary Humulock, Tobias Zrzavy, Patricia Conde-Sanroman, Mar Gacias, Zhiping Weng, Hao Chen, Emily Tjon, Fargol Mazaheri, Kristin Hartmann, Asaf Madi, Jason D. Ulrich, Markus Glatzel, Anna Worthmann, Joerg Heeren, Bogdan Budnik, Cynthia Lemere, Tsuneya Ikezu, Frank L. Heppner, Vladimir Litvak, David M. Holtzman, Hans Lassmann, Howard L. Weiner, Jordi Ochando, Christian Haass, and Oleg Butovsky. 2017. “The TREM2-APOE Pathway Drives the Transcriptional Phenotype of Dysfunctional Microglia in Neurodegenerative Diseases.” *Immunity* 47(3):566–81. doi: 10.1016/J.IMMUNI.2017.08.008.

Kudo, K., G. T. Emmons, E. W. Casserly, D. P. Via, L. C. Smith, J. St. Pyrek, and G. J. Schroepfer. 1989. “Inhibitors of Sterol Synthesis. Chromatography of Acetate Derivatives of Oxygenated Sterols.” *Journal of Lipid Research* 30(7):1097–1111. doi: 10.1016/S0022-2275(20)38296-1.

Kuhlmann, Tanja, Samuel Ludwin, Alexandre Prat, Jack Antel, Wolfgang Brück, and Hans Lassmann. 2017. “An Updated Histological Classification System for Multiple Sclerosis Lesions.” *Acta Neuropathologica* 133(1):13–24. doi: 10.1007/s00401-016-1653-y.

Kutzelnigg, Alexandra, Claudia F. Lucchinetti, Christine Stadelmann, Wolfgang Brück, Helmut Rauschka, Markus Bergmann, Manfred Schmidbauer, Joseph E. Parisi, and Hans Lassmann. 2005. “Cortical Demyelination and Diffuse White Matter Injury in Multiple Sclerosis.” *Brain* 128:2705–12. doi: 10.1093/brain/awh641.

de la Roche, Marianne, Claire Hamilton, Rebecca Mortensen, A. Arockia Jeyaprakash, Sanjay Ghosh, and Paras K. Anand. 2018. “Trafficking of Cholesterol to the ER Is Required for NLRP3 Inflammasome Activation.” *The Journal of Cell Biology* 217(10):3560–3676. doi: 10.1083/JCB.201709057.

Lampron, Antoine, Antoine Larochelle, Nathalie Laflamme, Paul Préfontaine, Marie Michèle Plante, Maria Gabriela Sánchez, V. Wee Yong, Peter K. Stys, Marie Ève Tremblay, and Serge Rivest. 2015. “Inefficient Clearance of Myelin Debris by Microglia Impairs Remyelinating Processes.” *The Journal of Experimental Medicine* 212(4):481–95. doi: 10.1084/JEM.20141656.

Lanz, Tobias V., R. Camille Brewer, Peggy P. Ho, Jae Seung Moon, Kevin M. Jude, Daniel Fernandez, Ricardo A. Fernandes, Alejandro M. Gomez, Gabriel Stefan Nadj, Christopher M.

Bartley, Ryan D. Schubert, Isobel A. Hawes, Sara E. Vazquez, Manasi Iyer, J. Bradley Zuchero, Bianca Teegen, Jeffrey E. Dunn, Christopher B. Lock, Lucas B. Kipp, Victoria C. Cotham, Beatrix M. Ueberheide, Blake T. Aftab, Mark S. Anderson, Joseph L. DeRisi, Michael R. Wilson, Rachael J. M. Bashford-Rogers, Michael Platten, K. Christopher Garcia, Lawrence Steinman, and William H. Robinson. 2022. "Clonally Expanded B Cells in Multiple Sclerosis Bind EBV EBNA1 and GlialCAM." *Nature* 603(7900):321–27. doi: 10.1038/S41586-022-04432-7.

Larocca, Jorge, N., and Williams, T. Norton. 2007. "Isolation of Myelin." *Current Protocols in Cell Biology* 33(1):3.25.1-3.25.19. doi: https://doi.org/10.1002/0471143030.cb0325s33.

Lassmann, H., C. S. Raine, J. Antel, and J. W. Prineas. 1998. "Immunopathology of Multiple Sclerosis: Report on an International Meeting Held at the Institute of Neurology of the University of Vienna." *Journal of Neuroimmunology* 86(2):213–17. doi: 10.1016/S0165-5728(98)00031-9.

Lassmann, Hans. 2018. "Multiple Sclerosis Pathology." *Cold Spring Harbor Perspectives in Medicine* 8(3). doi: 10.1101/CSHPERSPECT.A028936.

Lassmann, Hans, Wolfgang Brück, and Claudia Lucchinetti. 2001. "Heterogeneity of Multiple Sclerosis Pathogenesis: Implications for Diagnosis and Therapy." *Trends in Molecular Medicine* 7(3):115–21. doi: 10.1016/S1471-4914(00)01909-2.

Lassmann, Hans, Jack Van Horssen, and Don Mahad. 2012. "Progressive Multiple Sclerosis: Pathology and Pathogenesis." *Nature Reviews Neurology* 8(11):647–56. doi: 10.1038/NRNEUROL.2012.168.

Lee, Sun Hee, Jae Ho Lee, and Seung Soon Im. 2020. "The Cellular Function of SCAP in Metabolic Signaling." *Experimental & Molecular Medicine* 52(5):724–29. doi: 10.1038/s12276-020-0430-0.

Lejri, Imane, Amandine Grimm, François Hallé, Mustapha Abarghaz, Christian Klein, Michel Maitre, Martine Schmitt, Jean Jacques Bourguignon, Ayikoe Guy Mensah-Nyagan, Frederic Bihel, Anne Eckert, and Benedict Albensi. 2019. "TSPO Ligands Boost Mitochondrial Function and Pregnenolone Synthesis." *Journal of Alzheimer's Disease* 72(4):1045–58. doi: 10.3233/JAD-190127.

Leonarduzzi, Gabriella, Barbara Vizio, Barbara Sottero, Veronica Verde, Paola Gamba, Cinzia Mascia, Elena Chiarpotto, Giuseppe Poli, and Fiorella Biasi. 2006. "Early Involvement of ROS Overproduction in Apoptosis Induced by 7-Ketocholesterol." *Antioxidants & Redox Signaling* 8(3–4):375–80. doi: 10.1089/ARS.2006.8.375.

Leoni, Valerio, and Claudio Caccia. 2011. "Oxysterols as Biomarkers in Neurodegenerative Diseases." *Chemistry and Physics of Lipids* 164(6):515–24. doi: 10.1016/J.CHEMPHYSLIP.2011.04.002.

Leoni, Valerio, Dieter Lütjohann, and Thomas Masterman. 2005. "Levels of 7-Oxocholesterol in Cerebrospinal Fluid Are More than One Thousand Times Lower than Reported in Multiple Sclerosis." *Journal of Lipid Research* 46(2):191–95. doi: 10.1194/JLR.C400005-JLR200.

Leoni, Valerio, Caterina Mariotti, Sarah J. Tabrizi, Marta Valenza, Edward J. Wild, Susie M. D. Henley, Nicola Z. Hobbs, Maria Luisa Mandelli, Marina Grisoli, Ingemar Björkhem, Elena Cattaneo, and Stefano Di Donato. 2008. "Plasma 24S-Hydroxycholesterol and Caudate MRI in Pre-Manifest and Early Huntington's Disease." *Brain* 131(11):2851–59. doi: 10.1093/brain/awn212.

Lerner, Alan J., Steven E. Arnold, Erin Maxfield, Aaron Koenig, Maria E. Toth, Brooke Fortin, Natalia Mast, Bianca A. Trombetta, John Denker, Andrew A. Pieper, Curtis Tatsuoka, Sangeetha Raghupathy, and Irina A. Pikuleva. 2022. "CYP46A1 Activation by Low-Dose Efavirenz Enhances Brain Cholesterol Metabolism in Subjects with Early Alzheimer's Disease." *Alzheimer's Research and Therapy* 14(1):1–10. doi: 10.1186/S13195-022-01151-Z/FIGURES/2.

Levin, Lynn I., Kassandra L. Munger, Mark V. Rubertone, Charles A. Peck, Evelyne T. Lennette, Donna Spiegelman, and Alberto Ascherio. 2005. "Temporal Relationship between Elevation of Epstein-Barr Virus Antibody Titers and Initial Onset of Neurological Symptoms in Multiple Sclerosis." *JAMA* 293(20):2496–2500. doi: 10.1001/JAMA.293.20.2496.

Li, Dingfeng, Juan Zhang, and Qiang Liu. 2022. "Brain Cell Type-Specific Cholesterol Metabolism and Implications for Learning and Memory." *Trends in Neurosciences* 45(5):401–14. doi: 10.1016/J.TINS.2022.01.002.

Li, Qingyun, and Ben A. Barres. 2018. "Microglia and Macrophages in Brain Homeostasis and Disease." *Nature Reviews Immunology* 18(4):225–42.

Licht-Mayer, Simon, Graham R. Campbell, Marco Canizares, Arpan R. Mehta, Angus B. Gane, Katie McGill, Aniket Ghosh, Alexander Fullerton, Niels Menezes, Jasmine Dean, Jordon Dunham, Sarah Al-Azki, Gareth Pryce, Stephanie Zandee, Chao Zhao, Markus Kipp, Kenneth J. Smith, David Baker, Daniel Altmann, Stephen M. Anderton, Yolanda S. Kap, Jon D. Laman, Bert A. 't Hart, Moses Rodriguez, Ralf Watzlawick, Jan M. Schwab, Roderick Carter, Nicholas Morton, Michele Zagnoni, Robin J. M. Franklin, Rory Mitchell, Sue Fleetwood-Walker, David A. Lyons, Siddharthan Chandran, Hans Lassmann, Bruce D. Trapp, and Don J. Mahad. 2020. "Enhanced Axonal Response of Mitochondria to Demyelination Offers Neuroprotection: Implications for Multiple Sclerosis." *Acta Neuropathologica* 140(2):143–67. doi: 10.1007/S00401-020-02179-X.

Liddelow, Shane, Kevin Guttenplan, Laura E. clarke, Frederick Bennett, christopher Bohlen, Lucas Schirmer, Mariko L. Bennett, alexandra E. Münch, Won-Suk chung, Todd Peterson, Daniel K. Wilton, arnaud Frouin, Brooke napier, Beth Stevens, and Ben Barres. 2017. "Neurotoxic Reactive Astrocytes Are Induced by Activated Microglia." *Nature* 541(481). doi: 10.1038/nature21029.

Lindberg, Catharina, Milita Crisby, Bengt Winblad, and Marianne Schultzberg. 2005. "Effects of Statins on Microglia." *Journal of Neuroscience Research* 82(1):10–19. doi: 10.1002/JNR.20615.

Liu, Changlu, Xia V. Yang, Jiejun Wu, Chester Kuei, Neelakandha S. Mani, Li Zhang, Jingxue Yu, Steven W. Sutton, Ning Qin, Homayon Banie, Lars Karlsson, Siquan Sun, and Timothy W.

Lovenberg. 2011. “Oxysterols Direct B-Cell Migration through EBI2.” *Nature* 475(7357):519–23. doi: 10.1038/nature10226.

Liu, Liping, Abdelmadjid Belkadi, Lindsey Darnall, Taofang Hu, Caitlin Drescher, Anne C. Cotleur, Dolly Padovani-Claudio, Tao He, Karen Choi, Thomas E. Lane, Robert H. Miller, and Richard M. Ransohoff. 2010. “CXCR2-Positive Neutrophils Are Essential for Cuprizone-Induced Demyelination: Relevance to Multiple Sclerosis.” *Nature Neuroscience* 13(3):319–26. doi: 10.1038/nn.2491.

Liu, Ying, Zhuo Wei, Xingzhe Ma, Xiaoxiao Yang, Yuanli Chen, Lei Sun, Chuanrui Ma, Qing R. Miao, David P. Hajjar, Jihong Han, and Yajun Duan. 2018. “25-Hydroxycholesterol Activates the Expression of Cholesterol 25-Hydroxylase in an LXR-Dependent Mechanism.” *Journal of Lipid Research* 59(3):439–51. doi: 10.1194/JLR.M080440.

Loving, Bailey A., and Kimberley D. Bruce. 2020. “Lipid and Lipoprotein Metabolism in Microglia.” *Frontiers in Physiology* 11(393). doi: 10.3389/FPHYS.2020.00393.

Lubetzki, Catherine, and Bruno Stankoff. 2014. “Demyelination in Multiple Sclerosis.” *Handbook of Clinical Neurology* 122:99. doi: 10.1016/B978-0-444-52001-2.00004-2.

Lublin, Fred D., Dieter A. Häring, Habib Ganjgahi, Alex Ocampo, Farhad Hatami, Jelena Čuklina, Piet Aarden, Frank Dahlke, Douglas L. Arnold, Heinz Wiendl, Tanuja Chitnis, Thomas E. Nichols, Bernd C. Kieseier, and Robert A. Bermel. 2022. “How Patients with Multiple Sclerosis Acquire Disability.” *Brain : A Journal of Neurology* 145(9):3147–61. doi: 10.1093/brain/awac016.

Lublin, Fred, David H. Miller, Mark S. Freedman, Bruce A. C. Cree, Jerry S. Wolinsky, Howard Weiner, Catherine Lubetzki, Hans Peter Hartung, Xavier Montalban, Bernard M. J. Uitdehaag, Martin Merschhemke, Bingbing Li, Norman Putzki, Fonda C. Liu, Dieter A. Häring, and Ludwig Kappos. 2016. “Oral Fingolimod in Primary Progressive Multiple Sclerosis (INFORMS): A Phase 3, Randomised, Double-Blind, Placebo-Controlled Trial.” *Lancet (London, England)* 387(10023):1075–84. doi: 10.1016/S0140-6736(15)01314-8.

Lucchinetti, Claudia, Wolfgang Bruck, Joseph Parisi, Bernd Scheithauer, Moses Rodriques, and Hans Lassmann. 2000. “Heterogeneity of Multiple Sclerosis Lesions: Implications for the Pathogenesis of Demyelination.” *Ann Neurol* 47(6):707–17.

Lucchinetti, Claudia F., Bogdan F. G. Popescu, Reem F. Bunyan, Natalia M. Moll, Shanu F. Roemer, Hans Lassmann, Wolfgang Brück, Joseph E. Parisi, Bernd W. Scheithauer, Caterina Giannini, Stephen D. Weigand, Jay Mandrekar, and Richard M. Ransohoff. 2011. “Inflammatory Cortical Demyelination in Early Multiple Sclerosis.” *The New England Journal of Medicine* 365(23):2188. doi: 10.1056/NEJMOA1100648.

Luchetti, Sabina, Nina L. Fransen, Corbert G. van Eden, Valeria Ramaglia, Matthew Mason, and Inge Huitinga. 2018. “Progressive Multiple Sclerosis Patients Show Substantial Lesion Activity That Correlates with Clinical Disease Severity and Sex: A Retrospective Autopsy Cohort Analysis.” *Acta Neuropathologica* 135(4):511–28. doi: 10.1007/S00401-018-1818-Y.

Lund, Erik G., Joseph M. Guileyardo, and David W. Russell. 1999. “CDNA Cloning of Cholesterol 24-Hydroxylase, a Mediator of Cholesterol Homeostasis in the Brain.” *Proc. Natl. Acad. Sci* 96:7238–43.

Lund, Erik G., Chonglun Xie, Tiina Kotti, Stephen D. Turley, John M. Dietschy, and David W. Russell. 2003. “Knockout of the Cholesterol 24-Hydroxylase Gene in Mice Reveals a Brain-Specific Mechanism of Cholesterol Turnover.” *Journal of Biological Chemistry* 278(25):22980–88. doi: 10.1074/JBC.M303415200.

Luo, Chun, Chongdong Jian, Yuhan Liao, Qi Huang, Yuejuan Wu, Xixia Liu, Donghua Zou, and Yuan Wu. 2017a. “The Role of Microglia in Multiple Sclerosis.” *Neuropsychiatric Disease and Treatment* 13:1661–67. doi: 10.2147/NDT.S140634.

Luo, Chun, Chongdong Jian, Yuhan Liao, Qi Huang, Yuejuan Wu, Xixia Liu, Donghua Zou, and Yuan Wu. 2017b. “The Role of Microglia in Multiple Sclerosis.” *Neuropsychiatric Disease and Treatment* 13:1661. doi: 10.2147/NDT.S140634.

Luo, Chun, Chongdong Jian, Yuhan Liao, Qi Huang, Yuejuan Wu, Xixia Liu, Donghua Zou, and Yuan Wu. 2017c. “The Role of Microglia in Multiple Sclerosis.” *Neuropsychiatric Disease and Treatment* 13:1667. doi: 10.2147/NDT.S140634.

Lütjohann, Dieter, Olof Breuer, Gunvor Ahlborg, Inger Nennesmo, Åke Sidén, Ulf Diczfalusy, and Ingemar Björkhem. 1996. “Cholesterol Homeostasis in Human Brain: Evidence for an Age-Dependent Flux of 24S-Hydroxycholesterol from the Brain into the Circulation.” *Proc. Natl. Acad* 93(18):9799–9804. doi: 10.1073/PNAS.93.18.9799.

Lutjohann, Dieter, Olof Breuer, Gunvor Ahlborgt, Inger Nennesmot, Ake Side’n §, Ulf Diczfalusy, and Ingemar Bjdrkhem. 1996. “Cholesterol Homeostasis in Human Brain: Evidence for an Age-Dependent Flux of 24S-Hydroxycholesterol from the Brain into the Circulation (Cerebrospinal Fluid/Oxysterols/Plasma/Stable Isotopes).” *Medical Sciences* 93:9799–9804.

Maciak, Karina, Angela Dziedzic, and Joanna Saluk. 2023. “Remyelination in Multiple Sclerosis from the MiRNA Perspective.” *Frontiers in Molecular Neuroscience* 16:1–11.

Madill, Martin, Denise Fitzgerald, Kara E. O’Connell, Kumlesh K. Dev, Sanbing Shen, and Una FitzGerald. 2016. “In Vitro and Ex Vivo Models of Multiple Sclerosis.” *Drug Discovery Today* 21(9):1504–11.

Mado, Hubert, Monika Adamczyk-Sowa, and Paweł Sowa. 2023. “Role of Microglial Cells in the Pathophysiology of MS: Synergistic or Antagonistic?” *International Journal of Molecular Sciences 2023, Vol. 24, Page 1861* 24(3):142–67. doi: 10.3390/IJMS24031861.

Magliozzi, Roberta, Owain Howell, Abhilash Vora, Barbara Serafini, Richard Nicholas, Maria Puopolo, Richard Reynolds, and Francesca Aloisi. 2007. “Meningeal B-Cell Follicles in Secondary Progressive Multiple Sclerosis Associate with Early Onset of Disease and Severe Cortical Pathology.” *Brain* 130(4):1089–1104. doi: 10.1093/brain/awm038.

Magliozzi, Roberta, Owain W. Howell, Richard Nicholas, Carolina Cruciani, Marco Castellaro, Chiara Romualdi, Stefania Rossi, Marco Pitteri, Maria Donata Benedetti, Alberto Gajofatto, Francesca B. Pizzini, Stefania Montemezzi, Sarah Rasia, Ruggero Capra, Alessandra

Bertoldo, Francesco Facchiano, Salvatore Monaco, Richard Reynolds, and Massimiliano Calabrese. 2018. “Inflammatory Intrathecal Profiles and Cortical Damage in Multiple Sclerosis.” *Annals of Neurology* 83(4):739–55. doi: 10.1002/ANA.25197.

Magliozzi, Roberta, Owain W. Howell, Cheryl Reeves, Federico Roncaroli, Richard Nicholas, Barbara Serafini, Francesca Aloisi, and Richard Reynolds. 2010. “A Gradient of Neuronal Loss and Meningeal Inflammation in Multiple Sclerosis.” *Annals of Neurology* 68(4):477–93. doi: 10.1002/ana.22230.

Magnus, Tim, Andrew Chan, Oliver Grauer, Klaus V. Toyka, and Ralf Gold. 2001a. “Microglial Phagocytosis of Apoptotic Inflammatory T Cells Leads to Down-Regulation of Microglial Immune Activation.” *The Journal of Immunology* 167(9):5004–10. doi: 10.4049/jimmunol.167.9.5004.

Magnus, Tim, Andrew Chan, Oliver Grauer, Klaus V. Toyka, and Ralf Gold. 2001b. “Microglial Phagocytosis of Apoptotic Inflammatory T Cells Leads to Down-Regulation of Microglial Immune Activation.” *The Journal of Immunology* 167(9):5004–10. doi: 10.4049/JIMMUNOL.167.9.5004.

Mahad, Don H., Bruce D. Trapp, and Hans Lassmann. 2015. “Pathological Mechanisms in Progressive Multiple Sclerosis.” *The Lancet Neurology* 14(2):183–93. doi: 10.1016/S1474-4422(14)70256-X.

Mailleux, Jo, Tim Vanmierlo, Jeroen F. J. Bogie, Elien Wouters, Dieter Lütjohann, Jerome J. A. Hendriks, and Jack van Horssen. 2017. “Active Liver X Receptor Signaling in Phagocytes in Multiple Sclerosis Lesions.” *Multiple Sclerosis Journal* 24(3):279–89. doi: 10.1177/1352458517696595.

Malhotra, Sunny, Carme Costa, Herena Eixarch, Christian W. Keller, Lukas Amman, Helios Martínez-Banaclocha, Luciana Midaglia, Eduard Sarró, Isabel Machín-Díaz, Luisa M. Villar, Juan Carlos Triviño, Begoña Oliver-Martos, Laura Navarro Parladé, Laura Calvo-Barreiro, Fuencisla Matesanz, Koen Vandenbroeck, Elena Urcelay, María Luisa Martínez-Ginés, Amalia Tejeda-Velarde, Nicolás Fissolo, Joaquín Castilló, Alex Sanchez, Avril A. B. Robertson, Diego Clemente, Marco Prinz, Pablo Pelegrin, Jan D. Lünemann, Carmen Espejo, Xavier Montalban, and Manuel Comabella. 2020. “NLRP3 Inflammasome as Prognostic Factor and Therapeutic Target in Primary Progressive Multiple Sclerosis Patients.” *Brain : A Journal of Neurology* 143(5):1414–30. doi: 10.1093/BRAIN/AWAA084.

Marelli, Cecilia, Foudil Lamari, Dominique Rainteau, Alexandre Lafourcade, Guillaume Banneau, Lydie Humbert, Marie Lorraine Monin, Elodie Petit, Rabab Debs, Giovanni Castelnovo, Elisabeth Ollagnon, Julie Lavie, Julie Pilliod, Isabelle Coupry, Patrick J. Babin, Claire Guissart, Imen Benyounes, Urielle Ullmann, Gaetan Lesca, Christel Thauvin-Robinet, Pierre Labauge, Sylvie Odent, Claire Ewenczyk, Claude Wolf, Giovanni Stevanin, David Hajage, Alexandra Durr, Cyril Goizet, and Fanny Mochel. 2018. “Plasma Oxysterols: Biomarkers for Diagnosis and Treatment in Spastic Paraplegia Type 5.” *Brain* 141(1):72–84. doi: 10.1093/brain/awx297.

Mark, Martina B. Sintzel, Rametta Anthony, and T. Reder. 2018. “Vitamin D and Multiple Sclerosis: A Comprehensive Review.” *Neurol Ther* 7:59–85. doi: 10.1007/s40120-017-0086-4.

Marschallinger, Julia, Tal Iram, Macy Zardeneta, Song E. Lee, Benoit Lehallier, Michael S. Haney, John V. Pluvinage, Vidhu Mathur, Oliver Hahn, David W. Morgens, Justin Kim, Julia Tevini, Thomas K. Felder, Heimo Wolinski, Carolyn R. Bertozzi, Michael C. Bassik, Ludwig Aigner, and Tony Wyss-Coray. 2020. “Lipid-Droplet-Accumulating Microglia Represent a Dysfunctional and Proinflammatory State in the Aging Brain.” *Nature Neuroscience* 23(2):194–208. doi: 10.1038/S41593-019-0566-1.

Masanneck, Lars, Leoni Rolfes, Liesa Regner-Nelke, Alice Willison, Saskia Räuber, Falk Steffen, Stefan Bittner, Frauke Zipp, Philipp Albrecht, Tobias Ruck, Hans Peter Hartung, Sven G. Meuth, and Marc Pawlitzki. 2022. “Detecting Ongoing Disease Activity in Mildly Affected Multiple Sclerosis Patients under First-Line Therapies.” *Multiple Sclerosis and Related Disorders* 63(103927). doi: 10.1016/J.MSARD.2022.103927.

Mast, Natalia, Joseph B. Lin, and Irina A. Pikuleva. 2015. “Marketed Drugs Can Inhibit Cytochrome P450 27A1, a Potential New Target for Breast Cancer Adjuvant Therapy.” *Molecular Pharmacology* 88(3):428–36. doi: 10.1124/mol.115.099598.

Mast, Natalia, Aicha Saadane, Ana Valencia-Olvera, James Constans, Erin Maxfield, Hiroyuki Arakawa, Young Li, Gary Landreth, and Irina A. Pikuleva. 2017. “Cholesterol-Metabolizing Enzyme Cytochrome P450 46A1 as a Pharmacologic Target for Alzheimer’s Disease.” *Neuropharmacology* 123:465–76. doi: 10.1016/J.NEUROPHARM.2017.06.026.

Mathews, Emily, David Mawdsley, Macie Walker, Jacob Hines, Marina Pozzoli, and Bruce Appel. 2014. “Mutation of 3-Hydroxy-3-Methylglutaryl CoA Synthase I Reveals Requirements for Isoprenoid and Cholesterol Synthesis in Oligodendrocyte Migration Arrest, Axon Wrapping, and Myelin Gene Expression.” *The Journal of Neuroscience* 34(9):3409–12.

Mathews, Emily S., and Bruce Appel. 2016. “Cholesterol Biosynthesis Supports Myelin Gene Expression and Axon Ensheathment through Modulation of P13K/Akt/ MTor Signaling.” *J Neurosci* 36(29):7628–39. doi: 10.1523/JNEUROSCI.0726-16.2016.

Matsuda, Akihiro, Kohjiro Nagao, Michinori Matsuo, Noriyuki Kioka, and Kazumitsu Ueda. 2013. “24(S)-Hydroxycholesterol Is Actively Eliminated from Neuronal Cells by ABCA1.” *Journal of Neurochemistry* 126(1):93–101. doi: 10.1111/JNC.12275.

Matsushima, Glenn K., and Pierre Morell. 2001. “The Neurotoxicant, Cuprizone, as a Model to Study Demyelination and Remyelination in the Central Nervous System.” Pp. 107–16 in *Brain Pathology*. Vol. 11. International Society of Neuropathology.

Matthews, Paul M., Frederico Roncaroli, Adam Waldman, Maria Pia Sormani, Nicola De Stefano, Gavin Giovannoni, and Richard Reynolds. 2016. “A Practical Review of the Neuropathology and Neuroimaging of Multiple Sclerosis.” *Practical Neurology* 16(4):279–87. doi: 10.1136/PRACTNEUROL-2016-001381.

Mazein, Alexander, Steven Watterson, Wei Yuan Hsieh, William J. Griffiths, and Peter Ghazal. 2013. “A Comprehensive Machine-Readable View of the Mammalian Cholesterol

Biosynthesis Pathway." *Biochemical Pharmacology* 86(1):56–66. doi: 10.1016/j.bcp.2013.03.021.

McColgan, P., and S. J. Tabrizi. 2018. "Huntington's Disease: A Clinical Review." *European Journal of Neurology* 25(1):24–34. doi: 10.1111/ENE.13413.

McDonald, Jeffrey G., and David W. Russell. 2010. "Editorial: 25-Hydroxycholesterol: A New Life in Immunology." *Journal of Leukocyte Biology* 88(6):1071. doi: 10.1189/JLB.0710418.

McDonald, Jeffrey G., Daniel D. Smith, Ashlee R. Stiles, and David W. Russell. 2012. "A Comprehensive Method for Extraction and Quantitative Analysis of Sterols and Secosteroids from Human Plasma." *Journal of Lipid Research* 53(7):1399–1409. doi: 10.1194/JLR.D022285.

McGinley, Marisa P., Carolyn H. Goldschmidt, and Alexander D. Rae-Grant. 2021. "Diagnosis and Treatment of Multiple Sclerosis: A Review." *JAMA* 325(8):765–79. doi: 10.1001/JAMA.2020.26858.

McQuade, Amanda, Morgan Coburn, Christina H. Tu, Jonathan Hasselmann, Hayk Davtyan, and Mathew Blurton-Jones. 2018. "Development and Validation of a Simplified Method to Generate Human Microglia from Pluripotent Stem Cells." *Molecular Neurodegeneration* 13(1). doi: 10.1186/s13024-018-0297-x.

Meaney, Steve, Karl Bodin, Ulf Diczfalusy, and Ingemar Björkhem. 2002. "On the Rate of Translocation in Vitro and Kinetics in Vivo of the Major Oxysterols in Human Circulation: Critical Importance of the Position of the Oxygen Function." *Journal of Lipid Research* 43(12):2130–35. doi: 10.1194/jlr.M200293-JLR200.

Van Meerhaeghe, Tess, Antoine Néel, Sophie Brouard, and Nicolas Degauque. 2023. "Regulation of CD8 T Cell by B-Cells: A Narrative Review." *Frontiers in Immunology* 14:1–44. doi: 10.3389/FIMMU.2023.1125605/BIBTEX.

Meinl, Edgar, Chiara Cordiglieri, David Pitt, Gerald Ponath, and Calvin Park. 2018. "The Role of Astrocytes in Multiple Sclerosis." *Front. Immunol* 9. doi: 10.3389/fimmu.2018.00217.

Mellon, F. A. 2003. "MASS SPECTROMETRY | Principles and Instrumentation." *Encyclopedia of Food Sciences and Nutrition* 3739–49. doi: 10.1016/B0-12-227055-X/00746-X.

Melton, Elaina M., Haibo Li, Jalen Benson, Paul Sohn, Li Hao Huang, Bao Liang Song, Bo Liang Li, Catherine C. Y. Chang, and Ta Yuan Chang. 2019. "Myeloid Acat1/Soat1 KO Attenuates pro-Inflammatory Responses in Macrophages and Protects against Atherosclerosis in a Model of Advanced Lesions." *Journal of Biological Chemistry* 294(43):15836–49. doi: 10.1074/JBC.RA119.010564.

Mercadante, Anthony A., and Prasanna Tadi. 2022. *Neuroanatomy, Gray Matter*. StatPearls Publishing.

Merino-Serrais, Paula, Raul Loera-Valencia, Patricia Rodriguez-Rodriguez, Cristina Parrado-Fernandez, Muhammad A. Ismail, Silvia Maioli, Eduardo Matute, Eva Maria Jimenez-Mateos, Ingemar Björkhem, Javier Defelipe, and Angel Cedazo-Minguez. 2019. "27-

Hydroxycholesterol Induces Aberrant Morphology and Synaptic Dysfunction in Hippocampal Neurons." *Cerebral Cortex* 29(1):429–46. doi: 10.1093/CERCOR/BHY274.

Metz, Luanne M., David K. B. Li, Anthony L. Traboulsee, Pierre Duquette, Misha Eliasziw, Graziela Cerchiaro, Jamie Greenfield, Andrew Riddehough, Michael Yeung, Marcelo Kremenchutzky, Galina Vorobeychik, Mark S. Freedman, Virender Bhan, Gregg Blevins, James J. Marriott, Francois Grand'Maison, Liesly Lee, Manon Thibault, Michael D. Hill, and V. Wee Yong. 2017. "Trial of Minocycline in a Clinically Isolated Syndrome of Multiple Sclerosis." *New England Journal of Medicine* 376(22):2122–33. doi: 10.1056/NEJMOA1608889/SUPPL_FILE/NEJMOA1608889_DISCLOSURES.PDF.

Miron, Veronique E., Amanda Boyd, Jing Wei Zhao, Tracy J. Yuen, Julia M. Ruckh, Jennifer L. Shadrach, Peter Van Wijngaarden, Amy J. Wagers, Anna Williams, Robin J. M. Franklin, and Charles Ffrench-Constant. 2013. "M2 Microglia and Macrophages Drive Oligodendrocyte Differentiation during CNS Remyelination." *Nature Neuroscience* 16(9):1211–18. doi: 10.1038/nn.3469.

Miron, Veronique E., and Robin J. M. Franklin. 2014. "Macrophages and CNS Remyelination." *Journal of Neurochemistry* 130(2):165–71.

Miron, Veronique E., Tanja Kuhlmann, and J. P. Antel Jack P. 2011. "Cells of the Oligodendroglial Lineage, Myelination, and Remyelination." *Biochimica et Biophysica Acta - Molecular Basis of Disease* 1812(2):184–93.

Mitsche, Matthew A., Jeffrey G. McDonald, Helen H. Hobbs, and Jonathan C. Cohen. 2015. "Flux Analysis of Cholesterol Biosynthesis in Vivo Reveals Multiple Tissue and Cell-Type Specific Pathways." *ELife* 4(JUNE 2015):1–21. doi: 10.7554/eLife.07999.001.

Moore, Kathryn J., Frederick J. Sheedy, and Edward A. Fisher. 2013. "Macrophages in Atherosclerosis: A Dynamic Balance." *Nature Reviews Immunology 2013 13:10* 13(10):709–21. doi: 10.1038/nri3520.

Mulero, Patricia, Luciana, Midaglia, and Xavier Montalban. 2018. "Ocrelizumab: A New Milestone in Multiple Sclerosis Therapy." *Therapeutic Advances in Neurological Disorders* 11:1–6. doi: 10.1177/1756286418773025.

Muller, D., P. A. Buchs, and L. Stoppini. 1993. *Time Course of Synaptic Development in Hippocampal Organotypic Cultures*. Vol. 71.

Munoz, J. J., C. C. A. Bernard, and I. R. Mackay. 1984. *Elicitation of Experimental Allergic Encephalomyelitis (EAE) in Mica with the Aid of Pertussigen'*. Vol. 83.

Muñoz-Garcia, Javier, Denis Cochonneau, Stéphane Télétchéa, Emilie Moranton, Didier Lanoe, Régis Brion, Frédéric Lézot, Marie-Françoise Heymann, and Dominique Heymann. 2021. "The Twin Cytokines Interleukin-34 and CSF-1: Masterful Conductors of Macrophage Homeostasis." *HAL* 11(4):1568–93. doi: 10.7150/thno.50683ï.

Musella, Alessandra, Antonietta Gentile, Francesca Romana Rizzo, Francesca De Vito, Diego Fresegna, Silvia Bullitta, Valentina Vanni, Livia Guadalupi, Mario Stampanoni Bassi, Fabio Buttari, Diego Centonze, Georgia Mandolesi, Brandi Ormerod, Adelaide Fernandes, Daniel

Ortuño-Sahagún, De F. Vito, and Stampanoni M. Bassi. 2018. “Interplay Between Age and Neuroinflammation in Multiple Sclerosis: Effects on Motor and Cognitive Functions.” *Front. Aging Neurosci* 10. doi: 10.3389/fnagi.2018.00238.

Mutemberezi, Valentin, Owein Guillemot-Legris, and Giulio G. Muccioli. 2016. “Oxysterols: From Cholesterol Metabolites to Key Mediators.” *Progress in Lipid Research* 64:152–69. doi: 10.1016/j.plipres.2016.09.002.

Muzio, Luca, Alice Viotti, and Gianvito Martino. 2021. “Microglia in Neuroinflammation and Neurodegeneration: From Understanding to Therapy.” *Frontiers in Neuroscience* 15:1–25. doi: 10.3389/FNINS.2021.742065/BIBTEX.

Nair, Sunita, Siquan Sun, and Changlu Liu. 2015. “7α, 25-Dihydroxycholesterol-Mediated Activation of EBI2 in Immune Regulation and Diseases.” *Front. Pharmacol* 6(60). doi: 10.3389/fphar.2015.00060.

Naismith, Robert, T., Robert, Bermel, Christopher, S. Coffey, Andrew, D. Goodman, Janel Fedler, Marianne, Kearney, Eric, C. Klawiter, Kunio Nakanura, Sridar Narayanan, Christopher Goebel, Jon Yankey, Elizabeth Klinger, and Robert, J. Fox. 2021. “Effects of Ibudilast on MRI Measures in the Phase 2 SPRINT-MS Study Ibudilast: A Paradigm Shift for Progressive Multiple Sclerosis? Criteria for Rating Therapeutic and Diagnostic Studies NPub.Org/Coe.” *Neurology* 96(4):491–500. doi: 10.1212/WNL.0000000000011314.

Nayak, Debasis, Bernd H. Zinselmeyer, Kara N. Corps, and Dorian B. Mcgavern. 2012. “In Vivo Dynamics of Innate Immune Sentinels in the CNS.” *IntraVital* 1:95–106. doi: 10.4161/intv.22823.

Nazir, Faisal Hayat, Anna Wiberg, Malin Müller, Sara Mangsbo, and Joachim Burman. 2023. “Antibodies from Serum and CSF of Multiple Sclerosis Patients Bind to Oligodendroglial and Neuronal Cell-Lines.” *Brain Communications* 5(3). doi: 10.1093/braincomms/fcad164.

Newton, Jason, Nitai C. Hait, Michael Maceyka, Alexandria Colaco, Melissa Maczis, Christopher A. Wassif, Antony Cougnoux, Forbes D. Porter, Sheldon Milstien, Nicholas Platt, Frances M. Platt, and Sarah Spiegel. 2017. “FTY720/Fingolimod Increases NPC1 and NPC2 Expression and Reduces Cholesterol and Sphingolipid Accumulation in Niemann-Pick Type C Mutant Fibroblasts.” *FASEB J* 4:1719–30. doi: 10.1096/fj.201601041R.

Nieweg, Katja, Hubert Schaller, and Frank W. Pfrieger. 2009. “Marked Differences in Cholesterol Synthesis between Neurons and Glial Cells from Postnatal Rats.” *Journal of Neurochemistry* 109(1):125–34. doi: 10.1111/J.1471-4159.2009.05917.X.

Nikić, Ivana, Doron Merkler, Catherine Sorbara, Mary Brinkoetter, Mario Kreutzfeldt, Florence M. Bareyre, Wolfgang Brück, Derron Bishop, Thomas Misgeld, and Martin Kerschensteiner. 2011. “A Reversible Form of Axon Damage in Experimental Autoimmune Encephalomyelitis and Multiple Sclerosis.” *Nature Medicine* 17(4):495–99. doi: 10.1038/NM.2324.

Nimmerjahn, Axel. 2012. “Optical Window Preparation for Two-Photon Imaging of Microglia in Mice.” *Cold Spring Harbor Protocols* 7(5):587–93. doi: 10.1101/PDB.PROT069286.

Noda, Hiromi, Hideyuki Takeuchi, Tetsuya Mizuno, and Akio Suzumura. 2013. “Fingolimod Phosphate Promotes the Neuroprotective Effects of Microglia.” *Journal of Neuroimmunology* 256(1–2):13–18. doi: 10.1016/j.jneuroim.2012.12.005.

Nohturfft, Axel, Daisuke Yabe, Joseph L. Goldstein, Michael S. Brown, and Peter J. Espenshade. 2000. “Regulated Step in Cholesterol Feedback Localized to Budding of SCAP from ER Membranes.” *Cell* 102(3):315–23. doi: 10.1016/S0092-8674(00)00037-4.

Novakova, Lenka, Markus Axelsson, Clas Malmeström, Henrik Zetterberg, Ingemar Björkhem, Virginija Danylaité Karrenbauer, and Jan Lycke. 2015. “Reduced Cerebrospinal Fluid Concentrations of Oxysterols in Response to Natalizumab Treatment of Relapsing Remitting Multiple Sclerosis.” *Journal of the Neurological Sciences* 358(1–2):201–6. doi: 10.1016/j.jns.2015.08.1537.

Palavra, Filipe, Sofia D. Viana, Sara Henriques, João Dinis, João Martins, Maria H. Madeira, Raquel Santiago, Lorena Petrella, José Sereno, Miguel Castelo-Branco, Frederico C. Pereira, Luís Almeida, António F. Ambrósio, and Flávio Reis. 2022. “Defining Milestones for the Study of Remyelination Using the Cuprizone Mouse Model: How Early Is Early?” *Multiple Sclerosis and Related Disorders* 63. doi: 10.1016/j.msard.2022.103886.

Pan, Jie, and Jun Wan. 2020. “Methodological Comparison of FACS and MACS Isolation of Enriched Microglia and Astrocytes from Mouse Brain.” *Journal of Immunological Methods* 486. doi: 10.1016/J.JIM.2020.112834.

Paolicelli, Chiara Rosa, Kanchan Bisht, and Marie-Ève Tremblay. 2014. “Fractalkine Regulation of Microglial Physiology and Consequences on the Brain and Behavior.” *Front Cell Neuro* 8(129). doi: 10.3389/fncel.2014.00129.

Paolicelli, Rosa C., Giulia Bolasco, Francesca Pagani, Laura Maggi, Maria Scianni, Patrizia Panzanelli, Maurizio Giustetto, Tiago Alves Ferreira, Eva Guiducci, Laura Dumas, Davide Ragozzino, and Cornelius T. Gross. 2011. “Synaptic Pruning by Microglia Is Necessary for Normal Brain Development.” *Science (New York, N.Y.)* 333(6048):1456–58. doi: 10.1126/SCIENCE.1202529.

Parkhurst, Christopher N., Guang Yang, Ipe Ninan, Jeffrey N. Savas, John R. Yates, Juan J. Lafaille, Barbara L. Hempstead, Dan R. Littman, and Wen Biao Gan. 2013. “Microglia Promote Learning-Dependent Synapse Formation through Brain-Derived Neurotrophic Factor.” *Cell* 155(7):1596–1609. doi: 10.1016/J.CELL.2013.11.030.

Patsopoulos, Nikolaos A. 2018. “Genetics of Multiple Sclerosis: An Overview and New Directions.” *Cold Spring Harbor Perspectives in Medicine* 8(7). doi: 10.1101/CSHPERSPECT.A028951.

Patsopoulos, Nikolaos A., Sergio E. Baranzini, Adam Santaniello, Parisa Shoostari, Chris Cotsapas, Garrett Wong, Ashley H. Beecham, Tojo James, Joseph Replogle, Ioannis S. Vlachos, Cristin McCabe, Tune H. Pers, Aaron Brandes, Charles White, Brendan Keenan, Maria Cimpean, Phoebe Winn, Ioannis-Pavlos Panteliadis, Allison Robbins, Till F. M. Andlauer, Onigiusz Zarzycki, Bénédicte Dubois, An Goris, Helle Bach Søndergaard, Finn Sellebjerg, Per Soelberg Sorensen, Henrik Ullum, Lise Wegner Thørner, Janna Saarela, Isabelle Cournu-Rebeix, Vincent Damotte, Bertrand Fontaine, Lena Guillot-Noel, Mark Lathrop, Sandra Vukusic,

Achim Berthele, Viola Pongratz, Dorothea Buck, Christiane Gasperi, Christiane Graetz, Verena Grummel, Bernhard Hemmer, Muni Hoshi, Benjamin Knier, Thomas Korn, Christina M. Lill, Felix Luessi, Mark Mühlau, Frauke Zipp, Efthimios Dardiotis, Cristina Agliardi, Antonio Amoroso, Nadia Barizzone, Maria D. Benedetti, Luisa Bernardinelli, Paola Cavalla, Ferdinando Clarelli, Giancarlo Comi, Daniele Cusi, Federica Esposito, Laura Ferrè, Daniela Galimberti, Clara Guaschino, Maurizio A. Leone, Vittorio Martinelli, Lucia Moiola, Marco Salvetti, Melissa Sorosina, Domizia Vecchio, Andrea Zauli, Silvia Santoro, Nicasio Mancini, Miriam Zuccalà, Julia Mescheriakova, Cornelia van Duijn, Steffan D. Bos, Elisabeth G. Celius, Anne Spurkland, Manuel Comabella, Xavier Montalban, Lars Alfredsson, Izaura L. Bomfim, David Gomez-Cabrero, Jan Hillert, Maja Jagodic, Magdalena Lindén, Fredrik Piehl, Ilijas Jelčić, Roland Martin, Mirela Sospedra, Amie Baker, Maria Ban, Clive Hawkins, Pirro Hysi, Seema Kalra, Fredrik Karpe, Jyoti Khadake, Genevieve Lachance, Paul Molyneux, Matthew Neville, John Thorpe, Elizabeth Bradshaw, Stacy J. Caillier, Peter Calabresi, Bruce A. C. Cree, Anne Cross, Mary Davis, Paul W. I. de Bakker, Silvia Delgado, Marieme Dembele, Keith Edwards, Kate Fitzgerald, Irene Y. Frohlich, Pierre-Antoine Gourraud, Jonathan L. Haines, Hakon Hakonarson, Dorlan Kimbrough, Noriko Isobe, Ioanna Konidari, Ellen Lathi, Michelle H. Lee, Taibo Li, David An, Andrew Zimmer, Lohith Madireddy, Clara P. Manrique, Mitja Mitrovic, Marta Olah, Ellis Patrick, Margaret A. Pericak-Vance, Laura Piccio, Cathy Schaefer, Howard Weiner, Kasper Lage, Alastair Compston, David Hafler, Hanne F. Harbo, Stephen L. Hauser, Graeme Stewart, Sandra D'Alfonso, Georgios Hadjigeorgiou, Bruce Taylor, Lisa F. Barcellos, David Booth, Rogier Hintzen, Ingrid Kockum, Filippo Martinelli-Boneschi, Jacob L. McCauley, Jorge R. Oksenberg, Annette Oturai, Stephen Sawcer, Adrian J. Ivinson, Tomas Olsson, and Philip L. De Jager. 2019. "Multiple Sclerosis Genomic Map Implicates Peripheral Immune Cells and Microglia in Susceptibility." *Science* 365(6460). doi: 10.1126/science.aav7188.

Patsopoulos, Nikolaos A., Lisa F. Barcellos, Rogier Q. Hintzen, Catherine Schaefer, Cornelia M. van Duijn, Janelle A. Noble, Towfique Raj, Pierre Antoine Gourraud, Barbara E. Stranger, Jorge Oksenberg, Tomas Olsson, Bruce V. Taylor, Stephen Sawcer, David A. Hafler, Mary Carrington, Philip L. De Jager, Paul I. W. de Bakker, Luisa Bernardinelli, David Booth, Manuel Comabella, Alastair Compston, Sandra D'Alfonso, Bertrand Fontaine, An Goris, Jonathan Haines, Hanne Harbo, Steve Hauser, Clive Hawkins, Bernhard Hemmer, Adrian Ivinson, Christina Lill, Roland Martin, Filippo Martinelli-Boneschi, Annette Oturai, Aarno Palotie, Margaret PericakVance, Janna Saarela, Graeme Stewart, Frauke Zipp, Rodney J. Scott, Jeannette Lechner-Scott, Pablo Moscato, David R. Booth, Graeme J. Stewart, Robert N. Heard, Deborah Mason, Lyn Griffiths, Simon Broadley, Matthew A. Brown, Mark Slee, Simon J. Foote, Jim Stankovich, James Wiley, Melanie Bahlo, Victoria Perreau, Judith Field, Helmut Butzkueven, Trevor J. Kilpatrick, Justin Rubio, Mark Marriott, William M. Carroll1, and Allan G. Kermode. 2013. "Fine-Mapping the Genetic Association of the Major Histocompatibility Complex in Multiple Sclerosis: HLA and Non-HLA Effects." *PLoS Genetics* 9(11). doi: 10.1371/JOURNAL.PGEN.1003926.

Pereira, João Pedro, Lisa M. Kelly, and Jason G. Cyster jason. 2010. "Finding the Right Niche: B-Cell Migration in the Early Phases of T-Dependent Antibody Responses." *International Immunology* 22(6):413–19. doi: 10.1093/intimm/dxq047.

Peterson, John W., Lars Bö, Sverre Mörk, Ansi Chang, and Bruce D. Trapp. 2001. “Transected Neurites, Apoptotic Neurons, and Reduced Inflammation in Cortical Multiple Sclerosis Lesions.” *Annals of Neurology* 50(3):389–400. doi: 10.1002/ANA.1123.

Petrov, Alexey M., and Irina A. Pikuleva. 2019. “Cholesterol 24-Hydroxylation by CYP46A1: Benefits of Modulation for Brain Diseases.” *Neurotherapeutics* 16(3):635–48. doi: 10.1007/s13311-019-00731-6.

Poliani, Pietro Luigi, Yaming Wang, Elena Fontana, Michelle L. Robinette, Yoshinori Yamanishi, Susan Gilfillan, and Marco Colonna. 2015. “TREM2 Sustains Microglial Expansion during Aging and Response to Demyelination.” *Journal of Clinical Investigation* 125(5):2161–70. doi: 10.1172/JCI77983.

Ponath, Gerald, Calvin Park, and David Pitt. 2018. “The Role of Astrocytes in Multiple Sclerosis.” *Frontiers in Immunology* 9(FEB):1–12. doi: 10.3389/FIMMU.2018.00217/BIBTEX.

Ponath, Gerald, Sriram Ramanan, Mayyan Mubarak, William Housley, Seunghoon Lee, F. Rezan Sahinkaya, Alexander Vortmeyer, Cedric S. Raine, and David Pitt. 2017. “Myelin Phagocytosis by Astrocytes after Myelin Damage Promotes Lesion Pathology.” *Brain* 140(2):399–413. doi: 10.1093/BRAIN/AWW298.

Pooler, Amy M., Shijun C. Xi, and Richard J. Wurtman. 2006. “The 3-Hydroxy-3-Methylglutaryl Co-Enzyme A Reductase Inhibitor Pravastatin Enhances Neurite Outgrowth in Hippocampal Neurons.” *Journal of Neurochemistry* 97(3):716–23. doi: 10.1111/J.1471-4159.2006.03763.X.

Popescu, Bogdan F., Istvan Pirko, and Claudia F. Lucchinetti. 2013. “Pathology of Multiple Sclerosis: Where Do We Stand?” *Continuum* 19(4):902–21.

Prineas, J. W., and J. S. Graham. 1981. “Multiple Sclerosis: Capping of Surface Immunoglobulin G on Macrophages Engaged in Myelin Breakdown.” *Annals of Neurology* 10(2):149–58. doi: 10.1002/ANA.410100205.

Prineas, John W., Eunice E. Kwon, Eun Sook Cho, Leroy R. Sharer, Michael H. Barnett, Emilia L. Oleszak, Brad Hoffman, and Bryan P. Morgan. 2001. “Immunopathology of Secondary-Progressive Multiple Sclerosis.” *Annals of Neurology* 50(5):646–57. doi: 10.1002/ANA.1255.

Prinz, Marco, Steffen Jung, and Josef Priller. 2019. “Microglia Biology: One Century of Evolving Concepts.” *Cell* 179(2):292–311. doi: 10.1016/J.CELL.2019.08.053.

Procaccini, Claudio, Veronica De Rosa, Valentina Pucino, Luigi Formisano, and Giuseppe Matarese. 2015. “Animal Models of Multiple Sclerosis.” *European Journal of Pharmacology* 759:182–91.

Qin, Qi, Zhaoqian Teng, Changmei Liu, Qian Li, Yunsi Yin, and Yi Tang. 2021. “TREM2, Microglia, and Alzheimer’s Disease.” *Mechanisms of Ageing and Development* 195. doi: 10.1016/J.MAD.2021.111438.

Quek, Hazel, Carla Cuní-López, Romal Stewart, Tiziana Colletti, Antonietta Notaro, Tam Hong Nguyen, Yifan Sun, Christine C. Guo, Michelle K. Lupton, Tara L. Roberts, Yi Chieh Lim, Lotta E. Oikari, Vincenzo La Bella, and Anthony R. White. 2022. “ALS Monocyte-Derived Microglia-

like Cells Reveal Cytoplasmic TDP-43 Accumulation, DNA Damage, and Cell-Specific Impairment of Phagocytosis Associated with Disease Progression." *Journal of Neuroinflammation* 19(1):1–21. doi: 10.1186/S12974-022-02421-1/FIGURES/7.

Quek, Hazel, and Anthony White. 2023. "Patient-Specific Monocyte-Derived Microglia as a Screening Tool for Neurodegenerative Diseases." *Neural Regeneration Research* 18(5):955–58. doi: 10.4103/1673-5374.355740.

Ramagopalan, Sreeram V., David A. Dyment, M. Zameel Cader, Katie M. Morrison, Giulio Disanto, Julia M. Morahan, Antonio J. Berlanga-Taylor, Adam Handel, Gabriele C. De Luca, A. Dessa Sadovnick, Pierre Lepage, Alexandre Montpetit, and George C. Ebers. 2011. "Rare Variants in the CYP27B1 Gene Are Associated with Multiple Sclerosis." *Annals of Neurology* 70(6):881–86. doi: 10.1002/ANA.22678.

Ramanujam, Ryan, Anna Karin Hedström, Ali Manouchehrinia, Lars Alfredsson, Tomas Olsson, Matteo Bottai, and Jan Hillert. 2015. "Effect of Smoking Cessation on Multiple Sclerosis Prognosis." *JAMA Neurology* 72(10):1117–23. doi: 10.1001/JAMANEUROL.2015.1788.

Ramkumar, S., A. Raghunath, and S. Raghunath. 2016. "Statin Therapy: Review of Safety and Potential Side Effects." *Acta Cardiologica Sinica* 32(6):631–39. doi: 10.6515/ACS20160611A.

Rampler, Evelyn, Yasin El Abiead, Harald Schoeny, Felina Hildebrand, Veronika Fitz, and Gunda Koellensperger. 2021. "Recurrent Topics in Mass Spectrometry-Based Metabolomics and Lipidomics Standardization, Coverage, and Throughput." *Cite This: Anal. Chem* 93:545. doi: 10.1021/acs.analchem.0c04698.

Ransohoff, Richard M. 2023. "Multiple Sclerosis: Role of Meningeal Lymphoid Aggregates in Progression Independent of Relapse Activity." *Trends in Immunology* 44(4):266–75. doi: 10.1016/j.it.2023.02.002.

Reboldi, Andrea, Eric V. Dang, Jeffrey G. McDonald, Guosheng Liang, David W. Russell, and Jason G. Cyster. 2014. "25-Hydroxycholesterol Suppresses Interleukin-1-Driven Inflammation Downstream of Type I Interferon." *Science* 345(6197):679–84. doi: 10.1126/SCIENCE.1254790.

Reich, Daniel S., Claudia F. Lucchinetti, and Peter A. Calabresi. 2018. "Multiple Sclerosis." *New England Journal of Medicine* 378(2):169–80. doi: 10.1056/NEJMra1401483.

Reichert, F., U. Slobodov, C. Makranz, and S. Rotshenker. 2001. "Modulation (Inhibition and Augmentation) of Complement Receptor-3-Mediated Myelin Phagocytosis." *Neurobiology of Disease* 8(3):504–12. doi: 10.1006/NBDI.2001.0383.

Reichert, Fanny, and Shlomo Rotshenker. 1999. "Galectin-3/MAC-2 in Experimental Allergic Encephalomyelitis." *Experimental Neurology* 160(2):508–14. doi: 10.1006/EXNR.1999.7229.

Reynolds, Richard, Federico Roncaroli, Richard Nicholas, Bishan Radotra, Djordje Gveric, and Owain Howell. 2011. "The Neuropathological Basis of Clinical Progression in Multiple Sclerosis." *Acta Neuropathologica* 122(2):155–70. doi: 10.1007/S00401-011-0840-0/FIGURES/5.

Ricci, G., L. Volpi, L. Pasquali, L. Petrozzi, and G. Siciliano. 2009. “Astrocyte–Neuron Interactions in Neurological Disorders.” *Journal of Biological Physics* 35(4):336. doi: 10.1007/S10867-009-9157-9.

Riederer, F. 2017. “Ocrelizumab versus Placebo in Primary Progressive Multiple Sclerosis.” *Journal Fur Neurologie, Neurochirurgie Und Psychiatrie* 18(1):30–31. doi: 10.1056/NEJMoa1606468.

Rodgers, Jeff, Tim Friede, Frederick W. Vonberg, Cris S. Constantinescu, Alasdair Coles, Jeremy Chataway, Martin Duddy, Hedley Emsley, Helen Ford, Leonora Fisniku, Ian Galea, Timothy Harrower, Jeremy Hobart, Huseyin Huseyin, Christopher M. Kipps, Monica Marta, Gavin V. Mcdonnell, Brendan Mclean, Owen R. Pearson, David Rog, Klaus Schmierer, Basil Sharrack, Agne Straukiene, Heather C. Wilson, David V. Ford, Rod M. Middleton, and Richard Nicholas. 2022. “The Impact of Smoking Cessation on Multiple Sclerosis Disease Progression.” *Brain* 145(4):1368–78. doi: 10.1093/BRAIN/AWAB385.

Rosen, Haim, Ayeleth Reshef, Nobuyo Maeda, Andrea Lippoldt, Shoshi Shpizen, Liat Triger, Gösta Eggertsen, Ingemar Björkhem, and Eran Leitersdorf. 1998. “Markedly Reduced Bile Acid Synthesis but Maintained Levels of Cholesterol and Vitamin D Metabolites in Mice with Disrupted Sterol 27- Hydroxylase Gene.” *Journal of Biological Chemistry* 273(24):14805–12. doi: 10.1074/JBC.273.24.14805.

Ruan, Chunsheng, and Wassim Elyaman. 2022. “A New Understanding of TMEM119 as a Marker of Microglia.” *Frontiers in Cellular Neuroscience* 16. doi: 10.3389/FNCEL.2022.902372.

Rupprecht, Rainer, Vassilios Papadopoulos, Gerhard Rammes, Thomas C. Baghai, Jinjiang Fan, Nagaraju Akula, Ghislaine Groyer, David Adams, and Michael Schumacher. 2010. “Translocator Protein (18 KDa) (TSPO) as a Therapeutic Target for Neurological and Psychiatric Disorders.” *Nature Reviews Drug Discovery 2010 9:12* 9(12):971–88. doi: 10.1038/nrd3295.

Saez-Calveras, Nil, and Olaf Stuve. 2022. “The Role of the Complement System in Multiple Sclerosis: A Review.” *Frontiers in Immunology* 13:1–23. doi: 10.3389/FIMMU.2022.970486.

Saher, Gesine, Britta Brügger, Corinna Lappe-Siefke, Wiebke Möbius, Ryu-Ichi Tozawa, Michael C. Wehr, Felix Wieland, and Klaus-Armin Nave. 2005. “High Cholesterol Level Is Essential for Myelin Membrane Growth.” *Nature Neuroscince* 8(4):468–75. doi: 10.1038/nn1426.

Saher, Gesine, and Sina Kristin Stumpf. 2015. “Cholesterol in Myelin Biogenesis and Hypomyelinating Disorders.” *Biochimica et Biophysica Acta - Molecular and Cell Biology of Lipids* 1851(8):1083–94. doi: 10.1016/j.bbalip.2015.02.010.

Sarsby, Joscelyn, Nicholas J. Martin, Patricia F. Lalor, Josephine Bunch, and Helen J. Cooper. 2014. “Top-Down and Bottom-Up Identification of Proteins by Liquid Extraction Surface Analysis Mass Spectrometry of Healthy and Diseased Human Liver Tissue.” *Journal of the American Society for Mass Spectrometry* 25(11):1953–61. doi: 10.1007/S13361-014-0967-Z.

Sasmono, R. Tedjo, Delvac Oceandy, Jeffrey W. Pollard, Wei Tong, Paul Pavli, Brandon J. Wainwright, Michael C. Ostrowski, S. Roy Himes, and David A. Hume. 2003. “A Macrophage Colony-Stimulating Factor Receptor-Green Fluorescent Protein Transgene Is Expressed

throughout the Mononuclear Phagocyte System of the Mouse." *Blood* 101:1155–63. doi: 10.1182/blood.

Satoh, Jun ichi, Yoshihiro Kino, Naohiro Asahina, Mika Takitani, Junko Miyoshi, Tsuyoshi Ishida, and Yuko Saito. 2016. "TMEM119 Marks a Subset of Microglia in the Human Brain." *Neuropathology* 36(1):39–49. doi: 10.1111/neup.12235.

Scalfari, A., A. Neuhaus, M. Daumer, G. C. Ebers, and P. A. Muraro. 2011. "Age and Disability Accumulation in Multiple Sclerosis." *Neurology* 77(13):1246–52. doi: 10.1212/WNL.0B013E318230A17D.

Schüle, Rebecca, S. Siddique, Xiang Deng, Yi Yang, Sandra Donkervoort, Magnus Hansson, Ricardo E. Madrid, Nailah Siddique, Ludger Schöls, and Ingemar Björkhem. 2010. "Marked Accumulation of 27-Hydroxycholesterol in SPG5 Patients with Hereditary Spastic Paresis." *Journal of Lipid Research* 51(4):819–23. doi: 10.1194/jlr.M002543.

Segal, Benjamin M., Cris S. Constantinescu, Aparna Raychaudhuri, Lilianne Kim, Rosanne Fidelus-Gort, and Lloyd H. Kasper. 2008. "Repeated Subcutaneous Injections of IL12/23 P40 Neutralising Antibody, Ustekinumab, in Patients with Relapsing-Remitting Multiple Sclerosis: A Phase II, Double-Blind, Placebo-Controlled, Randomised, Dose-Ranging Study." *The Lancet Neurology* 7(9):796–804. doi: 10.1016/S1474-4422(08)70173-X.

Sellgren, C. M., S. D. Sheridan, J. Gracias, D. Xuan, T. Fu, and R. H. Perlis. 2017. "Patient-Specific Models of Microglia-Mediated Engulfment of Synapses and Neural Progenitors." *Molecular Psychiatry* 22(2):170–77. doi: 10.1038/mp.2016.220.

Shan, Hui, Jihai Pang, Shengrong Li, Tony B. Chiang, William K. Wilson, and George J. Schroepfer. 2003. "Chromatographic Behavior of Oxygenated Derivatives of Cholesterol." *Steroids* 68(3):221–33. doi: 10.1016/S0039-128X(02)00185-X.

Shields, Simon A., Jennifer M. Gilson, William F. Blakemore, and Robin J. M. Franklin. 1999. "Remyelination Occurs as Extensively but More Slowly in Old Rats Compared to Young Rats Following Gliotoxin-Induced CNS Demyelination." *GLIA* 28(1):77–83. doi: 10.1002/(SICI)1098-1136(199910)28:1<77::AID-GLIA9>3.0.CO;2-F.

Shimano, Hitoshi, and Ryuichiro Sato. 2017. "SREBP-Regulated Lipid Metabolism: Convergent Physiology - Divergent Pathophysiology." *Nature Reviews. Endocrinology* 13(12):710–30. doi: 10.1038/NRENDO.2017.91.

Sirtori, Cesare R. 2014. "The Pharmacology of Statins." *Pharmacological Research* 88:3–11. doi: 10.1016/j.phrs.2014.03.002.

Smith, M. E. 1993. "Phagocytosis of Myelin by Microglia in Vitro." *Journal of Neuroscience Research* 35(5):480–87. doi: 10.1002/JNR.490350504.

Smith, Marion E. 2001. "Phagocytic Properties of Microglia in Vitro: Implications for a Role in Multiple Sclerosis and EAE." *Microscopy Research and Technique* 54(2):81–94. doi: 10.1002/JEMT.1123.

Smith, Marion E., and Michelle T. Hoerner. 2000. “Astrocytes Modulate Macrophage Phagocytosis of Myelin in Vitro.” *Journal of Neuroimmunology* 102(2):154–62. doi: 10.1016/S0165-5728(99)00218-0.

Smith, R. Waddell. 2013. “Mass Spectrometry.” *Encyclopedia of Forensic Sciences: Second Edition* 603–8. doi: 10.1016/B978-0-12-382165-2.00250-6.

Solt, Laura, A., Naresh Kumar, Philippe Nuhant, Yongjun Wang, Janelle, L. Lauer, Jin Liu, Monica, A. Istrate, Theodore, M. Kamenecka, William ,R Roush, Dušica Vidović, Stephan, C. Schürer, Jihong Xu, Gail Wagoner, Paul, D. Drew, Patrick, R. Griffin, and Thomas, P. Burris. 2011. “Suppression of TH17 Differentiation and Autoimmunity by a Synthetic ROR Ligand.” *Nature* 472(7344):491–191. doi: doi:10.1038/nature10075.

Sonar, Sandip Ashok, and Girdhari Lal. 2017. “Differentiation and Transmigration of CD4 T Cells in Neuroinflammation and Autoimmunity.” *Frontiers in Immunology* 8(NOV):1–9. doi: 10.3389/fimmu.2017.01695.

Soroosh, Pejman, Jiejun Wu, Xiaohua Xue, Jiao Song, Steven W. Sutton, Marciano Sablad, Jingxue Yu, Marina I. Nelen, Xuejun Liu, Glenda Castro, Rosa Luna, Shelby Crawford, Homayon Banie, Rose A. Dandridge, Xiaohu Deng, Anton Bittner, Chester Kuei, Mandana Tootoonchi, Natasha Rozenkrants, Krystal Herman, Jingjin Gao, Xia V. Yang, Kacey Sachen, Karen Ngo, Wai Ping Fung-Leung, Steven Nguyen, Aimee De Leon-Tabaldo, Jonathan Blevitt, Yan Zhang, Maxwell D. Cummings, Tadimeti Rao, Neelakandha S. Mani, Changlu Liu, Murray McKinnon, Marcos E. Milla, Anne M. Fourie, and Siquan Sun. 2014. “Oxysterols Are Agonist Ligands of RORγt and Drive Th17 Cell Differentiation.” *Proceedings of the National Academy of Sciences of the United States of America* 111(33):12163–68. doi: 10.1073/pnas.1322807111.

Spittau, Björn, Yu Tang, Wai T. Wong, and Claudia Perez-Cruz. 2017. “Aging Microglia-Phenotypes, Functions and Implications for Age-Related Neurodegenerative Diseases.” *Front, Aging Neurosci* 9(194). doi: 10.3389/fnagi.2017.00194.

Stancu, Camélia, and Anca Sima. 2001. “Statins: Mechanism of Action and Effects.” *Journal of Cellular and Molecular Medicine* 5(4):378–87. doi: 10.1111/J.1582-4934.2001.TB00172.X.

Stevens, Beth, Nicola J. Allen, Luis E. Vazquez, Gareth R. Howell, Karen S. Christopherson, Navid Nouri, Kristina D. Micheva, Adrienne K. Mehalow, Andrew D. Huberman, Benjamin Stafford, Alexander Sher, Alan M. M. Litke, John D. Lambris, Stephen J. Smith, Simon W. M. John, and Ben A. Barres. 2007a. “The Classical Complement Cascade Mediates CNS Synapse Elimination.” *Cell* 131(6):1164–78. doi: 10.1016/j.cell.2007.10.036.

Stevens, Beth, Nicola J. Allen, Luis E. Vazquez, Gareth R. Howell, Karen S. Christopherson, Navid Nouri, Kristina D. Micheva, Adrienne K. Mehalow, Andrew D. Huberman, Benjamin Stafford, Alexander Sher, Alan M. M. Litke, John D. Lambris, Stephen J. Smith, Simon W. M. John, and Ben A. Barres. 2007b. “The Classical Complement Cascade Mediates CNS Synapse Elimination.” *Cell* 131(6):1164–78. doi: 10.1016/j.cell.2007.10.036.

Stoppini, L., P. A. Buchs, and D. Muller. 1993. *LESION-INDUCED NEURITE SPROUTING AND SYNAPSE FORMATION IN HIPPOCAMPAL ORGANOTYPIC CULTURES*. Vol. 57.

Tall, A. R. 2008. “Cholesterol Efflux Pathways and Other Potential Mechanisms Involved in the Athero-Protective Effect of High Density Lipoproteins.” *Journal of Internal Medicine* 263(3):256–73. doi: 10.1111/J.1365-2796.2007.01898.X.

Teng, Jon Ie, and Leland L. Smith. 1995. “High-Performance Liquid Chromatographic Analysis of Human Erythrocyte Oxyterols as Δ4-3-Ketone Derivatives.” *Journal of Chromatography A* 691(1–2):247–54. doi: 10.1016/0021-9673(94)00986-J.

Theofilopoulos, Spyridon, Ernest Arenas, Yuqin Wang, Spyridon Theofilopoulos, William J. Griffiths, Peter J. Crick, Shanzheng Yang, Anna Meljon, Michael Ogundare, Satish Srinivas Kitambi, Andrew Lockhart, Karin Tuschl, Peter T. Clayton, Andrew A. Morris, Adelaida Martinez, M. Ashwin Reddy, Andrea Martinuzzi, Maria T. Bassi, Akira Honda, Tatsuki Mizuochi, and Akihiko Kimura. 2014. “Cholestenoic Acids Regulate Motor Neuron Survival via Liver X Receptors Find the Latest Version : Cholestenoic Acids Regulate Motor Neuron Survival via Liver X Receptors.” *J Clin Invest* 124(11):4829–42. doi: 10.1172/JCI68506.adult.

Theofilopoulos, Spyridon, Yuqin Wang, Satish Srinivas Kitambi, Paola Sacchetti, Kyle M. Sousa, Karl Bodin, Jayne Kirk, Carmen Saltó, Magnus Gustafsson, Enrique M. Toledo, Kersti Karu, Jan Åke Gustafsson, Knut R. Steffensen, Patrik Ernfors, Jan Sjövall, William J. Griffiths, and Ernest Arenas. 2013. “Brain Endogenous Liver X Receptor Ligands Selectively Promote Midbrain Neurogenesis.” *Nature Chemical Biology* 9(2):126–33. doi: 10.1038/nchembio.1156.

Thomas, Stefani N. 2019. *Contemporary Practise in Clinical Chemistry*. 4th ed. Elsevier.

Thompson, Alan J., Brenda L. Banwell, Frederik Barkhof, William M. Carroll, Timothy Coetzee, Giancarlo Comi, Jorge Correale, Franz Fazekas, Massimo Filippi, Mark S. Freedman, Kazuo Fujihara, Steven L. Galetta, Hans Peter Hartung, Ludwig Kappos, Fred D. Lublin, Ruth Ann Marrie, Aaron E. Miller, David H. Miller, Xavier Montalban, Ellen M. Mowry, Per Soelberg Sorensen, Mar Tintoré, Anthony L. Traboulsee, Maria Trojano, Bernard M. J. Uitdehaag, Sandra Vukusic, Emmanuelle Waubant, Brian G. Weinshenker, Stephen C. Reingold, and Jeffrey A. Cohen. 2018. “Diagnosis of Multiple Sclerosis: 2017 Revisions of the McDonald Criteria.” *The Lancet Neurology* 17(2):162–73. doi: 10.1016/S1474-4422(17)30470-2.

Thompson, Alan J., Sergio E. Baranzini, Jeroen Geurts, Bernhard Hemmer, and Olga Ciccarelli. 2018. “Multiple Sclerosis.” *The Lancet* 391(10130):1622–36. doi: 10.1016/S0140-6736(18)30481-1.

Tiper, Irina V., James E. East, Priyanka B. Subrahmanyam, and Tonya J. Webb. 2016. “Sphingosine 1-Phosphate Signaling Impacts Lymphocyte Migration, Inflammation and Infection.” *Pathogens and Disease* 74(6). doi: 10.1093/FEMSPD/FTW063.

Del Toro, Daniel, Xavier Xifró, Albert Pol, Sandrine Humbert, Frédéric Saudou, Josep M. Canals, and Jordi Alberch. 2010. “Altered Cholesterol Homeostasis Contributes to Enhanced Excitotoxicity in Huntington’s Disease.” *Journal of Neurochemistry* 115(1):153–67. doi: 10.1111/j.1471-4159.2010.06912.x.

Travers, Brett S., Benjamin K. T. Tsang, and Joshua L. Barton. 2022. “Multiple Sclerosis: Diagnosis, Disease-Modifying Therapy and Prognosis.” *Reprinted from AJGP* 51(4):199–206.

Tremblay, Marie-E. `. Ve, Beth Stevens, Amanda Sierra, Hiroaki Wake, Alain Bessis, and Axel Nimmerjahn. 2011. “The Role of Microglia in the Healthy Brain.” *J. Neurosci* 31(45):16064–69. doi: 10.1523/JNEUROSCI.4158-11.2011.

Tur, Carmen, Pere Carbonell-Mirabent, Álvaro Cobo-Calvo, Susana Otero-Romero, Georgina Arrambide, Luciana Midaglia, Joaquín Castilló, Ángela Vidal-Jordana, Breogán Rodríguez-Acevedo, Ana Zabalza, Ingrid Galán, Carlos Nos, Annalaura Salerno, Cristina Auger, Deborah Pareto, Manuel Comabella, Jordi Río, Jaume Sastre-Garriga, Àlex Rovira, Mar Tintoré, and Xavier Montalban. 2023. “Association of Early Progression Independent of Relapse Activity With Long-Term Disability After a First Demyelinating Event in Multiple Sclerosis.” *JAMA Neurology* 80(2):151. doi: 10.1001/jamaneurol.2022.4655.

Ulland, Tyler K., and Marco Colonna. 2018. “TREM2 — a Key Player in Microglial Biology and Alzheimer Disease.” *Nature Reviews Neurology 2018 14:11* 14(11):667–75. doi: 10.1038/s41582-018-0072-1.

Umpierre, Anthony D., and Long-Jun Wu. 2021. “How Microglia Sense and Regulate Neuronal Activity.” *Glia* 69(7):1637–53. doi: 10.1002/glia.23961.

Vainchtein, Ilia D., and Anna V. Molofsky. 2020. “Astrocytes and Microglia: In Sickness and in Health.” *Trends in Neurosciences* 43(3):144–54. doi: 10.1016/J.TINS.2020.01.003.

Valenza, Marta, Jeffrey B. Carroll, Valerio Leoni, Lisa N. Bertram, Ingeman Björkhem, Roshni R. Singaraja, Stefano Di Donato, Dieter Lutjohann, Michael R. Hayden, and Elena Cattaneo. 2007. “Cholesterol Biosynthesis Pathway Is Disturbed in YAC128 Mice and Is Modulated by Huntingtin Mutation.” *Human Molecular Genetics* 16(18):2187–98. doi: 10.1093/HMG/DDM170.

Valenza, Marta, Jane Y. Chen, Eleonora Di Paolo, Barbara Ruozi, Daniela Belletti, Costanza Ferrari Bardile, Valerio Leoni, Claudio Caccia, Elisa Brilli, Stefano Di Donato, Marina M. Boido, Alessandro Vercelli, Maria A. Vandelli, Flavio Forni, Carlos Cepeda, Michael S. Levine, Giovanni Tosi, and Elena Cattaneo. 2015. “Cholesterol-Loaded Nanoparticles Ameliorate Synaptic and Cognitive Function in Huntington’s Disease Mice.” *EMBO Molecular Medicine* 7(12):1547–64. doi: 10.15252/EMMM.201505413.

Valenza, Marta, Valerio Leoni, Alessia Tarditi, Caterina Mariotti, Ingeman Björkhem, Stefano Di Donato, and Elena Cattaneo. 2007. “Progressive Dysfunction of the Cholesterol Biosynthesis Pathway in the R6/2 Mouse Model of Huntington’s Disease.” *Neurobiology of Disease* 28(1):133–42. doi: 10.1016/j.nbd.2007.07.004.

Vance, J. E., B. Karten, and H. Hayashi. 2006. “Lipid Dynamics in Neurons.” *Biochemical Society Transactions* 34(3):399–403. doi: 10.1042/BST0340399.

Varma, V.R., Büşra Lüleci, H., Oommen, A.M., Varma, S., Blackshear, C.T., Griswold, M.E., *et al.* (2021) Abnormal brain cholesterol homeostasis in Alzheimer’s disease—a targeted metabolomic and transcriptomic study. *NPJ Aging Mech Dis* **7**.

Vaughn, Caila B., Dejan Jakimovski, Katelyn S. Kavak, Murali Ramanathan, Ralph H. B. Benedict, Robert Zivadinov, and Bianca Weinstock-Guttman. 2019. “Epidemiology and Treatment of

Multiple Sclerosis in Elderly Populations." *Nature Reviews. Neurology* 15(6):329–42. doi: 10.1038/S41582-019-0183-3.

Volterra, Andrea, and Jacopo Meldolesi. 2005. "Astrocytes, from Brain Glue to Communication Elements: The Revolution Continues." *Nature Reviews Neuroscience* 6(8):626–40.

Voskuhl, Rhonda R., Noriko Itoh, Alessia Tassoni, Macy Akiyo Matsukawa, Emily Ren, Vincent Tse, Ellis Jang, Timothy Takazo Suen, and Yuichiro Itoh. 2019. "Gene Expression in Oligodendrocytes during Remyelination Reveals Cholesterol Homeostasis as a Therapeutic Target in Multiple Sclerosis." *Proceedings of the National Academy of Sciences of the United States of America* 116(20):10130–39. doi: 10.1073/PNAS.1821306116/SUPPL_FILE/PNAS.1821306116.SD03.XLSX.

Voskuhl, Rhonda R., R. Scott Peterson, Bingbing Song, Yan Ao, Laurie Beth J. Morales, Seema Tiwari-Woodruff, and Michael V. Sofroniew. 2009. "Reactive Astrocytes Form Scar-Like Perivascular Barriers to Leukocytes during Adaptive Immune Inflammation of the CNS." *The Journal of Neuroscience* 29(37):11522. doi: 10.1523/JNEUROSCI.1514-09.2009.

Voß, Elke Verena, Jelena Škuljec, Viktoria Gudi, Thomas Skripuletz, Refik Pul, Corinna Trebst, and Martin Stangel. 2012. "Characterisation of Microglia during De- and Remyelination: Can They Create a Repair Promoting Environment?" *Neurobiology of Disease* 45(1):519–28. doi: 10.1016/J.NBD.2011.09.008.

Wang, Fay, John Flanagan, Nan Su, Li Chong Wang, Son Bui, Allissa Nielson, Xingyong Wu, Hong Thuy Vo, Xiao Jun Ma, and Yuling Luo. 2012. "RNAscope: A Novel in Situ RNA Analysis Platform for Formalin-Fixed, Paraffin-Embedded Tissues." *The Journal of Molecular Diagnostics : JMD* 14(1):22–29. doi: 10.1016/J.JMOLDX.2011.08.002.

Wang, Yuqin, Eylan Yutuc, and William J. Griffiths. 2021. "Cholesterol Metabolism Pathways – Are the Intermediates More Important than the Products?" *The Febs Journal* 288(12):3727–45. doi: 10.1111/FEBS.15727.

Wang, Zhe, A. Dessa Sadovnick, Anthony L. L. Traboulsee, Jay P. P. Ross, Cecily Q. Q. Bernales, Mary Encarnacion, Irene M. M. Yee, Madonna de Lemos, Talitha Greenwood, Joshua D. D. Lee, Galen Wright, Colin J. J. Ross, Si Zhang, Weihong Song, and Carles Vilariño-Güell. 2016. "Nuclear Receptor NR1H3 in Familial Multiple Sclerosis." *Neuron* 90(5):948–54. doi: 10.1016/J.NEURON.2016.04.039.

Willey, Joshua Z., and Mitchell S. V. Elkind. 2010. "3-Hydroxy-3-Methylglutaryl–Coenzyme A Reductase Inhibitors in the Treatment of Central Nervous System Diseases." *Archives of Neurology* 67(9):1062–67. doi: 10.1001/ARCHNEUROL.2010.199.

Yang, Jennifer, Maysa Hamade, Qi Wu, Qin Wang, Robert Axtell, Shailendra Giri, and Yang Mao-Draayer. 2022. "Current and Future Biomarkers in Multiple Sclerosis." *International Journal of Molecular Sciences* 23(11). doi: 10.3390/IJMS23115877.

Yao, Rumeng, Ruiyuan Pan, Chao Shang, Xiaoheng Li, Jinbo Cheng, Jiangping Xu, and Yunfeng Li. 2020. "Translocator Protein 18 KDa (TSPO) Deficiency Inhibits Microglial Activation and Impairs Mitochondrial Function." *Frontiers in Pharmacology* 11. doi: 10.3389/FPHAR.2020.00986/BIBTEX.

Yeh, Felix L., Yuanyuan Wang, Irene Tom, Lino C. Gonzalez, and Morgan Sheng. 2016. “TREM2 Binds to Apolipoproteins, Including APOE and CLU/APOJ, and Thereby Facilitates Uptake of Amyloid-Beta by Microglia.” *Neuron* 91(2):328–40. doi: 10.1016/J.NEURON.2016.06.015.

Yong, Heather Y. F., and V. Wee Yong. 2021. “Mechanism-Based Criteria to Improve Therapeutic Outcomes in Progressive Multiple Sclerosis.” *Nature Reviews Neurology 2021 18:1* 18(1):40–55. doi: 10.1038/s41582-021-00581-x.

Young, Christina B., Emily Johns, Gabriel Kennedy, Michael E. Belloy, Philip S. Insel, Michael D. Greicius, Reisa A. Sperling, Keith A. Johnson, Kathleen L. Poston, and Elizabeth C. Mormino. 2023. “APOE Effects on Regional Tau in Preclinical Alzheimer’s Disease.” *Molecular Neurodegeneration* 18(1):1–14. doi: 10.1186/S13024-022-00590-4/FIGURES/4.

Yutuc, Eylan, Roberto Angelini, Mark Baumert, Natalia Mast, Irina Pikuleva, Jillian Newton, Malcolm R. Clench, David Skibinski, Owain W. Howell, Yuqin Wang, and William J. Griffiths. 2019. “Imaging Oxysterols in Mouse Brain by On-Tissue Derivatisation – Robotic Micro-Liquid-Extraction Surface Analysis – Liquid Chromatography Mass Spectrometry.” *BioRxiv* 450973. doi: 10.1101/450973.

Zhang, Hui, Andrew A. Jarjour, Amanda Boyd, and Anna Williams. 2011. “Central Nervous System Remyelination in Culture - A Tool for Multiple Sclerosis Research.” *Experimental Neurology* 230(1):138–48. doi: 10.1016/j.expneurol.2011.04.009.

Zhang, Jiquan, Anna Raper, Noriko Sugita, Ravi Hingorani, Mariolina Salio, Michael J. Palmowski, Vincenzo Cerundolo, and Paul R. Crocker. 2006. “Characterization of Siglec-H as a Novel Endocytic Receptor Expressed on Murine Plasmacytoid Dendritic Cell Precursors.” doi: 10.1182/blood-2005.

Zhang, Juan, and Qiang Liu. 2015. “Cholesterol Metabolism and Homeostasis in the Brain.” *Protein and Cell* 6(4):254–64. doi: 10.1007/s13238-014-0131-3.

Zhang, Z., D. Li, D. E. Blanchard, S. R. Lear, S. K. Erickson, and T. A. Spencer. 2001. “Key Regulatory Oxysterols in Liver: Analysis as Δ4-3-Ketone Derivatives by HPLC and Response to Physiological Perturbations.” *Journal of Lipid Research* 42(4):649–58. doi: 10.1016/S0022-2275(20)31174-3.

Zhu, Xiaoping, Tianyi Xu, Chen Peng, and Shihua Wu. 2022. “Advances in MALDI Mass Spectrometry Imaging Single Cell and Tissues.” *Frontiers in Chemistry* 9:1076–2002. doi: 10.3389/FCHEM.2021.782432/XML/NLM.

Zrzavy, Tobias, Simon Hametner, Isabella Wimmer, Oleg Butovsky, Howard L. Weiner, and Hans Lassmann. 2017. “Loss of ‘homeostatic’ Microglia and Patterns of Their Activation in Active Multiple Sclerosis.” *Brain* 140(7):1900–1913. doi: 10.1093/brain/awx113.